



Heath, Nikki (2015) *An investigation into the role of microvesicles in mutant p53 invasive gain-of-function*. PhD thesis.

<https://theses.gla.ac.uk/6895/>

Copyright and moral rights for this work are retained by the author

A copy can be downloaded for personal non-commercial research or study, without prior permission or charge

This work cannot be reproduced or quoted extensively from without first obtaining permission in writing from the author

The content must not be changed in any way or sold commercially in any format or medium without the formal permission of the author

When referring to this work, full bibliographic details including the author, title, awarding institution and date of the thesis must be given

Enlighten: Theses

<https://theses.gla.ac.uk/>
research-enlighten@glasgow.ac.uk

An investigation into the role of microvesicles in mutant p53 invasive gain-of-function

Nikki Heath

BSc (Hons)

Submitted in fulfilment of the requirements for the degree
of Doctor of Philosophy

Institute of Cancer Sciences
College of Medical, Veterinary and Life Sciences
University of Glasgow

September 2015

Abstract

p53 is a transcription factor with tumour suppressive attributes which is known to be mutated in over half of human cancers. As well as compromising the ability of p53 to function as a transcription factor, mutations in p53 often result in a gain-of-function phenotype which is characterised by increased ability of cancer cells to migrate and invade. This is mediated by the ability of mutant p53 to increase recycling of $\alpha 5\beta 1$ integrin and receptor tyrosine kinases (RTK) from endosomes to the plasma membrane; a process which is dependent on the Rab11 effector, Rab Coupling Protein (RCP) and the phosphatidic acid generating enzyme, diacylglycerol kinase- α (DGK α). Despite accumulating evidence linking RCP/DGK α -dependent receptor recycling to invasive migration, the mechanisms by which mutant p53 controls endosomal trafficking were still unclear when the current study was instigated.

Initial experiments indicated that the mutant p53 gain-of-function phenotype was not cell autonomous, and could be passed to p53 null cells by incubating them with conditioned medium from mutant p53 (R273H)-expressing cells. Furthermore, fractionation approaches indicated that the mutant p53 phenotype was transmitted between cells by a microvesicle vector. Upon treatment with microvesicles collected from mutant p53 expressing cells, p53 null cells displayed increased $\alpha 5\beta 1$ integrin and RTK recycling and the consequent invasive/migratory behaviour that was dependent on these RCP and DGK α -regulated trafficking events.

Despite a requirement for RCP in the response of p53 null cells to microvesicles, this Rab11 effector was not required for the production of pro-invasive microvesicles. Rather, mutant p53-expressing cells relied on Rab35 (but not Rab27a or Rab27b) for the production and/or release of microvesicles that were capable of transferring mutant p53's gain-of-function phenotype.

An in-depth RNA sequencing analysis indicated that microvesicles from mutant p53 cells influenced the endocytic trafficking and migratory characteristics of p53 null cells without detectably altering mRNA expression in these recipient cells. This indicated the possibility that microvesicles from mutant p53-expressing cells may act directly on the endomembrane system of recipient

cells. Immunoprecipitation experiments indicated that there was a physical interaction between Rab35 and podocalyxin (PODXL), a highly-charged sialomucin which is known to directly influence membrane organisation. Additionally, PODXL was detectable in microvesicular preparations by mass spectrometry. Microvesicles purified from mutant p53-expressing cells in which PODXL had been knocked down using siRNA, had significantly reduced capacity to promote integrin/RTK recycling and mutant p53-like migratory behaviour in p53 null cells, indicating that PODXL, as well as Rab35, is a key factor responsible for transmitting mutant p53's gain-of-function phenotype between cells. In addition to being incapable of influencing the migration of other cells, Rab35 knockdown cells themselves migrated with the characteristics of p53 null cells. Interestingly, microvesicles from mutant p53-expressing cells restored mutant p53-like migratory behaviour in these Rab35 knockdown cells. These data indicate that Rab35 and PODXL-dependent production of phenotype altering microvesicles not only influences the migration of neighbouring cells in a paracrine fashion, but may constitute an autocrine link between mutant p53 and integrin trafficking in the mutant p53 cells themselves. Finally, I have found that p53 null cells may be educated by microvesicles from mutant p53-expressing cells to themselves release cell migration-altering microvesicles, providing further evidence supporting the existence of microvesicle-based autocrine/paracrine mechanisms that may act to propagate mutant p53's invasive gain-of-function within both homogeneous and heterogeneous populations of tumour cells.

Table of Contents

Abstract	2
List of Tables	9
List of Figures	10
Acknowledgements	13
Author's declaration	14
Abbreviations	15
1 Introduction	18
1.1 Cancer	18
1.1.1 Hallmarks of cancer	18
1.1.2 Metastasis	19
1.1.3 Cell migration and invasion in cancer metastasis	21
1.1.3.1 Collective cell migration and invasion	22
1.1.3.2 Single cell migration and invasion.....	22
1.1.4 Integrin trafficking in cancer cell migration	24
1.1.4.1 Integrins	24
1.1.4.2 Integrin endocytosis.....	26
1.1.4.3 Rab-GTPases.....	26
1.1.4.4 Integrin trafficking routes	27
1.1.4.5 Integrin trafficking and cancer cell migration	29
1.2 p53	30
1.2.1 Historical perspective.....	30
1.2.2 Wild-type p53	31
1.2.2.1 Structure	31
1.2.2.2 Activation and regulation.....	32
1.2.2.3 Physiological effects of p53 activation.....	33
1.2.2.4 p53 loss and cell migration	36
1.2.3 Mutant p53.....	36
1.2.3.1 Mutant p53: transcriptional regulation	37
1.2.3.2 Gain-of-function mechanisms.....	38
1.2.3.3 Gain-of-function phenotypes.....	41
1.2.3.4 Targeting mutant p53 therapeutically	44
1.2.3.5 Concluding remarks	44
1.3 Microvesicles	45
1.3.1 Historical perspective.....	45
1.3.2 Biogenesis and subtypes	46
1.3.2.1 MVB-derived exosomes	46

1.3.2.2	Rab-GTPases.....	47
1.3.2.3	SNARE proteins	49
1.3.2.4	Plasma membrane-shed microvesicles.....	50
1.3.2.5	Stimuli leading to microvesicle release.....	52
1.3.2.6	Alteration of microvesicle contents	52
1.3.3	Microvesicle constituents.....	53
1.3.3.1	Proteins	53
1.3.3.2	Lipids	54
1.3.3.3	Nucleic acids.....	55
1.3.4	Microvesicle uptake by recipient cells	57
1.3.5	Microvesicle function.....	59
1.3.5.1	Modulation of immune responses.....	59
1.3.5.2	Modulation of immune function in cancer	59
1.3.5.3	Microvesicles in cancer immunotherapy.....	60
1.3.5.4	Microvesicles in cancer cell communication	61
1.3.5.5	Other microvesicle functions	63
1.4	Final concluding remarks	64
2	Methods	65
2.1	Cells and tissue culture	65
2.1.1	Cell line generation	65
2.1.1.1	H1299 p53 ^{-/-} and p53 ^{R273H/R175H}	65
2.1.1.2	H1299 p53 ^{-/-} GFP and p53 ^{R273H} m-cherry	66
2.1.1.2	MCF7 p53 ^{-/-} , p53 ^{R273H} and p53 ^{WT}	66
2.1.2	Tissue culture	67
2.1.2.1	H1299 and MCF7.....	67
2.1.2.2	A2780	67
2.1.2.3	Co-culture.....	67
2.1.2.4	Transfections and siRNA oligos.....	67
2.2	Conditioned medium and microvesicle collection.....	68
2.2.1	Conditioned medium collection	68
2.2.2	Microvesicle collection.....	68
2.2.2.1	Differential centrifugation	68
2.2.2.2	Sucrose density gradient.....	69
2.2.3	Conditioned medium or microvesicle pre-treatment of cells	70
2.2.3.1	Conditioned medium pre-treatment	70
2.2.3.2	Microvesicle pre-treatment	70
2.3	Microvesicle characterisation strategies	70

2.3.1	Protein content	70
2.3.2	Electron microscopy.....	71
2.3.3	Nanoparticle tracking analysis.....	71
2.4	Cell phenotype assays.....	72
2.4.1	Proliferation	72
2.4.2	Wound healing migration assay.....	72
2.4.3	Golgi-nucleus orientation Immunofluorescence	73
2.4.4	Inverted invasion assay	73
2.4.5	Recycling assay.....	74
2.4.5.1	Cell preparation	74
2.4.5.2	Internalisation.....	74
2.4.5.3	Recycling	75
2.4.5.4	ELISA.....	75
2.5	Screens	76
2.5.1	SILAC mass spectrometry of microvesicles	76
2.5.2	Lipidomic analysis of microvesicles.....	77
2.5.2.1	Lipid extraction	77
2.5.2.2	Liquid-chromatography-mass spectrometry	77
2.5.2.3	Data processing and multivariate statistical analysis	77
2.5.3	Next generation sequencing	78
2.5.3.1	RNA harvesting.....	78
2.5.3.2	cDNA library generation.....	78
2.5.3.3	Sequencing.....	78
2.5.3.4	Data analysis	79
2.6	Quantitative PCR.....	79
2.6.1	RNA isolation	79
2.6.2	cDNA synthesis	79
2.6.3	Quantitative PCR.....	80
2.7	Western blotting and antibodies	80
2.7.1	Cell lysis.....	80
2.7.2	Microvesicle preparation	80
2.7.3	Western blotting	81
2.8	Immunoprecipitation.....	81
2.8.1	Antibodies.....	82
2.9	Statistics	82
3	Microvesicle characterisation	83
3.1	Introduction	83
3.1.1	Microvesicles	83

3.1.2	Characterisation of microvesicles.....	85
3.2	Aims.....	87
3.3	Results.....	88
3.3.1	Microvesicle isolation optimisation	88
3.3.1.1	Differential centrifugation	89
3.3.1.2	Sucrose density gradient purification	91
3.3.1.3	Electron microscopy.....	92
3.3.1.4	Nanoparticle tracking.....	95
3.3.2	Characterisation of microvesicle constitution	97
3.3.2.1	Lipidomic screen	97
3.3.2.2	SILAC mass spectrometry screen	100
3.4	Discussion	106
3.4.1	The impact of mutant p53 expression on microvesicle release	106
3.4.2	Impact of mutant p53 expression on microvesicle content	107
3.4.2.1	Protein constituents.....	107
3.4.2.2	Lipid constituents.....	108
3.4.2.3	Screen limitations	109
3.4.2.4	Other microvesicle constituents.....	110
3.4.3	Concluding remarks	110
4	Influence of microvesicles from mutant p53-expressing cells on cell migration and invasion	112
4.1	Introduction	112
4.1.1	Non-cell-autonomous roles of p53	112
4.1.1.1	Protein secretion.....	112
4.1.1.2	MVB-derived exosome release.....	113
4.1.2	Non-cell autonomous role of mutant p53.....	114
4.1.3	Aims.....	114
4.2	Results.....	115
4.2.1	Mutant p53 expression in H1299 cells drives a gain-of-function migratory and invasive phenotype.....	115
4.2.2	Mutant p53 gain-of-function migratory phenotype is non-cell-autonomous	116
4.2.3	Microvesicles released by p53 ^{R273H} -expressing cells transfer the mutant p53 migratory phenotype to p53 ^{-/-} cells	122
4.2.3.1	Effect of microvesicles from p53 ^{R273H} -expressing cells on mRNA expression.....	127
4.2.3.2	RCP and DGK α are required for the response of H1299 cells to microvesicles from mutant p53-expressing cells, but not for generation of migration-altering microvesicles.....	129

4.2.3.3	Rab35 (but not Rab27) is required for production of migration-altering microvesicles.....	131
4.2.3.4	Podocalyxin is required for production of microvesicles that influence receptor trafficking and migration in recipient cells	134
4.2.3.5	Rab35 maintains the mutant p53 gain-of-function phenotype via an autocrine mechanism.....	137
4.3	Discussion	140
4.3.1	Mutant p53 microvesicles	140
4.3.1.1	Mutant p53 microvesicle release.....	140
4.3.1.2	Provenance of microvesicles from mutant p53 expressing cells.....	141
4.3.1.3	Microvesicles from p53 null cells.....	141
4.3.2	How are mutant p53 microvesicles exerting their effects?	142
4.3.2.1	Transcriptional regulation.....	142
4.3.2.2	Podocalyxin	142
4.3.2.3	Podocalyxin and cancer	143
4.3.2.4	Podocalyxin hypothesis.....	143
4.3.3	Mutant p53 microvesicles: Role in cell education and autocrine signalling.....	145
4.3.3.1	Microvesicles and education of neighbouring cells.....	145
4.3.3.2	Microvesicles and their autocrine role	146
4.4	Conclusion	146
5	Final discussion	148
5.1	Microvesicles from mutant p53-expressing cells and their role in cell migration	148
5.1.1	Microvesicles and cell migration	148
5.1.1.1	Microvesicles from mutant p53-expressing cells and cell migration: Integrins...149	
5.1.2	Microvesicles and cell migration and metastasis <i>in-vivo</i> : future aims	150
5.1.3	Microvesicles as diagnostic biomarkers	152
5.2	Mutant p53 gain-of-function mechanism.....	153
5.2.1	p63 and the mutant p53 gain-of-function	153
5.2.2	Achieving mutant p53 gain-of-function without alterations to mRNA expression	154
5.2.3	The roles of Rab35 and PODXL in microvesicle production and function	155
5.2.4	Autocrine and paracrine maintenance of the mutant p53 phenotype	156
5.2.4.1	Autocrine maintenance and paracrine transfer of the mutant p53 phenotype <i>in vivo</i> : future aims	157
	List of references	160

List of Tables

Table 2-1: p53 status of cell lines used in the study and their genetic modifications.	65
Table 2-2: Antibodies used in Western blotting, ELISA and IP.....	82
Table 3-1: Summary of MVB-derived exosome and plasma membrane-shed microvesicle characteristics.	84
Table 3-2: Protein categories expected to be present in MVB-derived exosomes and plasma membrane-shed microvesicles.	86
Table 3-3: In-depth analysis of lipid species detected in lipidomic screen.	99
Table 3-4: The most abundant proteins in microvesicles detected by mass spectrometry.	102
Table 3-5: Proteins present in microvesicles released by H1299 cells.	103
Table 3-6: Microvesicle SILAC mass spectrometry data.	105

List of Figures

Figure 1-1: Schematic diagram of the tumour microenvironment.	19
Figure 1-2: Overview of the metastatic cascade.	21
Figure 1-3: Cell migration modes.	24
Figure 1-4: Integrin families.	25
Figure 1-5: Diagram representing the cyclical activation and deactivation of Rab-GTPases.	27
Figure 1-6: Diagram depicting the main mechanisms of integrin trafficking in the cell.	29
Figure 1-7: Structure of p53 protein.....	31
Figure 1-8: MDM2 regulation of p53 protein stability.	33
Figure 1-9: Overview of stimuli that activate p53 and the subsequent responses that enable the maintenance of a healthy population of cells.....	34
Figure 1-10: Mutant p53 gain-of-function mechanisms.	40
Figure 1-11: Effect of mutant p53 on integrin and RTK trafficking.....	43
Figure 1-12: MVB-derived exosome biogenesis and release.....	50
Figure 1-13: Illustration of plasma membrane-shed microvesicle biogenesis and release.....	52
Figure 1-14: Diagram of microvesicle constituents.....	57
Figure 1-15: MVB-derived exosomes from cancer cells educate stromal cells to prime metastatic niches.	63
Figure 3-1: Diagram of microvesicle formation and release.	85
Figure 3-2: Diagram depicting the protocol used for the isolation of microvesicles by differential centrifugation and further purification by a sucrose density gradient.	88

Figure 3-3: The protein content of microvesicles collected by differential centrifugation from H1299-p53 ^{-/-} or H1299-p53 ^{R273H} cells is not different.	89
Figure 3-4: Western blot characterisation shows that there are no distinct differences in microvesicle marker or mutant p53 content in microvesicles derived from H1299 p53 ^{-/-} and H1299-p53 ^{R273H} cells.....	91
Figure 3-5: The distribution of CD63-positive microvesicles from H1299-p53 ^{-/-} and H1299-p53 ^{R273H} -expressing cells on a sucrose gradient.	92
Figure 3-6: Transmission electron microscopy analysis of microvesicles.	94
Figure 3-7: Nanoparticle tracking analysis of microvesicles released from p53 ^{-/-} and p53 ^{R273H} -expressing H1299 cells.	96
Figure 3-8: Lipidomic screen of microvesicles released by p53 ^{-/-} and p53 ^{R273H} -expressing H1299 cells revealed that there is no significant difference in the microvesicle lipid composition.	98
Figure 3-9: Experimental design of the microvesicle SILAC mass spectrometry analysis.	101
Figure 3-10: Gene enrichment analysis of protein constituents of microvesicles from H1299 p53 ^{-/-} and H1299-p53 ^{R273H} -expressing cells.	104
Figure 4-1: Mutant p53 expressing cells migrate with a lower forward migration index and display higher invasive capacity than cells null for p53.	116
Figure 4-2: Co-culture with p53 ^{R273H} -expressing cells reduces the forward migration index of H1299-p53 ^{-/-} cells.....	118
Figure 4-3: Schematic representation of conditioned medium experimental design.	119
Figure 4-4: Conditioned medium from p53 ^{R273H} -expressing cells transfers the mutant p53 gain-of-function migratory phenotype to p53 ^{-/-} cells.	121
Figure 4-5: Diagram depicting the experimental design of microvesicle pre-treatment experiments.	122

Figure 4-6: Microvesicles collected from p53 ^{R273H} and p53 ^{R175H} expressing cells can transfer the mutant p53 migratory phenotype to p53 ^{-/-} cells.	124
Figure 4-7: Microvesicles from p53 ^{R273H} expressing cells increase the receptor recycling rate and invasive capacity of p53 ^{-/-} cells.	126
Figure 4-8: Microvesicles from mutant p53-expressing cells are not able to detectably alter the mRNA expression profile of H1299 cells.	128
Figure 4-9: RCP and the activity of DGK α are required for response of H1299 cells to microvesicles from mutant p53-expressing cells.	130
Figure 4-10: Rab35 (but not Rab27) is required for release of migration-altering microvesicles from mutant p53-expressing cells.	132
Figure 4-11: Rab35 silencing has no detectable influence on the number or size of microvesicles released from mutant p53-expressing cells.	133
Figure 4-12: Podocalyxin co-immunoprecipitates with GFP-Rab35.	134
Figure 4-13: Podocalyxin is necessary for mutant p53 gain-of-function phenotype, and for transfer of the mutant p53 phenotype to p53 ^{-/-} cells via a microvesicle vector.	136
Figure 4-14: The mutant p53 gain-of-function migratory phenotype is maintained in p53 ^{R273H} -expressing cells and in microvesicle-educated p53 ^{-/-} cells in an autocrine/paracrine fashion.	139
Figure 4-15: Diagram illustrating mutant p53 non-cell-autonomous gain-of-function invasive phenotype model.	147
Figure 5-1: Diagram of potential mechanisms through which microvesicles influence cell migration.	150
Figure 5-2: A proposed mechanism for p53 gain-of-function.	159

Acknowledgements

I would like to thank my supervisor Jim Norman for giving me the opportunity to work on this project, and for teaching and supporting me throughout my PhD. Thank you to Cancer Research UK for the financial funding of this study.

Thank you to all collaborators without whom this project would not have progressed this far. Thank you to David Sumpton and Sara Zanivan for their SILAC and mass spectrometry expertise, Billy Clarke and Gabriela Kalna for RNA sequencing and bioinformatics analysis, Margaret O'Prey in the Beatson Advanced Imaging Resource and Margaret Mullin for her expertise in the electron microscopy facility at the University of Glasgow. Finally thank you to our collaborators external to the Beatson - Phil Whitfield and colleagues at the University of Highlands and Islands for their help in completing the lipidomic analysis of microvesicles.

A huge thank you to everyone in the R20 lab (past and present) for their excellent discussion and guidance, with a special thank you to Elena Rainero and Liane McGlynn for their advice whilst writing the thesis.

Lastly thank you to my amazing mum, dad and brother for their continuous support and encouragement throughout my studies. And thank you to my fabulous partner Tim for supporting and motivating me especially through this final year and writing up.

Finally I dedicate this thesis to the memory of Michael Braithwaite who lost his battle with cancer too young and inspired me to get to where I am today.

Author's declaration

I declare that I am the sole author of this thesis, except where explicit reference is made as to the work of others.

Nikki Heath.

Abbreviations

AMPK	Amp-activated protein kinase
ATM	Ataxia telangiectasia mutated gene
ATP	Adenosine triphosphate
BCL2	B-cell lymphoma 2
BSA	Bovine serum albumin
CAF	Cancer associated fibroblasts
cDNA	Complementary DNA
CLIC	Clathrin independent carriers
CM	Conditioned medium
CRISPR	Clustered regularly interspaced short palindromic repeats
DAG	Diacylglycerol
DGK	Diacylglycerol kinase
DMEM	Dulbecco's modified eagle medium
DMSO	Dimethyl sulfoxide
DNA	Deoxyribonucleic acid
ECM	Extracellular matrix
EE	Early endosome
EGF	Epidermal growth factor
EGFR	Epidermal growth factor receptor
ELISA	Enzyme linked immunosorbent assay
EMT	Epithelial mesenchymal transition
EPCAM	Epithelial cell adhesion molecule
ER	Endoplasmic reticulum
ESCRT	Endosomal sorting complex required for transport
FBS	Fetal bovine serum
FMI	Forward migration index
GAP	GTPase activating protein
GDF	GDP dissociation inhibitor
GDI	GDP dissociation inhibitor
GDP	Guanosine diphosphate
GEF	Guanine nucleotide exchange factor
GFP	Green fluorescent protein
GPI	Glycophosphatidylinositol
GTP	Guanosine triphosphate
HAX1	HS1-associated protein X-1
HGF	Hepatocyte growth factor
HIV	Human immunodeficiency virus
HRP	Horseradish peroxidase

HSP	Heat shock protein
IB	Immunoblot
ICAM1	Intracellular adhesion molecule-1
ILV	Intraluminal vesicles
IP	Immunoprecipitate
kDa	Kilodalton
LASP1	LIM and SH3 domain protein-1
LCMS	Liquid chromatography mass spectrometry
LIF	Leukaemia inhibitory factor
LMP1	Latent membrane protein-1
Lys	Lysosome
MAR	Matrix attachment region
MDM2	Mouse double minute 2
MDM4	Mouse double minute 4
MIF	Macrophage migration inhibitory factor
MMP	Matrix metalloproteinase
mRNA	Messenger RNA
miRNA	Micro RNA
MTOR	Mechanistic target of rapamycin
MV	Microvesicles
MVB	Multivesicular bodies
NFκB	Nuclear factor kappa-light-chain-enhancer of activated B cells
Nt	Non targeting
PA	Phosphatidic acid
PAGE	Polyacrylamide gel electrophoresis
PBS	Phosphate buffered saline
PCR	Polymerase chain reaction
PDAC	Pancreatic ductal adenocarcinoma
PDGF	Platelet derived growth factor
PI	Phosphatidylinositol
PKB	Protein kinase B
PKD	Protein kinase D
PM	Plasma membrane
PODXL	Podocalyxin
PUMA	p53 upregulated modulator of apoptosis
qPCR	Quantitative polymerase chain reaction
RCP	Rab coupling protein
RE	Recycling endosome
REP	Rab escort protein
RNA	Ribonucleic acid
ROCK	Rho-associated coiled-coil-containing protein kinase

RPM	Revolutions per minute
RTK	Receptor tyrosine kinase
SDS	Sodium dodecyl sulfate
SEM	Standard error of the mean
SILAC	Stable isotope labelling by amino acids in culture
siRNA	Small interfering RNA
SV40	Simian virus 40
TBS	Tris buffered saline
TBST	Tris buffered saline and tween 20
TCTP	Translationally controlled tumour protein
TGFB	Transforming growth factor beta
TNF	Tumour necrosis factor
TOP1	Topoisomerase 1
TSAP6	Tumour suppressor actuated pathway 6

1 Introduction

1.1 Cancer

1.1.1 Hallmarks of cancer

Cancer is a multifaceted disease characterised by growth of a primary tumour which progresses to invade, extravasate and metastasise to secondary visceral sites. The growth of chemotherapy-resistant secondary tumours at metastatic sites is responsible for most cancer-related deaths (Talmadge and Fidler, 2010, Hanahan and Weinberg, 2011). For this reason it is important to develop novel treatment strategies to prevent metastasis. To do this, characteristics of cancer growth and metastasis need to be thoroughly understood and the topic is extensively reviewed by Hanahan and Weinberg (2011). There are ten main hallmarks of cancer pathology that are displayed by most cancer types and collectively contribute to the progress of the disease. Primarily, cancer cells gain the ability to sustain proliferative signalling and acquire replicative immortality. In order for cancer cells to not only proliferate but also to survive, they need to be able to evade growth-suppressors and resist cell death. To sustain solid tumour growth and survival as the tumour mass increases, promotion of angiogenesis is essential to allow the necessary nutrient delivery to the cancer cells. Finally to progress to end-stages of the disease, the cells of solid tumours need to acquire an invasive migratory phenotype which allows cancer cells to extravasate and metastasise to secondary sites. More recently recognised hallmarks of cancer that are essential for tumour maintenance and survival include changes in energy metabolism, evasion of the immune response, genomic instability and promotion of an inflammatory environment.

Tumours are very complex tissues (as diagrammatically exemplified in figure 1-1) in which several stromal cell types are present in addition to the cancer cells, and these include endothelial cells, cancer-associated fibroblasts, immune inflammatory cells, cancer stem cells and bone marrow-derived progenitor cells. All these cell types co-operate to provide a microenvironment which sustains tumour growth and supports metastasis (Hanahan and Weinberg, 2011).

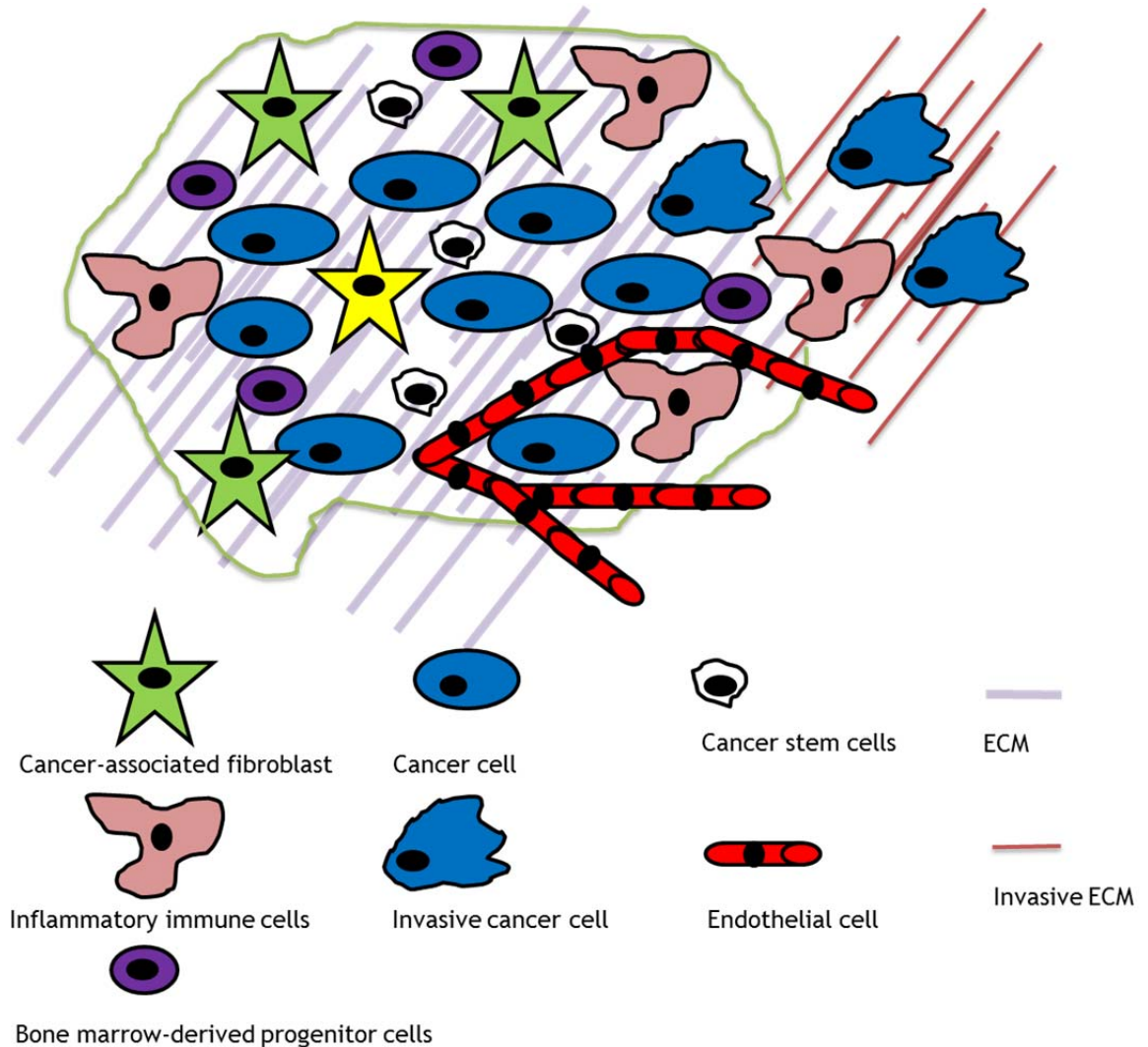


Figure 1-1: Schematic diagram of the tumour microenvironment.

A tumour is a complex environment in which the communication between several different cell types and the extracellular matrix (ECM) is essential to enable efficient tumour growth and metastasis. Cancer-associated fibroblasts (CAFs) enhance cancer progression and contribute to the production of cancer-associated ECM. Inflammatory immune cells including macrophages, neutrophils and lymphocytes support tumour progression by providing inflammatory signals, and by secreting factors that contribute to the degradation of the ECM allowing invasive cell migration to occur. Endothelial cells allow tumours to grow in size by providing vascularisation and, thereby, delivery of nutrients to tumour cells. Upon injection into mice, cancer stem cells are able to initiate the growth of new tumours and are extremely resilient to chemotherapy. Cancer stem cells are therefore thought to be one of the reasons for the high rates of cancer relapse after treatment. The presence of bone marrow progenitor cells in tumours is becoming increasingly recognised. In tumours, bone marrow progenitor cells are known to differentiate into various stromal cells that support tumour growth (Hanahan and Weinberg, 2011).

1.1.2 Metastasis

Tumour metastasis is a complex and multistep process which is reviewed in depth by Talmadge and Fidler (2010) and diagrammatically represented in figure 1-2. Briefly, once cells have undergone transformation, tumour growth is supported by angiogenesis which provides the necessary nutrients, and several different stromal cells, as discussed in the previous section (1.1.1). A small

number of cancer cells may acquire an invasive phenotype and migrate to a lymphatic vessel or blood vessel. Here, invasive cancer cells intravasate into the lumen of the lymphatic/blood vessel with the aid of tumour stromal cells. Subsequently tumour cells circulate within the lymph/blood until they adhere to the walls of the lymphatic or blood vessels. Once escaped tumour cells adhere to the vessel wall they can begin to extravasate from the vessel into the milieu of the secondary visceral site (for example the lung). The cancer cells then interact with the extracellular environment of the secondary organ and, if suitable proliferation occurs, followed by angiogenesis, and evasion of the immune response, a metastatic colony/secondary tumour can begin to grow in the secondary organ (Talmadge and Fidler, 2010).

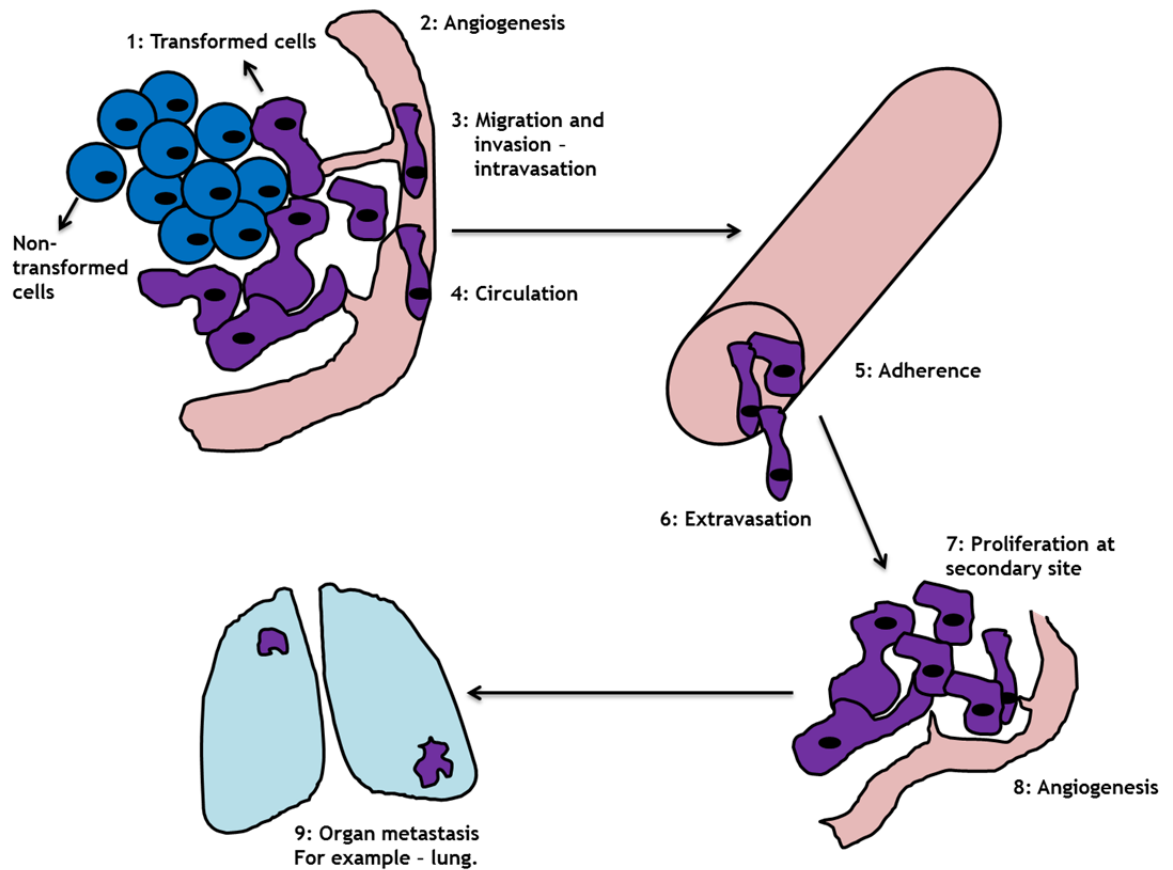


Figure 1-2: Overview of the metastatic cascade.

A small number of transformed cancer cells gain an invasive phenotype. Invasive cancer cells intravasate into lymphatic or blood vessels. Here they circulate until they adhere to a vessel wall and extravasate into a secondary organ (such as the lung) where proliferation and angiogenesis takes place allowing metastatic colony formation and growth of a secondary tumour (Talmadge and Fidler, 2010).

1.1.3 Cell migration and invasion in cancer metastasis

For transformed cancer cells to metastasise they need to acquire an invasive migratory phenotype. The exit of metastatic cells from primary tumours is thought to be a relatively rare event. Indeed, intra-vital imaging studies suggest that over the course of one hour, less than 0.01% of the cells in a tumour display a motile phenotype (Sahai, 2005). To acquire an invasive phenotype, cancer cells most probably acquire mutations and/or alterations to gene expression. A study that investigated gene expression of motile cells escaping from tumours found a distinct gene expression pattern which included changes in epidermal growth factor receptor (EGFR) and B1 integrin expression (Wang et al., 2004).

In addition to acquisition of an invasive migratory phenotype, communication between cancer cells, stromal cells and the extracellular environment is necessary for invasion and metastasis to occur. For example, mesenchymal stem

cells secrete chemokine (C-C ligand) motif (CCL5) which stimulates breast cancer cell invasion and metastasis through signalling of breast cancer cell chemokine receptor (CCR5) (Karnoub et al., 2007). Alternatively, tumour-associated macrophages of pancreatic tumours are activated by interleukin-4 to release the extracellular protease cathepsin which promotes cancer cell growth, angiogenesis and invasion (Gocheva et al., 2010). Additionally, fibroblasts and macrophages have been shown to secrete matrix metalloproteinases to degrade the extracellular matrix to aid cancer cell motility and invasion (Sameni et al., 2003, Grimshaw et al., 2004). As a final example, breast cancer-associated macrophages release epidermal growth factor (EGF) which stimulates carcinoma cells to express colony-stimulating factor-1 (CSF-1) which subsequently drives EGF expression in macrophages. This paracrine loop between macrophages and carcinoma cells has positive feedback characteristics and promotes both macrophage and carcinoma cells to become invasive (Goswami et al., 2005).

1.1.3.1 Collective cell migration and invasion

There are several modes of cancer cell migration that have been documented and these are illustrated in figure 1-3. A cluster of cells can become detached from the tumour and begin to migrate and invade collectively. This mode of migration is characterised by the maintenance of cell-cell adhesions between cells which can migrate in narrow linear strands with one leading cell, or alternatively as a broad sheet with several leading cells. This is quite a slow mechanism of invasion with cell migration speeds which range between 0.01 and 0.1 $\mu\text{m}/\text{minute}$. (Clark and Vignjevic, 2015, Khalil and Friedl, 2010).

A different form of collective migration has been described called multicellular streaming. In this type of migration, a collection of cells which are loosely linked to one another, migrate in long straight paths at a slightly faster speed (1-2 $\mu\text{m}/\text{minute}$) than is observed during collective migration (Clark and Vignjevic, 2015, Friedl and Alexander, 2011).

1.1.3.2 Single cell migration and invasion

Some metastatic cells (10 - 40 %) display the hallmarks of epithelial mesenchymal transition (EMT). Cells that have undergone EMT have low E-cadherin expression, spindle morphology and increased motility. They also resist

apoptosis and express matrix-degrading enzymes that facilitate invasion (Klymkowsky and Savagner, 2009, Sahai, 2005). The expression of the transcription factor Slug promotes EMT initiation. For example upon Slug expression, E-cadherin expression and its localisation at cell-cell junctions is decreased (Bolos et al., 2003). Consequently, decreased E-cadherin expression results in weaker cell-cell junction strength and increased ability of tumour cells to migrate individually and metastasise (Derksen et al., 2006).

After undergoing EMT, cells display a mesenchymal mode of migration. Mesenchymal cell migration occurs on relatively stiff 2D substrates and so can be easily studied *in vitro*. During mesenchymal-type migration, cells are elongated, polarised, and their translocation through 3D microenvironments depends upon ECM degradation by secreted proteases (Sahai, 2005). Activation of receptor tyrosine kinases such as cMET leads to increased Rac signalling which is important for a mesenchymal-like mode of cell motility (De Wever et al., 2004, Sahai and Marshall, 2003, Vial et al., 2003). Increased Rac activity at the leading edge promotes activation of the Scar/WAVE complex and Arp-2/3. Arp-2/3 serves to increase actin nucleation allowing formation of lamellipodia, pseudopods and filopodia at the cell front. These protrusions then promote migration by attaching to the ECM through focal contacts. This attachment, in combination with cell rear contraction allows the cell body to move forward and thus the cell migrates through the ECM (Sahai, 2005, Pollard and Borisy, 2003).

Alternatively cells can migrate in an amoeboid fashion where they assume a rounded morphology. This mode of migration can be mediated by Rho-ROCK mediated cell blebbing (Lorentzen et al., 2011). Cells exhibiting amoeboid migration have weak cell-ECM adhesions (Friedl and Alexander, 2011) and migrate independently of matrix degradation (Wolf et al., 2003). This is because rounded amoeboid cells can squeeze through gaps of the ECM matrix.

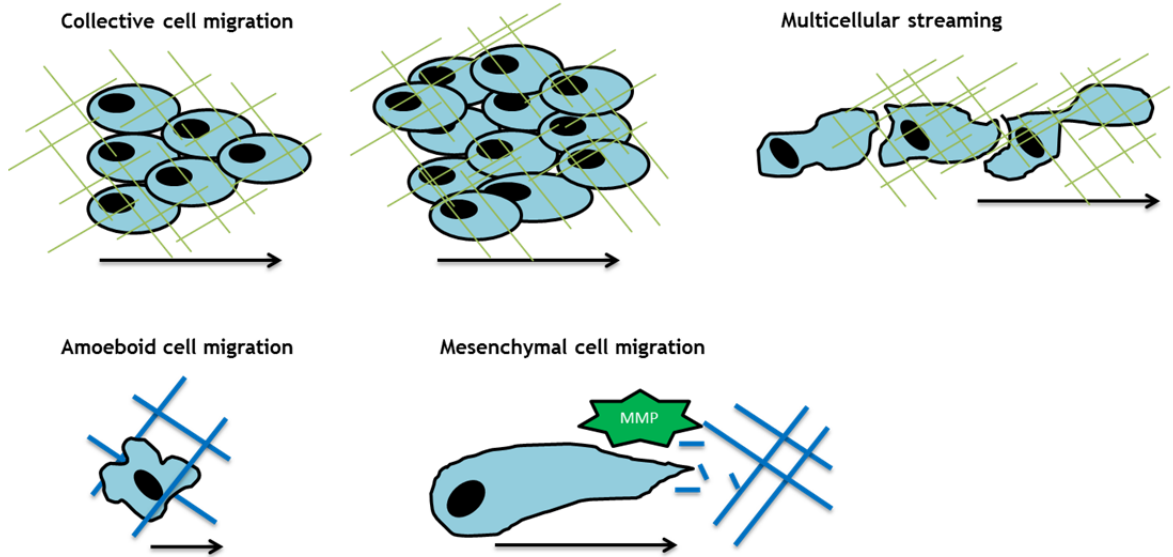


Figure 1-3: Cell migration modes.

Cancer cells migrate and invade through the extracellular matrix (ECM) during metastasis using several different modes of migration. Primarily, cells can migrate collectively either with one leading cell or with several leading cells (collective cell migration). In this case collective migrating cells maintain their cell-cell contacts. Alternatively cells migrate together with weak cell-cell contacts in a multicellular streaming migration mode. Cells also migrate singularly in an amoeboid fashion in which membrane blebbing propels cell migration through ECM gaps. Finally cells migrate with a mesenchymal phenotype which is dependent upon matrix metalloproteinase (MMP) degradation of the ECM.

1.1.4 Integrin trafficking in cancer cell migration

It is very important to thoroughly understand the mechanisms of cancer cell migration in order to be able to target the cells therapeutically to prevent invasion and metastasis. Our lab is interested in the role that integrins play in cell migration. This section therefore discusses integrins, their endocytosis, trafficking and the importance of these processes in cancer cell migration.

1.1.4.1 Integrins

As reviewed by (Hynes, 2002) integrins are heterodimer transmembrane receptors composed of an alpha subunit (of which there are 18) and a beta subunit (of which there are 8). Integrins localise in focal adhesions (alongside hundreds of other proteins) and serve to link the cell cytoskeleton with the ECM by association with extracellular ligands such as collagen, laminin, vitronectin and fibronectin (figure 1-4) (Humphries et al., 2006). Integrins that are bound to an extracellular ligand assume an extended (open) conformation, whereas the bent (closed) state of integrins has a low affinity for extracellular ligands. The activation state of integrins can contribute to the role they play in bi-directional

signalling. Extracellular ligand occupancy mediates intracellular cell signalling (outside-in) whereas binding of intracellular proteins such as talin and kindlin to the intracellular C-terminus of integrins regulates integrin activation state (inside-out signalling) (Legate et al., 2009). Integrin activation and signalling have several physiological consequences that can be exerted both immediately and also in the longer term through changes in gene expression (Legate et al., 2009). Integrin signalling controls many different cellular processes; the main one of interest here is the role of integrins in controlling cell migration and invasion. How integrin receptors control migration and invasion is dependent upon their localisation within the cell - whether they are available and functional at the plasma membrane to link the ECM with the actin cytoskeleton, or present inside internal vesicles during their transportation and trafficking (Bridgewater et al., 2012, Hynes, 2002).

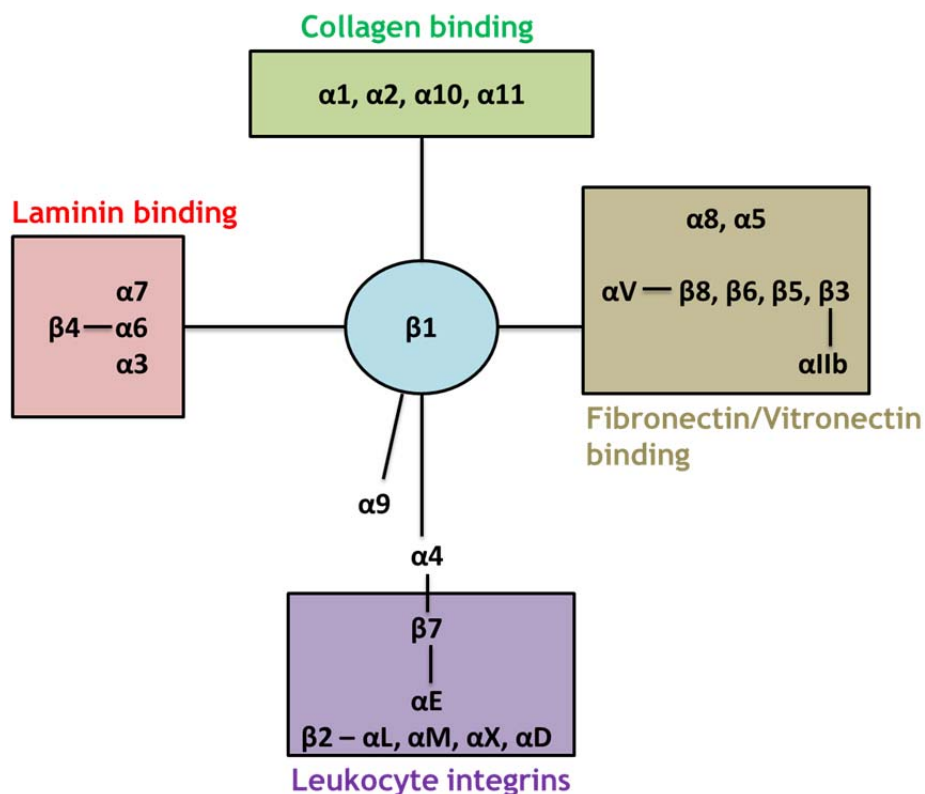


Figure 1-4: Integrin families.

Integrin α and β subunits form 24 different heterodimers that specifically bind to extracellular ligands. There are integrin families that are collagen-binding, RGD-binding (fibronectin and vitronectin), laminin-binding and finally there are integrins expressed specifically by leukocytes that bind ligands such as E-cadherin, adapted from (Margadant et al., 2011).

1.1.4.2 Integrin endocytosis

Integrins are endocytosed from the plasma membrane via both clathrin-dependent and clathrin-independent mechanisms (Bridgewater et al., 2012). Clathrin-dependent endocytosis is mediated by recruitment of AP-2, cargo-specific adaptor proteins, clathrin and dynamin to the plasma membrane (McMahon and Boucrot, 2011). Adaptor proteins specifically involved in mediating clathrin-dependent endocytosis of integrins include DAB2, ARH and NUMB which bind to the NPxY motif on the integrin tail of the β -subunit (Teckchandani et al., 2012, Nishimura and Kaibuchi, 2007, Calderwood et al., 2003, Ezratty et al., 2009). Upon clathrin assembly a vesicle can be formed and dynamin polymerisation initiates the vesicle neck scission allowing formation of an endosome (McMahon and Boucrot, 2011). Alternatively integrins can be internalised by clathrin-independent endocytosis which can be mediated through caveolae association with $\alpha 2\beta 1$ integrin (Upla et al., 2004), by macropinocytosis after dorsal ruffle formation (Mayor and Pagano, 2007), or via a distinct set of endosomes termed clathrin-independent carriers (CLICs) (Howes et al., 2010, Lakshminarayan et al., 2014).

1.1.4.3 Rab-GTPases

After internalisation, integrins are located within the endosomal system where their fate is determined. Integrins can either be recycled back to the plasma membrane or targeted for degradation. These processes will be discussed in further detail next in section (1.1.4.4), however here I will introduce the Rab GTPases which are key mediators of vesicular trafficking and are known to contribute to endosomal trafficking of integrins in a way that influences integrin function.

Rab-GTPases are master regulators of intracellular vesicle trafficking. Shortly after synthesis Rab-GTPases bind to Rab escort proteins (REPs) which present the Rab to geranylgeranyl transferase for lipid modification (prenylation) which allows subsequent association of Rab proteins to membranes. Once they have been lipid-modified, Rab proteins can undergo activation from the GDP to the GTP bound state; a process which is catalysed by guanine nucleotide exchange factors (GEFs). In the GTP-bound state, Rab-GTP proteins are recognised and

bound by Rab effector proteins enabling the Rab protein to carry out its functions in vesicular transport. GTPase activating proteins (GAPs) then promote the hydrolysis of Rab-associated GTP to GDP. Geranylgeranylated Rab-GDPs interact with GDP dissociation inhibitors (GDIs) which stabilises the proteins in its inactive soluble form and maintain their solubility in the cytosol. The Rab-GDI complex may be targeted to specific membrane compartments by association with membrane bound GDI displacement factors (GDF). Once returned to their original membrane and dissociated from GDIs, Rab-GDP proteins can again then be activated. This process is summarised in figure 1-5. Rab-GTPase proteins contribute to the control of the exocytic, endocytic and transcytic transport in a cell. Rab proteins are characterised by their localisation within vesicular compartments of the cell and contribute to many cellular processes including cell motility, proliferation and differentiation (Bhuin and Roy, 2014, Stenmark, 2009).

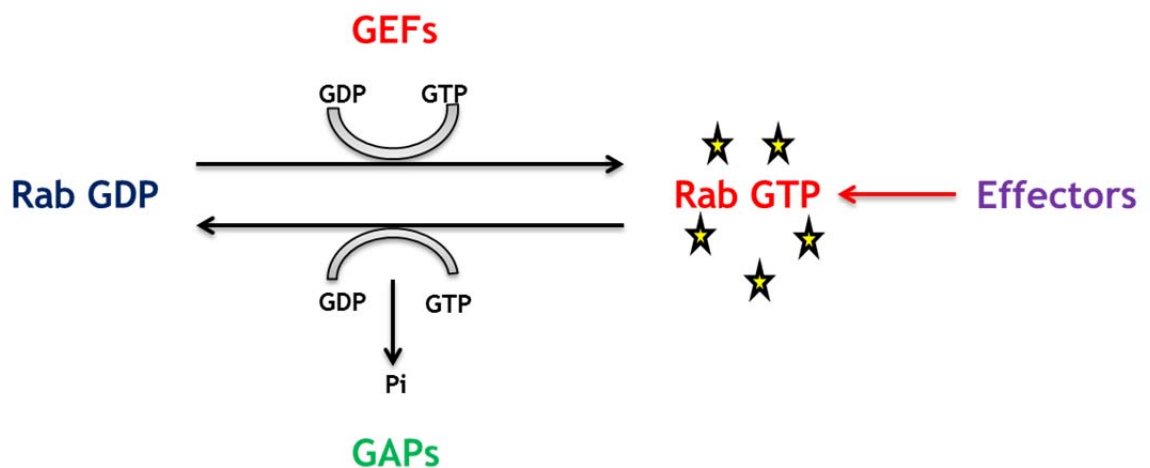


Figure 1-5: Diagram representing the cyclical activation and deactivation of Rab-GTPases. Inactive Rab-GDP is activated by guanine nucleotide exchange factors (GEFs) to yield the active GTP-loaded Rab. Effectors can interact with Rab-GTP in its active state, enabling Rab-GTP to carry out its biological functions in vesicular transport. GTPase activating proteins (GAPs) then deactivate Rab-GTP to the Rab-GDP inactive state again.

1.1.4.4 Integrin trafficking routes

After internalisation from the plasma membrane into early endosomes there are several routes which the integrin can take. $\alpha\text{v}\beta\text{3}$ integrins can be recycled back to the plasma membrane from Rab4-positive early endosomes via a route that has been termed the 'short loop' pathway (Roberts et al., 2001). The short-loop is subject to tight control by growth factor-activated kinases. In the presence of

growth factors (such as PDGF), Protein Kinase D1 (PKD1) is autophosphorylated promoting its interaction with the C-terminus of $\beta 3$ integrin. PKD1 then phosphorylates Rabaptin-5 (dual Rab4/Rab5 effector) at serine 407 which favours its association with Rab4 over Rab5 and this drives $\alpha\beta 3$ integrin recycling through the Rab4 positive compartment promoting persistent fibroblast and endothelial cell migration (di Blasio et al., 2010, White et al., 2007, Christoforides et al., 2012).

$\alpha 5\beta 1$ integrins, on the other hand, do not follow the short-loop back to the plasma membrane, but are trafficked from early endosomes to recycling endosomes in the perinuclear region of the cell and then returned to the plasma membrane by the 'long loop' Rab11-positive pathway. After internalisation, Rab21 is displaced from the cytoplasmic tail of $\alpha 5$ integrin by p120RasGAP, this in turn promotes $\alpha 5\beta 1$ delivery to recycling endosomes and recycling to the plasma membrane via the Rab11 dependent long loop (Mai et al., 2011). Other regulators of the long loop pathway of integrin recycling include PKB/AKT (Roberts et al., 2004) and ARF6 (Powelka et al., 2004). Activation of PKB/AKT leads to phosphorylation and inactivation of glycogen synthase kinase 3 (GSK-3) which consequently drives $\alpha 5\beta 1$ and $\alpha\beta 3$ recycling to the plasma membrane from the Rab11 compartment and regulates cell spreading (Roberts et al., 2004). Furthermore, Arf6 is also known to contribute to Rab11-dependent recycling of $\alpha 5\beta 1$ following growth factor stimulation. This mechanism of integrin trafficking contributes to cancer cell motility (Powelka et al., 2004). The short loop and long loop of integrin recycling dictate the way that a cell can migrate. For example, short loop recycling of $\alpha\beta 3$ promotes directional cell migration, whereas inhibition of $\alpha\beta 3$ recycling promotes $\alpha 5\beta 1$ recycling to the plasma membrane and drives cells to migrate with a decreased persistence (White et al., 2007).

Finally $\alpha 5\beta 1$ integrins can arrive in the late endosomal compartment where they can either be degraded in lysosomes, or in Rab25 expressing cells integrins can be recycled back to the plasma membrane from late endosomes/lysosomes in a CLIC3-dependent manner (Dozynkiewicz et al., 2012, Caswell et al., 2007). The main routes of integrin trafficking are diagrammatically reviewed in figure 1-6.

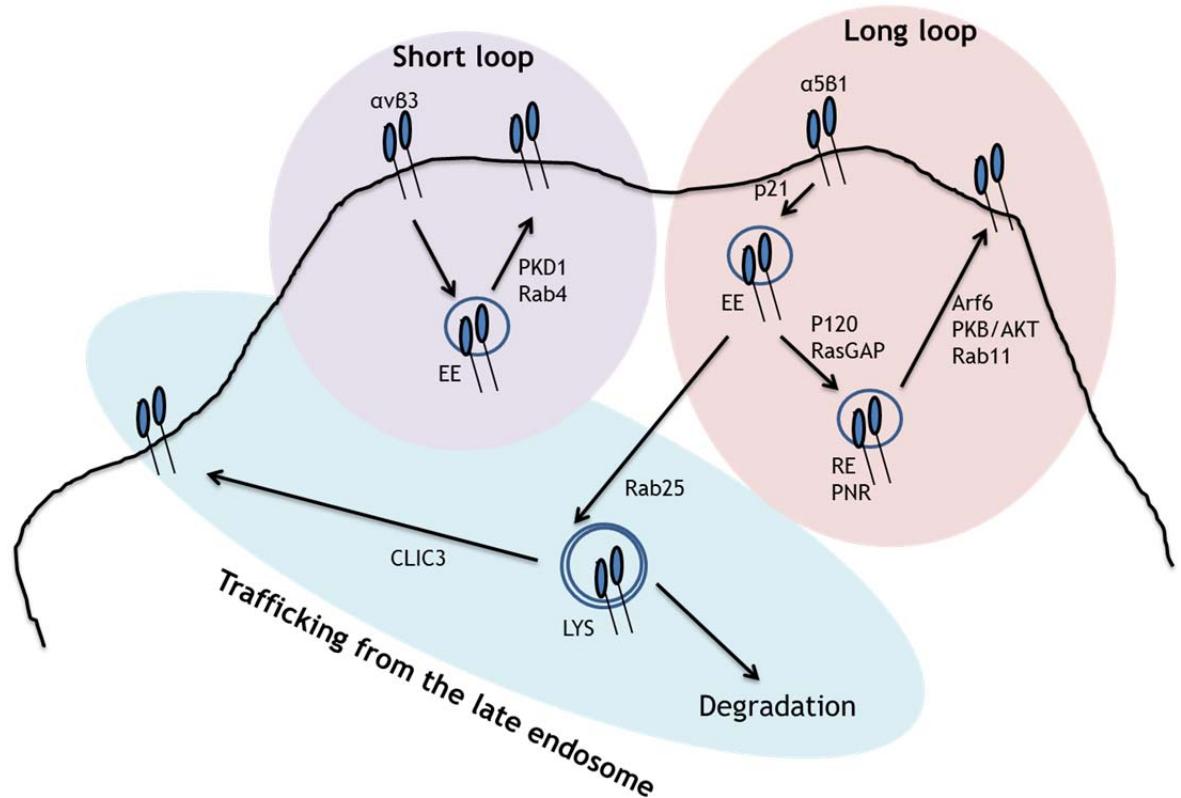


Figure 1-6: Diagram depicting the main mechanisms of integrin trafficking in the cell.

After internalisation integrins are directed through the cells endocytic compartment. They can quickly be recycled back to the plasma membrane from early endosomes via the short loop in a Rab4 positive compartment. Alternatively the Rab11 dependent long loop, returns integrins from recycling endosomes to the plasma membrane. Finally in Rab25 expressing cells integrins in late endosomes can be targeted for degradation or recycled back to the plasma membrane in a CLIC3 dependent manner. EE – early endosome. RE – recycling endosome. PNR – perinuclear region. Lys – lysosome.

1.1.4.5 Integrin trafficking and cancer cell migration

In cancer biology integrin trafficking has been found to have an important role in determining the invasive nature of migration that cancers cell exhibit. For example, hypoxia increases invasion of breast cancer cells via $\alpha 6 \beta 4$ recycling which is dependent upon the Rab11 long loop recycling pathway (Yoon et al., 2005). Additionally $\alpha \nu \beta 6$ interaction with HS1-associated protein X-1 (HAX1) promotes clathrin-dependent endocytosis and integrin trafficking driving an invasive mode of migration in oral squamous cell carcinoma cells (Ramsay et al., 2007). The role of Rab25-mediated $\alpha 5 \beta 1$ integrin trafficking has an important role in cancer cell migration. Rab25 has been found to be overexpressed in aggressive forms of ovarian cancer (Cheng et al., 2004) and has been shown to promote spatially-restricted $\alpha 5 \beta 1$ integrin recycling at the tips of invasive pseudopods to promote pseudopod extension and cell invasion (Caswell et al.,

2007). Subsequently it was shown that Rab25 promotes $\alpha 5\beta 1$ integrin localisation into late endosomes, from whence it is recycled back to the plasma membrane at the rear of the cell in a CLIC3-dependent manner. This allows the retraction of the cell rear and promotes forward cell migration and invasion of ovarian cancer cells (Dozynkiewicz et al., 2012).

Expression of the oncogene mutant p53 or inhibition of $\alpha v\beta 3$ recycling using cilengitide both increase the recycling rate of $\alpha 5\beta 1$ integrin to the plasma membrane in an RCP (a Rab11 effector)-dependent manner leading to less persistent and more invasive cancer cell migration (Muller et al., 2009, Caswell et al., 2008). Additionally localisation of RCP at the invasive pseudopod tip is dependent upon phosphatidic acid generation by DGK α which consequently promotes $\alpha 5\beta 1$ integrin recycling to the pseudopod plasma membrane (Rainero et al., 2012). Receptor tyrosine kinases (RTKs) such as epidermal growth factor receptor (EGFR) and cMET are recycled to the plasma membrane alongside $\alpha 5\beta 1$ integrins. The activation of RTKs at the cell surface results in increased AKT signalling which promotes the cell migration and invasive phenotype that can support metastasis (Muller et al., 2013, Muller et al., 2009, Caswell et al., 2008).

1.2 p53

As discussed previously, mutant p53 has an important role in promoting invasive cell motility by driving $\alpha 5\beta 1$ integrin and RTK recycling. It is therefore essential to understand mutant p53 in the context of cancer cell migratory behaviour in order to develop an anti-metastatic therapeutic strategy that could potentially target 50 % of cancer cases. Here we discuss wild-type p53, mutant p53 and the role that mutant p53 plays in cancer cell migration and invasion.

1.2.1 Historical perspective

p53 is part of a family of transcription factors which also includes p63 and p73. All members of this family have important tumour suppressor functions through their control of gene expression (Freed-Pastor and Prives, 2012). The p53 protein was first discovered in 1979 in simian virus 40 (SV40) transformed cells, when it co-immunoprecipitated with the SV40 encoded T-antigen (Lane and

Crawford, 1979, Linzer and Levine, 1979). There was initial confusion regarding the role of p53, it appeared that there were high expression levels of p53 in transformed cancer cells which led to speculation that it was functioning as an oncoprotein (Rotter, 1983, DeLeo et al., 1979). It was finally realised that mutant forms of p53 were being investigated rather than wild-type p53 - which is usually expressed at low levels in healthy cells. After initial experiments showing that overexpression of wild-type p53 inhibited cell transformation, it became firmly established that wild-type p53 functions as a tumour suppressor, and that mutant forms of p53 contribute to tumorigenesis (Levine and Oren, 2009, Hinds et al., 1989, Hinds et al., 1990, Eliyahu et al., 1989). The tumour-suppressing activity of wild-type p53 has been demonstrated by mouse models in which removal of p53 expression promotes spontaneous tumour development (Donehower et al., 1992).

1.2.2 Wild-type p53

1.2.2.1 Structure

As reviewed in figure 1-7 and by Meek and colleagues (2015), the p53 protein consists of two transactivation domains at the N-terminus, followed by a proline rich region important for both p53 response to ionising radiation, and p53-driven apoptosis of tumour cells (Campbell et al., 2013, Baptiste et al., 2002). The core DNA-binding domain is essential for the ability of p53 to bind DNA and control the transcription of tumour suppressive genes. Finally the C-terminus of the protein contains many functionally important domains:- a nuclear localisation signal, a tetramerisation domain, and a regulatory region which can be modified post-translationally and controls the turnover of the p53 protein (Meek, 2015).

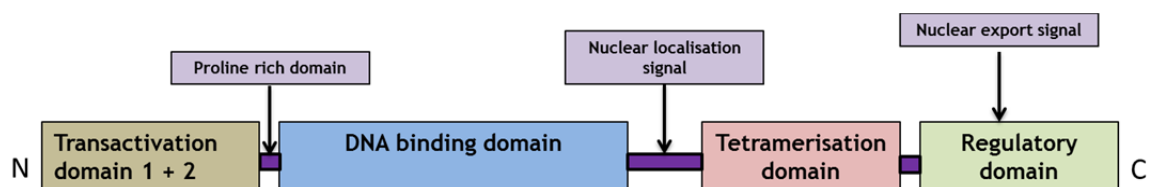


Figure 1-7: Structure of p53 protein
Adapted from (Meek, 2015).

1.2.2.2 Activation and regulation

The role of p53 in tumour suppression becomes particularly evident upon its activation by cell stressors such as DNA damage, hypoxia and oncogene activation (Vousden and Lu, 2002). Upon activation, p53 tetramers bind to response elements on DNA and either promote or repress gene transcription (Laptenko and Prives, 2006). This transcriptional control has an impact on several cellular processes such as cell cycle arrest, senescence, apoptosis and metabolism - specific examples of which are discussed in the next section (Vousden and Ryan, 2009, Freed-Pastor and Prives, 2012, Vousden and Lu, 2002). This stringent regulation of cellular activity by p53 that occurs upon exposure to stressful stimuli provides a mechanism by which healthy non-transformed cell populations are maintained.

In the absence of cellular stresses, p53 is maintained at low levels by a negative feedback loop. p53 stimulates transcription of the E3 ubiquitin ligase MDM2, subsequently MDM2 promotes ubiquitination and degradation of p53 (Barak et al., 1993, Marine and Lozano, 2010). Upon activation of p53 by cell stress, MDM2 is inhibited and this leads to alleviation of p53 inhibition. This allows high levels of p53 to be sustained and permits the execution of p53-dependent cell stress responses (Levine and Oren, 2009).

There are several mechanisms by which MDM2 maintains low levels of p53 in normal low stress conditions. Primarily, as already discussed, an interaction between the N-terminus of both MDM2 and p53, leads to p53 ubiquitination and proteasomal degradation (Kussie et al., 1996, Marine and Lozano, 2010). MDM2 also has an interactor called MDM4, which further exacerbates/activates MDM2 mediated polyubiquitination and degradation of p53 (Wang et al., 2011). Additionally MDM2 can promote degradation of the ribosomal protein, L26 which is responsible for translation of transcripts encoding p53 (Ofir-Rosenfeld et al., 2008). Finally MDM2 can bind to the core domain of the p53 protein and decrease its ability to bind DNA and regulate transcription (Cross et al., 2011).

Upon cell stress, p53 is activated and becomes stably expressed at high levels within the cell. The processes through which this occurs have been extensively reviewed (Hu et al., 2012). For example, upon genotoxic stress MDM2 is

phosphorylated by ATM kinase, inhibiting the association between p53 and MDM2. This allows p53 levels to increase in the cell (Maya et al., 2001).

Alternatively upon oncogene activation, p19ARF transcription is increased, which promotes p19ARF binding to MDM2 and sequesters it in the nucleolus, inhibiting its capacity to ubiquitinate p53 for degradation (Weber et al., 1999). MDM2 regulation of p53 levels is diagrammatically reviewed in figure 1-8.

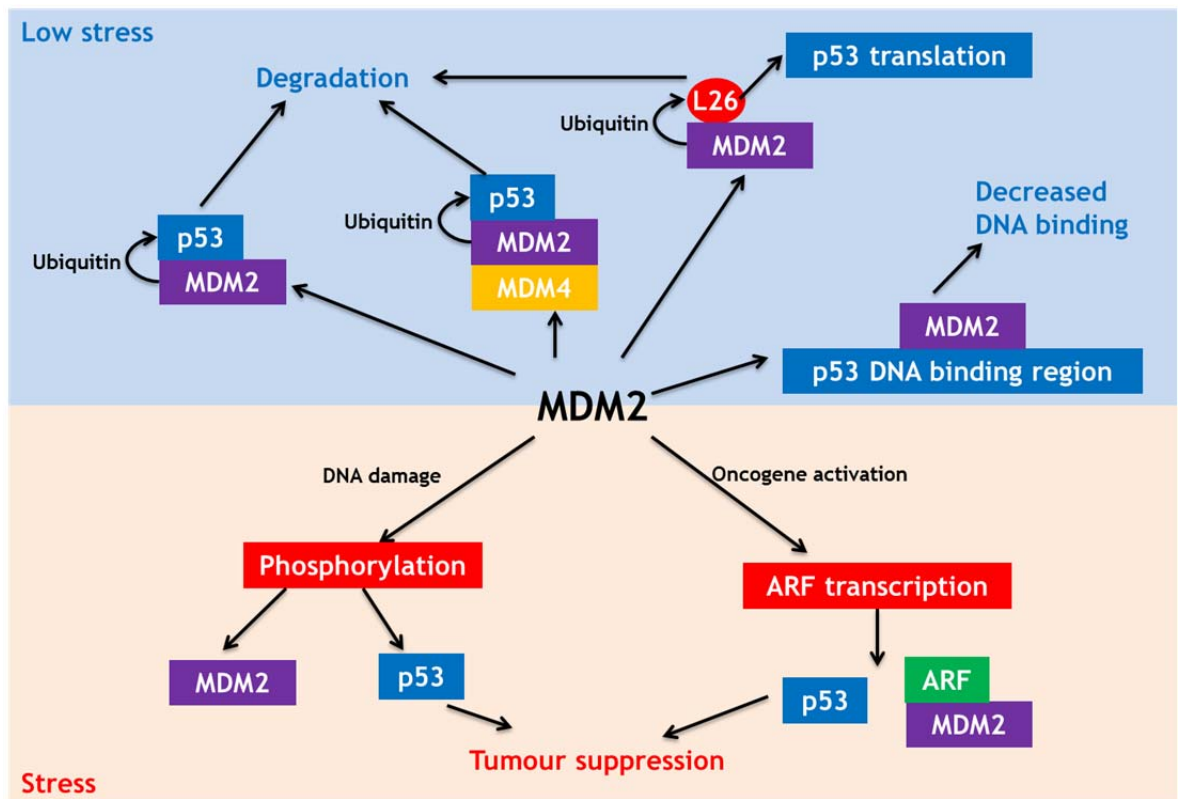


Figure 1-8: MDM2 regulation of p53 protein stability.

In conditions of low cellular stress, MDM2 maintains low levels of p53 by binding to and promoting ubiquitination and degradation of p53 with or without the aid of MDM4. MDM2 drives the degradation of ribosomal L26 which leads to a decreased rate of p53 translation. This keeps p53 at low levels. Alternatively MDM2 can bind p53 in the DNA binding region, inhibiting its ability to bind to DNA and exert its tumour-suppressing effects. Following stressful stimuli, phosphorylation of MDM2 decreases its association with and ubiquitination of p53, allowing the levels of functional p53 protein to increase. Alternatively, oncogene activation increases p19ARF transcription which binds and sequesters MDM2, decreasing the degradation of p53 and allowing it to become stably expressed in the cell.

1.2.2.3 Physiological effects of p53 activation

Wild-type p53 performs physiological functions to maintain homeostasis at its non-stimulated basal/physiological level. For example it suppresses inflammatory immune responses through NF- κ B antagonism (Komarova et al., 2005), maintains a healthy population of non-transformed stem cells (Aloni-Grinstein et al.,

2014), and it can control fertility and implantation by regulating leukaemia inhibitory factor (LIF) transcription (Levine et al., 2011).

Upon activation by stressful stimuli, p53 is present at higher levels which allow it to perform its tumour suppressor function. There is some evidence that p53 can perform tumour suppressive functions independently of transcriptional regulation. For example p53 is thought to have a pro-apoptotic function through BCL2 protein interactions (Vousden and Lane, 2007). More often however, tumour suppression is exerted through p53 transcriptional regulation to initiate apoptosis, cell cycle arrest, senescence, DNA repair, alteration of cell metabolism or to decrease angiogenesis (figure 1-9).

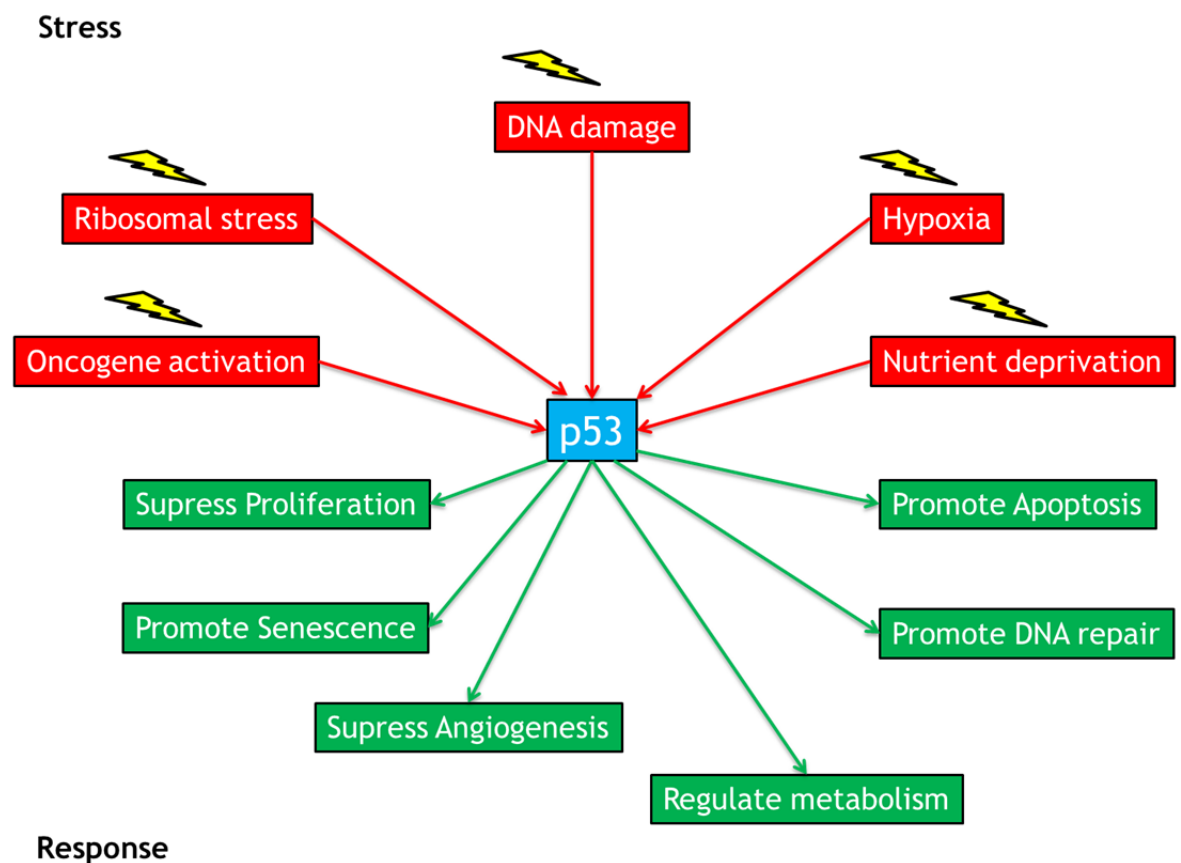


Figure 1-9: Overview of stimuli that activate p53 and the subsequent responses that enable the maintenance of a healthy population of cells.

p53 has been found to promote transient cell cycle arrest in response to stressful stimuli which enable cells to survive until the stress stimulus has been removed, or until the damage has been repaired. For example, p53-inducible genes are involved in decreasing the quantity of reactive oxygen species, thus protecting

the cell from DNA damage, genome instability and even decreasing the tendency of the cell to undergo apoptosis (Bensaad et al., 2006). Similarly, to inhibit fibroblast proliferation upon DNA damage, p53 increases transcription of the cyclin dependent kinase inhibitor p21, to initiate G1 cell cycle arrest (Dulic et al., 1994). Additionally p53 can initiate cellular DNA repair, so that once DNA damage has been rectified, the repaired cells can re-join the population of healthy cells (Gatz and Wiesmuller, 2006). This transient arrest/DNA repair process is a risky strategy because in the event of inaccurate DNA repair this may promote malignant transformation. In these cases, activation of irreversible cell cycle arrest is preferable - a process called senescence - which can be activated by p21 in a p53-dependent manner (Van Nguyen et al., 2007). Interestingly, if wild-type p53 is reintroduced into p53 null tumours, the senescence programme is activated leading to tumour regression and clearance (Xue et al., 2007, Ventura et al., 2007). Alternatively, p53 can trigger cell apoptosis. One well-defined mechanism of p53-driven apoptosis is through the upregulation of p53-upregulated modulator of apoptosis (PUMA) transcription. PUMA interacts with apoptosis regulatory Bcl-2 proteins, and initiates cell apoptosis via induction of mitochondrial dysfunction *in vitro* and *in vivo* (Yu et al., 2003).

According to Vousden and Prives (2009) whether p53 dictates either transient cell cycle inhibition to allow the damage to be resolved and the cell to survive, or whether p53 evokes permanent cell cycle arrest (senescence) or cell death by apoptosis, depends on the type of cell stress that the cell experiences. Low levels of transient stress normally promote repair and survival, whereas high stress levels trigger apoptosis and senescence (Vousden and Prives, 2009).

Finally wild-type p53 also exerts tumour suppression through control of cell metabolism. For example the mTOR complex responds to cell stressors, such as nutrient deprivation to control protein synthesis and cell growth. Upon genotoxic stress the p53 products, sestrin1 and sestrin2, activate AMP-activated protein kinase (AMPK) which leads to inhibition of mTOR activity and consequent inhibition of cell growth (Budanov and Karin, 2008). This suggests that one of p53's tumour suppressing mechanisms is via inhibition of the mTOR activity. Additionally p53 can promote energy production to sustain cellular function through mitochondrial respiration (Ma et al., 2007) and limit the amount of

energy contributed by cellular glycolysis (Kawauchi et al., 2008, Bensaad et al., 2006). Such metabolic regulation is thought to prevent cells reverting to anaerobic glycolysis, a process which normally supports cancer cell metabolism.

1.2.2.4 p53 loss and cell migration

Upon loss of p53 expression from a cell, an important regulator of tumour suppression is absent. p53 loss promotes epithelial mesenchymal transition (EMT) which is discussed in more detail in section (1.1.3.2). EMT is characterised by decreased apoptosis and senescence, and changes the migratory phenotype of cells, all with the aim of promoting tumour formation. Wild-type p53 suppresses expression of the EMT-associated transcription factor Twist (Shiota et al., 2008), and enhances MDM2-mediated degradation of the EMT-associated transcription factor Slug (Wang et al., 2009b). Therefore loss of p53 expression allows both Twist and Slug levels to increase. Increased Slug expression drives a decrease in E-cadherin transcription. Loss of E-cadherin at cell-cell junctions is a marker of EMT (Bolos et al., 2003, Shih et al., 2005). Indeed, loss of E-cadherin from cancer cells is known to increase the rate of metastasis *in vivo* (Shih et al., 2005, Derksen et al., 2006). Additionally in the absence of p53, cells that undergo EMT acquire a more motile phenotype. Upon loss of p53, Ras-driven cell migration is exacerbated (Xia and Land, 2007). Additionally RhoA and ROCK signalling (which is normally suppressed by p53) promotes an amoeboid mode of cell migration (Gadea et al., 2007). Overall loss of p53 expression causes loss of tumour suppression and allows EMT cell phenotypes to be displayed that can contribute to tumorigenesis.

1.2.3 Mutant p53

p53 is mutated in over half of all cancers (Vogelstein et al., 2000). Many mutations are missense amino acid substitutions and occur in the hotspot DNA binding region of p53. p53 mutations are sub-categorised into structural mutations that occur in the DNA binding domain, such as the R273H substitution, resulting in an inability of p53 to bind DNA. Alternatively, mutations may occur outwith the DNA binding region, such as R175H substitution, and these inhibit the ability of p53 to bind DNA by affecting protein conformation (Olivier et al., 2003, Cho et al., 1994, Petitjean et al., 2007). Mutations in p53 that result in

reduced DNA-binding, lead to loss of the transcriptional regulation that is important for tumour suppression (Cho et al., 1994, O'Farrell et al., 2004). Moreover, expression of a single allele of mutant p53 has been shown to exert a dominant negative effect over the remaining wild-type p53 allele. There is debate as to how this occurs; one hypothesis is that wild-type p53 is forced into a mutant p53 conformation within a heterotetramer that can consequently no longer bind DNA (Milner and Medcalf, 1991, Brosh and Rotter, 2009). Alternatively, low levels of wild-type p53 remaining in the cell can aggregate with mutant p53 thus silencing its tumour suppressing function (Silva et al., 2013, Ano Bom et al., 2012).

Despite the fact that mutant p53s are, in principle, susceptible to MDM2-dependent and independent degradation, these oncogenic mutants are more commonly found at very high levels within the cell (Haupt et al., 1997, Lukashchuk and Vousden, 2007). Subjecting wild-type p53-expressing cells to stresses such as ionising radiation, stabilises p53 so it can complete its tumour suppressive functions. These same cell stressors (many of which will be present in the environment in which cancer cells reside) also stabilise mutant p53 through similar pathways. The stable nature of mutant p53 is essential for the gain-of-function metastatic phenotype (discussed in 1.2.3.2) to be exhibited and this is likely to be reliant on suppression of the p53 degradation system. Supporting this, mice in which MDM2 is silenced exhibit stable expression of mutant p53 which consequently promotes early onset of tumour development (Terzian et al., 2008).

1.2.3.1 Mutant p53: transcriptional regulation

O'Farrell et al (2004) via microarray analysis, found that mutant p53-expressing cells retain only 5 % of the transcriptional regulatory activities that wild-type p53 can perform. This study also shows that cells expressing mutant p53 (R175H) may increase the mRNA expression of some novel genes not normally regulated by wild-type p53. This demonstrates that mutant p53 not only loses wild-type functions but may also acquire functions of its own that lead to changes in mRNA expression (O'Farrell et al., 2004). For example Weisz et al (2004), via microarray analysis, found that mutant p53 (R175H) expression increases mRNA expression of the transcription factor, early growth response-1

(EGR1) which is involved in cell cycle regulation, by physically interacting with the EGR1 promoter. Upregulation of EGR1 expression results in transformation and resistance to apoptosis of mutant p53-expressing cells. This demonstrates a role of mutant p53 in transcriptional control of the gain-of-function phenotype (Weisz et al., 2004).

1.2.3.2 Gain-of-function mechanisms

Here we discuss how mutations in p53 not only oppose the function of wild-type p53, but also contribute to new gain-of-function mechanisms and the phenotypes that arise from this. First of all we will discuss the mechanisms by which mutant p53 exerts these gain-of-function phenotypes. Firstly mutant p53 has a decreased ability to bind DNA at response elements that binds wild-type p53 to control transcription (Ludwig et al., 1996). However mutant p53 is able to bind to DNA at matrix attachment regions (MARs). MARs are 200 base pair long regions of DNA that bind the nuclear matrix forming chromatin loops and are sites of replication, transcription and repair (Wang et al., 2010). Proteins (such as mutant p53) have been found to interact with MARs and may perhaps regulate gene transcription. This could be one explanation as to how mutant p53 can exert gain-of-function transcriptional effects within a cell, and it may also be another reason as to why mutant p53 is so stable within a cell (Will et al., 1998, Gohler et al., 2005). Additionally mutant p53 can influence gene expression by binding to other transcription factors and altering their activity. For example, after DNA damage, mutant p53 forms a complex at the NF-Y promoter with the transcription factor NF-Y and transcriptional co-factor p300. This drives transcription of NF-Y genes that are involved in regulation of the cell cycle. The changed gene expression profile causes disruption to the cell cycle, allowing mutant p53-expressing cells to gain a more malignant and proliferative phenotype (Di Agostino et al., 2006). Mutant p53 also upregulates transcription of genes involved in the mevalonate pathway by binding the transcription factor SREBP. This results in increased expression of sterol genes which consequently alter the morphology of breast cancer acini (Freed-Pastor et al., 2012).

Mutant p53 can bind the tumour suppressing transcription factors p63 and p73 and inhibit their DNA binding capacity and function (Strano et al., 2002, Gaiddon et al., 2001). Inhibition of p63/p73 can contribute to the mutant p53 gain-of-

function phenotype. One mechanism by which this occurs is via TGF β -stimulated association of mutant p53 with p63 and SMAD. Formation of this complex decreases the ability of p63 to control transcriptional regulation and consequently allows increased cell invasion and metastasis to occur (Adorno et al., 2009). Additionally, the mutant p53-driven increased rate of integrin and RTK recycling and the resulting migration and invasion can be both dependent and independent of mutant p53 mediated suppression the p63 axis (Muller et al., 2014, Muller et al., 2009).

Finally mutant p53 can carry out its gain-of-function by binding to other proteins and causing a change in the protein function. For example, conformational mutants of p53 associate with the cell cycle regulator B-cell translocation gene-2 (BTG2). This association inhibits BTG2's ability to deactivate HRAS, allowing HRAS-driven cancer promoting genes to be expressed (Solomon et al., 2012). Additionally upon mutant p53 expression, the balance between the activation and repression of DNA repair is lost through mutant p53 association with topoisomerase-1 (TOP1). The resulting hyper-recombination of DNA causes genome instability - a tumour promoting hallmark of mutant p53 (Restle et al., 2008). The mechanisms by which mutant p53 exerts its gain-of-function phenotype are diagrammatically reviewed in figure 1-10.

Mutant p53 gain-of-function mechanisms

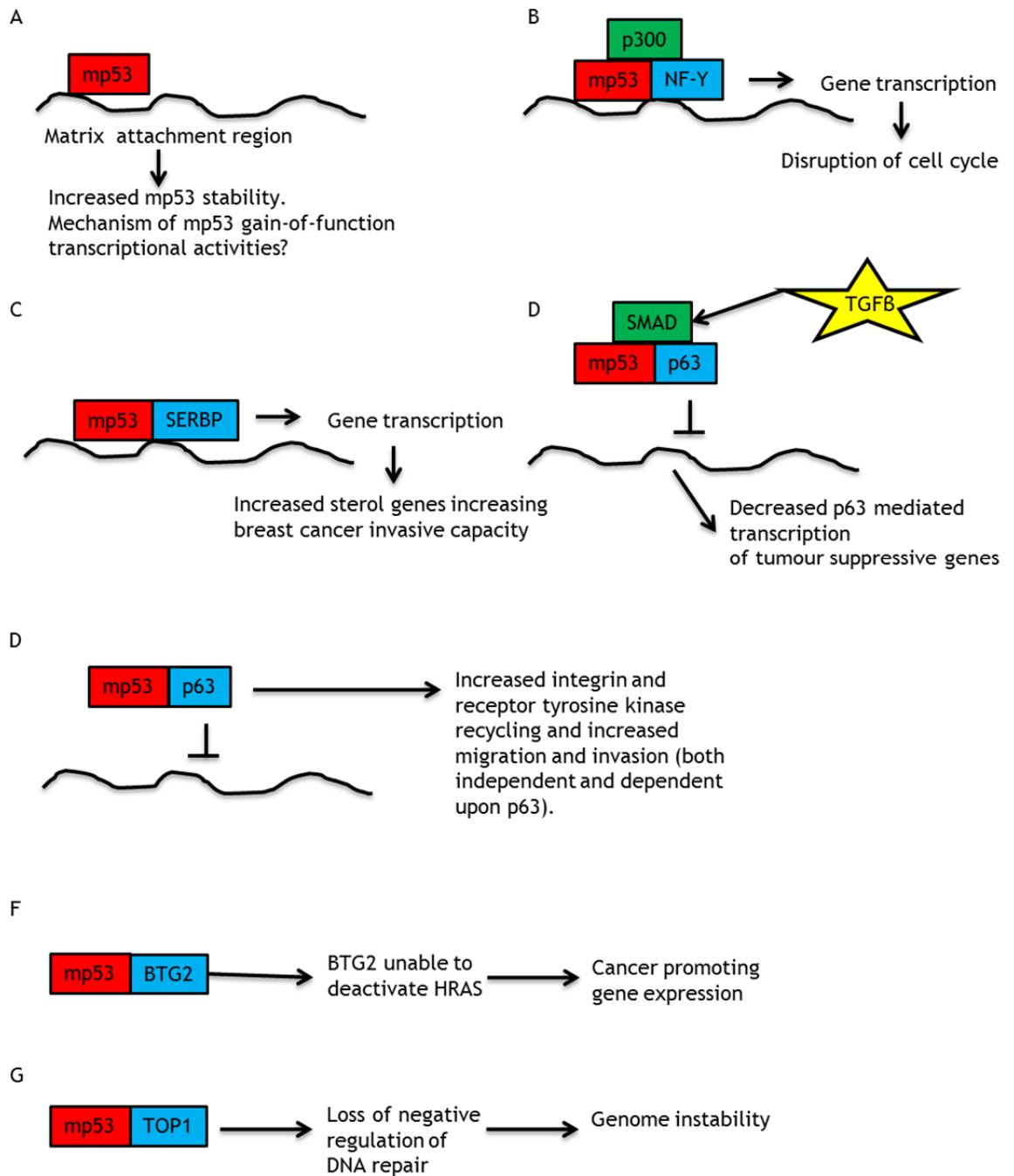


Figure 1-10: Mutant p53 gain-of-function mechanisms.

(A) Mutant p53 (mp53) can bind to matrix attachment regions to increase its stability and acquire gain-of-function transcriptional control. (B) Mutant p53 associates with the transcription factor NF-Y and transcriptional co-regulator p300 upon DNA damage to initiate gene transcription that disrupts the cell cycle. (C) Mutant p53 and transcription factor SERBP association drives transcription of sterol-related genes increasing cancer like morphology of breast cancer. (D) TGFβ-stimulated formation of the SMAD, p53 and p63 complex, inhibits tumour-suppressing transcription by p63, increasing the migratory and invasive phenotype of cancer cells. (E) Mutant p53 association with p63 enhances integrin and receptor tyrosine kinase receptor recycling contributing to migratory and invasive phenotype (this can also be independent of p63). (F) Mutant p53 binding to BTG2 means that BTG2 cannot deactivate HRAS. Constitutively active HRAS leads to increased expression of cancer promoting genes. (G) Mutant p53 association with TOP1 leads to exacerbated DNA repair and genome instability.

1.2.3.3 Gain-of-function phenotypes

Initial experiments identified a mutant p53 gain-of-function by showing that mutant p53 expression alone is sufficient to transform p53 null cells to display enhanced growth in soft agar (anchorage-independent conditions) and as xenografts in mice (Dittmer et al., 1993). One key gain-of-function hallmark exhibited by mutant p53-expressing cells is genomic instability. Indeed, mutant p53's disruption of spindle checkpoint control leads to the generation of cells with polyploid genomes *in vitro* (Gualberto et al., 1998). Additionally, *in vivo* expression of mutant p53 promotes aneuploidy in tumours (Caulin et al., 2007). Another hallmark of mutant p53 gain-of-function is suppression of apoptosis. Initial findings indicated that cMyc driven apoptosis is suppressed by mutant p53 expression (Lotem and Sachs, 1995). Additionally, upon growth factor deprivation or exposure of cells to chemotherapeutic agents, expression of mutant p53 was able to suppress apoptosis (Peled et al., 1996, Li et al., 1998).

A number of *in vivo* studies have provided key evidence to support mutant p53's role in cancer cell invasion and metastasis. The mouse model of Li-Fraumeni syndrome, in which a mutant form of p53 (p53^{R175H}) is knocked-in to the appropriate endogenous locus, displays many characteristics of the human disease. Moreover, the spectrum of tumours contracted by these animals generally assumes a more invasive phenotype than the malignancies which are found in p53 null mice - an observation which is consistent with a pro-invasive gain-of-function for mutant p53 (Olive et al., 2004, Lang et al., 2004). More recently, comparison of the invasive phenotypes of p53 loss and p53 mutation in a mouse model of pancreatic cancer has reinforced this view. The Hingorani/Tuveson model of pancreatic cancer comprises a transgenic animal co-expressing mutant alleles of KRAS (LSL-KRAS^{G12D}) and p53 (LSL-p53^{R172H}) under control of a pancreatic-specific Cre recombinase (Pdx-Cre). These animals develop a form of pancreatic cancer which is highly invasive, and which metastasises to the liver in the majority of animals (Hingorani et al., 2005). However, transgenic mice which express mutant KRAS in combination with a floxed allele of p53 under control of Pdx-Cre (which implements p53 loss in the pancreas) develop pancreatic adenocarcinoma with high penetrance, but these tumours are less invasive than those from Hingorani/Tuveson animals and never form metastases. Moreover, when studied *ex vivo* cells derived from these

tumours display invasive characteristics that are dictated by their mutant p53 status, thus confirming the ability of mutant p53 to drive an invasive and metastatic gain-of-function phenotype *in vivo* (Morton et al., 2010).

Finally, several studies have identified the mechanisms by which mutant p53 exerts its gain-of-function invasive migratory phenotype. Mutant p53 expression increases TGF β -dependent migration, invasion and metastasis *in vitro* and *in vivo* (Adorno et al., 2009). Furthermore mutant p53 expression inhibits the wild-type p53 transcriptional suppression of LASP1 expression. The consequent increased expression of actin binding protein LIM and SH3 domain protein-1 (LASP1) promotes migration and invasion of hepatocellular carcinoma cells (Wang et al., 2009a). Additionally, studies from our lab have identified a mutant p53 gain-of-function invasive and migratory phenotype which is achieved via the ability of mutant p53 to increase rates of α 5 β 1 integrin, epidermal growth factor receptor (EGFR) and cMET recycling and signalling (Muller et al., 2009, Rainero et al., 2012). This increase in receptor recycling is dependent upon the Rab11 effector, Rab coupling protein (RCP) and the phosphatidic acid producing enzyme, diacylglycerol kinase alpha (DGK α). Furthermore, the mechanism linking increased RCP/DGK α -dependent recycling to the cellular machinery responsible for driving invasion have been elucidated by Jacquemet (2013). Indeed, when mutant p53 drives RCP/DGK α -dependent recycling of α 5 β 1 and RTKs, this leads to activation of the Akt signalling axis, in particular Akt2. Akt2 then promotes phosphorylation of RacGAP1 at threonine-249, which recruits it to the front of the cells. RacGAP1 phosphorylation then leads to inhibition of Rac-GTPase which, in turn, activates RhoA at the cell front. This spatially-restricted pool of activated RhoA then drives extension of invasive pseudopod protrusion and invasive migration of mutant p53-expressing cells through the ECM (Jacquemet et al., 2013).

These findings are strongly supported in a study by Timpson et al (2011) which carried out intra-vital imaging of pancreatic ductal adenocarcinoma (PDAC) tumours that were either expressing mutant p53^{R172H} or were p53 null. Imaging of these tumours identified an increased RhoA activity at the leading edge and rear of mutant p53-expressing invasive PDAC cells, this was absent from p53 null (non-invasive) cells. Furthermore treatment of mutant p53 expressing tumours with anti-invasive drug Dasatanib inhibited the spatial distribution of RhoA in

mutant p53 expressing cells indicating that it is the spatial distribution of RhoA is important for the invasive potential of cells (Timpson et al., 2011).

An additional component to mutant p53's gain-of-function migratory phenotype is mediated via down-regulation of transcription of the endoribonuclease, DICER. Suppression of DICER promotes increased RCP-dependent integrin, EGFR and cMET trafficking rates as well as resulting in decreased processing of some miRNAs (Muller et al., 2014). These comprehensive mechanisms of mutant p53 driven invasive migration are shown in figure 1-11.

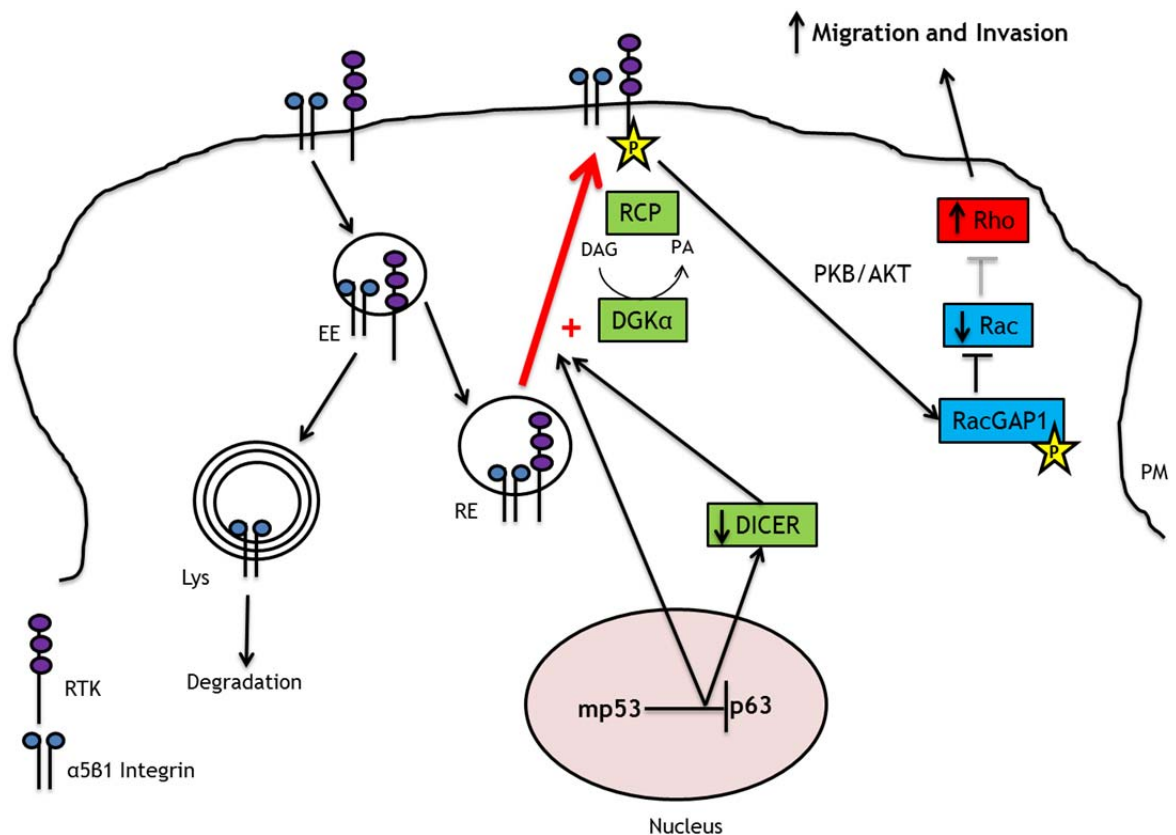


Figure 1-11: Effect of mutant p53 on integrin and RTK trafficking.

Mutant p53 expression increases integrin and receptor tyrosine kinase (RTK) recycling to the plasma membrane (this can be both dependent and independent of p63 suppression). This increased recycling rate is dependent upon DGKα activity allowing phosphatidic acid (PA) generation from diacylglycerol (DAG), which promotes tethering of RCP to invasive pseudopod tips driving increased integrin and RTK recycling. Additionally decreased DICER expression mediated by mutant p53 suppression of p63 transcriptional activity drives increased RTK and integrin recycling. Integrin and RTK presence and activation at the plasma membrane leads to increased AKT signalling, which phosphorylates RacGAP1, decreasing Rac and increasing RhoA activity. RhoA activity at the leading edge of a migrating cell allows invasive cell migration supporting a pro-tumorigenic phenotype. EE – early endosome. RE- recycling endosome. Lys – lysosome.

1.2.3.4 Targeting mutant p53 therapeutically

Due to the fact that p53 is mutated in so many cancers, there have been many investigations into how mutant p53 could be targeted therapeutically to prevent cancer progression. One strategy that has been investigated is the re-activation of wild-type p53 function. The drug PRIMA1 was found to restore the mutant p53 protein conformation back to the DNA binding conformation allowing wild-type p53 function to be restored (Bykov et al., 2002). This is a particularly attractive prospect due to the fact that re-activation of wild-type p53 in tumours has been shown to cause tumour regression (Xue et al., 2007).

Strategies to de-stabilise mutant p53 have also been considered, for example by rescuing MDM2-mediated ability to degrade mutant p53 (Li et al., 2011) or by disrupting mutant p53 interactions with transcription factors (Kravchenko et al., 2008). A drug called RETRA has been identified to be useful in disrupting p53-p73 interaction to restore some of p73's tumour suppressive activity (Kravchenko et al., 2008). Additionally, peptides targeted to the C-terminus of p53 have been shown to impart apoptosis-promoting capabilities to mutant p53's (Selivanova et al., 1997). However targeting p53 therapeutically is not without its problems. For instance, wild-type p53-stabilising therapies have been shown to also stabilise mutant p53 in mice resulting in a very poor outcome (Suh et al., 2011). Therefore p53-targeted therapies should be considered and tested carefully before being translated into the clinic.

1.2.3.5 Concluding remarks

Overall, here we have reviewed the importance of the role that mutant p53 has in cancer cell invasion and metastasis - the mechanisms of which are becoming well established. Directly targeting mutant p53 therapeutically is difficult and sometimes not a desirable option. Therefore, further understanding of the mechanisms through which mutant p53 drives invasion is necessary, and investigation of the role of mutant p53 in novel fields of research should be encouraged. Microvesicle biology is currently attracting a huge amount of attention in the field of cancer research due to the role that microvesicles have in cell-cell communication and the transfer of oncogenic phenotypes between cells. Surprisingly, even though mutant p53 is recognised as an oncogene, it has not yet been investigated in the context of microvesicle biology. Next we

review the field of microvesicles and the important role that they have in normal physiology as well as in diseases such as cancer.

1.3 Microvesicles

1.3.1 Historical perspective

The presence of membrane-enclosed vesicles in the extracellular environment has been recognised since the 1970s when they were isolated from fluids such as blood (platelet-derived microparticles) and semen (prostasomes) (Crawford, 1971, Stegmayr and Ronquist, 1982). The analysis of the constituents of platelet-derived microparticles suggested that they were membrane-derived and showed that they displayed ATPase activity. Additionally the isolated prostasomes also displayed ATPase activity and had the functional capacity to aid the motility of sperm. It was later identified that microvesicles can be shed from the plasma membrane of cancer cells and display functional 5' nucleotidase and pro-coagulant activities (Trams et al., 1981, Dvorak et al., 1981).

Release of microvesicles derived from the endosomal system was identified in the 1980s. During maturation of reticulocytes into erythrocytes, membrane proteins such as the transferrin receptor are lost. Electron microscopy studies have shown that the transferrin receptor is exported from cells during reticulocyte maturation via the release of small vesicles (Harding et al., 1983, Pan and Johnstone, 1983, Pan et al., 1985). Subsequently the trafficking of the endocytosed transferrin receptor through the cell was followed, and it was shown to travel through the endosomal system to arrive in intraluminal vesicles (ILVs) which form via inward budding of the multivesicular body (MVB) limiting membrane. The transferrin-positive ILVs were subsequently released into the extracellular environment via an exocytic mechanism. MVB-derived exosomes that are released from reticulocytes had some of the functional properties that are related to reticulocyte function. Therefore the process whereby proteins are lost from the reticulocyte plasma membrane via MVB-derived exosomes, was hypothesised to allow the removal of proteins important in reticulocyte function to allow maturation into erythrocytes (Johnstone et al., 1987, Pan et al., 1985).

1.3.2 Biogenesis and subtypes

There are two main routes by which microvesicles can be released into the extracellular environment. MVB-derived exosome is the name given to vesicles formed within the endosomal system and they are typically under 100 nm in size. Alternatively microvesicles can be shed directly from the plasma membrane by a budding process. These are referred to as plasma membrane-shed microvesicles and these are generally greater than 100 nm in size (Colombo et al., 2014). Accordingly, throughout this thesis I will refer to MVB-derived exosomes, plasma membrane-shed microvesicles, and a mixture of both types will collectively be referred to as microvesicles. Furthermore, in reviewing studies that have not conclusively determined whether they are dealing specifically with either MVB-derived or plasma membrane-shed structures, I will also use the generic term, 'microvesicles'.

1.3.2.1 MVB-derived exosomes

The endosomal compartment is a complex system which is essential for the intracellular transport of proteins. After endocytosis from the plasma membrane, most protein cargoes are delivered to early endosomes. Early endosomes can then mature into late endosomes. Inward budding of the late endosomal limiting membrane then occurs to result in the formation of MVBs which contain a number of ILVs (Stoorvogel et al., 1991). The contents of MVBs can either be degraded by fusion with lysosomes, or they may be released as exosomes into the extracellular environment by exocytic fusion of the MVB with the plasma membrane (Johnstone et al., 1987, Piper and Katzmann, 2007). This process is diagrammatically summarised in figure 1-12.

Inward budding of the late endosomal membrane - which leads to the formation of ILVs - may be catalysed by endosomal sorting complex (ESCRT)-dependent, or ESCRT-independent mechanisms as comprehensively reviewed by Hanson and Cashikar (Hanson and Cashikar, 2012). The ESCRT complex is a large family of proteins sub-divided into groups 0, I, II and III. Each group of the family assembles into a complex to direct inward budding from the endosomal limiting membrane. During ILV formation, ESCRT 0, I and II have the role of targeting and clustering ubiquitinated protein cargo in the late endosomal membrane.

This 'cluster model' leads to the inward deformation of the endosomal membrane forming a vesicle connected to the endosome limiting membrane by a neck. Subsequently, upon stimulation and recruitment to the endosomal membrane, monomeric ESCRT III components are polymerised into filamentous structures, a process that is most commonly described as being driven by vacuolar protein sorting 4 (VPS4). These ESCRT III filaments then drive the final stages of vesicle formation promoting the scission of the neck; however it is not yet known how membrane scission is achieved.

Other processes have been implicated in MVB and ILV biogenesis which are independent of the ESCRT machinery. One of these involves sphingomyelinase-induced ceramide synthesis which triggers cargo sorting and membrane curvature to promote ILV formation (Trajkovic et al., 2008). Conversely tetraspanins have been shown to participate in MVB/ILV biogenesis by contributing to sorting of correct cargo into ILVs before they are released into the extracellular environment. Persistent Epstein Barr virus infection is maintained by constitutive activation of NF- κ B by latent membrane protein-1 (LMP1). LMP1 avoids degradation and maintains its constitutive activity both inside and outside infected cells by CD63-dependent trafficking to ILVs and subsequent release into the extracellular environment in MVB-derived exosomes (Verweij et al., 2011). The tetraspanins CD82 and CD9 suppress tumour metastasis by decreasing Wnt signalling. The tetraspanins do this by promoting the export of β -catenin out of the cell via MVB-derived exosome release (Chairoungdua et al., 2010). Finally a mass spectrometric analysis of MVB-derived exosomes released from CD81 silenced cells and an *in vivo* screen of CD81 knockout mice, showed that CD81 has an important role in sorting cargo into exosomes without having any effect upon the number of MVB-derived exosomes released (Perez-Hernandez et al., 2013).

1.3.2.2 Rab-GTPases

Rab-GTPases are essential participants in mediating the transport of MVBs to the plasma membrane for docking and exocytic fusion, thus allowing the release of ILVs as MVB-derived exosomes into the extracellular environment. MVB-derived exosome release requires transport of MVBs to the plasma membrane using the cytoskeleton, molecular motors, Rab-GTPases and exocytic fusion machinery,

such as SNARE proteins (Cai et al., 2007). The Rab GTPases that have been most investigated in regard of MVB-derived exosome release are Rab27a and Rab27b. Silencing of both Rab27a and Rab27b results in decreased MVB-derived exosome release from HeLa cells. It is believed that Rab27a and Rab27b collaborate to promote MVB docking to the plasma membrane by allowing fusion with the plasma membrane and release of their contents into the extracellular environment (Ostrowski et al., 2010). Rab27-dependent MVB-derived exosome release may have an important role in mammary carcinogenesis *in vivo*. Rab27 knockdown in xenografted mammary carcinoma cells leads to decreased tumour growth and reduced metastatic dissemination to the lung, indicating the possibility that Rab27a driven exosome release is involved in these aspects of tumour progression (Bobrie et al., 2012). Rab9 has been shown to participate in the release of tumour necrosis factor from melanoma cells via an exosome-mediated route (Soderberg et al., 2007). Furthermore, other Rabs such as Rabs 5 and 2 have been identified by siRNA screens to potentially have an impact upon microvesicle release, however this has so far not been intensively investigated (Ostrowski et al., 2010).

Rab11 has been found to be involved in MVB-derived exosome release. As previously discussed, the process of membrane protein-shedding is integral to reticulocyte maturation. They do this by MVB formation of ILVs that are subsequently released as MVB-derived exosomes (Johnstone et al., 1987). Rab11 overexpression has been found to increase MVB-derived exosome release from haematopoietic leukaemia cells and, consistently, expression of dominant negative Rab11 decreases MVB-derived exosome release from these cells (Savina et al., 2002). Other studies looking at the role of exosomes in Wnt signalling in *Drosophila* S2 cells have reaffirmed the role of Rab11 in 'exosome like' microvesicle release (Beckett et al., 2013, Koles et al., 2012).

Hsu and colleagues overexpressed different Rab-GAPs to identify Rabs whose activity is important in MVB-derived exosome release. These workers found that the catalytic activity of the Rab-GAP TBC1D10A-C, was essential for MVB-derived exosome release from oligodendrocytes. TBC1D10A-C is an effector of Rab35, and, consistently this study found that suppression of Rab35 increased endosome accumulation within the cell and decreased MVB-derived exosome release. The presence of vesicles at Rab35-expressing domains at the plasma membrane

suggests that Rab35 may have a role in vesicle tethering/docking (Hsu et al., 2010). This observation is supported by another study showing that the glutamate neurotransmitter stimulates MVB-derived exosome release from oligodendrocytes in a Rab35-dependent manner. These MVB-derived exosomes are taken up into neurons by endocytosis and the transfer of MVB-derived exosome protein/mRNA content increases neurone viability following stressful stimuli (Fruhbeis et al., 2013a).

1.3.2.3 SNARE proteins

Once MVBs have been transported to the cell periphery they need to dock and fuse with the plasma membrane in order for ILVs to be released as exosomes. SNARE proteins on the endosomal vesicle form a complex with target SNAREs on the target membrane with which the vesicle is destined to dock and fuse (Zylbersztein and Galli, 2011). Vamp7 has been identified as having a role in directing the fusion of MVBs with the plasma membrane in K562 leukaemia cells. This allows the release of acetylcholinesterase-containing MVB-derived exosomes into the extracellular space (Fader et al., 2009). Studies in *Drosophila* have identified two other SNARE proteins, Ykt6 and syntaxin1A, as being responsible for the release of exosomes (Koles et al., 2012, Gross et al., 2012). The processes involved in MVB/ILV biogenesis, MVB transport to and fusion with the plasma membrane, and release of ILVs into the extracellular environment as MVB-derived exosomes are diagrammatically summarised in figure 1-12.

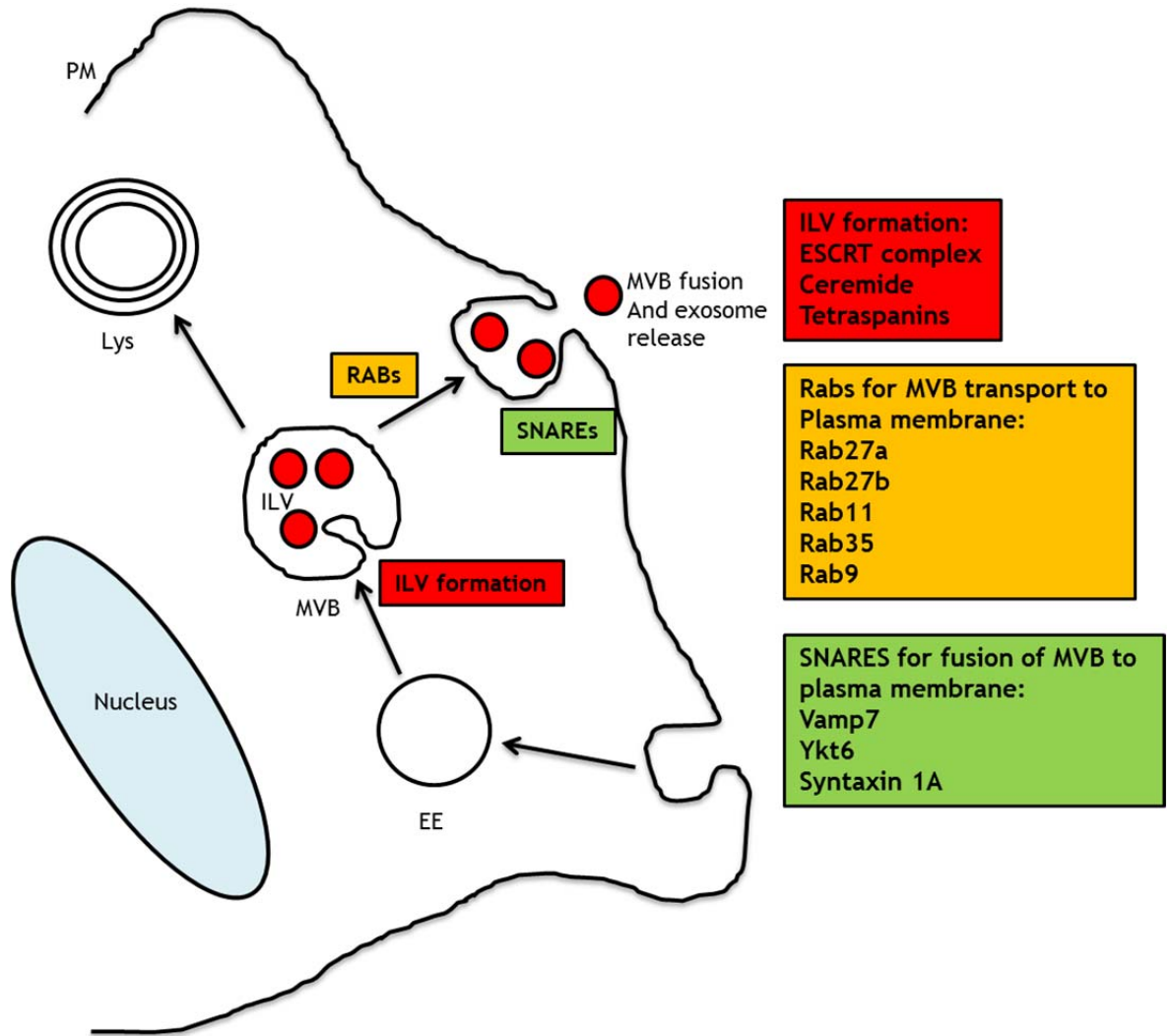


Figure 1-12: MVB-derived exosome biogenesis and release.

Brief outline of how early endosomes (EE) mature into multivesicular bodies (MVB) upon ESCRT, ceramide or tetraspanin dependent intraluminal vesicle (ILV) formation. MVB's are then transported to the plasma membrane via Rab-GTPase proteins where they dock and fuse via interactions between vesicular SNARE proteins and target membrane SNARE proteins. This membrane fusion allows ILV release into the extracellular environment as MVB-derived exosomes.

1.3.2.4 Plasma membrane-shed microvesicles

The way that plasma membrane-shed microvesicles are formed and released into the extracellular environment has been extensively studied. Similar to MVB-derived exosome biogenesis, the ESCRT complex has also been shown to be involved in plasma membrane-shed microvesicle biogenesis. The HIV retrovirus promotes plasma membrane budding events that are catalysed by recruitment of the HIV Gag protein. The HIV Gag protein is recruited to domains on the plasma membrane that are rich in endosomal proteins including members of the ESCRT complex such as Class E VPS proteins and TSG101. These ESCRT components are functionally important in the vesicle budding process within the endosomal

system, and their presence at plasma membrane domains at which Gag-mediated budding occurs, suggests that ESCRT may also be functionally important in plasma membrane-derived microvesicle release (Booth et al., 2006). Additionally, regulation of actin dynamics by Arf6 expression results in plasma membrane-derived microvesicle release (Muralidharan-Chari et al., 2009). Arf6-GTP activates phospholipase-D which recruits ERK to the plasma membrane. Here, ERK phosphorylates myosin light chain kinase which, in turn, phosphorylates myosin light chain allowing acto-myosin contraction of the microvesicle necks. This allows release of integrin and protease-rich microvesicles from the plasma membrane. Furthermore, decreased expression of the actin nucleating protein, diaphanous related formin 3, promotes plasma membrane-derived microvesicle budding from prostate cancer cells (Di Vizio et al., 2009).

Calcium signalling activates the phospholipid pumps - floppase and scramblase - which causes membrane phospholipid re-distribution and plasma membrane-derived microvesicle shedding (Hugel et al., 2005). Additionally, calcium influx and signalling in platelets activates the protease calpain, which is important in platelet microvesicle shedding (Pasquet et al., 1996).

As in MVB-derived exosome biogenesis, lipids have an important role in the biogenesis and release of plasma membrane-shed microvesicles. Activation of purinergic P2X7 receptor in glial cells initiates phosphorylation of p38 which, in turn, activates acid sphingomyelinase. Acid sphingomyelinase activity in the plasma membrane results in conversion of sphingomyelin to ceramide which has a role in plasma membrane-derived microvesicle release as well as MVB-derived exosome biogenesis (although MVB-derived exosome biogenesis relies upon a neutral sphingomyelinase rather than acid sphingomyelinase for ceramide synthesis) (Trajkovic et al., 2008, Bianco et al., 2009). Finally hypoxia-induced increase in Rab22a expression results in an increased release of plasma membrane-derived microvesicles from breast cancer cells. In this study Rab22a was seen to localise to the sites of plasma membrane budding, therefore the authors hypothesised that Rab22a may have a role in hypoxia-driven microvesicle biogenesis (Wang et al., 2014). Although it is not known how Rab22a mechanistically contributes to microvesicle biogenesis, it is known that the resulting microvesicles can promote breast cancer invasion and metastasis. The

processes involved in plasma membrane-shed microvesicle biogenesis are reviewed in figure 1-13.

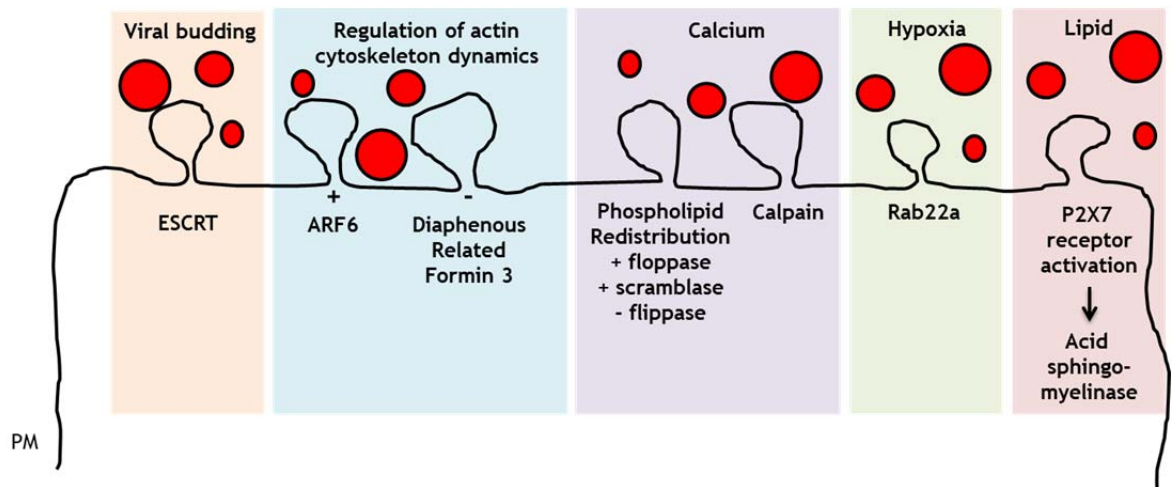


Figure 1-13: Illustration of plasma membrane-shed microvesicle biogenesis and release
 During viral budding the plasma membrane-shed microvesicles are released possibly with the aid of ESCRT machinery. Budding from the plasma membrane is also regulated by the actin cytoskeleton in ARF6 and Diaphanous related formin 3 dependent mechanisms. Calcium can stimulate microvesicle budding from the plasma membrane, this is dependent upon calcium signalling activation of calpain or phospholipid re-distribution. Hypoxia promotes Rab22A dependent microvesicle release from the plasma membrane and finally P2X7 receptor activation activates acid sphingomyelinase which alters membrane dynamics resulting in the budding of microvesicles.

1.3.2.5 Stimuli leading to microvesicle release

Plasma membrane-shed microvesicle and MVB-derived exosome release can be enhanced by environmental factors. Early studies indicated that exposure of cells to serum increased shedding of microvesicles that display metalloproteinase activities from the plasma membrane of breast carcinoma cells (8701-BD and MCF7) (Dolo et al., 1994). Depolarisation of neurons can also stimulate the release of microvesicles from primary cortical neurones (Faure et al., 2006). Finally DNA damage by irradiation stimulates MVB-derived exosome release via p53-dependent transcription of tumour suppressor-activated pathway 6 (TSAP6) which is involved in the regulation of protein trafficking and secretory pathways (Lespagnol et al., 2008).

1.3.2.6 Alteration of microvesicle contents

As discussed above certain stimuli can alter the quantity of microvesicles released from cells, but in addition to this there are a number of factors that can more selectively influence the constitution of microvesicles. For example,

several reports have shown that the microvesicle proteome is changed by expression of oncogenes, such as KRAS and EGFRvIII (Demory Beckler et al., 2013, Al-Nedawi et al., 2008). Inflammatory mediators, such as TNF- α or INF- γ also alter the miRNA and protein content of microvesicles released from endothelial cells and mesenchymal stromal cells respectively (de Jong et al., 2012, Kilpinen et al., 2013). Additionally, acidity (Parolini et al., 2009) and hypoxia (Kucharzewska et al., 2013), which are conditions often associated with the tumour microenvironment, change microvesicle release and composition. For example, acidity increases microvesicle release from melanoma cells, changes their lipid content as well as increasing the ability of microvesicles to deliver clathrin to recipient cells (Parolini et al., 2009). Secondly glioma cells exposed to hypoxic conditions release microvesicles that are enriched in hypoxia-stimulated protein and mRNA constituents (for example matrix metalloproteinases and caveolin-1) (Kucharzewska et al., 2013).

1.3.3 Microvesicle constituents

Microvesicles contain lipids, proteins and nucleic acids, but are generally devoid of cellular organelles. Many studies of microvesicle constituents are now accessible on two public databases; exocarta (www.exocarta.org) and vesiclepedia (www.microvesicles.org). Here, published microvesicle lipid, protein and nucleic content from a variety of cell types/clinical samples are accessible (Mathivanan et al., 2012, Simpson et al., 2012).

1.3.3.1 Proteins

Proteins present in microvesicle samples were originally identified by Western blotting and immuno-gold electron microscopy techniques. Then, in 1999, a more advanced screening was performed on exosomes collected from dendritic cells, which were analysed by trypsin digestion and protein mapping (They et al., 1999, They et al., 2001). It is now commonplace for microvesicles to be analysed using mass spectrometry-based proteomics to allow identification of proteins within the sample and to confirm the absence of contaminants (Lotvall et al., 2014). Microvesicle characterisation and classification by protein composition is discussed in detail in chapter 3. Briefly, the protein constituents of microvesicles commonly include endosomal, cytoplasmic and plasma

membrane-derived proteins. It is less common to find endoplasmic reticulum, Golgi, nuclear or mitochondrial proteins in microvesicles (Colombo et al., 2014). The proteins that are present in microvesicles vary depending upon the cell type from which they are derived (Mathivanan et al., 2010b). For example Mathivanan and colleagues found that there were markers (such as members of the ESCRT complex and tetraspanins) that were common to microvesicles collected from mouse mast cells, colorectal cancer derived cells and human urine, while some proteins were specific to the microvesicles released from colorectal cancer cells such as A33, cadherin-17 and EpCAM (Mathivanan et al., 2010b). Analysis of microvesicle contents from 19 different studies has been used to identify ubiquitous microvesicle protein markers including certain Rabs, Annexins, and tetraspanins (CD63, CD81, CD9), members of the ESCRT complex (ALIX, TSG101) and heatshock proteins (HSP70) (Mathivanan et al., 2010a).

Colombo and colleagues found that microvesicle contents can be influenced by whether they arise from MVBs or whether they are produced by shedding from the plasma membrane. For example upon Rab27a silencing (which has a well-defined role in MVB-derived exosome release), the release of CD63 positive MVB-derived exosomes is decreased, whereas the microvesicular CD9 content is not changed. This indicates that CD63 is enriched in exosomes generated in MVBs whereas CD9 may be more abundant in plasma membrane-shed microvesicles (Bobrie et al., 2012). However, as most microvesicle marker proteins are present in both MVB-derived exosomes and plasma membrane-derived microvesicles, these observations are more likely indicative of a heterogeneous population of microvesicles being released by different cell types, rather than indicating the cellular provenance of released microvesicles. Therefore, there are still no distinctive markers that can unambiguously discriminate between MVB-derived exosomes and plasma membrane-shed microvesicles; however several groups of proteins can be used as an indicator of microvesicle purity.

1.3.3.2 Lipids

Several studies have compared enrichment of lipid constituents in microvesicles from various cell types. Cholesterol, sphingomyelin, phosphatidylserine and ceramide are consistently reported to be enriched in MVB-derived exosomes (Llorente et al., 2013, Trajkovic et al., 2008, Wubbolts et al., 2003, Laulagnier

et al., 2005). Furthermore a study analysing 'exosome like' microvesicles from prostate cells (prostasomes) showed enrichment of sphingomyelin, cholesterol and glycosphingolipids (Brouwers et al., 2013). The fact that lipid raft components such as cholesterol and sphingolipids are sometimes enriched in microvesicles, may indicate the existence of a relationship between lipid rafts and microvesicle biogenesis. Lipid rafts are structures in the plasma membrane that are rich in cholesterol, sphingolipids and signalling proteins, such as Src family kinases. Lipid rafts are important mediators of protein-protein and protein-lipid interactions. Through these interactions lipid rafts mediate protein sorting and vesicle formation for endocytosis driving efficient intracellular transport of proteins (Ikonen, 2001). Therefore there is some speculation around the involvement of lipid raft domains in microvesicle biogenesis and the sorting of cargo proteins into microvesicles. The presence of lipid raft-associated GPI-anchored proteins in detergent resistant microvesicles supports this observation (Rabesandratana et al., 1998, Wubbolts et al., 2003). Indeed, there is evidence that exosomes from mesenchymal stem cells derive from lipid raft domains endocytosed from the plasma membrane (Tan et al., 2013).

1.3.3.3 Nucleic acids

RNA species such as mRNA and miRNAs are present in microvesicles (Ratajczak et al., 2006, Valadi et al., 2007). Experiments with RNases indicated that RNA is present both inside (resistant to RNase) and on the outside (sensitive to RNase) of microvesicles (Valadi et al., 2007, Deregibus et al., 2007). Interestingly RNAs present in microvesicles appear to be functional, and it is clear that they can be transferred to and alter gene expression in recipient cells and consequently change the recipient cell phenotype. Several studies have shown successful suppression of gene expression in recipient cells by miRNA transferred via microvesicles (Pegtel et al., 2010, Montecalvo et al., 2012, Ismail et al., 2013). Additionally, mRNA transferred via microvesicles has been shown to be translated into functional protein in recipient cells (Valadi et al., 2007). It appears that some RNA species are enriched in microvesicles compared to the donor cell, suggesting that there is an RNA sorting mechanism that takes place. Indeed, there is some speculation as to the involvement of a putative RNA sorting sequence that targets RNA for extracellular transport (Batagov et al., 2011), however this postulate is yet to be tested.

As well as RNA, genomic DNA has been identified in microvesicles. DNA fragments from which mutant forms of KRAS and p53 have been identified on circulating microvesicles from pancreatic cancer patients and medium conditioned by pancreatic cancer cell lines (Kahlert et al., 2014). The presence of genomic DNA on circulating microvesicles is a promising avenue for diagnostic blood tests for a spectrum of diseases. A schematic diagram showing a generic overview of the constituents of microvesicles (MVB-derived exosomes and plasma membrane-shed microvesicles) is shown in figure 1-14.

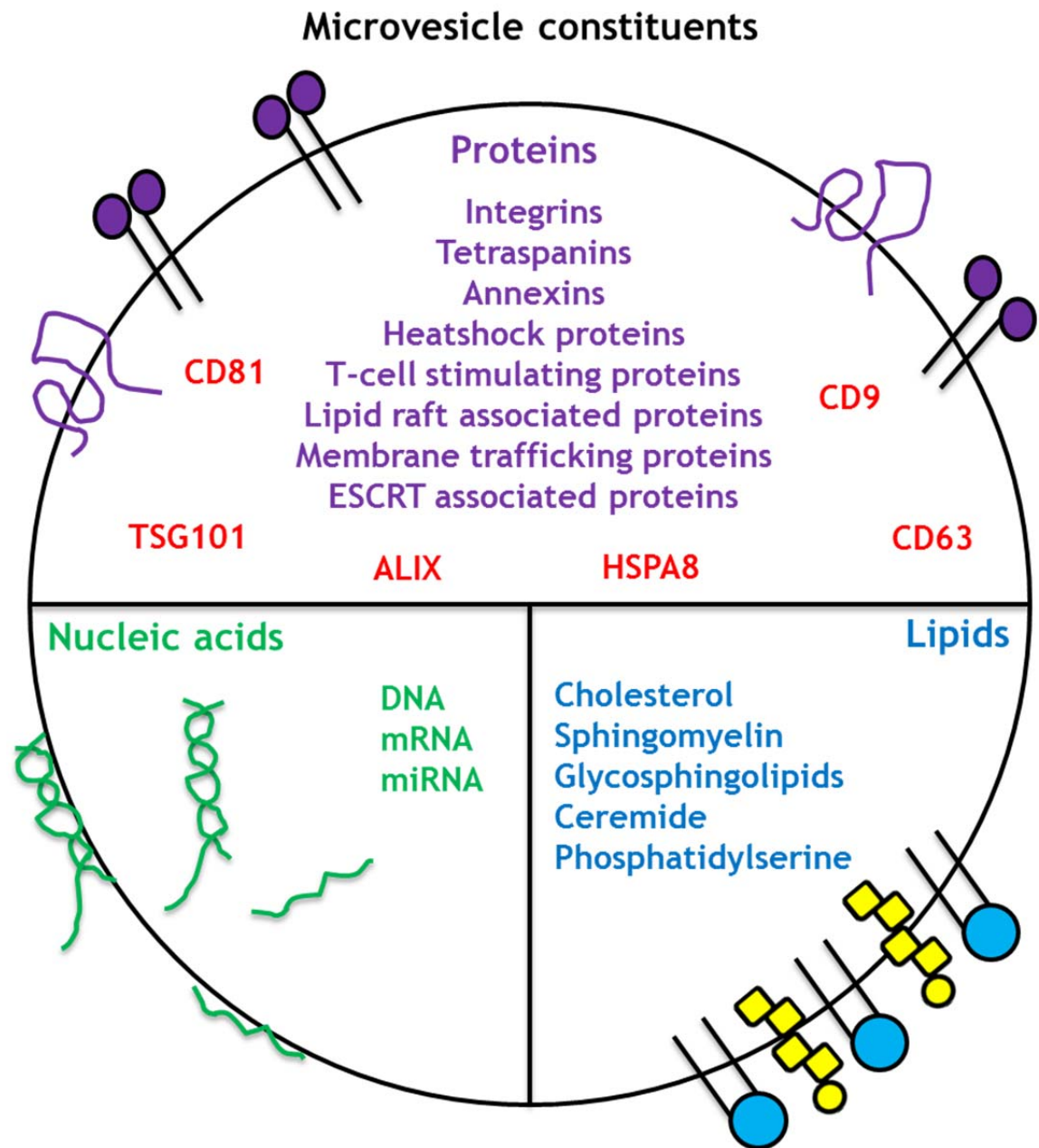


Figure 1-14: Diagram of microvesicle constituents.

Microvesicles contain proteins, lipids and nucleic acids. Proteins involved in adhesion, lipid raft domains, membrane trafficking, ILV biogenesis and antigen presentation are commonly found. Additionally shown in red are common proteins found in all microvesicles and can be referred to as microvesicle markers. Microvesicles are often enriched in cholesterol, sphingomyelin, ceramides and phosphatidylserine compared to the plasma membrane from the cells that they are released from. Microvesicles have also been shown to contain mRNA, miRNA and DNA nucleic acid species.

1.3.4 Microvesicle uptake by recipient cells

There is evidence indicating that microvesicles can be targeted to the surface of recipient cells via ligand-receptor interactions. For example, galectin-5 on rat reticulocyte MVB-derived exosomes targets their uptake into macrophages (Barres et al., 2010). Microvesicle capture by dendritic cells has been

hypothesised to be dependent on the interaction of ICAM1 ligand (on the microvesicle) with lymphocyte function-associated antigen (LFA-1) (on the surface of many immune cells including dendritic cells and T-cells) (Segura et al., 2005). Additionally blocking antibodies against α v integrin, β 3 integrin, CD9 and CD81 decrease bone marrow dendritic cell microvesicle capture and uptake by recipient dendritic cells (Morelli et al., 2004). Finally, the capture of B-cell derived microvesicles bearing α 2,3-sialic acid by macrophages is dependent on expression of the lectin adhesion molecule sialoadhesin in the macrophages (Saunderson et al., 2014).

In some instances ligand-receptor mediated association of microvesicles with the surface of recipient cells is sufficient for microvesicle to influence recipient cell function. Indeed, microvesicles from dendritic cells can effectively present antigens to T cells without being internalised (Segura et al., 2007). However, in most cases it is thought to be necessary for the microvesicle and its contents to enter the cell for the microvesicle to be able to exert any functional effects. It is possible that microvesicles may be able to fuse with the plasma membrane of the recipient cell; however it is more likely that endocytic mechanisms mediate the delivery of microvesicular cargoes into recipient cells. There are several reported mechanisms through which microvesicles can be taken into a cell and these include phagocytosis (Feng et al., 2010), dynamin-dependent macropinocytosis (Fitzner et al., 2011), receptor-mediated endocytosis (Morelli et al., 2004), clathrin-dependent endocytosis (Fruhbeis et al., 2013a), lipid raft-dependent endocytosis (Svensson et al., 2013) and caveolae-dependent endocytosis (Nanbo et al., 2013).

Once the microvesicle has been taken up into the cell by endocytosis, it is thought that fusion of the microvesicle with an endosomal membrane must occur if its cargo is to reach the cytosol of the recipient cell. The nanometre size of microvesicles and limitations of the resolution of current microscopy have precluded direct visualisation of microvesicle-endosome fusion events. However global fusion events can be indirectly visualised using lipid dyes which alter their fluorescence yield following dilution by fusion with another membrane (Montecalvo et al., 2012).

Additionally microvesicles may exert their effects through interactions with the extracellular matrix. For example, MMP-loaded microvesicles from tumour cells have been shown to enhance cell migration by binding to and degrading the extracellular matrix (Muralidharan-Chari et al., 2009).

1.3.5 Microvesicle function

1.3.5.1 Modulation of immune responses

Many of the key functions of microvesicles are related to regulation of the immune system. Antigen presenting cells release MVB-derived exosomes that contain MHC class II antigen peptide complexes that can then present these peptides to T-cells, triggering an immune response (Raposo et al., 1996). Furthermore, it is thought that MVB-derived exosomes containing MHC II peptide complexes are released by dendritic cells, and these need to be internalised by other dendritic cells in order for them to acquire the functional capacity to initiate T cell activation and induce an immune response (Thery et al., 2002). Microvesicles are also thought to be relevant to tumour immunology. Microvesicles released by cancer cells contain tumour-derived antigens. In the presence of dendritic cells, these microvesicle-associated tumour antigens can be transferred to dendritic cells to be incorporated into the MHC class II complex which then stimulates T-cell activation and initiates an anti-tumour immune response (Wolfers et al., 2001, Andre et al., 2002).

Antigens and MHC complexes are not the only means by which microvesicles can modulate the immune system. Microvesicles that are positive for Fas ligand (FasL) have been shown to be released by tumour cells and immune cells and these can initiate immune suppression by promoting T-cell apoptosis (Monleon et al., 2001, Andreola et al., 2002). Alternatively, pathogen infected macrophages can release microvesicles that, when taken up by recipient macrophages, initiate the secretion of pro-inflammatory cytokines to initiate an immune response (Bhatnagar and Schorey, 2007).

1.3.5.2 Modulation of immune function in cancer

It has been observed that increased levels of microvesicles are commonly detected in the blood of cancer patients, this indicates the possibility that

microvesicles are released at an increased rate by cancer cells (Taylor and Gercel-Taylor, 2008). This has triggered a wealth of important work identifying roles for microvesicles in cancer pathology. The shedding of microvesicles from the plasma membrane in cancer cells was originally documented many years ago (Poutsika et al., 1985), but it is only recently that progress is being made in characterising microvesicle release by cancer cells, and understanding the physiological roles of cancer cell-derived microvesicles. The first role ascribed to tumour-derived microvesicles was suppression of the immune response which enhanced tumour cell survival (Poutsika et al., 1985, Taylor and Gercel-Taylor, 2005). Microvesicles which are shed from the plasma membrane of melanoma cells have the ability to decrease expression of 1a antigen in macrophages, which is potentially the reason for their role in suppression of an immune response (Poutsika et al., 1985). Additionally microvesicles from tumour cells can promote T-cell apoptosis, which may decrease the immune response against the tumour (Taylor and Gercel-Taylor, 2005). Finally, MVB-derived exosomes from cancer cells can have a role in promoting immune cell infiltration to promote tumorigenesis (Bobrie et al., 2012).

MVB-derived exosomes released by tumours are also able to promote an immune response directed against the tumour. MVB-derived exosomes released by tumour cells have been found to act as a vector for tumour antigen peptide presentation to dendritic cells which consequently enhances the anti-tumour immune response (Wolfers et al., 2001). Additionally EGFRvIII-positive microvesicles isolated from glioblastoma cells also have the ability to induce anti-tumour responses (Graner et al., 2009). There is still much discrepancy as to how tumour-derived microvesicles impact on the immune system *in vivo*. However the potential role of microvesicles in enhancing immune responses against tumours has attracted the attention of immunologists in investigating the possibility of using microvesicles as an immunotherapy treatment of cancer.

1.3.5.3 Microvesicles in cancer immunotherapy

There have been numerous reports discussing an important role of microvesicles in promoting or inhibiting tumour progression *in vivo*. Interestingly MVB-derived exosomes collected from dendritic cells that have been pulsed with tumour antigens are able to initiate a T-lymphocyte anti-tumour immune response *in*

in vivo resulting in tumour clearance (Zitvogel et al., 1998). Phase 1 clinical trials so far have been performed in lung cancer (Morse et al., 2005) and melanoma (Escudier et al., 2005) patients. These trials showed that injection of microvesicles from dendritic cells pulsed with tumour antigens were safe and well-tolerated in patients. The treatment even led to regression/stabilisation of some tumours. This is a promising start to identifying possible therapeutic uses of microvesicles in the clinic.

1.3.5.4 Microvesicles in cancer cell communication

As well as the impact that tumour-derived microvesicles have on the immune system, they have more recently been identified as having a role in tumour cell invasion *in vitro* and metastasis *in vivo*. Cancer cell-derived microvesicles have been shown to be capable of transferring oncogene products and their associated proteins from cancer cells to other cells. Subsequently, the recipient cells gain a pro-tumorigenic phenotype that supports cancer progression (Al-Nedawi et al., 2008, Demory Beckler et al., 2013). Microvesicles shed from the plasma membrane of tumour cells are known to be loaded with matrix metalloproteinases and are able to interact with and degrade the extracellular matrix to enhance migration and invasion of tumour cells (Muralidharan-Chari et al., 2009). Furthermore microvesicles released from cancer-associated fibroblasts can help to drive breast cancer cell invasive capacity *in vitro* and metastasis *in vivo* through the autocrine maintenance of the wnt-planar cell polarity signalling pathway in breast cancer cells (Luga et al., 2012).

Finally, tumour-derived microvesicles have been shown to have an important role in co-ordinating and directing metastasis. Microvesicles released by melanoma cells have the ability to prime lymph nodes for melanoma cell metastasis by enhancing angiogenesis and extracellular-matrix deposition in the lymph node, as well as increasing the recruitment of melanoma cells to the metastatic site (Hood et al., 2011). Exciting studies from David Lydon's lab (exemplified schematically in figure 1-15), demonstrated a novel and very important role for microvesicles in mediating metastasis by priming the secondary visceral site to support the metastatic growth. cMET-containing MVB-derived exosomes from melanoma cancer cells irreversibly educate bone marrow progenitor cells when injected into mice. Melanoma MVB-derived exosomes

promote bone marrow progenitor cell mobilisation to the metastatic site, the lung, where they promote a pro-angiogenic environment allowing secondary metastatic colony formation (Peinado et al., 2012). It was later found that pancreatic ductal adeno carcinoma (PDAC) cells release MVB-derived exosomes that contain migration inhibitory factor (MIF). These MVB-derived exosomes educate kupffer cells at the liver metastatic site. This education results in TGF β signalling and increased fibronectin deposition which recruits bone marrow derived macrophages to take part in forming a fibrotic environment to support PDAC secondary tumour metastatic growth in the liver (Costa-Silva et al., 2015). These exciting studies show that microvesicles released by cancer cells have a very important role in directing metastasis *in vivo* and are, therefore, a potentially very important anti-metastatic therapeutic target.

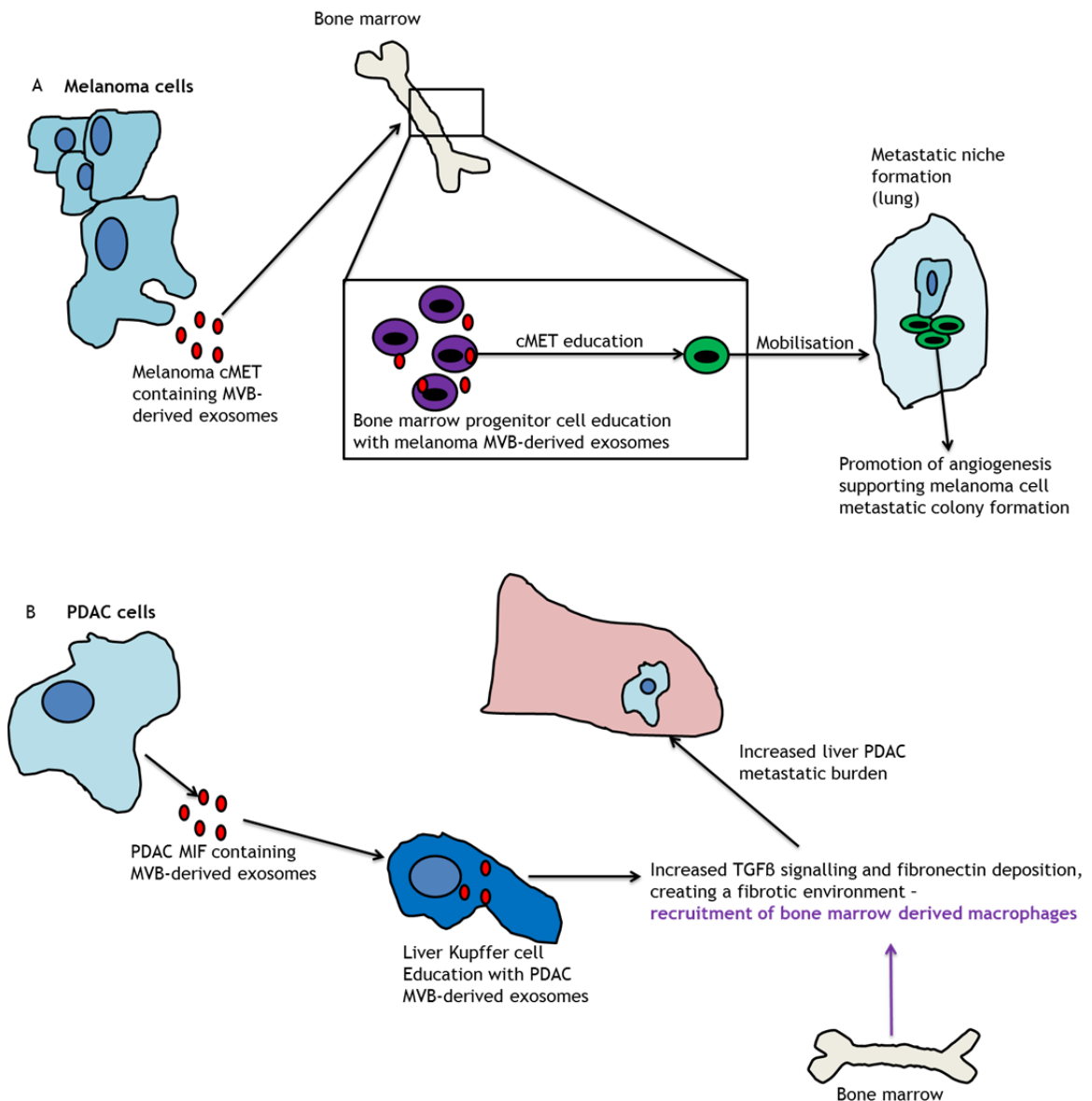


Figure 1-15: MVB-derived exosomes from cancer cells educate stromal cells to prime metastatic niches.

(A) shows how melanoma cells release MVB-derived exosomes that contain cMET, which educate bone marrow progenitor cells to mobilise to and prime, the metastatic organ to be pro-angiogenic and thus supportive of secondary tumour growth (Peinado et al., 2012). (B) shows that pancreatic ductal adenocarcinoma (PDAC) MVB-derived exosomes which contain migratory inhibitory factor (MIF), educate visceral cells at the metastatic site to promote a fibrotic pro-metastatic environment (Costa-Silva et al., 2015).

1.3.5.5 Other microvesicle functions

Cell types other than cancer cells and those of a haematopoietic lineage have been identified as being capable of releasing microvesicles. For example, cultured neurons release microvesicles upon depolarisation (Faure et al., 2006). Additionally plasma membrane-shed microvesicles and MVB-derived exosomes that are released by glial cells are of emerging importance in neuron-glial cell communication and act to control neuron viability (Mao et al., 2015, Fruhbeis et

al., 2013b, Fruhbeis et al., 2013a). Finally epithelial cells from the intestine release microvesicles that contain MHC class II peptides and may potentially be involved in antigen presentation (van Niel et al., 2001).

1.4 Final concluding remarks

As we have discussed, cancer cell migration and invasion away from the primary tumour is necessary for metastasis to secondary sites, and it is this metastasis and secondary tumour growth that causes the majority of deaths from cancer. It is well established that p53 is mutated in over half of all cancer cases, and it is therefore a very important protein to understand in cancer progression. Studies from our lab and several others have elucidated an important role for the oncogene mutant p53 in integrin and RTK receptor recycling and consequent promotion of cancer cell invasion. Additionally it is evident that oncogene expression has an impact upon microvesicle biology, and can alter the content of microvesicles to such an extent that microvesicles from oncogene expressing cells can transfer oncogenic phenotypes to other cells. The oncogenic mutant p53 has not yet been investigated in the context of microvesicle biology and, as will be discussed in chapter four, p53 has important non-cell-autonomous functions. Therefore this study investigates the role that mutant p53 expression has upon cancer cell microvesicle release, content and function within the extracellular environment.

2 Methods

2.1 Cells and tissue culture

2.1.1 Cell line generation

The following cells were all purchased from ATCC: H1299 (null for p53), MCF7 (express wild-type p53) and A2780 (express wild-type p53). H1299 and MCF7 cells were then genetically modified to express mutant p53 as described below. The p53 status of each of the cell lines and the genetically modified cell lines used in this study are reviewed in table 2-1.

Cell line	p53 status	Genetic modifications
H1299	Null	p53 ^{R273H/R175H}
MCF7	Wild-type	p53 ^{-/-} and p53 ^{R273H}
A2780	Wild-type	none

Table 2-1: p53 status of cell lines used in the study and their genetic modifications.

2.1.1.1 H1299 p53^{-/-} and p53^{R273H/R175H}

H1299 non-small cell lung carcinoma cells null for p53^{-/-} or stably expressing mutant p53^{R273H/R175H} were generated as previously described (Noske et al., 2009). Briefly empty plasmid pCB6 or pCB6 plasmid containing p53^{R273H/R175H} were transfected into H1299 cells using Effectene (Qiagen) according to manufacturer's instructions. Successfully transfected cells were selected using DMEM containing 600 µg/ml of G418 (Life Technologies) until stable polyclonal cell lines expressing pCB6-(empty) or pCB6-p53^{R273H/R175H} were produced.

Site directed mutagenesis was performed to mutate p53 in pCB6 p53 containing constructs. The following oligos were used for mutagenesis: p53^{R175H} forward AGC GAG GTT GTG AGG CAC TGC CCC CAC CAT GAG CGC TGC CCC CAC CAT GAG CGC TGC T and reverse AGC AGC GCT CAT GGT GGG GGC AGT GCC TCA CAA CCT CCG T; p53^{R273H} forward GGA ACA GCT TTG AGG TGC ATG TTT GTG CCT GTC CTG G and reverse CCA GGA CAG GCA CAA ACA TGC ACC TCA AAG CTG TTC C.

2.1.1.2 H1299 p53^{-/-} GFP and p53^{R273H} m-cherry

H1299 cells stably expressing both p53^{-/-} and GFP or p53^{R273H} and m-cherry, were generated as previously described (Muller et al., 2014). A GFP expressing plasmid (Clontech) was co-transfected with pCB6 empty plasmid, whilst an m-cherry expressing plasmid (Clontech) was co-transfected with a pCB6-p53^{R273H} expressing plasmid using Genejuice Transfection Reagent (Millipore). Colonies were picked and cells maintained under selection by growing in medium containing 600 µg/ml G418.

2.1.1.2 MCF7 p53^{-/-}, p53^{R273H} and p53^{WT}

MCF7, breast adenocarcinoma cells (ATCC) which express wild-type p53 were genetically engineered to be null for p53 using a CRISPER-Cas9 nickase system according to manufacturer's instructions (Addgene) (Ran et al., 2013). The CRISPER plasmid (expressing Cas9-D10A nuclease along with the p53 guide RNA), was transfected into MCF7 cells using Lipofectamine (Life Technologies). A double nick was introduced into p53 exon 4, which after non-homologous end joining resulted in a frameshift/deletion/stop codon in the endogenous p53 gene to inhibit wild-type p53 translation. CRISPER oligo's for p53 guide RNA: gRNA-1: ACCAGCAGCTCCTACACCGG. gRNA-2: GGCATTCTGGGAGCTTCATC. Clones null for p53 were selected for by growing them in medium containing in 5 µm Nutlin. Nutlin causes cell cycle arrest and apoptosis in cells expressing wild-type p53, therefore only cells null for p53 should grow in its presence.

Mutant p53^{R273H} was introduced into the MCF7 p53^{-/-} cells using a Phoenix cell retroviral transduction protocol. Briefly Phoenix cells (ATCC) were transfected with plasmid pWZL-blast-p53^{R273H} using Genejuice Transfection Reagent. Conditioned medium containing virus particles with the packaged p53^{R273H} construct was collected 48 hours post-transfection and was subject to a 45 µm filtration. MCF7 p53^{-/-} cells were transfected with ecotropic receptor using Lipofectamine to enable viral infection, 24 hours later they were treated with the collected virus particles allowing retroviral infection. Infected cells were grown under selection with medium containing 2 µg/ml blasticidin (Millipore) to kill all non-transfected cells, resulting in MCF7 cell lines stably expressing

mutant p53 (cells made by Flore Kruiswijk. The Beatson Institute for Cancer Research).

2.1.2 Tissue culture

2.1.2.1 H1299 and MCF7

H1299 (p53^{-/-} and p53^{R273H/R175H}) and MCF7 cells were cultured in Dulbecco's Modified Eagle Medium (DMEM, Life Technologies) supplemented with 10 % FBS (Gibco), 1 mM L-glutamine, 100 µg/ml streptomycin and 100 U/ml penicillin. Cells were maintained at 37 °C in 10 % CO₂. All tissue culture products were purchased from Life Technologies. Cells were routinely passaged by washing with PBS (137 mmol/L NaCl, 2.7 nm/L KCl, 10 mmol/L Na₂HPO₄, 1.8 mmol/L KH₂PO₄ - fisher scientific) followed by 3 minute incubation in 0.25 % trypsin (Life Technologies) to detach cells from plates. The trypsin was quenched using 10 % FBS containing DMEM. H1299 cells were split at a ratio of 1:10 whereas MCF7 cells were split at a ratio of 1:3 every three days.

2.1.2.2 A2780

A2780 cells were cultured in RPMI (Life Technologies) supplemented with 10 % FBS, 1 mM L-glutamine, 100 µg/ml streptomycin and 100 U/ml penicillin. Cells were maintained in 10 % CO₂ at 37 °C. Cells were routinely passaged as previously described (2.1.2.1) at a ratio of 1:5 every five days.

2.1.2.3 Co-culture

H1299 p53^{-/-} cells stably expressing GFP or p53^{R273H} cells expressing m-cherry proliferated at the same rate as one another. Therefore they were co-cultured by plating each cell type at a density of 1x10⁶ cells in a 15 cm plate to grow to confluence together over 72 hours. Cells were maintained in DMEM containing 600 mg/ml G418 for continuous selection.

2.1.2.4 Transfections and siRNA oligos

H1299 cells were transfected using AMAXA transfection kit V according to manufacturer's instructions. Briefly, each siRNA transfection required approximately 6x10⁶ cells, the equivalent to an 80% confluent 15cm dish. Cells

were washed with PBS and trypsinised. Trypsin was quenched and cells re-suspended in DMEM containing 10 % FBS. Cells were pelleted by centrifugation at 1000 rpm for 5 minutes. The cell pellet was washed with PBS and re-pelleted before being re-suspended in 100 µl solution V plus siRNA for each transfection (18 µl supplement solution, 82 µl solution-V and 10 - 15 µl 20 µM siRNA). Cells were electroporated by AMAXA using the X-001 programme. Transfected cells were re-suspended in DMEM before being re-plated at an appropriate density for further experimentation.

For 24 hour knockdowns, 10 µl of a 20 µM stock siRNA was used. For 72 hour knockdowns 15 µl from the 20 µM stock siRNA was used (except for the Rab27a and Rab27b simultaneous knockdown which used 10 µl of each siRNA oligo).

For p53 the siRNA oligo used was- GACUCCAGUGGUAUACUU, whereas for RCP, DGKα, PODXL, Rab35, Rab27a, Rab27b SMARTpool siRNAs were used (Dharmacon).

2.2 Conditioned medium and microvesicle collection

2.2.1 Conditioned medium collection

H1299 p53^{-/-} and p53^{R273H} cells were grown to 90 % confluence over a 72 hour period (1×10^6 cells were plated per 15 cm plate). The conditioned medium was then collected and subjected to differential centrifugation at 300 g for 10 minutes, 2000 g for 10 minutes and 10,000 g for 30 minutes to remove live cells, dead cells and cell debris respectively; this is hereby referred to as conditioned medium. At this point conditioned medium was ready to use in experiments or could be stored at 4 °C for 24 hours.

2.2.2 Microvesicle collection

2.2.2.1 Differential centrifugation

For microvesicle collection a previously published protocol was followed and adapted (They et al., 2006a). For each collection, nine 15 cm dishes of H1299 p53^{-/-} and p53^{R273H} cells were grown to 90 % confluence over a period of 72 hours (the initial seeding density was 1×10^6 cells per 15 cm plate for H1299 cells and

2×10^6 for MCF7 cells). Cells were re-fed 24 hours after plating with 15 ml 5 % FBS microvesicle depleted DMEM. The 5 % FBS DMEM was depleted of serum microvesicles by an overnight ultra-centrifugation at 100,000 g in SW32 rotor using 36 ml polyallomer centrifuge tubes (Beckman).

Conditioned medium from the confluent cells was collected 48 hours after re-feeding. To collect microvesicles, conditioned medium was subject to differential centrifugation as previously described (2.2.1). This was followed by further ultra-centrifugation steps. Conditioned medium was centrifuged at 100,000 g for 70 minutes to pellet microvesicles. The supernatant was removed and the microvesicle pellet was washed in PBS and re-pelleted by centrifugation at 100,000 g for 70 minutes. The supernatant was removed and the microvesicle pellet re-suspended in 200 μ l PBS. For all centrifugation steps 36 ml polyallomer tubes and a SW32 rotor were used to ensure optimal yield during microvesicle collection and to prevent lipid bound microvesicles adsorbing onto the tube. The collected pellet comprised of a heterogeneous population of microvesicles. The microvesicle pellet could be used immediately for further experimentation or purified further by sucrose density gradient. Alternatively the microvesicle pellet could be stored for 24 hours at 4 °C. Generally pellets were not stored at -20 °C unless specified.

2.2.2.2 Sucrose density gradient

For further purification and characterisation, the microvesicle pellet was subject to a sucrose density gradient. The microvesicle pellet was re-suspended in 1 ml of 2.5 M sucrose (2.5 M sucrose (Thermo Scientific), 20 nM HEPES (Sigma), pH 7.4) and transferred to the bottom of a 12 ml polyallomer centrifuge tube (Beckman). Serial dilutions of sucrose from 2 M - 0.4 M were prepared in 20 nM HEPES solution (pH 7.4), from a starting concentration of 2.5 M. Each sucrose fraction was carefully applied one at a time, on top of the microvesicle layer, with the lowest sucrose concentration at the top and the highest concentration at the bottom. The sucrose gradient was ultra-centrifuged at 200,000 g for 16 hours in a SW40 rotor. Different microvesicle populations were separated according to their specific densities. Each microvesicle population was collected by separating the gradient fractions. Each fraction was diluted in 11 ml of PBS and centrifuged at 100,000 g for 70 minutes in an SW40 rotor. Pelleted

microvesicle fractions were then re-suspended in a small volume of PBS (50 - 200 μ l) and used for further experimentation.

2.2.3 Conditioned medium or microvesicle pre-treatment of cells

2.2.3.1 Conditioned medium pre-treatment

Conditioned medium was collected from p53^{-/-} and p53^{R273H} cells as previously described (section 2.2.1) and supplemented with DMEM (1:1). 1×10^6 cells were seeded into 15 cm plates and cultured in the collected conditioned medium for 72 hours until they reached 90 % confluence. Pre-treated cells were then re-plated into DMEM, for further experimentation.

2.2.3.2 Microvesicle pre-treatment

For microvesicle pre-treatment, 1×10^6 cells were seeded into 15 cm plates containing complete DMEM supplemented with freshly collected microvesicles. The volume of microvesicles used for treatment, was three times more than would be collected from the total treatment volume, to account for any material lost during centrifugation. For example if the treatment volume was 20 ml of DMEM, microvesicles collected from 60 ml conditioned medium were used to supplement the DMEM. Cells were grown to confluence in microvesicle supplemented DMEM for 72 hours before being plated into fresh DMEM for subsequent experiments. Alternatively for shorter term experiments cells were treated with microvesicle supplemented medium overnight.

2.3 Microvesicle characterisation strategies

2.3.1 Protein content

The protein content of microvesicles was analysed using Qubit protein assay (Life Technologies) according to the manufacturer's instructions. Briefly, the collected microvesicle pellet was re-suspended in 200 μ l of PBS. To quantify protein concentration, 10 μ l of the re-suspended pellet was used in the assay. To normalise for the presence of PBS, 10 μ l of PBS was added to each of the protein standards. The protein content of microvesicles released by 1×10^6 cells was subsequently calculated.

2.3.2 Electron microscopy

Microvesicles collected from nine 15 cm dishes of H1299 cells were re-suspended and fixed in 100 μ l of 2 % paraformaldehyde (Thermo Scientific Pierce). Subsequently 5 μ l of fixed microvesicles were adsorbed onto Formvar carbon coated EM grids overnight at 4 °C. Grids were washed with 100 μ l PBS and treated with 1 % glutaraldehyde (Sigma) solution for 5 minutes. This was followed by eight washes with distilled water. Microvesicles were visualised by negative staining, grids were incubated with uranyl oxalate (Polysciences) for 5 minutes and subsequently methyl cellulose-UA (Sigma) for 10 minutes at 4 °C. Air dried grids were imaged on the transmission electron microscope FEI Tecnai T20 running at 200 kV using Olympus Soft Imaging System software.

Alternatively if immuno-gold staining was required, adsorbed microvesicles were subject to four blocking washes with PBS/50 mM glycine (Sigma) after initial adsorption onto grids. A second blocking step was then carried out using PBS/5 % BSA (Sigma) for 10 minutes. Microvesicles were then exposed to CD63 primary antibody (Pelicluster, 1:200) or mouse IgG1 isotype control antibody (Pierce, 1:200) diluted in PBS/1 % BSA for 30 minutes. Grids were washed in PBS/0.1 % BSA six times for 5 minutes each. Grids were then incubated with anti-mouse 10 nm protein A-gold conjugate secondary antibodies (Cell Microscopy Centre) for 30 minutes before eight PBS washes. From this point onwards the fixation and negative staining protocol was performed as described above. (Preparation of microvesicles for electron microscopy and image acquisition was performed by Margaret Mullin, the University of Glasgow).

Acquired Images were analysed using ImageJ (National Institutes of Health) to determine the microvesicle size.

2.3.3 Nanoparticle tracking analysis

Nanoparticle tracking analysis was carried out using the NanoSight LM10 instrument according to manufacturer's instructions. Prepared microvesicles in 200 μ l of PBS were diluted 1:30 in filtered PBS before being introduced into the instrument for measurement. Three fields of view per sample were imaged and

tracked (over 1000 tracks were analysed per condition/per experiment to enable reliable analysis).

Nanoparticle tracking analysis uses information acquired from light scattering and Brownian motion to calculate particle size and concentration. Briefly a laser beam was passed through the sample chamber. Particles within the sample scattered light to a level that could be detected by a 20 times microscope objective. The camera took images at a rate of 30 frames per second and the software tracked and analysed the Brownian movement of each of the detected particles. A Stokes-Einstein equation was then used by the software to calculate particle size and concentration.

2.4 Cell phenotype assays

2.4.1 Proliferation

Cells were plated at a low density of 5000 cells/well in 24 well plates. Proliferation assays were performed over 4 days. Each day cells were trypsinised and counted using a CASYcounter. The medium was refreshed every second day so nutrients would always be available for cells to grow. Each experimental condition was counted in triplicate.

2.4.2 Wound healing migration assay

For wound healing assays, 6×10^5 H1299/A2780 cells were plated in 6 well plates and grown into a confluent monolayer over 24 hours. A wound was created using a p200 pipette tip, wounded cells were washed twice using warm DMEM. Once the plate had acclimatised to the microscope stage and temperatures, time-lapse microscopy acquired images of cells closing the wound every 10 minutes for 16 hours at 5 % CO₂ and 37 °C. Images were captured using a Nikon time-lapse Z6011, CoolSNAP HQ camera (photometrics) and metamorph software (molecular devices).

Data was then tracked and quantified using ImageJ to analyse single cell forward migration index which represents the ability of cells to migrate in a forward direction when closing the wound. Data sets were handled in Excel and analysed statistically using Prism.

2.4.3 Golgi-nucleus orientation Immunofluorescence

H1299 cells were treated with conditioned medium for 72 hours before 5×10^5 cells were plated onto glass bottomed MatTeck dishes. A wound was formed in the cell monolayer 24 hours later and cells were washed and medium refreshed using warm DMEM. Cells were left to recover and migrate for 2 hours before being fixed in 4 % paraformaldehyde in PBS for 10 minutes and permeabilised with 0.2 % triton-X100 (Sigma) in PBS for 10 minutes. Cells were washed twice with PBS and blocked using 1 % BSA in PBS.

The primary antibody GM130 (1:100, BD transduction lab) which labels the golgi was applied to cells in 1 % BSA/PBS for 1 hour. After 3 washes in PBS, the secondary goat anti mouse FITC antibody (1:100, Southern Biotech) and phalloidin (1:200 Life Technologies) was applied for 30 minutes in 1 % BSA/PBS. After 3 washes with PBS, soft set Vectashield with DAPI was used to mount samples.

Samples were then visualised by confocal microscopy using Olympus Fluoview FV1000. Ten images per condition were analysed for golgi orientation. Every cell in each of the images was scored according to whether the golgi was oriented in front, behind or to the side of the nucleus.

2.4.4 Inverted invasion assay

Invasion assays were carried out as previously described but with a few alterations (Hennigan et al., 1994, Caswell et al., 2008). Geltrex (reduced growth factor basement membrane matrix - Life Technologies) was diluted 1:1 in ice cold PBS and supplemented with 25 $\mu\text{g}/\text{ml}$ fibronectin (Sigma) and left to polymerise in a transwell chamber for 1 hour at 37 °C. The chambers were inverted and 4×10^4 cells were plated onto the bottom of the transwell membrane and left to attach for 3 hours. After two washes, the transwell chamber was placed in 1ml of serum free medium, whilst 100 μl of 10 % FCS DMEM supplemented with 10 ng/ml HGF (Sigma) was added to the top of the Geltrex plug.

Cells were allowed to invade along the chemotactic gradient for 72 hours before being stained with 4 $\mu\text{g}/\text{ml}$ calcein-AM (Life Technologies) for 1 hour. The

percentage of invading cells was then analysed by acquiring confocal images of the cells at 15 μm intervals through the plug starting from the transwell membrane. Images were acquired using the Olympus Fluoview FV1000 at 20 times magnification. ImageJ was used to quantify percentage of cells invading > 30 μm through the Geltrex plug by analysing total fluorescence intensity.

2.4.5 Recycling assay

2.4.5.1 Cell preparation

Before starting the recycling assay, H1299 p53^{-/-} cells were pre-treated with microvesicles from p53^{-/-} or p53^{R273H} cells for 72 hours and re-plated for a further 72 hours in DMEM until 80 % confluence was reached. Alternatively microvesicles were collected from p53^{R273H} siRNA treated cells, and used to pre-treat p53^{-/-} cells for 24 hours before the assay took place. For recycling assays investigating the effects of siRNA silencing of a protein, p53^{R273H} cells were transfected with the appropriate siRNA and allowed to grow for 24 hours to 80 % confluence before starting the assay. Internalisation of $\alpha 5\text{B1}$ integrin, c-met and EGFR was investigated using recycling ELISA assays previously described (Caswell et al., 2008, Roberts et al., 2001).

2.4.5.2 Internalisation

Medium was aspirated from plates and the plates were immediately transferred to ice. Cells were washed twice in ice cold PBS before incubating with 0.2 mg/ml NHS-SS-Biotin (Thermo Fisher Scientific) in PBS for 1 hour at 4 °C to label surface proteins. Labelled cells were washed in ice cold PBS and then incubated in DMEM for 30 minutes at 37 °C to enable internalisation of labelled proteins. Medium was aspirated and dishes were put back on ice and washed twice with ice cold PBS. Biotin was removed from remaining surface labelled proteins by incubating with 20 mM MesNa (20 mM sodium 2-mercaptoethanesulphonate (Sigma), 50 nM Tris (Melford), 100 nM NaCl (Fisher Scientific), pH 8.6.) for 15 minutes at 4 °C. Cells were then incubated with 20 mM iodoacetamide for 10 minutes, (Sigma) to quench the remaining MesNa.

2.4.5.3 Recycling

After the remaining biotin was removed from the cell surface and MesNa was quenched, internalised biotinylated receptor recycling back to the plasma membrane was chased by incubating cells at 37 °C for various time points up to 30 minutes. At each time point medium was removed and cells were put on ice, washed twice with ice cold PBS and biotin was removed from recycled biotinylated proteins at the cell surface using MesNa. Cells from each time point were then lysed using non-denaturing lysis buffer (Lysis buffer: 200 nM NaCl, 75 nM Tris, 15 mM NaF (Sigma), 1.5 mM Na₂VO₄ (Fisher Scientific), 7.5 mM EDTA (Sigma), 7.5 mM EGTA (Sigma), 1.5 % Triton X-100, 0.75 % NP40 (Sigma), 50 µg/ml leupeptin (Melford), 50 µg/ml aprotinin (Sigma), 1 mM 4-(2-aminoethyl)benzynesulphonyl fluoride - AESBF (Melford)). Lysates were homogenised using a 25-gauge needle and debris pelleted by centrifugation at 10,000 rpm for 10 minutes at 4 °C. The quantity of remaining biotinylated protein was then analysed by ELISA (enzyme-linked immunosorbent assay) capture of collected cell lysates.

2.4.5.4 ELISA

96 well plates (Maxisorp Life Technologies) were coated with antibody of interest by adding 50 µl 0.05 M Na₂CO₃ (Fisher Scientific), pH 9.6 plus 5 µg/ml antibody to each well and incubating overnight at 4 °C with constant rocking. Antibodies used included integrin α5, EGFR and cMET as detailed in Table 2-2. One hour before starting the assay each well was blocked with 50 µl 5 % BSA in PBS-T (PBS plus 0.05 % Tween 20 - Sigma) at 4 °C. After washing twice with PBS-T and removing as much liquid as possible, 50 µl of each cell lysate sample was added to the plate in triplicate to allow protein capture. The plate was incubated at 4 °C with constant rocking, overnight.

The next day the plate was washed 4 times with PBS-T to remove excess/unbound protein. Each well was incubated with 50 µl of the appropriate species of HRP secondary antibody conjugated with streptavidin (GE healthcare) in 1 % BSA PBS-T for 1 hour at 4 °C, with constant rocking. Four PBS-T washes followed and residual liquid was removed. Each well was then exposed to ortho-phenylenediamine (0.56 mg/ml ortho-phenylenediamine (Sigma), 25.4 mM

Na₂HPO₄ (Fisher Scientific), 12.3 mM citric acid (Sigma), pH 5.4 with 0.003% H₂O₂ (Sigma)) for 10 minutes at room temperature before the absorbance of each well was quantified using a plate reader at wave length 490 nm. Recycling assays done by Jim Norman, the Beatson Institute for Cancer Research.

2.5 Screens

2.5.1 SILAC mass spectrometry of microvesicles

H1299 cells were cultured in SILAC (Single Isotope Labelling by Amino acids in Culture) medium (Life Technologies) with 10 % 10 kDa cut off dialysed FBS (Life Technologies), 1 mM L-glutamine, 100 µg/ml streptomycin, 100 U/ml penicillin and 1:1000 amino acid isotopes (heavy: lysine⁸, argenine¹⁰ or medium: lysine⁴, argenine⁶ - Cambridge Isotope Labs). The following experiments were set up, the forward experiment consisted of p53^{-/-} cells labelled with medium amino acid isotopes and p53^{R273H} cells labelled with heavy amino acid isotopes and the reverse experiment consisted of p53^{-/-} cells labelled with heavy amino acid isotopes and p53^{R273H} cells labelled with medium amino acid isotopes. Once amino acid isotopes were fully incorporated, p53^{-/-} and p53^{R273H} cells (both heavy and light) were plated for microvesicle isolation. Conditioned medium from each condition of the forward and the reverse experiment was collected and mixed together (eg p53^{-/-} medium and p53^{R273H} heavy) at the very beginning of microvesicle collection protocol to minimise any variation between the conditions during collection. Microvesicles were prepared as previously described (section 2.2.2.1) and the final pellet was re-suspended in 6M urea for mass spectrometry analysis. During mass spectrometry analysis, proteins detected in microvesicles from p53^{-/-} cells and p53^{R273H} expressing cells could be distinguished from one another in the sample due to the different amino acid isotope labelling.

In preparation for mass spectrometry, microvesicle proteins were reduced (10 mM dithiothreitol), alkylated (55 mM iodoacetamide) and digested (Lys C and trypsin). Peptides were cleaned using stage tips and re-dissolved in 5 % acetonitrile/0.25 % formic acid. Protein samples were then used directly on the Orbitrap Elite (LC-MS). Data was searched and quantified against Swissprot (Human) database using MaxQuant software. All mass spectrometry experiments

were performed in collaboration with David Sumpton, The Beatson Institute for Cancer Research.

2.5.2 Lipidomic analysis of microvesicles

Microvesicles were collected from p53^{-/-} and p53^{R273H} cells, re-suspended in 100 µl PBS and then frozen before undergoing lipidomic analysis. All lipidomic analyses were performed in the lab of Phil Whitfield, University of Highlands and Islands, using their standard protocols below.

2.5.2.1 Lipid extraction

Microvesicles were suspended in 100µL PBS. The lipids were then extracted according to the Folch method (Folch et al., 1957). Briefly microvesicles were mixed with 3 mL chloroform/methanol (2/1, v/v). The mixture was incubated at room temperature for 1 h. The samples were partitioned by the addition of 670 µL of 0.1 M KCl and the mixture centrifuged to facilitate phase separation. The lower chloroform layer was evaporated to dryness under nitrogen gas and reconstituted in 160 µL methanol containing 5 mM ammonium formate. (All solvents were of HPLC grade and were purchased from Thermo-Fisher Scientific).

2.5.2.2 Liquid-chromatography-mass spectrometry

The lipids were analysed by liquid chromatography-mass spectrometry (LC-MS). All analyses were performed using a Thermo Exactive Orbitrap mass spectrometer (Thermo Scientific). All samples were analysed in both positive and negative ion mode.

2.5.2.3 Data processing and multivariate statistical analysis

The raw LC-MS data were processed with Progenesis CoMet software (Non-linear Dynamics) and searched against LIPID MAPS (www.lipidmaps.org) for identification. The processed data were Pareto scaled and subjected to principal component analysis (PCA) using SIMCA-P v13.0 (Umetrics).

2.5.3 Next generation sequencing

Cells null for p53 were treated with microvesicles collected from p53^{-/-} and p53^{R273H} expressing cells for 72 hours. Pre-treated cells were then re-plated in DMEM to grow to confluence in a 6 well plate.

2.5.3.1 RNA harvesting

RNA was harvested using RNAeasy kit (Qiagen) according to manufacturer's instructions. Collected RNA was re-suspended in 30 µl RNase free water and quantified using the nanodrop. The RNA was checked for quality and degradation using the nano Agilent chip bioanalysis, according to manufacturer's instructions.

2.5.3.2 cDNA library generation

RNA (4 µg) was used to create cDNA libraries using the TruSeq RNA sample Prep Kit, v.0 (Illumina) by Billy Clarke, Beatson Institute for Cancer Research. This protocol was previously described (Fisher et al., 2011). Briefly RNA was purified and fragmented to allow first strand cDNA synthesis to take place using random primers and reverse transcriptase. The second strand synthesis replaced remaining RNA strand with a cDNA strand creating double stranded DNA. The overhangs from fragmentation process were repaired before the 3' end was adenylated to prevent ligation of fragments. Adaptors for hybridisation onto the sequencing flow cell were ligated to the ends of each fragment before PCR amplification was used to amplify each fragment with their adaptors. The Library was finally validated by Agilent DNA 1000 before being normalised and pooled ready for cluster generation and sequencing.

2.5.3.3 Sequencing

The library cDNA fragments were loaded into a flow cell and captured by oligos complimentary to the adaptors ligated to cDNA fragments. Cluster generation of library samples took place on the C-bot, generating around 1000 identical copies of each cDNA fragment by bridge amplification. After annealing of the sequencing primers to the DNA, the sequencing protocol then took place using the Genome Analyser 11x. Sequencing reagents and fluorescent nucleotides

began the addition of nucleotides to each DNA molecule, and after each nucleotide addition the flow cell was imaged so the base added could be identified. The sequencing settings used were 2x36 cycles, single index, paired end and this was done by Billy Clarke, Beatson Institute for Cancer Research. Real time analysis of sequencing was done by the machine software before the data was then used for bioinformatics analysis.

2.5.3.4 Data analysis

Quality control of the raw RNASeq data files was performed by fastqc and reads were aligned to the human genome (GRCh37) using TopHat2. Resulting bam files were processed with easyRNASeq package in R. The final counts were normalised and analysed with DESeq. Statistically significant differences in gene expression were determined with a false discovery rate of 5% or 10%. This was carried out in collaboration with Gabriela Kalna, Beatson Institute for Cancer Research.

2.6 Quantitative PCR

Rab27b knockdown was analysed using quantitative PCR due to the lack of an effective antibody for Western blotting.

2.6.1 RNA isolation

RNA was isolated from a confluent 6 well plate at 24, 48 and 72 hours after transfection with si-Rab27b or control si-nt. Cells were washed twice with PBS and put on ice before commencing RNA extraction using RNeasy spin columns according to manufacturer's instructions. The concentration of RNA collected was quantified using 2 µl on the nanodrop machine.

2.6.2 cDNA synthesis

1 µg RNA was used to synthesise cDNA using the Promega Reverse Transcription system following manufacturer's instructions. Briefly 1 µg RNA was mixed with 0.5 µg oligo-DT and made up to a total volume of 10 µl with water. Samples were heated to 70 °C for 5 minutes before being chilled to 4 °C. At which point 10 µl of a master mix containing (1 µl ImPromII reverse transcriptase, 5 times

reaction buffer, 20 U RNasin, 0.5 mM each dNTP, 25 mM MgCl) was added to each tube and samples were subjected to a reverse transcription cycle of: annealing 25 °C for 5 minutes, extension 42 °C for 60 minutes and inactivation 70 °C for 5 minutes. The resultant cDNA was stored at - 20 °C or used immediately in further experimentation.

2.6.3 Quantitative PCR

1 µl of synthesised cDNA in 7 µl H₂O was then used in a quantitative PCR (qPCR) reaction with 10 µl PerfeCTa SYBR green master mix (Quanta bioscience) and 2 µl QuantiTect primers (Qiagen) for Rab27b or GAPDH (housekeeping gene), according to manufacturer's instructions. Samples were loaded into a Biorad 96 well plate in triplicate. Quantitative PCR was run on the Biorad C1000 thermal cycler. DNA was denatured at 95 °C for 5 minutes. Then the cycle of denaturation at 95 °C for 30 seconds, annealing at 60 °C for 30 seconds and extension at 72 °C for 30 seconds was repeated 40 times before the final extension time of 5 minutes at 72 °C.

Data was analysed using Biorad software using CT cycle values. Rab27b levels were normalised to GAPDH levels and the fold change of Rab27b cycle number in si-nt (control) versus si-Rab27b conditions was calculated.

2.7 Western blotting and antibodies

2.7.1 Cell lysis

Medium was aspirated from plates and cells were put on ice. Cells were washed twice with ice cold PBS before being exposed to 50 mM tris/1 % SDS lysis buffer. Cells were scraped and homogenised using Qia-shredder columns (Qiagen). Cell lysate was then mixed with 4 times loading SDS buffer (NuPage, Life Technologies) and boiled for 5 minutes at 95 °C. Samples were centrifuged at 10,000 rpm for one minute and loaded onto gel.

2.7.2 Microvesicle preparation

Microvesicles in PBS were mixed with 4 times SDS loading buffer and boiled for 5 minutes at 95 °C. After a final centrifugation samples were ready to load.

2.7.3 Western blotting

To resolve proteins by size, NuPage pre-cast SDS (sodium dodecyl sulphate-polyacrylamide) gels were used (Life Technologies). Samples were loaded onto NuPage pre-cast gradient gels (4 - 12 %) (Life Technologies) alongside a protein standard (Biorad). Gels were ran using NuPage MOPS running buffer and under non-reducing conditions (essential for some antibodies used in this study) at 100 V for 2 hours.

Proteins were transferred from the gel onto methanol activated PVDF membrane (Millipore) in NuPage transfer buffer (Life Technologies) at 30 V for 90 minutes. The membrane was blocked in 5 % Milk (Marvel) or 3 % BSA in TBS-T (10 mM Tris-HCl (pH7.4), 150 mM NaCl, 0.1 % Tween-20) for one hour at room temperature under agitation. The antibody of interest (see Table 2-2 for details) was then applied to the membrane in 1 % milk/BSA in TBS-T overnight at 4 °C.

Membranes were washed with TBS-T three times (10 minutes each) before secondary Licor infra-red fluorescent antibodies of the appropriate species (1:10000) were applied for 30 minutes, at room temperature (antibodies detailed in table 2-2). Three more TBS-T washes were carried out followed by a distilled water wash before the Licor Odyssey system was used to expose the blots and visualise protein bands.

2.8 Immunoprecipitation

H1299 cells were lysed in non-denaturing lysis buffer (recipe in section 2.4.5.3). The H1299 lysates were passed through a 27-gauge needle three times before being clarified by centrifugation at 10,000 x g for 10 minutes at 4 °C. Magnetic beads conjugated to sheep anti-mouse IgG (Dynabeads, Life Technologies) were bound to anti-GFP antibody (Abcam). GFP-Antibody coated beads were then incubated with lysates for 2 hours at 4 °C whilst being subjected to constant rotation. Washing of the beads in lysis buffer removed any unbound proteins, so that specifically associated proteins could be eluted from the beads by boiling for 10 minutes in sample buffer (Sigma). Proteins were resolved by SDS-PAGE and analysed by Western blotting. The immunoprecipitation (IP) method was adapted from (Rainero et al., 2012). Antibodies that were used in the

immunoprecipitation (mouse anti-GFP) and used for Western blotting (rabbit anti-GFP and anti-Podocalyxin) are shown in table 2-2.

2.8.1 Antibodies

Antibody (species)	Company	Dilution (use)
CD63 (mouse)	Pelicluster	1:1000 (WB)
p53 (mouse)	*DO-1 antibody	1:10,000 (WB)
TSG101 (rabbit)	GeneTex	1:1000 (WB)
HSPA8 (rabbit)	Cell Signalling	1:1000 (WB)
Integrin B1 (mouse)	BD Pharmingen	1:2000 (WB)
Rab35 (rabbit)	Cell Signalling	1:100 (WB)
Rab27a (mouse)	Abcam	1:1000 (WB)
DGK α Rabbit)	Proteintech	1:500 (WB)
RCP (rabbit)	In house antibody RCP ³⁷⁹⁻⁶⁴⁹	1:1000 (WB)
Podocalyxin (rabbit)	Abcam	1:1000 (WB)
cMET (goat)	R+D systems	1:100/5 μ g/ml (WB/ELISA)
β -actin (mouse)	Sigma	1:10,000 (WB)
EGFR (rabbit)	BD Pharmingen	5 μ g/ml (ELISA)
Integrin α 5 (mouse)	BD Pharmingen	5 μ g/ml (ELISA)
GFP (mouse)	Abcam	1:1000 (IP)
GFP (mouse)	Abcam	1:10,000 (WB)
IR Dye 680 (anti mouse)	Licor	1:10,000 (WB)
IR Dye 680 (anti rabbit)	Licor	1:10,000 (WB)
IR Dye 680 (anti goat)	Licor	1:10,000 (WB)
IR Dye 800 (anti mouse)	Licor	1:10,000 (WB)
IR Dye 800 (anti rabbit)	Licor	1:10,000 (WB)
IR Dye 800 (anti goat)	Licor	1:10,000 (WB)

Table 2-2: Antibodies used in Western blotting, ELISA and IP.

*The p53 antibody has been described previously (Vojtesek et al., 1992).

2.9 Statistics

All statistical analyses were performed using Prism. I did not test if the data was normally distributed therefore the following statistical tests were used. The non-parametric Mann-Whitney test was used to analyse data sets of two conditions. For data sets with multiple conditions the non-parametric Kruskal Wallis test was used to compare all conditions with one another. Finally for data sets with two conditions but multiple time points, a two-way ANOVA statistical test was used.

3 Microvesicle characterisation

3.1 Introduction

3.1.1 Microvesicles

Microvesicles are lipid enclosed vesicles that contain many cellular components including protein, lipid, DNA, mRNA and miRNA. They are released from the cell into the extracellular environment in two main ways; either by budding off the plasma membrane (plasma membrane-shed microvesicles), or by being released from the cell following their prior formation in multivesicular bodies (MVB) within the endosomal system (MVB-derived exosomes) (Raposo and Stoorvogel, 2013, Colombo et al., 2014).

Plasma membrane-shed microvesicles (typically >100 nm in diameter) bud directly from the plasma membrane, a process that is dependent upon cytoskeleton regulation, lipid signalling, Rab-GTPase proteins or ESCRT machinery (Booth et al., 2006, Muralidharan-Chari et al., 2009, Trajkovic et al., 2008, Wang et al., 2014, Bianco et al., 2009). Alternatively, MVB-derived exosomes are formed in late endosomes which mature into multivesicular bodies (MVB) by inward budding of the endosome's limiting membrane to form intraluminal vesicles (ILVs) (Futter et al., 2001). This is often an ESCRT and/or ceramide-dependent process (Trajkovic et al., 2008, Colombo et al., 2014). MVBs are then transported to and dock with the plasma membrane, a process which is dependent upon Rab-GTPase proteins such as Rab27a, Rab27b, Rab35 and Rab11, and SNARE proteins such as VAMP7 (Hsu et al., 2010, Savina et al., 2002, Ostrowski et al., 2010, Fader et al., 2009). Fusion of MVBs with the plasma membrane allows the release of ILVs into the extracellular environment as MVB-derived exosomes (<100 nm in diameter). These processes are discussed in greater detail in chapter 1. The characteristics of MVB-derived exosomes and plasma membrane-shed microvesicles are summarised in table 3-1 and diagrammatically reviewed in figure 3-1. We will subsequently, collectively refer to MVB-derived exosomes and plasma membrane-shed microvesicles as microvesicles, unless stated otherwise.

	MVB-derived exosomes	Plasma membrane-shed microvesicles
Site of origin and release	MVB exocytosis	Plasma membrane budding
Composition	Protein, lipid and nucleic acids	Protein, lipid and nucleic acids
Size	<100 nm	>100 nm
Mechanism of biogenesis	ESCRT, ceramide, tetraspanin	Cytoskeletal regulation, lipid signalling, Rab-GTPase, ESCRT
Mechanism of release	Rab-GTPase, SNARE	

Table 3-1: Summary of MVB-derived exosome and plasma membrane-shed microvesicle characteristics.

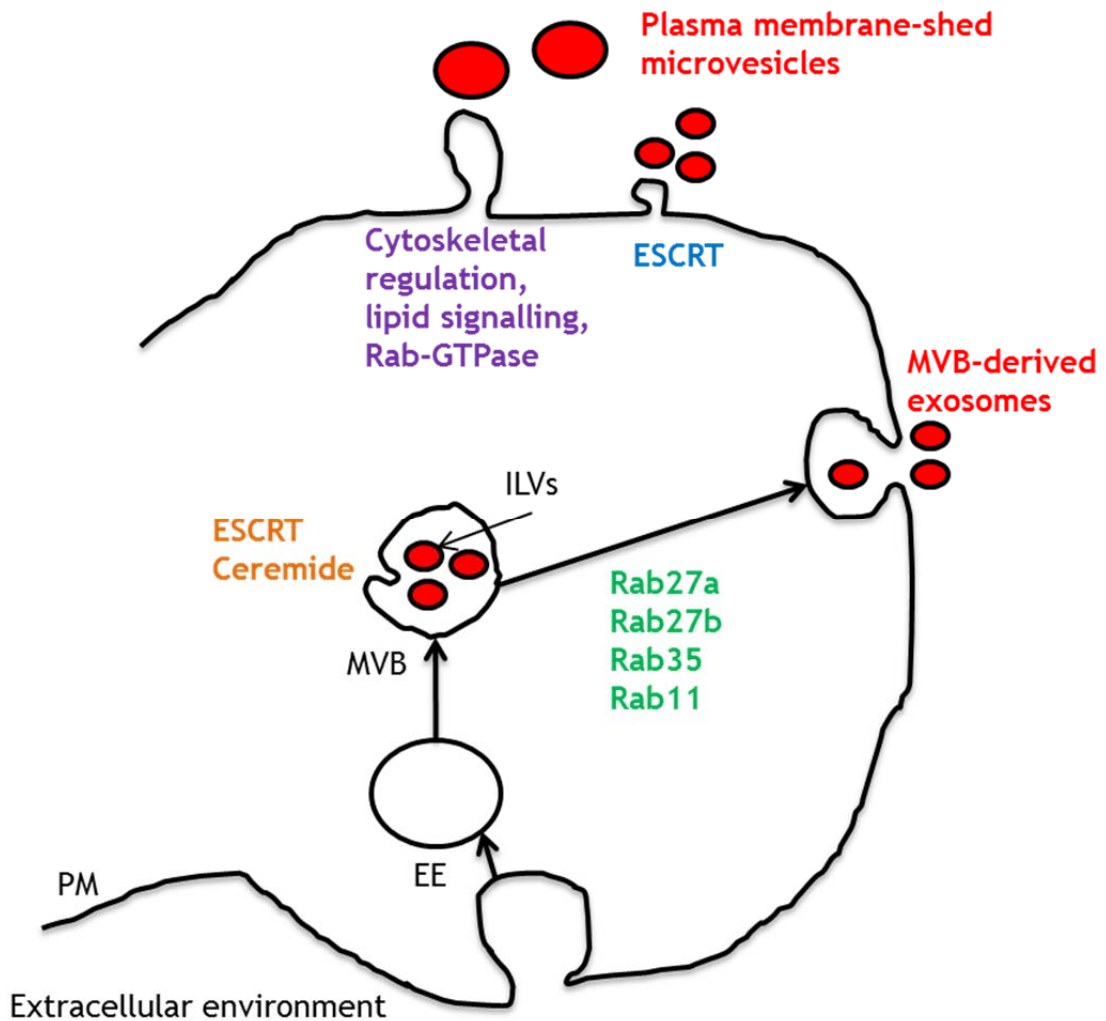


Figure 3-1: Diagram of microvesicle formation and release.

EE – early endosome. MVB – multivesicular body. ILVs – intra luminal vesicles. PM – plasma membrane. Early endosomes mature into MVBs upon ESCRT/ceramide mediated inward budding of the endosome limiting membrane forming ILVs. MVBs are then transported to the plasma membrane in a Rab-GTPase dependent manner where fusion allows ILVs to be released into the extracellular environment as MVB-derived exosomes. Alternatively plasma membrane-shed microvesicles bud directly from the plasma membrane. This process can be driven by ESCRT components, cytoskeletal regulation, lipid signalling and Rab-GTPases.

3.1.2 Characterisation of microvesicles

When investigating microvesicles, it is very important to perform thorough and comprehensive characterisation of their physical characteristics. A report published from the International Society for Extracellular Vesicles described the steps an investigator should take to characterise microvesicles (Lotvall et al., 2014). Briefly, microvesicle protein components should be characterised by Western blot and mass spectrometry to identify the presence of microvesicle markers (table 3-2). Additionally, isolated microvesicles should be characterised by both electron microscopy and nanoparticle tracking analysis (or other related

methods, such as atomic force microscopy, dynamic light scattering and resistive pulse sensing) to identify that a pure preparation of microvesicles is being collected and so their size can be quantified. Finally experiments should be well-controlled to eliminate any potential consequences of the isolation of serum microvesicles.

	Transmembrane and lipid bound proteins	Cytosolic proteins	Intracellular proteins	Extracellular proteins
What protein presence indicates	Membrane present	Proteins with membrane or receptor binding capacity	Proteins from other cell compartments	Proteins bind to microvesicle membrane and co-isolate during centrifugation
Status	Present in MVB-derived exosomes and plasma membrane-shed microvesicles	Present in MVB-derived exosomes and plasma membrane-shed microvesicles	Lower presence in MVB-derived exosomes. More likely to be found in plasma membrane-shed microvesicles	Variable
Examples	Tetraspanin, integrin, growth factor receptor	Endosomal proteins, membrane binding proteins (ESCRT/Rabs)	ER, Golgi, mitochondria and nucleus associated proteins	Albumin, growth factors, ECM components, MMPs

Table 3-2: Protein categories expected to be present in MVB-derived exosomes and plasma membrane-shed microvesicles.

Adapted from (Lotvall et al., 2014).

These characterisation strategies are useful for determining that microvesicle preparations are free from larger membrane fragments, blebs and cell debris. However, it is not possible to determine the origin of microvesicles (i.e. whether they are generated by plasma membrane-shedding or via intraluminal budding within MVBs) by measuring their size. Indeed, although plasma membrane-shed microvesicles are generally accepted to be bigger than MVB-derived exosomes, the involvement of the ESCRT complex in plasma membrane-shedding indicates the possibility that these latter structures may be somewhat smaller than 100 nm (Booth et al., 2006). Moreover, although analysing protein constituents commonly found in microvesicles may give more confidence in the purity of the

microvesicle isolation, the cell compartment of origin still cannot be extrapolated from these data as most microvesicle markers are common to more than one microvesicle type. Therefore, one must conclude that, although a stringent microvesicle characterisation regimen will provide information as to the complexity and purity of the preparations used for experimentation (and thus lend transparency to the published work), these procedures will not inform meaningfully as to the provenance of the microvesicles in question, nor the cellular processes that lead to their generation. Therefore, the main purpose of the microvesicle characterisation that is carried out in this study is to ensure that our preparations are largely free from contaminants such as cell debris and apoptotic blebs, and to determine whether mutant p53 has the ability to influence the size distribution and constitution of released microvesicles.

3.2 Aims

As discussed in chapter 1 the field of microvesicle biology is an up-and-coming area of cancer research due to the important role of microvesicles in cell communication, and their utility in diagnostic biomarker discovery. Studies have identified that oncogene-expressing cancer cells release microvesicles that transfer certain oncoproteins (KRAS/EGFRvIII) and their interactors to neighbouring cells. These cancer cell-derived microvesicles can change the phenotype of the recipient cells to promote cancer progression (Al-Nedawi et al., 2008, Demory Beckler et al., 2013). Our research focuses on the oncogene mutant p53 control of integrin and receptor tyrosine kinase trafficking, and the consequent regulation of invasive cell migration. The role of mutant p53 in microvesicle biology has not yet been investigated despite the important role the oncogene has in over 50 % of cancer cases (Vogelstein et al., 2000). Therefore our interest became focused around mutant p53 and any potential role it has in microvesicle release, content and function.

Microvesicle collection from non-small cell lung carcinoma H1299 cells either null for p53^{-/-} or expressing mutant p53^{R273H} was optimised. The effect of p53^{R273H} expression on microvesicle quantity, size (using electron microscopy and nanoparticle tracking analysis) and content (using proteomics and lipidomics), enabled both analysis of the microvesicle preparation purity, and observation of any effect mutant p53 expression may have upon microvesicle content.

3.3 Results

3.3.1 Microvesicle isolation optimisation

Initially we optimised the collection of microvesicles from H1299 cells, a human non-small cell lung carcinoma cell line, which are null for p53^{-/-} or that have been engineered to express mutant p53^{R273H}. A previously-published method was used to collect microvesicles by differential centrifugation and to purify them further using a sucrose density gradient as described in chapter 2 (section 2.2.2) and diagrammatically reviewed in figure 3-2 (They et al., 2006a).

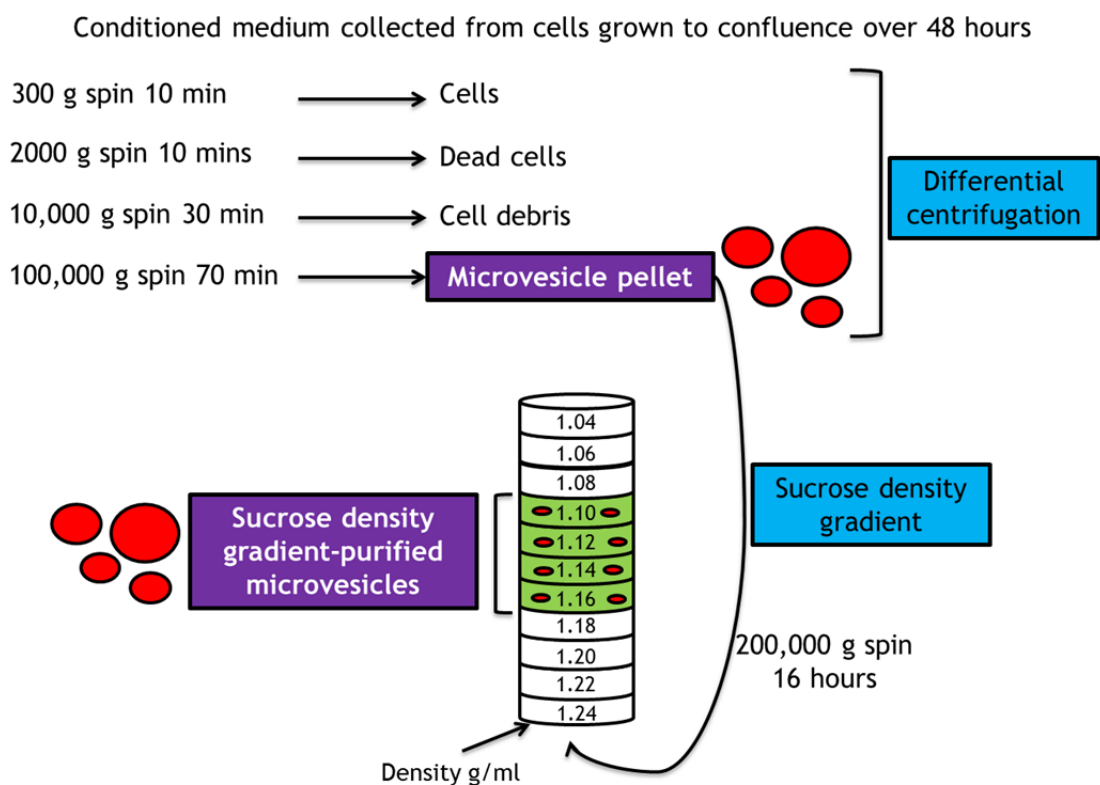


Figure 3-2: Diagram depicting the protocol used for the isolation of microvesicles by differential centrifugation and further purification by a sucrose density gradient.

H1299 cells null for p53^{-/-} or expressing mutant p53^{R273H} were grown to confluence over 48 hours in microvesicle depleted DMEM. Conditioned medium was collected and subjected to centrifugation to remove live cells (300 g), dead cells (2000 g) and finally to remove cell debris and larger lipid membrane fragments (10,000 g). Microvesicles were then pelleted using a 100,000 g centrifugation in a SW32 rotor. The pellet was washed in PBS before a final pelleting centrifugation at 100,000 g, after which microvesicles were re-suspended in a small volume of PBS. Microvesicles were mixed with 1 ml of a 2.5 M solution of sucrose at the bottom of a 12 ml centrifugation tube. Eleven layers of sucrose decreasing in concentration were added to the top of the microvesicle layer (from 2 M to 0.4 M sucrose using 20 mM HEPES as the diluent). The gradient was spun at 200,000 g overnight using an SW40 rotor. Microvesicles floated to a specific density within the gradient dependent upon microvesicle density. Microvesicles were collected from each gradient fraction by a final centrifugation in PBS at 100,000 g.

3.3.1.1 Differential centrifugation

Medium conditioned over 48 hours by H1299 p53^{-/-} and p53^{R273H} cells was collected and depleted of dead cells and cell debris by a series of centrifugation steps conducted at 300 g, 2000 g and 10,000 g. Following this, microvesicles were pelleted by centrifugation at 100,000 g. The expression of p53^{R273H} did not affect the protein content of the microvesicle pellet collected from H1299 cells (figure 3-3).

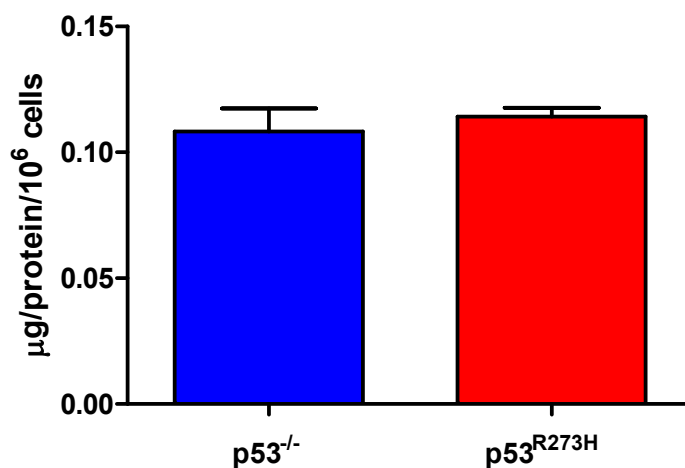


Figure 3-3: The protein content of microvesicles collected by differential centrifugation from H1299-p53^{-/-} or H1299-p53^{R273H} cells is not different.

Microvesicles were pelleted from approximately 7×10^7 H1299 p53^{-/-} and p53^{R273H} cells by differential centrifugation and re-suspended in 200 µl PBS. Subsequently the protein content of the microvesicle pellet was analysed using a Qubit protein assay (Life Technologies) according to manufacturer's instructions. The protein concentration of microvesicles released per 1×10^6 cells was calculated. n=6. Values are mean \pm SEM.

To determine whether p53^{R273H} expression affects the microvesicle constitution, the abundance of several microvesicle markers was determined by Western blotting. Figure 3-4 (A) shows that microvesicle markers CD63, HSPA8 and TSG101 were present in equal quantities in microvesicles released from H1299-p53^{-/-} and H1299-p53^{R273H} cells. We tried to identify other markers such as CD9 and CD81 within the microvesicle pellet; however they were not present in sufficient quantities to be detectable (data not shown). Importantly, there were no microvesicle markers present in the medium-only control condition. This suggested that the differential centrifugation approach yielded a preparation of H1299 microvesicles that was effectively free of serum microvesicle contaminants.

It was next essential to investigate whether mutant p53 or any of its effectors such as RCP, DGK α , cMET and β 1 integrin were detectable in microvesicles released by H1299-p53^{R273H} cells (Rainero et al., 2012, Muller et al., 2013, Muller et al., 2009). Integrin β 1 was present in equal quantities in microvesicles collected from p53^{-/-} or p53^{R273H} cells. However p53^{R273H}, RCP, cMET and DGK α were not detectable in microvesicles from either H1299-p53^{-/-} or p53^{R273H}-expressing H1299 cells (figure 3-4 A + B). Finally as part of the preliminary study of microvesicle constituents, the presence of Rab27a and Rab35 (mediators of microvesicle release) in the microvesicle pellet was determined (Hsu et al., 2010, Ostrowski et al., 2010). Even though Rab27a and Rab35 were equally expressed in H1299-p53^{-/-} and H1299-p53^{R273H} cells, neither of these proteins were detected in microvesicles released from these cells (figure 3-4 B).

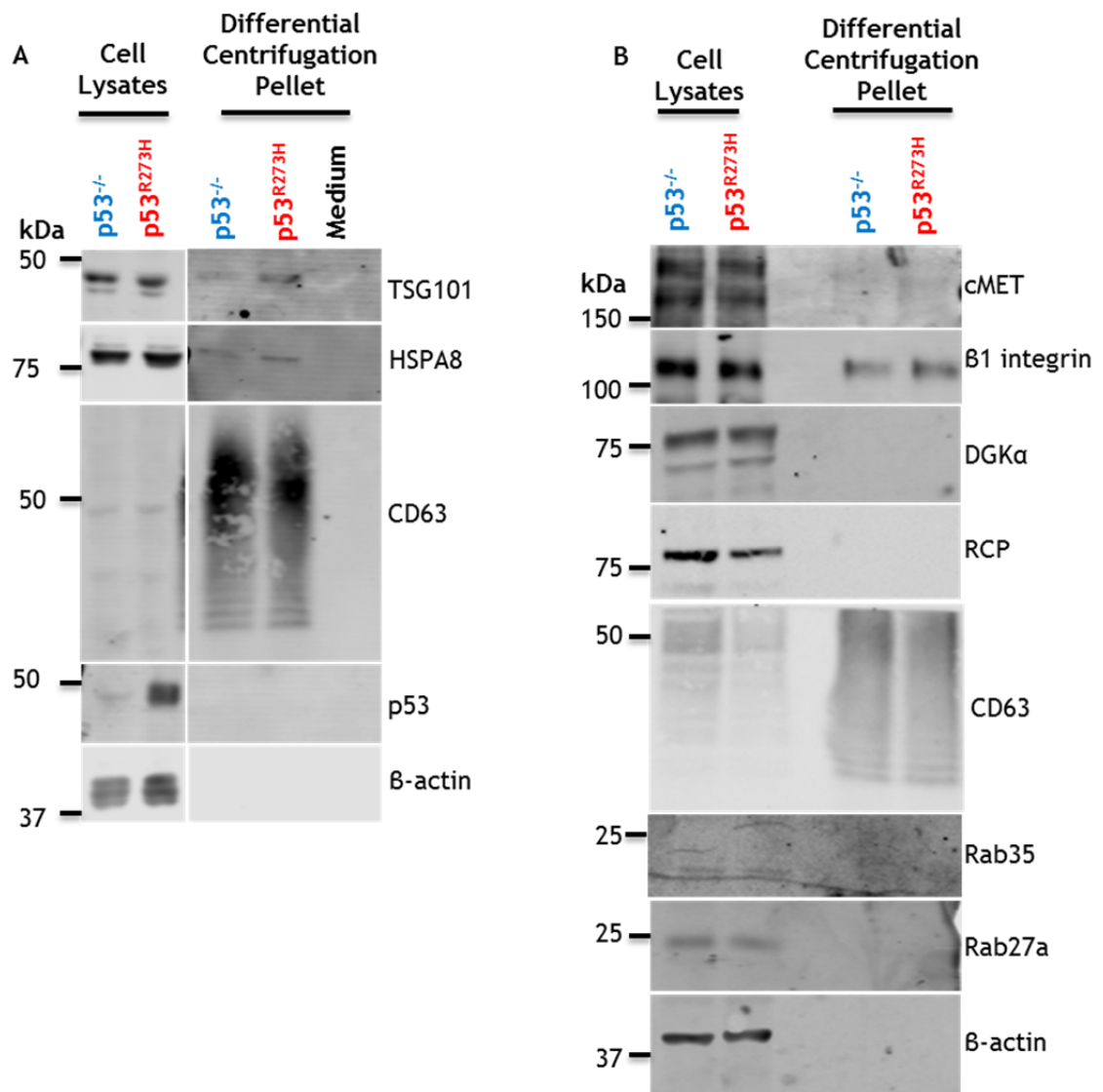


Figure 3-4: Western blot characterisation shows that there are no distinct differences in microvesicle marker or mutant p53 content in microvesicles derived from H1299 p53^{-/-} and H1299-p53^{R273H} cells.

Cell lysates and microvesicles were collected from H1299 p53^{-/-} and p53^{R273H} expressing cells and prepared for Western blot analysis. Cell lysates were harvested in 1 % SDS/50 mM Tris lysis buffer and microvesicles in PBS. Both cell lysates and microvesicles were further lysed in 4x SDS loading buffer before being boiled at 95 °C for 5 minutes. Samples were loaded and ran on pre-cast 4 – 12 % gradient gels under non-reducing conditions (essential for detection of CD63 with this antibody). Blots were probed for microvesicle markers (A) and proteins involved in the mutant p53 gain-of-function invasive phenotype (B). n=3.

3.3.1.2 Sucrose density gradient purification

As protein aggregates and other membrane fragments can co-sediment with microvesicles during a 100,000 g centrifugation, we further purified the 100,000 g differential centrifugation microvesicle pellet using sucrose density gradient flotation. Microvesicles float in the gradient in a way that is dictated by their density, whereas protein aggregates sediment through sucrose (Colombo et al., 2014, Raposo et al., 1996). Analysis of CD63-positive microvesicle

distribution across a sucrose gradient enabled investigation of whether there were specific sub-populations of microvesicles being released by H1299-p53^{R273H} cells that were distinguishable from those released from H1299-p53^{-/-} cells (figure 3-5).

Sucrose density gradient centrifugation indicated that there was no reproducible difference in the density distribution of the CD63 positive microvesicle populations isolated from H1299-p53^{-/-} cells and H1299-p53^{R273H}-expressing cells. Finally it became apparent that the sucrose density gradient method, lead to a significant loss of material making further experimentation difficult. Therefore we used differential centrifugation microvesicle pellets for future characterisation and experimentation.

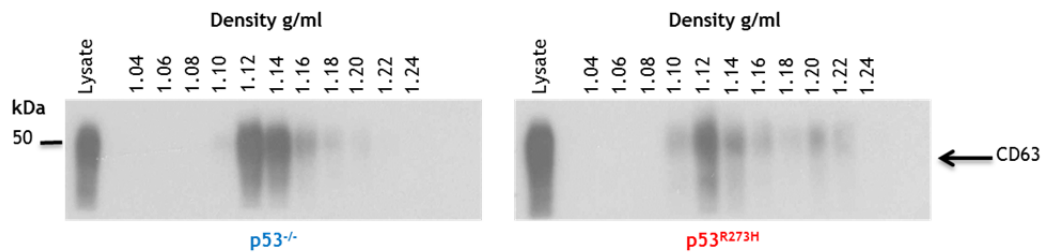


Figure 3-5: The distribution of CD63-positive microvesicles from H1299-p53^{-/-} and H1299-p53^{R273H}-expressing cells on a sucrose gradient.

Microvesicles were collected from H1299-p53^{-/-} and p53^{R273H}-expressing cells by differential centrifugation. The microvesicle pellet was re-suspended in 1ml of 2.5 M sucrose. This was put into the bottom of a 12 ml Beckman polyallomer centrifuge tube and 11 layers of sucrose decreasing in concentration to 0.4 M (diluent = 20 nM Tris) was carefully added onto the top of the microvesicle layer. The gradient was subject to a 200,000 g centrifugation for 16 hours before gradient fractions were collected, diluted in PBS and pelleted by a final 100,000 g centrifugation. Each fraction was re-suspended in a small volume of PBS before being ran on a gel for Western blot analysis under non-reducing conditions, probing for CD63. n=5.

3.3.1.3 Electron microscopy

To determine the purity and the size distribution of microvesicles collected from p53^{-/-} and p53^{R273H}-expressing H1299 cells, conditioned medium from each cell type was subjected to differential centrifugation and the resulting microvesicle pellet was then analysed using transmission electron microscopy. Figure 3-6 shows representative images of microvesicles that were fixed and subjected to negative staining (A) as well as immuno-gold staining for CD63 (D). Upon visualisation cup-shaped microvesicles were present, and preparations were free of larger membrane fragments. CD63 was also present on microvesicles, further supporting successful isolation.

As shown in figure 3-6 (A and B) there was a large variation in the size distribution of microvesicles (30-500 nm) which suggested that the differential centrifugation pellet was a mixture of plasma membrane-shed microvesicles (>100 nm) and MVB-derived exosomes (<100 nm). Despite this variation, the average size of microvesicles released from p53^{-/-} and p53^{R273H}-expressing cells was 253 nm and 218 nm respectively, indicating that p53^{R273H}-expressing H1299 cells release microvesicles of a significantly smaller size than H1299-p53^{-/-} cells. Indeed, size distribution analysis indicated that expression of p53^{R273H} selectively promoted release of a population of microvesicles that were less than 50 nm in diameter (figure 3-6 C).

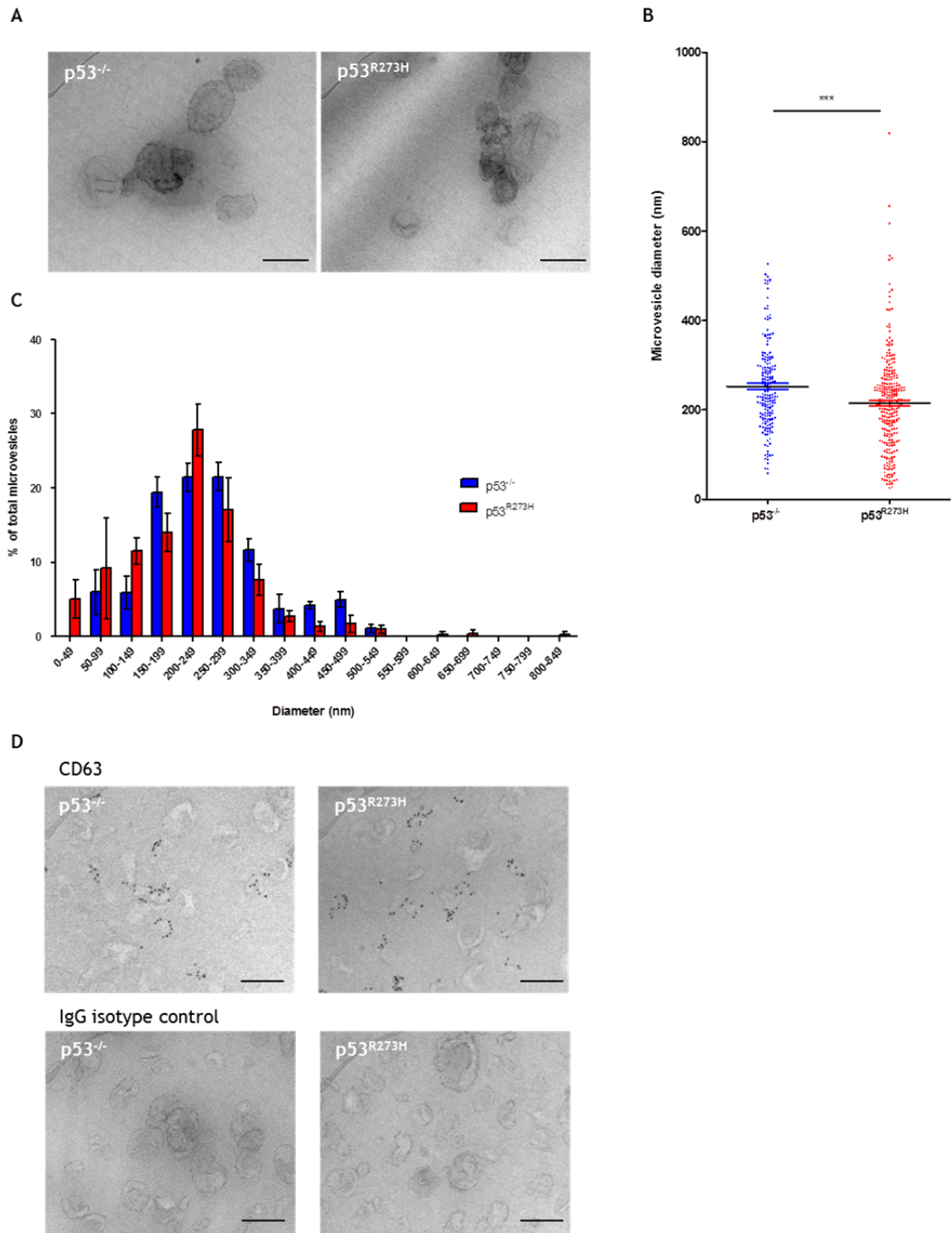


Figure 3-6: Transmission electron microscopy analysis of microvesicles.

(A) Microvesicles were collected from H1299-p53^{-/-} and H1299-p53^{R273H}-expressing cells by differential centrifugation. The microvesicle pellet was fixed in 2 % paraformaldehyde, adsorbed onto formvar electron microscopy grids and subsequently negatively stained with uranyl oxalate and methyl cellulose. Transmission electron microscope FEI Tecnai T20 was used to acquire images running at 200 Kv. Scale bars 200 nm. (B & C) ImageJ was used to measure the diameter of each microvesicle in acquired images. Data was used to plot the size distribution of measured microvesicles. n=3. Values are mean \pm SEM. Mann-Whitney. ***p<0.0001. (D) After microvesicle fixation and adsorption onto the grid, microvesicles were incubated with anti-CD63 antibody or IgG isotype control followed by a 10 nm gold particle secondary, before the negative staining protocol was carried out. Scale bars 200 nm. n=3. Data was acquired in collaboration with Margaret Mullin, electron microscopy department, University of Glasgow.

3.3.1.4 Nanoparticle tracking

The NanoSight LM10 was used to carry out Nanoparticle tracking analysis of microvesicles released from p53^{-/-} or p53^{R273H}-expressing H1299 cells.

Nanoparticle tracking analysis is described in detail in the chapter 2. Briefly the technology uses light scattering (from a laser passing through an optical prism into the microvesicle sample) and the Brownian motion of particles, to measure the concentration and size of microvesicles within a fluidic sample. Figure 3-7 (A) shows a representative image of the particles detected in the microvesicle pellet by this technique. Upon analysis on the NanoSight we found that microvesicles from H1299-p53^{-/-} and H1299-p53^{R273H}-expressing cells did not differ in their size distribution (B), average size (C) and particle concentration (D). A PBS (microvesicle diluent) only control indicated that the background particle concentration was very low.

Nanoparticle tracking analysis indicated that the average size of microvesicles from H1299-p53^{-/-} cells was 161 nm, and from p53^{R273H}-expressing H1299 cells this was 158 nm. This is noticeably smaller than the diameters of 253 nm and 218nm measured by electron microscopy for microvesicles released from p53^{-/-} and p53^{R273H}-expressing H1299 cells respectively. Additionally the size distribution of microvesicles analysed using the NanoSight, suggests that very few structures in the microvesicle pellets are less than 50 nm in size, indicating a discrepancy between results from electron microscopy and nanoparticle tracking.

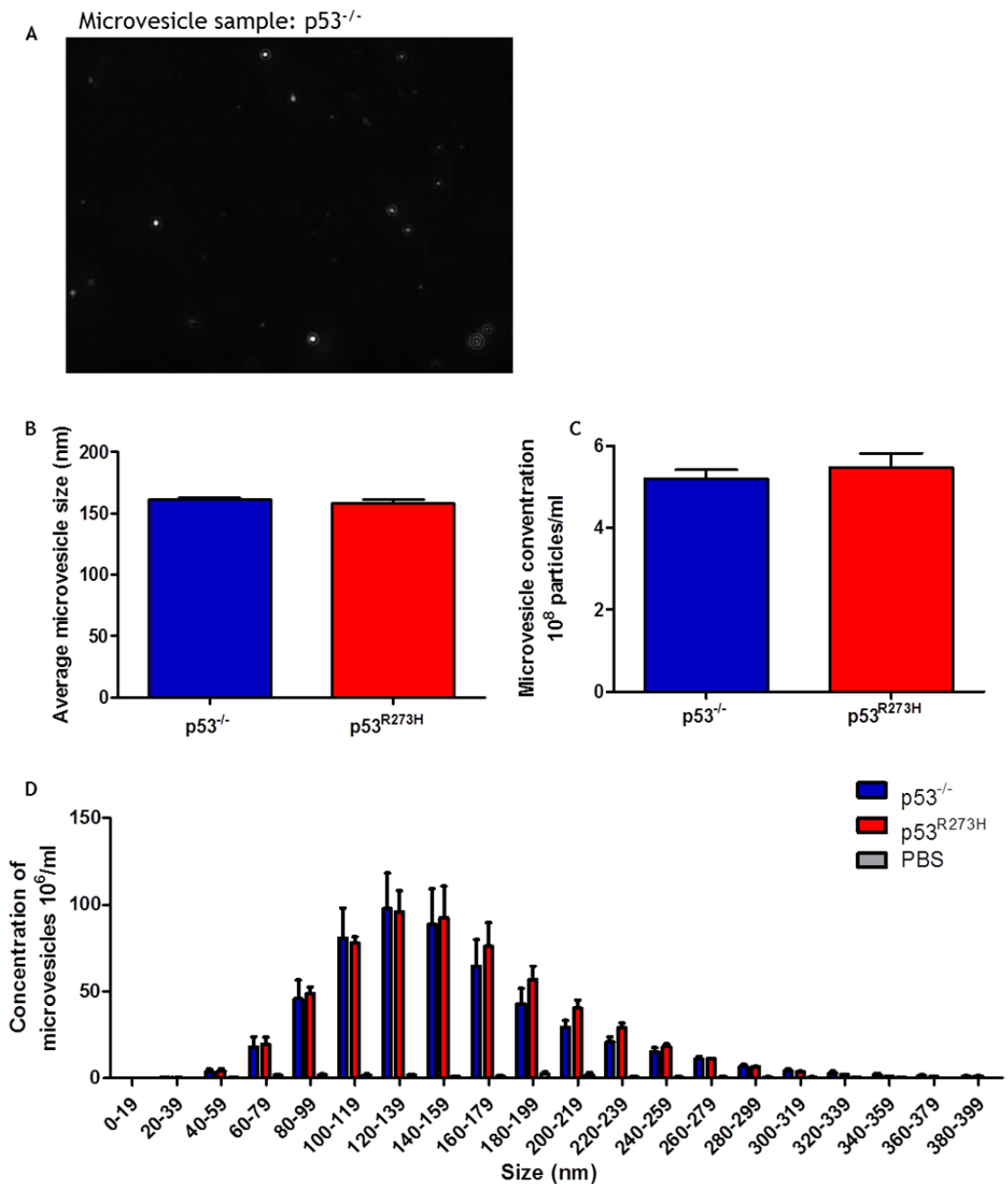


Figure 3-7: Nanoparticle tracking analysis of microvesicles released from p53^{-/-} and p53^{R273H}-expressing H1299 cells.

Microvesicles from H1299 p53^{-/-} and H1299-p53^{R273H} cells were collected by normal protocol and diluted 1:30 in PBS before applying to the NanoSight instrument (the use of which is described in chapter 2). Over 1000 particles per condition, per experiment, were tracked to achieve quantitative results. (A) A representative image of microvesicle particles from H1299-p53^{-/-} cells as detected by the NanoSight instrument is shown. The data acquired from particle tracking was used to determine the average size (B), particle concentration (C) and the size distribution (D) of microvesicles released by both p53^{-/-} and p53^{R273H}-expressing H1299 cells alongside a PBS only control. n=3. Values are mean \pm SEM.

3.3.2 Characterisation of microvesicle constitution

3.3.2.1 Lipidomic screen

Several reports have identified an important role of p53 in lipid metabolism as well as a role of lipids in microvesicle biogenesis (Goldstein and Rotter, 2012, Trajkovic et al., 2008). Therefore it seemed important to investigate the lipid constituents of microvesicles collected from p53^{-/-} and p53^{R273H}-expressing H1299 cells.

Liquid chromatography mass spectrometry (LCMS) lipidomic analysis of microvesicles collected from p53^{-/-} and p53^{R273H}-expressing H1299 cells indicated that they both had similar lipid content with no significant differences found between the two. Figure 3-8 (A) shows the chromatograms from the negative and the positive ion LCMS modes. The chromatograms represent very similar lipid detection signatures of microvesicles from p53^{-/-} and p53^{R273H}-expressing H1299 cells. Principal component analysis (B) revealed that microvesicles from H1299-p53^{-/-} and H1299-p53^{R273H} cells did not group into specific clusters indicating they both have similar lipid composition and complexity. Additionally, the lack of clustering within a condition in the principal component analysis, suggests that there was some variation between technical replicates.

The data set was subject to further in-depth analysis of specific species from lipid families in which we had a particular interest. Any discreet differences between lipid species that could not be detected globally may be identified this way. In particular, we were interested in closer analysis of diacylglycerol and phosphatidylinositol species due to their importance in the mutant p53 gain-of-function invasive phenotype (Rainero et al., 2012). Additionally ceramides and sphingomyelins were analysed as they have been found to be important in MVB-derived exosome biogenesis (Trajkovic et al., 2008). Despite some variation in the proportion of certain lipid species found in microvesicles from p53^{-/-} and p53^{R273H}-expressing H1299 cells, this in-depth analysis indicated that there were no significant differences in the categories of lipids that we had considered likely to contribute to mutant p53 function and/or microvesicle biogenesis (table 3-3).

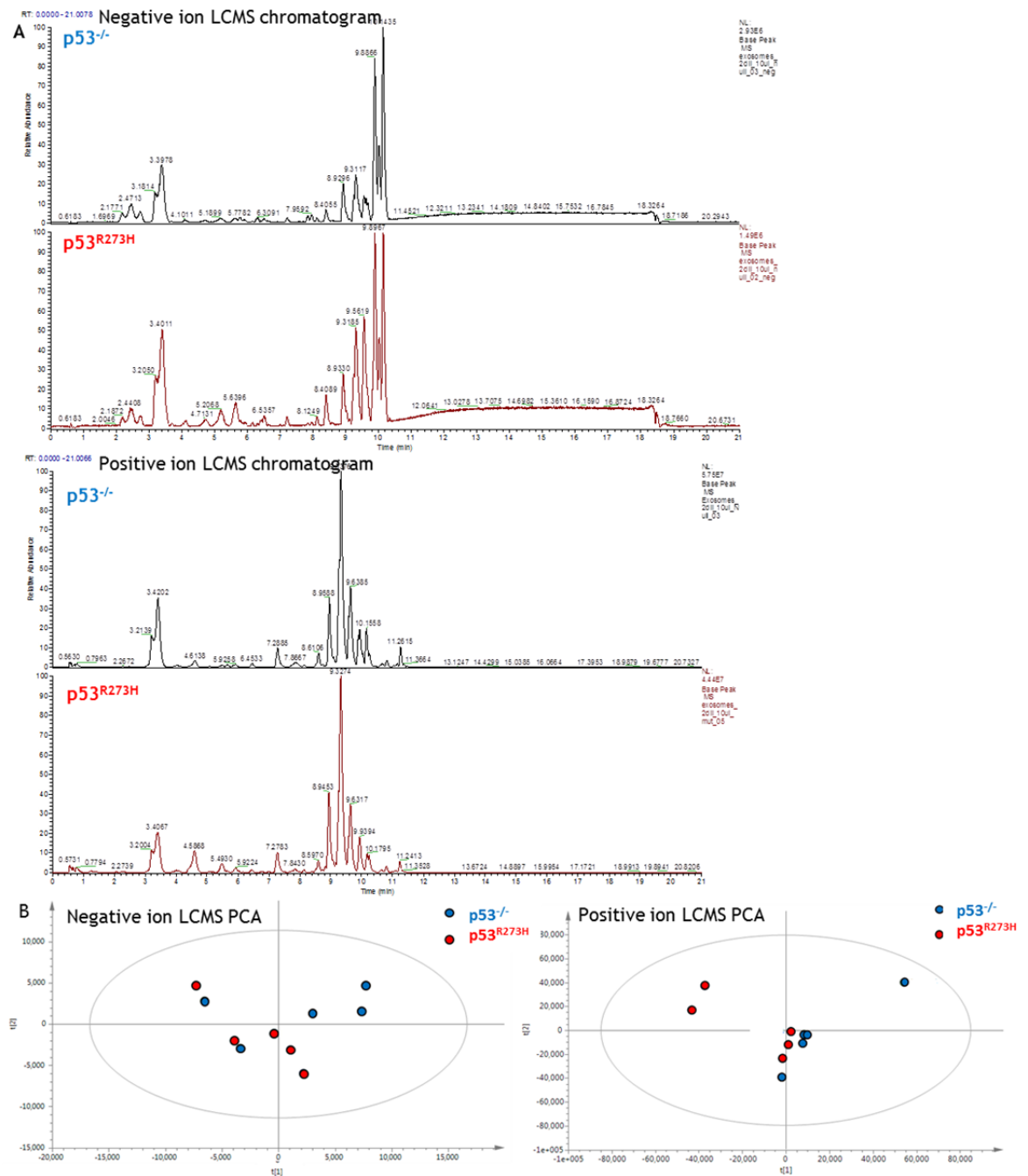


Figure 3-8: Lipidomic screen of microvesicles released by p53^{-/-} and p53^{R273H}-expressing H1299 cells revealed that there is no significant difference in the microvesicle lipid composition.

Microvesicles from H1299-p53^{-/-} and H1299-p53^{R273H}-expressing cells were isolated by differential centrifugation and subject to lipidomic analysis by Phil Whitfield and team in the University of Highlands and Islands. We present here the positive and negative ion LMSC chromatography results (A) alongside the principle component analysis (PCA) (B). n=5.

DAG	Identification	m/z	Anova (P)
Positive ion	DG(36:0)	647.6	0.109
	DG(P-32:1)	551.5	0.125
	DG(36:5)	653.5	0.148
	DG(40:7)	689.5	0.170
	DG(36:1)	640.6	0.178
Negative ion	DG(44:11)	759.5	0.276
	DG(42:6)	677.6	0.593
	DG(36:4)	661.5	0.906
	DG(32:3)	543.4	0.944
	DG(42:7)	675.5	0.996
Ceramide			
Positive ion	LacCer(d32:1)	856.6	0.070
	GlCCer(d40:2)	836.6	0.074
	Cer(d40:1)	638.6	0.145
	Cer(d40:1)	638.6	0.147
	GalCer(d40:1)	806.6	0.156
Negative ion	Cer(d44:2)	674.6	0.128
	Cer(d44:1)	676.7	0.202
	Cer(t42:0)	664.6	0.321
	LacCer(d36:0)	912.6	0.341
	PE-Cer(d37:2)	715.5	0.346
PI			
Positive ion	PI(36:5)	879.5	0.095
	PI-Cer(t-36:0)	859.6	0.100
	PI(34:1)	854.6	0.155
	PI-Cer(t-36:0)	859.6	0.183
	PI(30:0)	800.5	0.250
Negative ion	PI(O-40:4)	921.6	0.067
	PI(36:8)	831.4	0.201
	PI(P-38:6)	887.5	0.246
	PI-Cer(d40:0)	910.6	0.300
	PI(O-34:4)	837.5	0.339
SM			
Positive ion	SM(d36:2)	751.6	0.187
	SM(d32:0)	699.5	0.317
	SM(d32:0)	699.5	0.361
	SM(d32:0)	699.5	0.369
	SM(d36:1)	731.6	0.377
Negative ion	SM(d40:3)	763.6	0.253
	SM(d42:3)	855.7	0.514
	SM(d38:1)	803.6	0.585
	SM(d36:1)	775.6	0.594
	SM(d40:3)	763.6	0.697

Table 3-3: In-depth analysis of lipid species detected in lipidomic screen.

The data from the lipidomic analysis of microvesicles released by p53^{-/-} and p53^{R273H}-expressing cells was further analysed for specific lipid species within the diacylglycerol kinase (DAG), ceramide, phosphatidylinositol (PI) and sphingomyelin (SM) lipid families. None of the species were significantly changed between p53^{-/-} and p53^{R273H}-expressing cells according to their ANOVA p-value. n=5.

3.3.2.2 SILAC mass spectrometry screen

We used mass spectrometry approaches to investigate the protein constituents of microvesicles from H1299-p53^{-/-} and H1299-p53^{R273H}-expressing cells. A single isotope labelling by amino acids in culture (SILAC) mass spectrometry screen was carried out; this is described in more detail in chapter 2. Microvesicles were collected from H1299 p53^{-/-} and H1299-p53^{R273H}-expressing cells that had been labelled with either heavy amino acid or medium amino acid isotopes. Proteins present in microvesicles collected from these cells were SILAC-labelled and any unlabelled serum contaminants from the culture serum were able to be excluded from the analysis (experimental design is shown in figure 3-9). Using SILAC labelled cells enabled the conditioned media from H1299-p53^{-/-} and H1299-p53^{R273H}-expressing cells to be combined at an early stage during the microvesicle collection protocol, decreasing the amount of variability between the two conditions. Finally, SILAC also provided a quantitative way of analysing the protein constituents of the microvesicles.

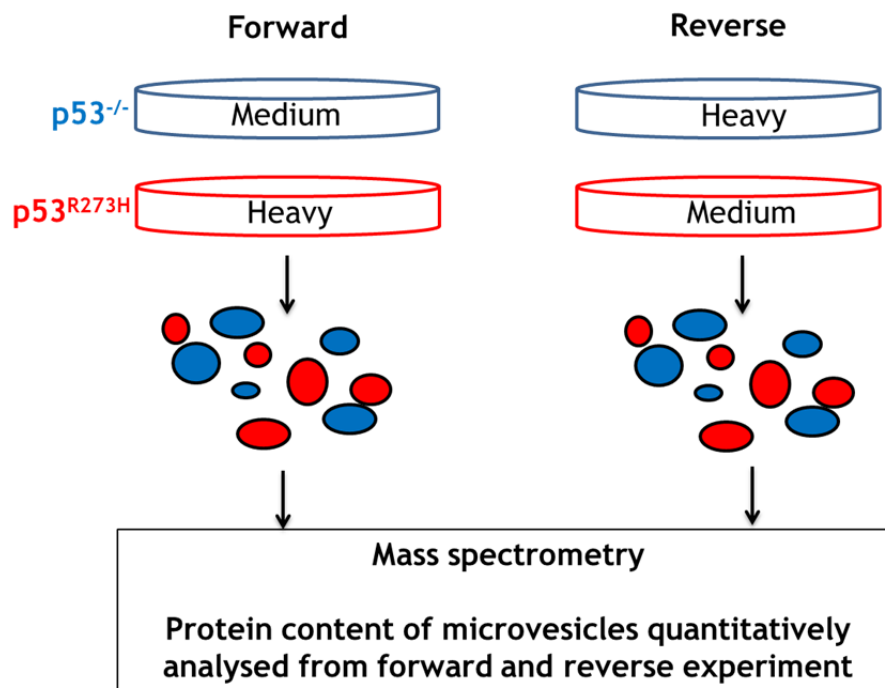


Figure 3-9: Experimental design of the microvesicle SILAC mass spectrometry analysis. H1299 p53^{-/-} and H1299-p53^{R273H}-expressing cells were cultured in SILAC medium containing heavy or medium amino acid isotopes. Once cells had fully incorporated the amino acid isotopes, microvesicles were collected from them by differential centrifugation. For the forward experiment, conditioned medium from H1299-p53^{-/-} cells SILAC labelled with medium amino acids, and H1299-p53^{R273H} cells SILAC labelled with heavy amino acids, was mixed together and microvesicles were collected. The relative abundance of protein constituents was quantitatively analysed by mass spectrometry. The same protocol was carried out for the reverse experiment except H1299-p53^{-/-} cells were SILAC labelled with heavy amino acids, and H1299-p53^{R273H} cells were SILAC labelled with medium amino acids, to ensure that different isotope labelling did not alter the functions and physiology of the cells. Forward and reverse microvesicle pellets were re-suspended in 6 M urea before they were reduced, alkylated and digested in preparation for mass spectrometry analysis. Samples were run directly on the Orbitrap Velos (LC-MS). Swissprot and MaxQuant were used to analyse and quantify data.

Having determined that the medium or heavy amino acid isotopes had been fully incorporated into cellular protein, microvesicles were collected and subjected to one-shot mass spectrometry. Table 3-4 shows a list of proteins determined to be the most abundant from our screen: the most abundant proteins present were often membrane-associated proteins or microvesicle-associated proteins. Additionally table 3-5 shows a more comprehensive list of proteins detected in the screen (irrespective of their abundance). There were numerous proteins present in the microvesicle preparations that are plasma membrane-associated, involved in membrane transport and additionally several microvesicle markers were detected. These data of microvesicle protein constituents, support the fact that our preparations were microvesicular in nature and largely free of any contaminants (Colombo et al., 2014).

Protein	log10 Intensity	Protein	log10 Intensity
ITGA3	9.38868721	YWHAZ	8.739129122
ITGB1	9.347369051	YWHAE	8.733165153
ATP1A1	9.166666883	CYR61	8.712994644
ENO1	9.09635376	CPNE8	8.696810544
HSPA8	9.095587747	CD9	8.684908168
MFGE8	9.09509958	HSPA6;HSPA7	8.641424531
GAPDH	9.088455045	NT5E	8.63905796
UBB	9.081239261	GNG12	8.627150705
VIM	9.080590414	PFN1	8.620614869
CD59	9.049838001	ANXA1	8.583765368
EEF1A1;EEF1A1P5	9.047586357	SLC1A5	8.581858673
MSN	9.024526714	EZR	8.575072326
HIST1H4A	8.849585237	EPHA2	8.564050279
CD44	8.843014641	UTRN	8.552558716
PDCD6IP	8.841891062	PKM;PKM2	8.542078146
HSP90AA1	8.816108671	ALDOA	8.54052968
CD151	8.806078174	MYH9	8.533517862
EEF2	8.784674339	STOM	8.531478917
CFL1	8.769916167	TSPAN4	8.521778588
CALM1;CALM2;CALM3	8.755569981	GNB1	8.504185317

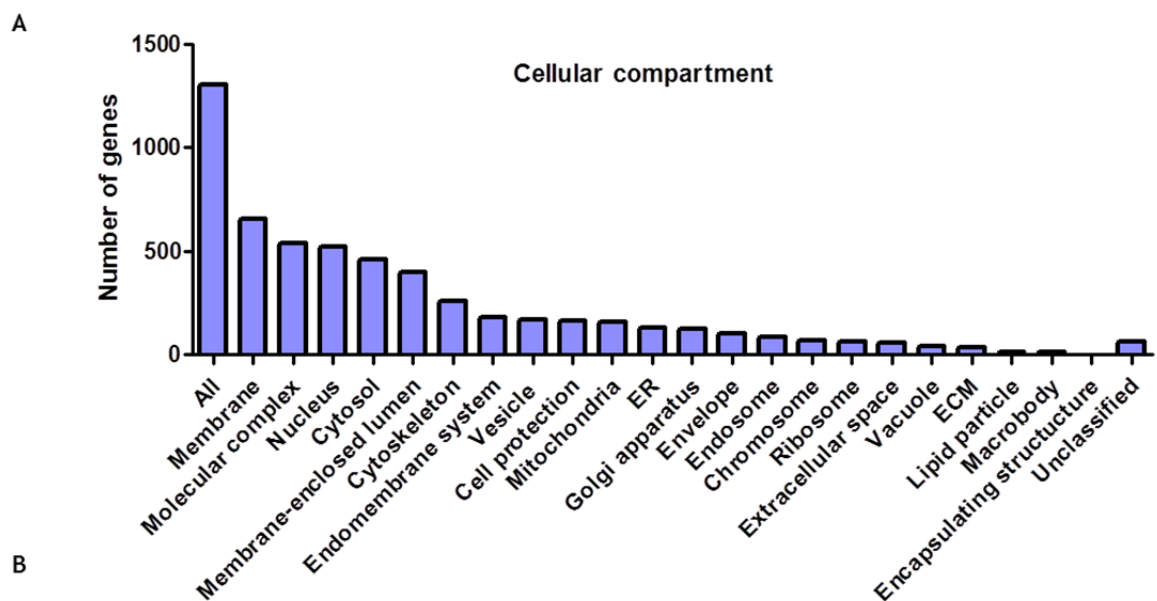
Table 3-4: The most abundant proteins in microvesicles detected by mass spectrometry. Microvesicles from p53^{-/-} and p53^{R273H} expressing cells were subject to mass spectrometry, the most abundant proteins as determined by their log10 intensity are listed. Proteins highlighted in purple are known to be either transmembrane proteins, membrane-associated proteins or microvesicle related proteins.

Protein Group	Protein	Protein Group	Protein
Transmembrane proteins involved in adhesion	ITGA6	Membrane transport	ANXA6
	ITGA4		ANXA1
	ITGA3		ANXA5
	ITGB1		ANXA4
	ITGAV		ANXA7
	ITGA6		ANXA2;ANXA2P2
	ITGA5		ANXA11
	ITGB5		FLOT2
	ITGB6		FLOT1
	ITGA2		ARF3;ARF1
	TSPAN6		ARF4
	TSPAN4		ARF6
	TSPAN14		ARF5
	TSPAN9		RAB23
	TSPAN5		RAB35
TSPAN15	RAB10		
Other transmembrane proteins	LAMP1	RAB12	
	TFRC	RAB5C	
	EGFR	RAB7A	
Antigen presentation	MICA;MICB	RAB11B;RAB11A	
Microvesicle markers	CD63	RAB1A	
	TSG101	RAB14	
	HSPA8	RAB34	
	CD9	RAB6A	
	CD81	RAB8A	
Cytosolic protein examples	HIST2H3A	RAB13	
	H2AFZ	RAB22A	
	RBBP7	RAB5B	
	HIST2H2AA3	RAB18	
	H2AFX	RAB2A;RAB2B	
	RRBP1	RAB3A	
		RAB3B	
		RAB32;	
		RAB8B	
		RAB1B	
		RAB21	
		CLTC	
	CLTA		
	CLTB		

Table 3-5: Proteins present in microvesicles released by H1299 cells.

This table shows proteins, often enriched in microvesicles, that were found in the SILAC mass spectrometry screen of microvesicles from H1299 p53^{-/-} and H1299-p53^{R273H}-expressing cells (Colombo et al., 2014).

From the proteins identified in the mass spectrometry screen, gene enrichment analysis was carried out. Figure 3-10 (A) shows the cellular compartment from which the microvesicle proteins were derived. Over half of the identified proteins were classed as being membrane-derived, a positive indicator that the microvesicles are derived from membrane compartments. Additionally there was particular enrichment in protein groups present in microvesicles from H1299 cells that are involved in several pathways in which we are interested; including endocytosis, regulation of the actin cytoskeleton and focal adhesion dynamics (figure 3-10 B).



KEGG pathway analysis of microvesicle proteins

- Ribosome
- **Regulation of actin cytoskeleton**
- Metabolic pathways
- **Endocytosis**
- Protein processing in endoplasmic reticulum
- **Focal adhesion**
- Spliceosome
- Phagosome
- Tight Junction
- Pathogenic E.coli infection

Figure 3-10: Gene enrichment analysis of protein constituents of microvesicles from H1299 p53^{-/-} and H1299-p53^{R273H}-expressing cells.

(A) Genes associated with proteins identified in the mass spectrometry analysis were categorised from which cellular compartment they were known to reside (WebGestalt). (B) The same data was used to complete KEGG pathway analysis. The pathways in which proteins from the screen of microvesicles are enriched within are noted. Highlighted in red are the protein groups in our microvesicles involved in pathways that may be in our interest.

The proteomic screen indicated that microvesicles from H1299-p53^{-/-} and H1299-p53^{R273H}-expressing cells were very similar to one another in terms of their overall protein constituents (Table 3-6). Although some proteins present in microvesicles collected from H1299-p53^{-/-} and H1299-p53^{R273H}-expressing cells were at apparently different levels, the changes were not reproducible between the forward and reverse experiments.

Gene name	Mol. weight [kDa]	Ratio H/M normalized FWD	1/[Ratio H/M normalized REV]	FWD A significant	REV A significant
ANXA2	38.604	5.72	NaN	+	
PODXL	58.635	-1.31	-0.70		+
MLLT4	206.8	-0.09	0.96		+
HSPG2	468.83	0.02	0.76		+
CPM	50.513	NaN	0.64		+
MME	85.513	-1.50	0.32		
COL12A1	333.14	-1.25	NaN		
MATN2	106.84	-1.24	-0.43		
CPNE3	60.13	-1.21	0.08		
FAM129A	103.13	-1.17	0.05		
SLC1A4	55.722	-1.13	-0.25		
PSEN1	52.667	-1.07	NaN		
MFGE8	43.122	-1.05	-0.03		
ITGA6	126.63	-1.03	NaN		
RFTN1	63.145	-0.99	0.00		
ADAM10	84.141	-0.99	0.03		
DSG2	122.29	-0.97	0.13		
KIF4A	139.88	-0.95	0.20		
CACNA2D1	124.57	-0.94	0.28		
FAS	37.732	-0.92	0.02		

Table 3-6: Microvesicle SILAC mass spectrometry data.

This table depicts the top 20 most changed proteins in microvesicles from H1299 p53^{-/-} vs H1299-p53^{R273H} cells. Forward experiment = H1299-p53^{-/-} cells labelled with medium amino acids and H1299-p53^{R273H} cells with heavy amino acids. Reverse experiment (an experimental replicate) = H1299-p53^{-/-} cells labelled with heavy amino acids and H1299-p53^{R273H}-expressing cells with medium amino acids. The ratios are expressed in a log2 scale. The inverse ratio is calculated for the reverse experiment prior to logging, for ease of interpretation. Therefore if the ratio is a negative value in both the forward and reverse experiment, the protein is present at an increased level in microvesicles from H1299-p53^{-/-} cells. However none of these proteins were reproducibly or significantly different within microvesicles isolated from p53^{-/-} or p53^{R273H}-expressing H1299 cells.

3.4 Discussion

3.4.1 The impact of mutant p53 expression on microvesicle release

Although other studies have investigated the effect of expression of several oncogenes on microvesicle release, this is the first study to investigate the role of mutant p53 expression on microvesicle release and content. We chose to characterise and compare microvesicles released by H1299 cells null for p53^{-/-} or those expressing mutant p53^{R273H}.

Analysis of the concentration, size and microvesicle marker content determined that similar microvesicle populations are released by each cell type regardless of mutant p53 expression. Microvesicle markers TSG101, HSPA8 and CD63 identified the presence of microvesicles in the 100,000 g pellet. None of the markers are capable of discriminating between MVB-derived exosomes or those shed from the plasma membrane, although the majority of microvesicles are present at a density of 1.1 - 1.16 g/ml. This is the density at which MVB-derived exosomes (which are <100 nm in diameter) are commonly found (Colombo et al., 2014, Raposo et al., 1996). However, transmission electron microscopy and nanoparticle tracking analysis data suggested that we are isolating microvesicles of such heterogeneity in terms of their size (from 30 nm to 500 nm) that it is likely that our microvesicle preparations contain both MVB-derived exosomes and plasma membrane-shed microvesicles. Thus, it is possible that MVB-derived exosomes and plasma membrane-shed microvesicles released by H1299 cells are of similar densities to one another even though they are very different sizes. This would render it impossible to separate the two microvesicle populations from one another using sucrose density gradients. Perhaps successful isolation of MVB-derived exosomes (<100 nm in size) by sucrose density gradients is dependent upon cell type, and relies upon cells that do not release large quantities of plasma membrane-shed microvesicles into the extracellular environment.

Electron microscopy suggested that p53^{R273H}-expressing H1299 cells release a population of microvesicles that have a smaller average size than those released by H1299-p53^{-/-} cells. Additionally a distinct population of microvesicles that

were less than 50 nm in diameter (which would most likely correspond to exosomes generated in MVBs) are released by p53^{R273H}-expressing H1299 cells. However nanoparticle tracking analysis was unable to support this result and this may be due to detection limitations of this technique. A previous study showed that nanoparticle tracking analysis can reliably detect and track microvesicles over 70 nm in size, our study agrees with this, as the NanoSight detects very few microvesicles that are less than 50 nm in our microvesicle preparations (Soo et al., 2012). Therefore we conclude that, for the population of microvesicles we are interested in, nanoparticle tracking analysis is unlikely to be useful in supporting the electron microscopy analysis. Additionally it is also important to remember that analysis of microvesicle characteristics by transmission electron microscopy has been reported to be complicated by artefacts that occur during sample preparation. These artefacts are thought to introduce distortions into the microvesicle structure. Indeed, because cryo-electron microscopy (which has a different sample work-up from transmission electron microscopy) yields microvesicle structures that appear to be spherical, it is thought that the cup-shape ascribed to microvesicles using transmission electron microscopy may be erroneous (Raposo et al., 1996, Conde-Vancells et al., 2008, Raposo and Stoorvogel, 2013).

Taken together, these data indicate that H1299-p53^{-/-} and p53^{R273H}-expressing H1299 cells release a heterogeneous population of microvesicles whose size distribution corresponds to a mixture of both MVB-derived exosomes and plasma membrane-shed microvesicles. Electron microscopy analysis of microvesicle size suggests that a small population of microvesicles less than 50 nm in diameter are being specifically released, by p53^{R273H}-expressing H1299 cells. Although this is not conclusive and needs to be further supported by a different technique, I think that there is sufficient evidence to suggest that mutant p53 expression promotes the release of a specific sub-population of microvesicles.

3.4.2 Impact of mutant p53 expression on microvesicle content

3.4.2.1 Protein constituents

Expression of mutant KRAS is thought to considerably alter the proteome of microvesicles. Mutant KRAS itself is packaged into microvesicles alongside other

factors, and transferred from colon cancer cells to neighbouring non-transformed cells which leads to increased invasive capacity of these neighbouring cells (Demory Beckler et al., 2013). Additionally lipid raft-associated microvesicles can transfer the EGFRvIII oncoprotein between glioma cells. These EGFRvIII-rich microvesicles initiate oncogenic activity in recipient cells via activation of signalling pathways such as the ERK/MAPK and PI3K/AKT axes to allow morphological transformation and growth (Al-Nedawi et al., 2008). These studies set a precedent for the packaging of oncogene products and proteins with oncogenic properties into microvesicles. However, despite the fact that p53^{R273H} certainly qualifies as an oncogene product, we have been consistently unable to detect its presence in any of the microvesicle preparations used in this study. Additionally, proteins such as α 5B1, RCP, DGK α , and cMET, whose functions are associated with mutant p53's gain-of-function, were either absent from microvesicles, or were present in equal quantities in microvesicles from p53^{-/-} and p53^{R273H}-expressing cells.

The mutant p53 gain-of-function phenotype has been found to be dependent upon many other proteins. Therefore, the next step was to carry out a comprehensive analysis of the microvesicle protein constituents. However SILAC mass spectrometry showed no significant reproducible differences in the protein constituents present in microvesicles collected from p53^{-/-} and p53^{R273H}-expressing cells.

3.4.2.2 Lipid constituents

There are reports indicating that wild-type p53 has a role in inhibiting lipid anabolism and promoting the catabolism of lipids (Goldstein and Rotter, 2012). Interestingly there is evidence that mutant p53 enhances lipid anabolism which contributes to breast cancer aggressiveness. Mutant p53 promotes flux through the mevalonate pathway which is involved in cholesterol production, and upregulates the expression of genes involved in fatty acid synthesis (Freed-Pastor et al., 2012). However the lipidomic screen carried out on microvesicles released by p53^{-/-} and p53^{R273H}-expressing cells, showed that mutant p53 expression had no significant impact upon their lipid composition.

Mutant p53 expression increases integrin recycling to promote an invasive phenotype in a DGK α -dependent manner. DGK α exerts its effect via specific regulation of the 38:4 DAG species, but not total DAG levels (Rainero et al., 2012). We were interested to determine whether DAG levels were increased in microvesicles released from p53^{R273H}-expressing cells which could account for any pro-migratory/functional effects that they may elicit in recipient p53^{-/-} cells. However upon closer analysis of the lipidomic data for specific lipid species, there was no 38:4 DAG species detectable in the microvesicles and overall DAG levels were similar in microvesicles from both p53^{-/-} and p53^{R273H}-expressing cells.

3.4.2.3 Screen limitations

The global analysis of protein and lipid constituents of the microvesicles surprisingly revealed that mutant p53 expression has no detectable effect upon lipid composition and minimal effect on their protein constituents. However, lack of clustering of technical repeats as demonstrated by the principal component analyses, suggested a degree of variation that would prevent detection of small differences in lipid or protein content. This may be owing to losses incurred during the multi-step process of microvesicle isolation. It may also be owing to there being insufficient quantity of relevant material obtained from the microvesicle preparations to attain the detection limits of the assays. Therefore experiments on a larger scale might be informative. Finally, as it is possible that changes in the constitution of a minority subpopulation of microvesicles may be masked by more abundant microvesicle populations, it would be necessary to physically separate MVB-derived exosomes from plasma membrane-shed microvesicles in order to identify any effect that mutant p53 may have on microvesicle constitution.

Separation of microvesicle populations into MVB-derived exosomes and plasma membrane-shed microvesicles has been shown to be achieved using sucrose density gradients (Thery et al., 2006a, Raposo et al., 1996). However, we have found that a microvesicle population with a very broad size distribution is present within a narrow band of density (1.1 g/ml - 1.16 g/ml) collected from the sucrose density gradient (data not shown). This indicates that, in our hands, this technique is not capable of resolving MVB-derived exosomes from plasma

membrane-derived microvesicles. Microvesicle populations can alternatively be separated using immuno-affinity capture deploying antibodies for specific microvesicle markers or microvesicle proteins of interest (Tauro et al., 2012). This technique allows the enrichment and separation of a specific population of microvesicles from the overall population so that their composition can be analysed with greater sensitivity.

3.4.2.4 Other microvesicle constituents

Past studies have shown microvesicles to be rich in nucleic acids including DNA, mRNA and miRNA (Colombo et al., 2014). Double stranded DNA encoding the mutants of KRAS and p53 has been identified on microvesicles isolated from pancreatic cancer cell lines and in serum from pancreatic cancer patients (Kahlert et al., 2014). Therefore it would be interesting to check whether DNA encoding mutant p53 is present in microvesicles collected from p53^{R273H}-expressing cells. RNA-containing microvesicles can transfer functional RNA to neighbouring cells where it alters the gene expression and phenotype (Valadi et al., 2007, Skog et al., 2008). For example mRNA encoding the luciferase protein has been shown to be delivered to recipient cells via a microvesicle vector. The transferred mRNA is then translated by the recipient cell to generate a functionally active product (Skog et al., 2008). Additionally the transfer of mouse mRNA to human cells via microvesicles results in the translation of functional mouse proteins in the recipient human cells (Valadi et al., 2007). Finally the transfer of miRNA to recipient cells has been shown to suppress gene expression in recipient cells (Montecalvo et al., 2012). Preliminary data (not shown) indicated the presence of small RNAs in microvesicles from H1299 cells. As mutant p53 has a well-characterised role in reducing DICER expression and suppressing mature miRNA processing, it would be interesting to identify whether mutant p53 expression causes differential sorting of small RNAs into microvesicles (Muller et al., 2014).

3.4.3 Concluding remarks

After initial characterisation of microvesicles from p53^{-/-} and p53^{R273H}-expressing cells we can confirm that we can isolate microvesicle preparations which are positive for several microvesicle markers and free of large membrane fragments

or debris contaminants. The microvesicles collected from both p53^{-/-} and p53^{R273H}-expressing cells are released in similar concentrations. Furthermore, the microvesicles are heterogeneous in size indicating that they are a mixture of MVB-derived exosomes and plasma membrane-shed microvesicles. Although not supported by nanoparticle tracking analysis (due to detection threshold limitations), transmission electron microscopy indicated that mutant p53 expression promotes the release of a specific sub-population of small microvesicles (<50 nm). However extensive screening revealed that mutant p53 expression has no global effect upon the microvesicle protein or lipid constituents. Finally we have not been able to separate microvesicle populations of different size using sucrose density gradient flotation. Other techniques such as immuno-affinity capture will need to be trialled in the future to enable further experimentation on separate microvesicle populations.

There are technical limitations to the global analysis we have conducted on microvesicles from p53^{-/-} and p53^{R273H}-expressing cells, and the microvesicles have yet to be screened for their nucleic acid content. However transmission electron microscopy indicates that mutant p53-expressing cells release a population of small (< 50 nm) microvesicles that is not detectable in medium conditioned by p53 null cells. Therefore going forward, the next step was to ascertain whether microvesicles from cells with various p53 statuses have different functional effects in recipient cells. In particular, we wanted to investigate whether microvesicles released by mutant p53-expressing cells are capable of influencing the behaviour of p53^{-/-} cells. Mass spectrometry indicated that the microvesicles contained protein groups related to actin dynamics, focal adhesions and endocytosis. These processes are known to be altered by mutant p53-expression and contribute to enhanced integrin and receptor tyrosine kinase recycling and signalling resulting in an invasive migratory phenotype. Therefore, we investigated the ability of microvesicles from mutant p53-expressing cells to evoke these phenotypic parameters in p53^{-/-} recipient cells, and these findings are described in the following chapter.

4 Influence of microvesicles from mutant p53-expressing cells on cell migration and invasion

4.1 Introduction

In chapter 3 we identified that expression of mutant p53 in H1299 cells has no detectable effect on the protein or lipid constituents of microvesicles. Despite this, transmission electron microscopy indicated that mutant p53 expression promotes release of a sub-population of MVB-derived exosomes that are smaller than 50 nm in diameter. The fact that these small microvesicles represent a minority of the total microvesicle population, would render it difficult to determine their constitution using the purification protocols and analytical approaches described in the previous chapter. We hypothesise that this small microvesicle population may have distinct biological properties; we therefore wished to investigate whether microvesicles collected from mutant p53-expressing cells are capable of transferring the mutant p53 gain-of-function phenotype to other cells.

4.1.1 Non-cell-autonomous roles of p53

The mechanisms by which p53 acts as a tumour suppressor in a cell-autonomous way are well established and already described in chapter 1. There is also evidence indicating that p53 can promote tumour suppression through non-cell-autonomous mechanisms, primarily by modifying transcription of genes for secreted proteins. Additionally there are limited, although convincing, studies regarding p53's involvement in MVB-derived exosome release. However, there is only limited evidence for any non-cell-autonomous functions of mutant p53.

4.1.1.1 Protein secretion

One of the first studies reporting a non-cell-autonomous role of wild-type p53 showed that p53 promotes thrombospondin-1 gene transcription, and the consequent secretion of its protein product, which leads to inhibition of angiogenesis in the extracellular environment (Dameron et al., 1994). Additionally, irradiation of cells activates p53 and increases p53-dependent transcription of genes for secreted proteins that are involved in cell cycle regulation. Consequently, conditioned medium collected from p53-activated

cells has the ability to deliver growth suppressive stimuli to neighbouring cells, and this demonstrates a second non-cell-autonomous role of p53 in maintaining a tumour suppressive environment (Komarova et al., 1998). Furthermore p53 exerts non-cell-autonomous tumour suppression between different cell types. Exemplifying this, stromal fibroblasts that express p53 suppress cancer cell growth *in vivo*. MCF7 breast cancer cells co-injected with p53-deficient fibroblasts into immunocompromised mice results in the growth of tumours that are larger and more aggressive by comparison with co-injection of MCF7 cells with fibroblasts expressing wild type p53 (Kiaris et al., 2005).

Finally, non-cell-autonomous tumour suppressive roles of p53 are closely associated with cell senescence. Hepatocellular carcinoma tumours regress upon re-activation of p53 expression. This is attributed to p53-dependent activation of a cellular senescence programme. *In vitro*, p53-mediated activation of cellular senescence leads to differentiation and the suppression of proliferation. *In vivo*, activation of senescence is additionally characterised by the secretion of pro-inflammatory cytokines which recruit immune cells to the tumour site and initiate cancer cell clearance (Xue et al., 2007). Furthermore, in a mouse model of liver damage, inhibition of the p53-induced senescence programme in hepatic stellate cells increases the rate of liver fibrosis and hepatocellular carcinoma formation (Lujambio et al., 2013). This study by Lujambio and colleagues showed that wild-type p53 maintains a tumour suppressive environment through non-cell-autonomous control of macrophage polarisation. Wild-type p53-expressing senescent liver stellate cells secrete factors into the extracellular environment that promote macrophage-mediated destruction of senescent cells, maintaining a tumour-suppressive environment. Upon removal of p53 expression, the stellate cells proliferate and secrete factors that polarise macrophages to a state which can promote proliferation of pre-malignant cells to support tumour formation (Lujambio et al., 2013).

4.1.1.2 MVB-derived exosome release

Wild-type p53 promotes release of MVB-derived exosomes into the extracellular environment. The release of translationally-controlled tumour protein (TCTP) into the extracellular environment via MVB-derived exosomes is enhanced by tumour suppressor activated pathway 6 (TSAP6) expression, the transcription of

which is under the control of p53 (Amzallag et al., 2004). Later studies confirmed that DNA damage-induced p53 activation, increases MVB-derived exosome release, and that this increase is dependent upon p53 activation of TSAP6 transcription (Yu et al., 2006). TSAP6 null mice display abnormal reticulocyte maturation - a process in which MVB-derived exosome release is essential (Johnstone et al., 1991). Additionally, the increased rate of MVB-derived exosome release upon DNA damage is abrogated in TSAP6 null mice (Lespagnol et al., 2008).

A recent study has identified that treatment of lung cancer cells with β -elemene (a naturally-occurring compound that is currently under investigation as a potential cancer therapy) inhibits cancer cell growth and increases cancer cell apoptosis. After β -elemene treatment, cancer cells upregulate p53 expression which enhances anti-proliferative MVB-derived exosome release. The treatment of other cancer cells with these MVB-derived exosomes suppresses their proliferation (Li et al., 2014). These studies identify a potentially important role that p53 may have in MVB-derived exosome release and function.

4.1.2 Non-cell autonomous role of mutant p53

One study so far has indicated a non-cell-autonomous role for mutant p53. This study found that conditioned medium from H1299 cells stably expressing a ponasterone-A inducible mutant of p53 (p53^{R248Q}) was able to promote invasiveness of p53 null H1299 and ZR751 cells (Nielsen et al., 2011). Although this study identifies many mutant p53-activated genes that are, in principle, capable of influencing cell migration, the pro-invasive components of the 'mutant p53 secretome' are yet to be identified.

4.1.3 Aims

This chapter aims to explore the non-cell-autonomous nature of the mutant p53 gain-of-function phenotype. We have investigated the impact of conditioned medium from mutant p53-expressing cells on the migratory and invasive characteristics (this includes directional cell migration, cell polarity, invasiveness and integrin trafficking) of p53 null cells, and the role that microvesicles play in these processes.

4.2 Results

4.2.1 Mutant p53 expression in H1299 cells drives a gain-of-function migratory and invasive phenotype

Expression of mutant p53 in H1299 cells drives a gain-of-function migratory and invasive phenotype (Noske et al., 2009). Figure 4-1 (A) shows that cells expressing p53^{R273H} migrate with a lower forward migration index (FMI) in wound healing migration assays and that they have a higher invasive capacity as determined by inverted invasion assays (Figure 4-1 B) than do p53^{-/-} cells, effectively reproducing previously published results. The migration speed of H1299 cells expressing p53^{R273H} was also increased compared to cells null for p53^{-/-} (data not shown). Once the protocols used to analyse cell migration and invasion were in place and working effectively, we wanted to investigate whether the gain-of-function migratory phenotype is truly cell-autonomous or if it can be transferred from cell to cell in a non-cell-autonomous fashion.

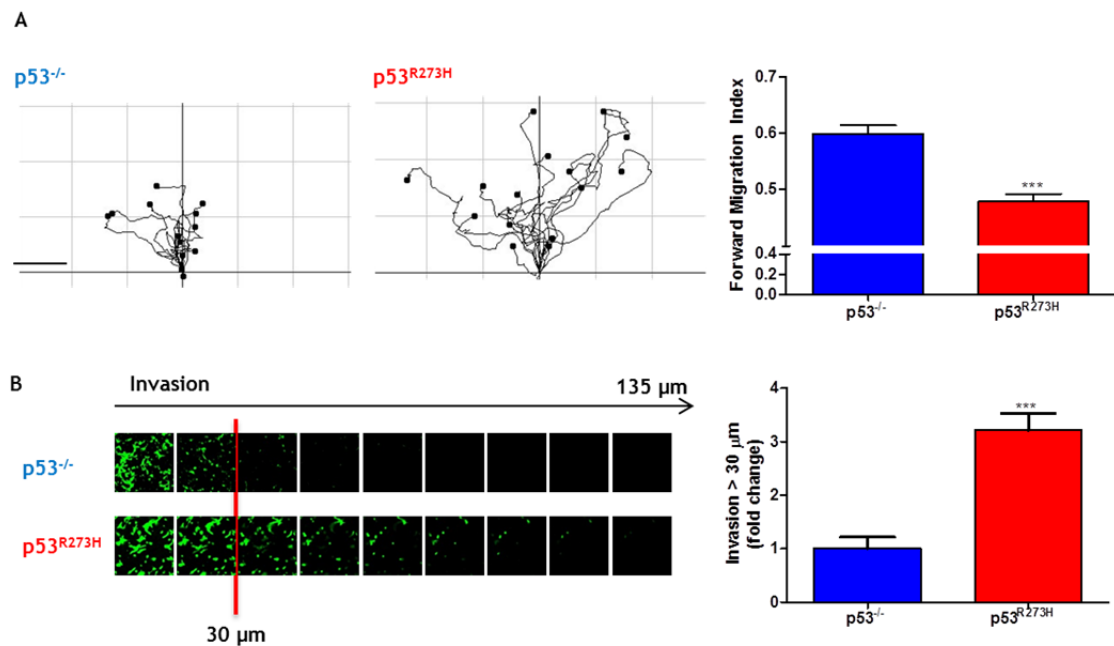


Figure 4-1: Mutant p53 expressing cells migrate with a lower forward migration index and display higher invasive capacity than cells null for p53.

(A) H1299 p53^{-/-} and p53^{R273H}-expressing cells were plated onto plastic plates. Once a confluent monolayer was formed, a wound was made using a pipette tip. Time-lapse microscopy was used to image the migration of cells into the wound, with frames being captured every 10 minutes over 16 hours at 10x magnification. The movement of individual cells was tracked and the resulting data were used to measure the forward migration index using ImageJ (protocol further described in materials and methods). Over 60 cells per condition were tracked in 3 independent experiments (unless otherwise stated). This protocol was used for all subsequent wound-healing analyses. n=3. Values are mean ± SEM. Mann-Whitney. ***p<0.0001. Representative track-plots (with the starting position of each cell aligned to the origin) are displayed to illustrate the migratory characteristics of p53^{-/-} and p53^{R273H}-expressing cells. Scale bar = 100 μm. (B) H1299 p53^{-/-} and p53^{R273H}-expressing cells were plated onto a transwell membrane and allowed to invade through a plug of Geltrex (a Matrigel substitute) supplemented with 25 μg/ml fibronectin towards a chemotactic gradient of serum supplemented with 10 ng/ml HGF. 72 hours later cells were visualised with 4 μg/ml Calcein-AM and confocal images were captured using an Olympus Fluoview FV1000 microscope at 20x magnification. Optical sections were captured at 15 μm intervals, and are presented as a sequence in which the individual optical sections are placed alongside one another with increasing depth from left to right as indicated. Invasiveness was quantitated by measuring the fluorescence intensity (as a percentage of total cell fluorescence) of cells penetrating the Geltrex to depths of 30 μm and greater using ImageJ. Data is expressed as a fold change in invasion over 30 μm. n=3. Values are mean ± SEM. Mann-Whitney. ***p<0.0001.

4.2.2 Mutant p53 gain-of-function migratory phenotype is non-cell-autonomous

The non-cell-autonomous nature of the mutant p53 migratory phenotype was investigated using a co-culture experimental design. H1299-p53^{-/-} cells stably expressing GFP were cultured individually or together with H1299-p53^{R273H} cells stably expressing mCherry (Muller et al., 2013). After 72 hours of co-culture, cells were plated for wound healing analysis - the stable expression of GFP and mCherry in p53^{-/-} and p53^{R273H}-expressing cells respectively, allowed each cell

type to be individually tracked in co-culture experiments. When cultured independently, the mCherry-expressing H1299-p53^{R273H} cells displayed the mutant p53 gain-of-function migratory phenotype. They migrated with significantly lower forward migration index (FMI) than the GFP-expressing p53^{-/-} cells, indicating that expression of these fluorescent proteins did not alter the migratory behaviour of H1299 cells. However, when p53^{-/-} cells were mixed with mutant p53-expressing cells, the p53^{-/-} cells migrated with a significantly reduced FMI, thus displaying a mutant p53 migratory phenotype (figure 4-2). This indicated that the mutant p53 migratory phenotype is not cell-autonomous and can be transferred to neighbouring cells.

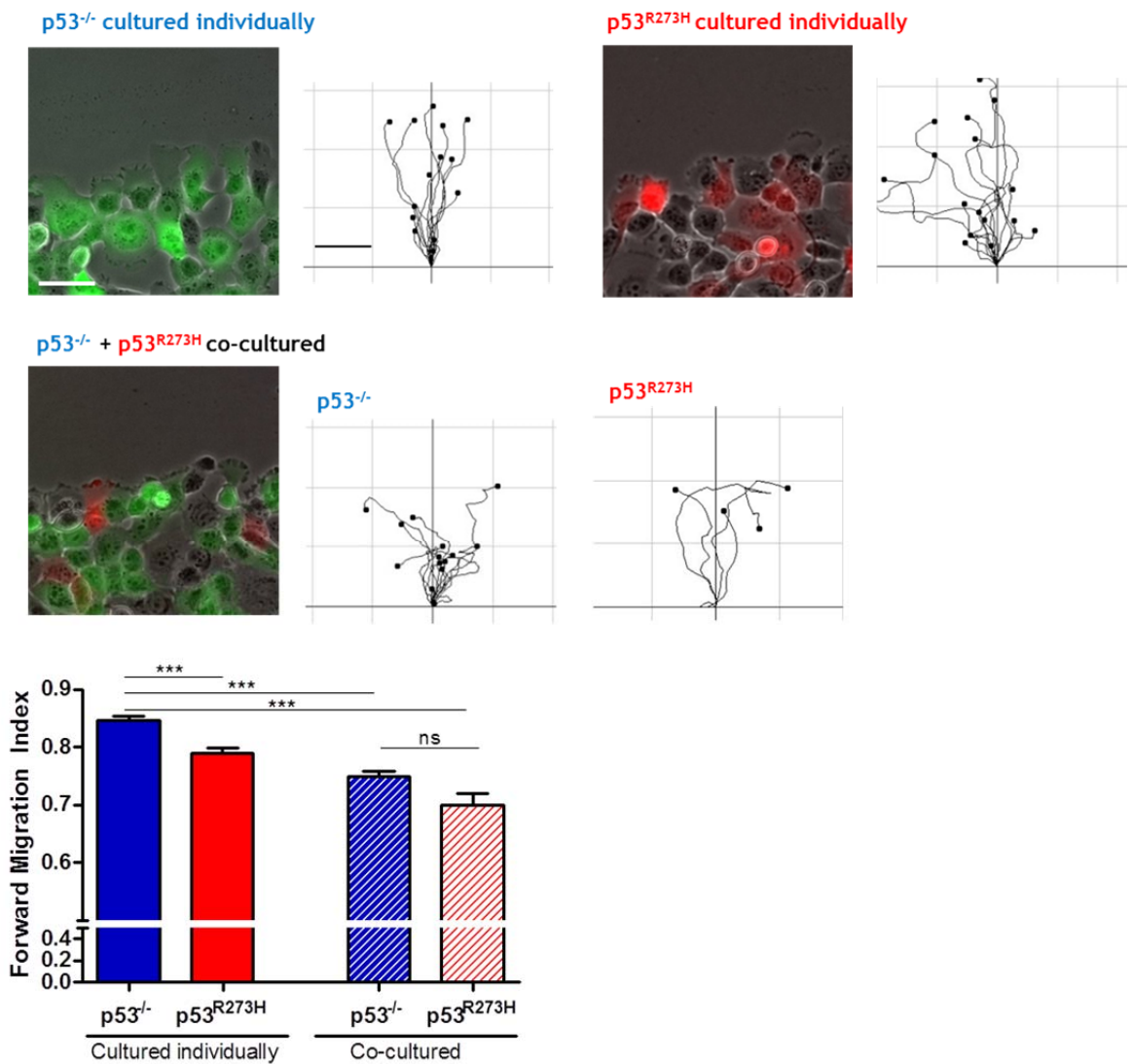


Figure 4-2: Co-culture with p53^{R273H}-expressing cells reduces the forward migration index of H1299-p53^{-/-} cells.

H1299-p53^{-/-} cells stably expressing GFP and H1299-p53^{R273H} cells stably expressing mCherry were cultured individually or were co-cultured for 72 hours as represented by fluorescent images, (scale bar=20 μ m). Cells were plated onto plastic surfaces and 24 hours later the confluent monolayer was wounded using a pipette tip. The closure of the wound was imaged by time-lapse microscopy capturing bright-field, GFP and m-cherry fluorescent images every 15 minutes for 16 hours. Each cell type was identified by their GFP or mCherry expression and tracked using ImageJ. Data were used to determine the forward migration index of cell migration. Track plots representing the cell migration characteristics in each condition are shown (scale bar = 100 μ m). n=3. Values are mean \pm SEM. Kruskal Wallis. ***p<0.0001.

The ability of p53^{R273H}-expressing cells to influence the FMI of p53^{-/-} cells may require direct cell-cell contact, or may be transmitted via the release of secreted factor(s). To distinguish between these two possibilities, we compared the ability of conditioned medium from p53^{-/-} and p53^{R273H}-expressing cells to influence the migratory behaviour of p53^{-/-} cells (figure 4-3).

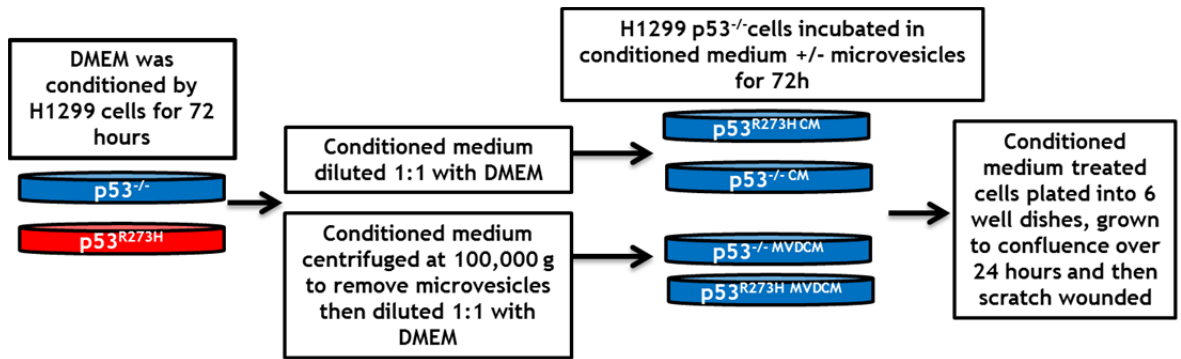


Figure 4-3: Schematic representation of conditioned medium experimental design.

DMEM conditioned by donor H1299 p53^{R273H}-expressing cells and p53^{-/-} cells was collected and depleted of cell debris by differential centrifugation (300 g, 2000 g, and 10,000 g). The conditioned medium was then used 1:1 with DMEM to treat recipient p53^{-/-} cells for 72 hours. Alternatively conditioned medium was subject to an extra centrifugation spin at 100,000 g to deplete the conditioned medium of any released microvesicles (microvesicle depleted conditioned medium - MVDCM) before using to pre-treat p53^{-/-} cells. After a 72 hour pre-treatment with conditioned medium, p53^{-/-} cells were re-plated for further experimentation.

Pre-treatment of p53^{-/-} H1299 cells with medium conditioned by p53^{R273H}-expressing cells decreased their FMI to that normally displayed by mutant p53-expressing cells, whereas conditioned medium from p53^{-/-} cells was ineffective in this regard (figure 4-4 A). Depletion of mutant p53 expression using siRNA (but not non-targeting siRNAs) yielded conditioned medium that did not alter the FMI of p53^{-/-} cells, indicating that it is mutant p53-expression (and not an unrelated characteristic of the H1299-p53^{R273H} cell line) that is responsible for generating conditioned medium capable of altering the migratory behaviour of recipient cells (Figure 4-4 B). It is well-established that the Golgi complex is orientated towards a cell's leading edge (They et al., 2006b). Previously published work has indicated that H1299 cells are able to effectively orientate their Golgi complex as they prepare to migrate into scratch-wounds, and that expression of mutant p53 significantly disturbs this indicator of cell polarity (Noske et al., 2009). We confirmed this observation, and also found that pre-treatment of p53^{-/-} cells with medium conditioned by p53^{R273H}-expressing cells was sufficient to significantly reduce the ability of p53^{-/-} cells to orientate their Golgi towards scratch-wounds (Figure 4-4 C). Thus, in regard of two key quantitative read-outs of cell migratory behaviour - FMI and Golgi orientation - the mutant p53-migratory phenotype may be communicated between cells via factor(s) that are released into the medium.

Wild-type p53 has a role in MVB-derived exosome release (Yu et al., 2006, Lespagnol et al., 2008). To test whether microvesicles might be responsible for

transfer of mutant p53's gain-of-function migratory phenotype, p53^{-/-} H1299 cells were pre-treated with medium conditioned by either p53^{-/-} or p53^{R273H}-expressing cells which had been depleted of microvesicles by differential centrifugation (figure 4-4 D). Depletion of microvesicles significantly reduced the ability of conditioned medium collected from p53^{R273H} cells to reduce the FMI of p53^{-/-} H1299 cells, indicating the likelihood that the released factor(s) responsible for transfer of mutant p53's migratory gain-of-function is/are associated with microvesicles.

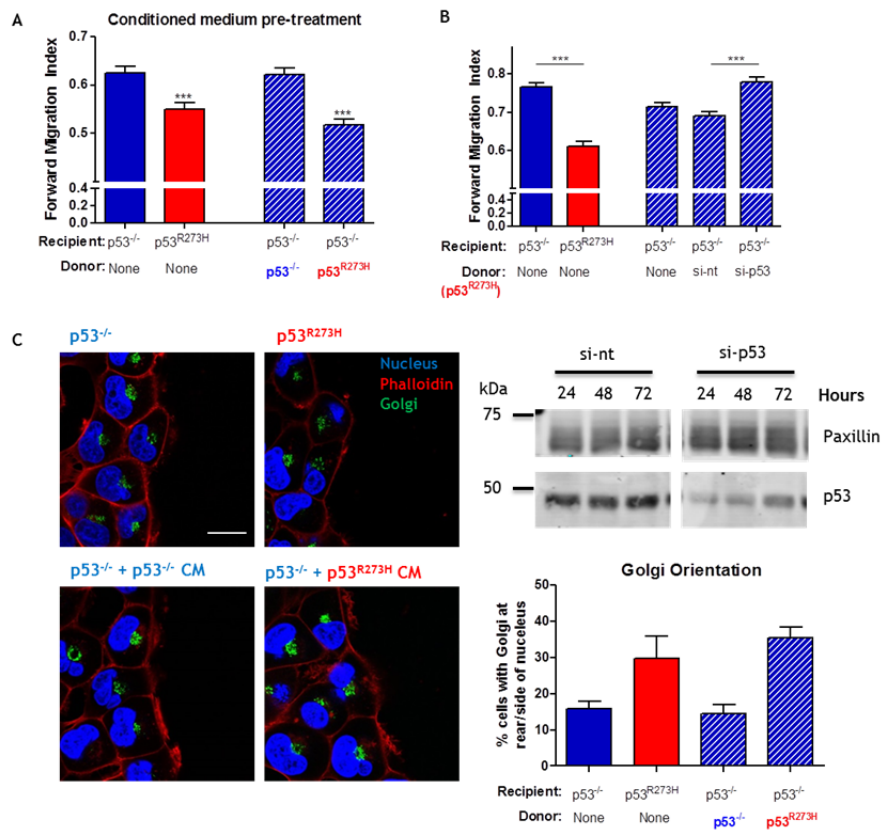


Figure 4-4: Conditioned medium from p53^{R273H}-expressing cells transfers the mutant p53 gain-of-function migratory phenotype to p53^{-/-} cells.

(A) Conditioned medium was collected from donor p53^{-/-} and p53^{R273H}-expressing cells and used to treat p53^{-/-} recipient cells for 72 hours. Cells were then re-plated and allowed to grow to confluence overnight. Confluent monolayers were wounded and migration of cells into the wound was followed by time-lapse microscopy as described in figure 4-1. n=4. Values are mean ± SEM. Kruskal Wallis. ***p<0.0001. (B) p53^{-/-} cells were subject to AMAXA transfection in the absence of siRNA (si-mock), with non-targeting siRNA (si-nt) or siRNAs targeting p53 (si-p53). These donor cells were then allowed to condition medium for 72 hours. Conditioned medium (mixed 1:1 with DMEM) was used to treat recipient p53^{-/-} cells for 72 hours before they were plated on plastic. The confluent monolayer was wounded 24 hours later and migration of cells closing the wound was imaged by time-lapse microscopy as in figure 4-1. n=3. Values are mean ± SEM. Kruskal Wallis. ***p<0.0001. The ability of siRNAs targeting p53 to reduce levels of mutant p53 in H1299 cells was confirmed using Western blotting. (C) Conditioned medium (CM) collected from p53^{-/-} and p53^{R273H}-expressing cells were used to treat p53^{-/-} cells for 72 hours. Cells were re-plated and the confluent monolayer was wounded 24 hours later. Cells were allowed to migrate for 2 hours before fixing using 4 % PFA, permeabilising with 0.5 % TritonX-100 and staining for F-actin (phalloidin), Golgi (GM130) and the nucleus (DAPI). Images were acquired by confocal microscopy at 60x magnification and the Golgi orientation with respect to the nucleus was scored. n=3. Values are mean ± SEM. Scale bar = 20 μm. (D) p53^{-/-} cells were treated with conditioned medium depleted of microvesicles collected from p53^{-/-} and p53^{R273H}-expressing cells, for 72 hours. The pre-treated cells were plated on plastic and a confluent monolayer was wounded 24 hours later. The migration of cells closing the wound was imaged by time-lapse microscopy as in figure 4-1. n=3. Values are mean ± SEM. Kruskal Wallis. ***p<0.0001.

4.2.3 Microvesicles released by p53^{R273H}-expressing cells transfer the mutant p53 migratory phenotype to p53^{-/-} cells

Having determined that microvesicles must be present within conditioned medium in order for mutant p53's migratory phenotype to be transferred to p53 null cells, we next wanted to establish whether the microvesicles isolated from p53^{R273H} expressing cells can function independently of other secreted factors within the conditioned medium. Therefore we isolated microvesicles from p53^{-/-} and p53^{R273H}-expressing cells and compared their ability to alter the migratory behaviour of p53^{-/-} cells. The experimental design is shown in figure 4-5.

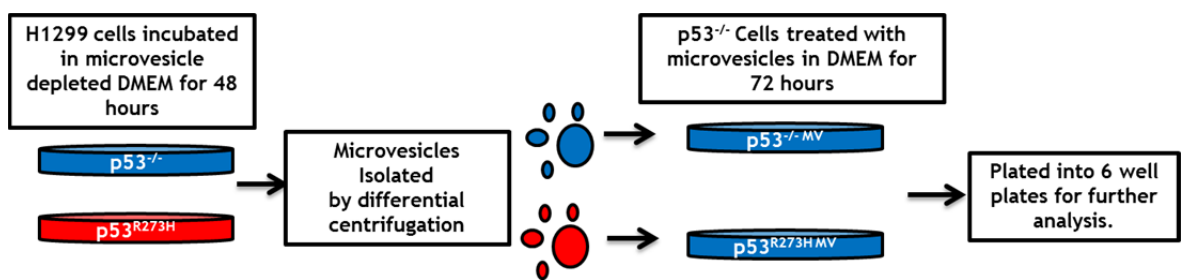


Figure 4-5: Diagram depicting the experimental design of microvesicle pre-treatment experiments.

Microvesicles were collected from p53^{-/-} and p53^{R273H} cells by differential centrifugation. Subsequently microvesicles were added to p53^{-/-} cells for 72 hours before cells were re-plated for further experimentation.

Pre-treatment of p53^{-/-} H1299 cells with microvesicles from p53^{R273H}-expressing cells reduced their FMI such that their movement was indistinguishable from that of mutant p53-expressing cells, whereas microvesicles from p53 null cells were ineffective in this regard (figure 4-6 A + B). Another characteristic of mutant p53 expressing cell migration is that they migrate with increased speed. As well as decreasing the FMI of cell migration, treatment of p53^{-/-} cells with microvesicles collected from p53^{R273H}-expressing cells also increases the cell migration speed of p53^{-/-} cells (data not shown). However, because the ability of conditioned medium from mutant p53-expressing cells to influence the migration speed of p53 null cells was not reproducibly demonstrable, I have elected not to present data pertaining to migration speed and have focussed on the consistently reproducible changes that I have observed in the FMI of conditioned medium and microvesicle-treated cells.

To determine whether the effect we observed was restricted to one particular p53 mutation (in this case R273H within the DNA binding region of p53), we

purified microvesicles from a H1299 cell line expressing the R175H p53 mutant, which is a conformational mutation that lies outside the DNA binding region (Freed-Pastor and Prives, 2012), and tested their ability to influence the migration of p53^{-/-} cells. Figure 4-6 (C) shows that microvesicles collected from H1299 cells expressing p53^{R175H} were as effective as those released by p53^{R273H}-expressing cells in reducing the FMI of p53^{-/-} cells. Furthermore, we wished to determine whether microvesicles from mutant p53-expressing cells were able to influence the migratory behaviour of cells other than H1299s. Treatment of A2780 ovarian cancer cells (which express wild-type p53) with microvesicles from H1299-p53^{R273H}-expressing cells significantly reduced the FMI of A2780 cells during migration into scratch-wounds, whereas microvesicles from H1299-p53^{-/-} cells were ineffective in this regard (Figure 4-6 D).

We wished to determine whether cell types other than the H1299 cell line were able to produce migration-altering microvesicles upon manipulation of their p53 status. To address this, we used MCF7 breast cancer cells which express wild-type p53 to generate an MCF7 cell line in which endogenous p53 expression was disrupted using CRISPR gene editing. We then used a retroviral expression system to express the R273H mutant of p53 in these MCF7-p53 null cells. Western blotting confirmed the CRISPR-mediated deletion of p53 in MCF7 cells, and showed the expression levels of both wild-type and mutant p53 in the MCF7 cells (Figure 4-6 F). We then collected microvesicles from the parental MCF7 cells and our engineered MCF7-p53^{-/-} and MCF7-p53^{R273H} cells and measured the influence of these on migration of H1299-p53^{-/-} cells into scratch-wounds. Pre-treatment with microvesicles from mutant p53-expressing MCF7 cells significantly reduced the FMI of H1299-p53^{-/-} cells migrating into scratch-wounds to much the same extent as did microvesicles from H1299-p53^{R273H} cells, whereas microvesicles from parental MCF7 cells or MCF-p53^{-/-} cells were ineffective in this regard (Figure 4-6 E). Taken together, these data indicate that mutant p53 is able to promote the generation of microvesicles through which a *bona fide* gain-of-function effect may be transmitted to other cells. Conversely, deletion of wild-type p53 does not significantly influence the ability of a cell to generate microvesicles that influence the FMI of other cells.

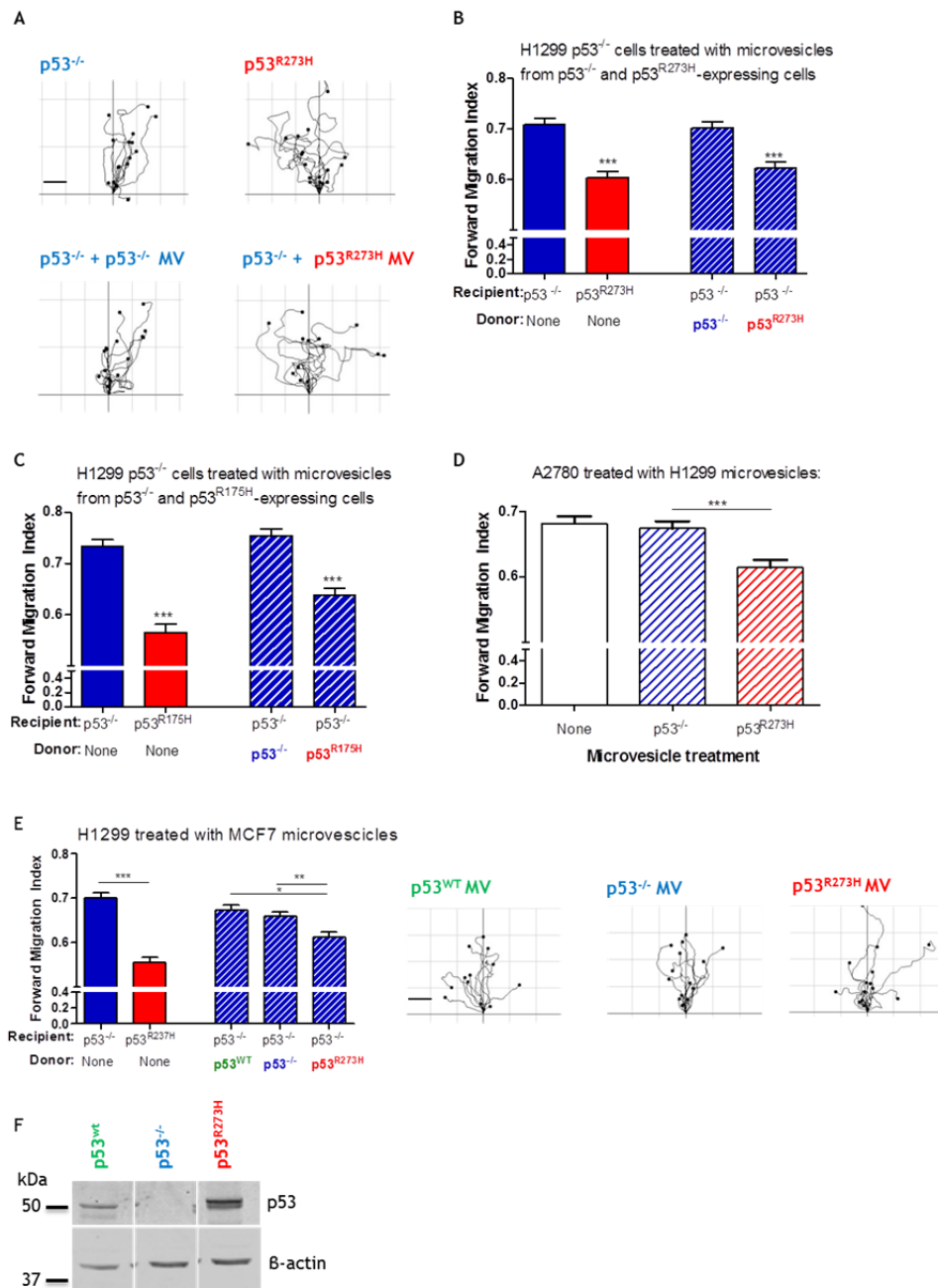


Figure 4-6: Microvesicles collected from p53^{R273H} and p53^{R175H} expressing cells can transfer the mutant p53 migratory phenotype to p53^{-/-} cells.

(A + B) Microvesicles were collected from p53^{-/-} and p53^{R273H} H1299 cells and used to pre-treat p53^{-/-} H1299 cells for 72 hours. Pre-treated cells were re-plated on plastic and their migration closing a wound analysed as in figure 4-1. Track-plots represent the migratory phenotypes of each condition (scale bar = 100 μ m). n=4. Values are mean \pm SEM. Kruskal Wallis. ***p<0.0001. (C) Microvesicles were collected from p53^{-/-} and p53^{R175H} expressing H1299 cells and protocol followed as in A & B. n=2. Values are mean \pm SEM. Kruskal Wallis. ***p<0.0001. (D) A2780 cells were treated with microvesicles collected from H1299 cells null for p53^{-/-} or H1299 cells expressing mutant p53^{R273H}. H1299 cells were plated on plastic and the confluent monolayer wounded 24 hours later. Migration of cells closing the wound was analysed as in figure 4-1. n=3. Values are mean \pm SEM. Kruskal Wallis. ***p<0.0001. (E) H1299 p53^{-/-} cells were pre-treated with microvesicles collected from parental MCF7 (p53^{WT}) cells, MCF7 cells with p53 deleted using CRISPR gene editing (p53^{-/-}) and MCF7-p53^{-/-} cells with retrovirally expressed mutant p53 (p53^{R273H}). Again the migration of H1299 cells closing the wound was analysed as in figure 4-1, track-plots are shown to represent the migration of H1299 p53^{-/-} cells in each condition. Scale bar = 100 μ m. n=4. Values are mean \pm SEM. Kruskal Wallis. *p=0.01. **p=0.001. ***p<0.0001. (F) The p53 status of parental and genetically engineered MCF7 cells is shown by Western blotting.

The FMI of cells migrating into scratch-wounds can be measured relatively quickly and easily, and the ability of mutant p53 to alter this metric of migratory behaviour greatly facilitated our identification of microvesicles as a potential vector for mutant p53's pro-invasive gain-of-function. However, in order to fully test the postulate that microvesicles can transfer mutant p53's pro-invasive gain-of-function we needed to perform a more comprehensive analysis of the cellular functions known to be influenced by mutant p53. Expression of p53^{R273H} has previously been shown to increase the rate at which internalised α 5B1 integrin, EGFR and cMET are returned (or recycled) to the plasma membrane and this is thought, in turn, to drive increased invasiveness in 3D microenvironments (Noske et al., 2009, Muller et al., 2013). We therefore pre-treated H1299-p53^{-/-} cells with microvesicles from either p53^{-/-} or p53^{R273H}-expressing cells. Following this, receptors were labelled at the plasma membrane and allowed to internalise into endosomes for 30 minutes. We then measured the rate at which these internalised receptors returned to the cell surface. In H1299 p53^{-/-} cells pre-treated with microvesicles collected from p53^{R273H}-expressing cells, α 5B1, EGFR1 and cMET returned to the plasma membrane significantly more rapidly than in p53^{-/-} cells pre-treated with p53^{-/-} microvesicles (Figure 4-7 A). To determine whether this marked alteration to receptor trafficking was accompanied by increased invasion, we measured the ability of microvesicle pre-treated cells to penetrate Geltrex (a Matrigel substitute). Indeed, H1299 p53^{-/-} cells pre-treated with microvesicles from p53^{R273H}-expressing cells invaded significantly further into Geltrex plugs than did the same cells pre-treated with microvesicles from p53^{-/-} cells (Figure 4-7 B).

It is thought that estimates of invasiveness using assays such as the inverted invasion assay may be influenced by the proliferation rate of the cells plated into the assay. We, therefore, determined whether microvesicle pre-treatment altered growth of H1299 cells. However, H1299 cells proliferated at identical rates irrespective of their mutant p53 status and whether or not they had been pre-treated with microvesicular preparations from p53^{-/-} or p53^{R273H}-expressing cells (Figure 4-7 C).

Taken together, these data indicate that microvesicles can transfer mutant p53's pro-invasive and migratory gain-of-function behaviour between cells (without affecting their proliferative capacity), and that this is likely mediated

via the ability of microvesicles from mutant p53-expressing cells to increase recycling of integrins and RTKs in recipient cells.

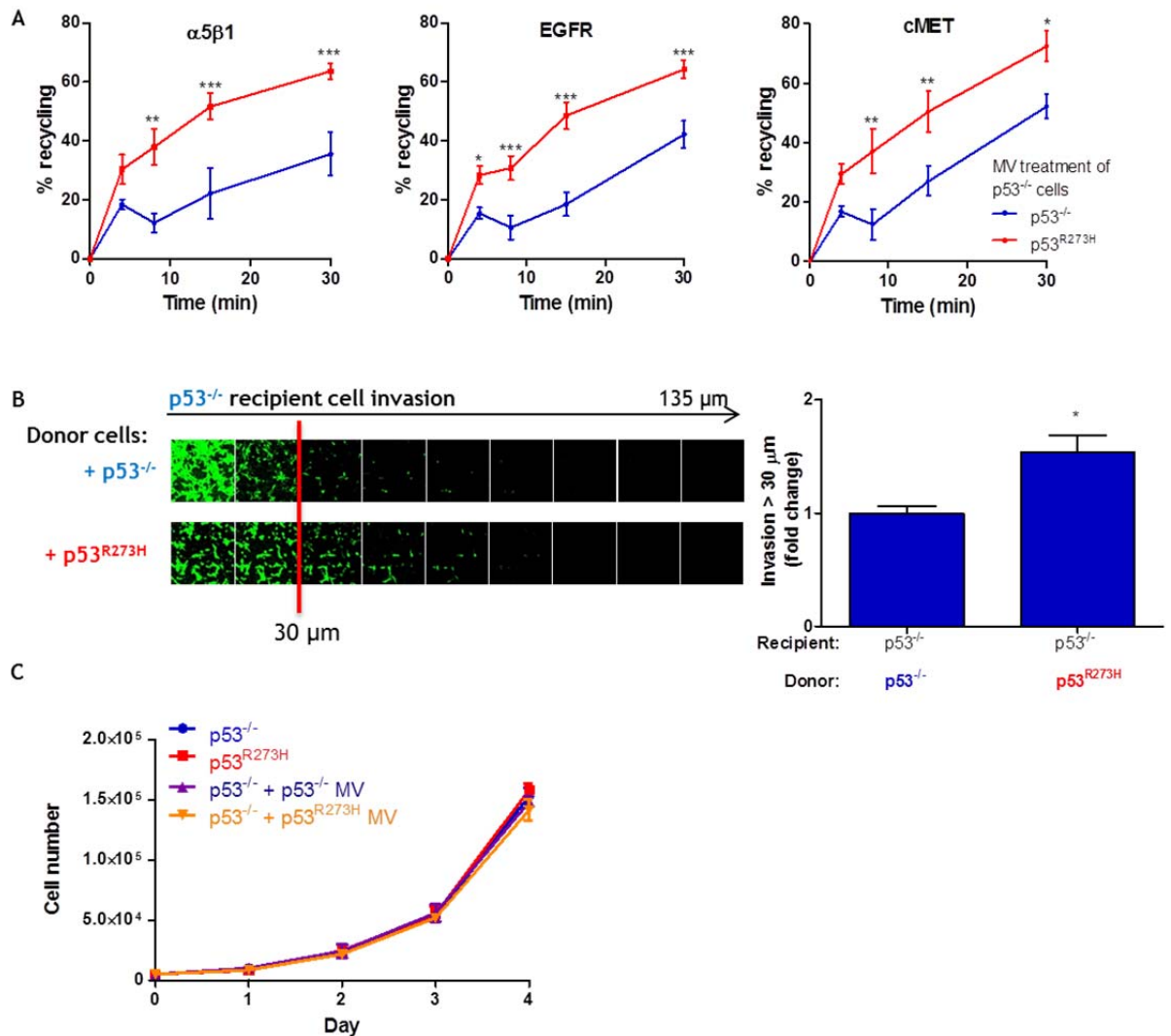


Figure 4-7: Microvesicles from p53^{R273H} expressing cells increase the receptor recycling rate and invasive capacity of p53^{-/-} cells.

(A) p53^{-/-} H1299 cells were treated with microvesicles collected from p53^{R273H}-expressing or p53^{-/-} H1299 cells for 72 hours. Cells were then re-plated onto 10cm plastic dishes and allowed to grow to 80 % confluence for 72 hours. Surface proteins were biotinylated using NHS-SS-biotin at 4 °C and allowed to internalise for 30 minutes at 37 °C. Biotin remaining at the cell surface was removed by cell surface reduction at 4°C, and internalised receptors were allowed to recycle to the plasma membrane for the indicated times. A second reduction step was used to remove biotin from receptors that had returned to the cell surface and the amount of biotinylated receptors (α5β1, EGFR1, and cMET) remaining within the cells was determined by capture-ELISA. n=3. Values are mean ± SEM. Two way ANOVA. **p<0.01. ***p<0.001. (B) p53^{-/-} H1299 cells were pre-treated with microvesicles collected from p53^{-/-} and p53^{R273H} expressing H1299 cells before being plated on a transwell membrane for an inverted invasion assay as described in figure 4-1. Briefly cells were allowed to invade through a Geltrex plug supplemented with 25 μg/ml fibronectin for 72 hours. Cells were visualised and imaged using a 4 μg/ml Calcein-AM treatment and confocal microscopy acquiring images every 15 μm starting from the transwell membrane. Olympus Fluoview FV1000 microscope was used at 20x magnification. n=4. Values are mean ± SEM. Mann-Whitney. *p<0.0249. (C) p53^{-/-} cells were treated with microvesicles collected from either p53^{-/-} or p53^{R273H}-expressing cells and plated at a low density to assess proliferation. Cells were counted every day for 4 days until cells reached confluence. n=2. Values are mean ± SEM.

4.2.3.1 Effect of microvesicles from p53^{R273H}-expressing cells on mRNA expression

After firmly establishing that microvesicles released by p53^{R273H} expressing cells have the ability to transfer the mutant p53 gain-of-function invasive migratory phenotype to cells null for p53, it was subsequently necessary to examine the mechanism by which microvesicles from p53^{R273H} cells exert their effects. Expression of p53^{R273H} can alter the gene expression of cells due to its decreased capacity to bind DNA and to act as a transcription factor (O'Farrell et al., 2004, Cho et al., 1994). Some of the transcriptional changes exerted by mutant p53 expression contribute to gain-of-function phenotypes (Di Agostino et al., 2006). The mechanism through which this occurs is discussed in detail in chapter one but, as an example, our lab has found that mutant p53 expression can exert its gain-of-function invasive phenotype by inhibiting the transcriptional activity of tumour suppressor p63 (Muller et al., 2009). Therefore we investigated whether microvesicles from p53^{R273H}-expressing cells are able to potentially alter the gene expression profile of p53^{-/-} cells. An in-depth RNASeq analysis showed that p53^{-/-} and p53^{R273H} cells have very different patterns of mRNA expression from one another. However, in spite of marked alterations to their receptor trafficking and cell migratory and invasive characteristics, H1299 cells treated with microvesicles from p53^{R273H}-expressing cells displayed a mRNA expression profile that was indistinguishable from cells treated with microvesicles from p53^{-/-} cells. This suggested that the transferred mutant p53 gain-of-function migratory phenotype was not attributable to any overt changes in gene transcription (figure 4-8).

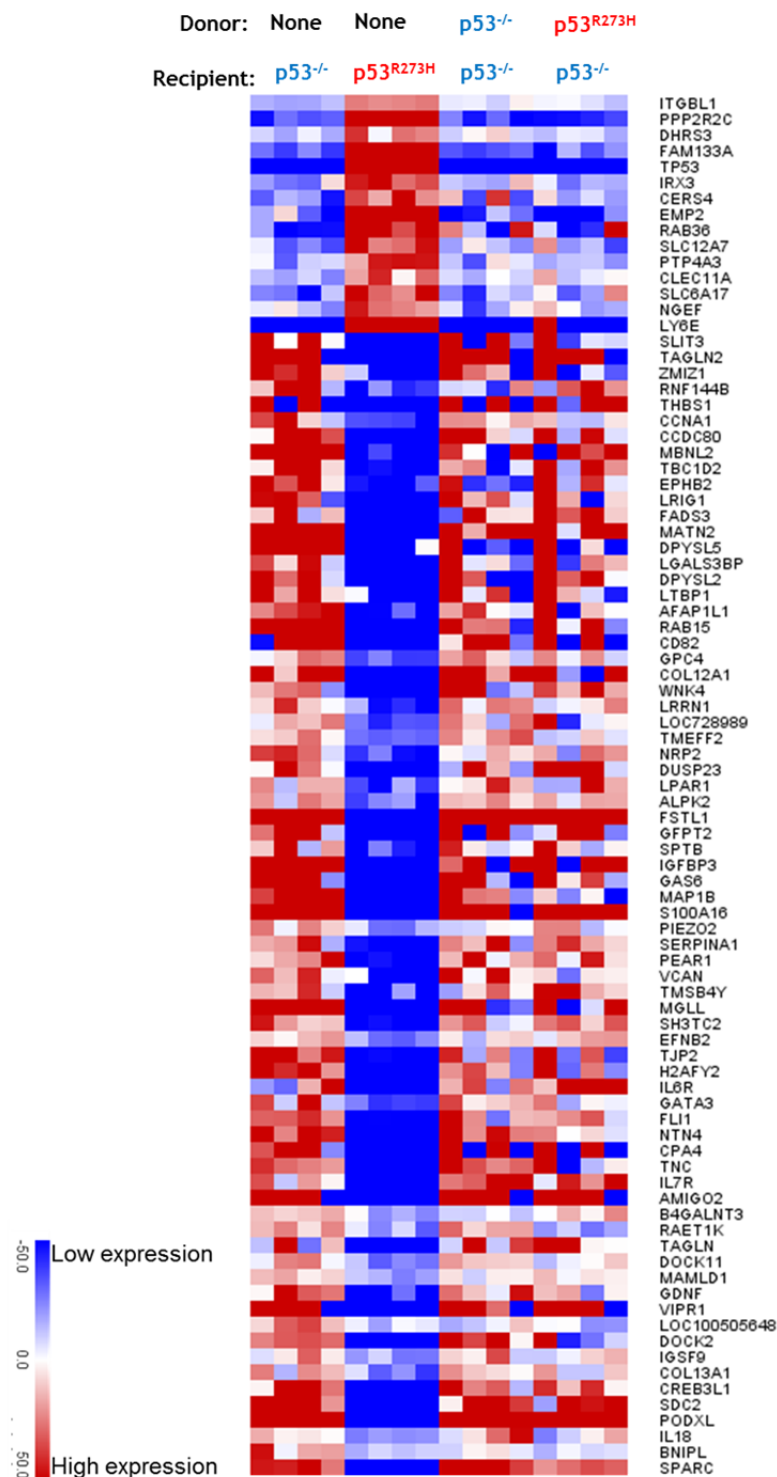


Figure 4-8: Microvesicles from mutant p53-expressing cells are not able to detectably alter the mRNA expression profile of H1299 cells.

H1299 cells null for p53^{-/-} were treated with microvesicles from p53^{-/-} or p53^{R273H}-expressing H1299 cells for 72 hours. Cells were then re-plated and RNA was collected 24 hr later. RNA concentration was determined by Qubit assay and its quality by Agilent bioanalysis. 4 µg RNA was used to create cDNA libraries for next generation RNA sequencing using the Genome Analyser 11x. Shown is a heatmap of the mRNA transcripts that are the most significantly changed between p53^{-/-} and p53^{R273H}-expressing H1299 cells. n=4. RNA sequencing and bioinformatic analysis was performed in collaboration with Billy Clark and Gabriela Kalna at the Beatson Institute for Cancer Research.

4.2.3.2 RCP and DGK α are required for the response of H1299 cells to microvesicles from mutant p53-expressing cells, but not for generation of migration-altering microvesicles.

Many aspects of the mutant p53 migratory phenotype, including increased integrin and RTK recycling, reduced FMI, and increased invasiveness, are dependent upon RCP. Moreover, we have shown that the function of RCP relies on DGK α to generate a source of PA which associates with RCP's C2 domain to allow docking of recycling vesicles with the plasma membrane. Thus it is possible that RCP and DGK α contribute to the generation of microvesicles which are capable of transferring mutant p53's gain-of-function migratory phenotype. To investigate this, we used siRNA to knock down RCP or DGK α in H1299-p53^{R273H} cells and tested the ability of conditioned medium collected from these donor cells to influence migration of recipient H1299-p53^{-/-} cells. This indicated that knockdown of either RCP or DGK α did not affect the ability of mutant p53-expressing cells to release microvesicles with the capacity to reduce the FMI of p53^{-/-} cells (figure 4-9 A + B). In view of this we proposed that RCP and DGK α may be required for recipient cells to mount a migratory response to microvesicles from mutant p53-expressing cells. To investigate this, we used siRNA to silence RCP expression, or a pan DGK inhibitor (R59022) to inhibit DGK activity in recipient H1299 cells, and tested their ability to respond to microvesicles from mutant p53-expressing cells. This indicated that siRNA of RCP or pharmacological inhibition of DGK α ablated the ability of p53^{-/-} recipient cells to reduce their FMI in response to microvesicles from mutant p53-expressing cells, whereas non-targeting siRNAs or a vehicle control (DMSO) were ineffective in this regard (Figure 4-9 C + D). Taken together these data indicate that DGK α and RCP are not required in p53^{R273H}-expressing cells for the production of microvesicles with the capacity to evoke the mutant p53 gain-of-function phenotype. However, H1299-p53^{-/-} cells do need to express RCP and DGK α in order to alter their cell migration in response to microvesicles from mutant p53-expressing cells.

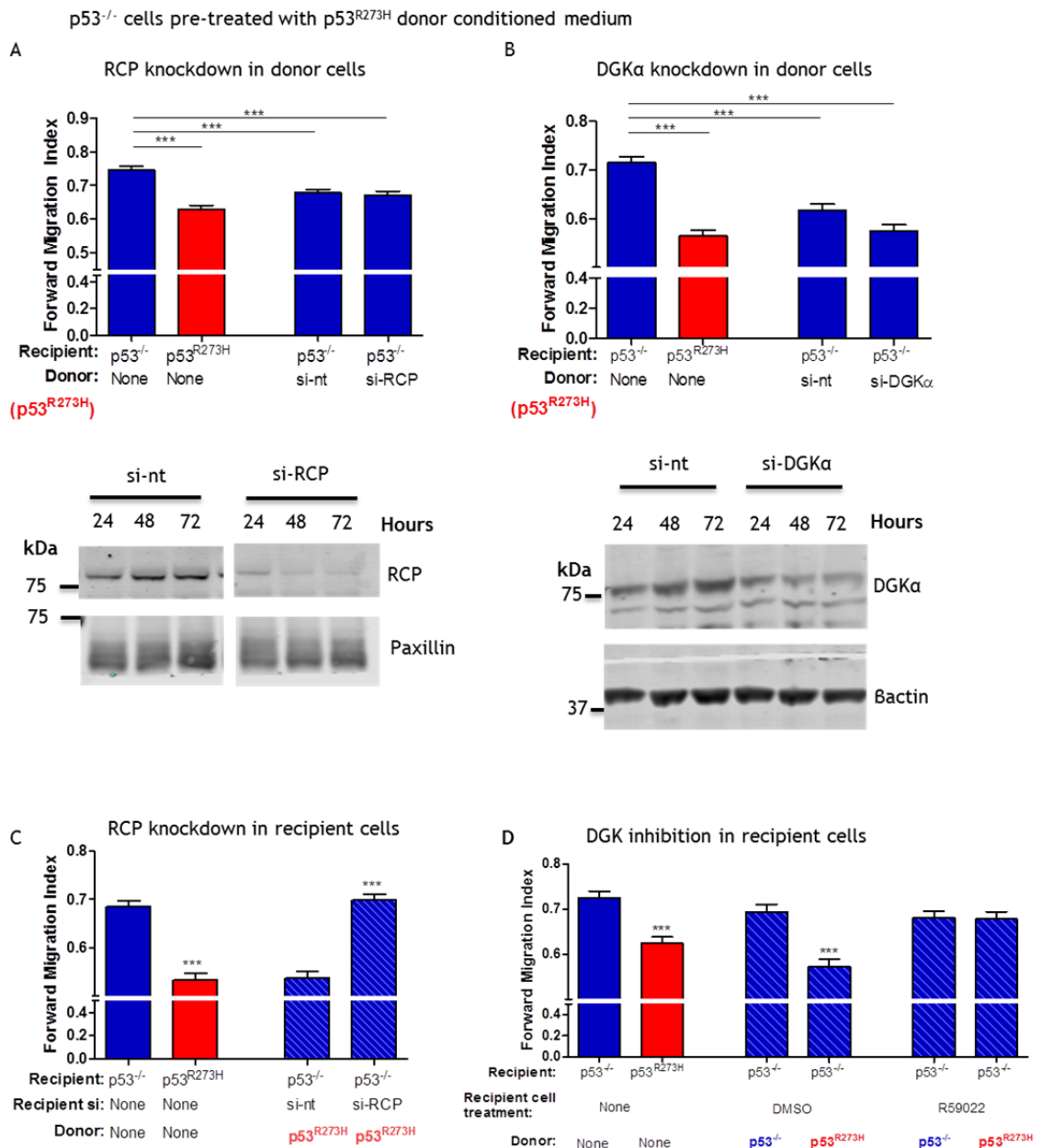


Figure 4-9: RCP and the activity of DGKα are required for response of H1299 cells to microvesicles from mutant p53-expressing cells.

(A + B) p53^{R273H} expressing H1299 cells were transfected with siRNAs targeting RCP (si-RCP), DGKα (si-DGKα) and a non-targeting control (si-nt). Conditioned medium collected from these cells was used to treat p53^{-/-} H1299 cells for 72 hours. The pre-treated cells were then plated onto plastic, allowed to grow to confluence and then scratch-wounded. Cell migration during wound closure was analysed as described in figure 4-1. Representative Western blot images are shown to demonstrate RCP and DGKα knockdown at 24, 48 and 72 hours after transfection of donor p53^{R273H}-expressing cells with siRNAs targeting RCP or DGKα or a non-targeting control (si-nt). n=3. Values are mean ± SEM. Kruskal Wallis. ***p<0.0001. (C) p53^{-/-} H1299 cells were treated with microvesicles from p53^{R273H}-expressing H1299 cells for 72 hours. Cells were then transfected with si-RNAs targeting RCP (si-RCP) or a non-targeting control (si-nt) before being plated onto plastic. The confluent monolayer was then wounded and migration of cells analysed as in figure 4-1. n=3. Values are mean ± SEM. Kruskal Wallis. ***p<0.0001. (D) p53^{-/-} cells were treated with microvesicles from p53^{-/-} or p53^{R273H}-expressing cells for 72 hours. Cells were plated on plastic and the confluent monolayer was wounded and treated with 10 μM of a DGK inhibitor (R59022) or vehicle control (DMSO). The migration of cells closing the wound was tracked as in figure 4-1. n=4. Values are mean ± SEM. Kruskal Wallis. ***p<0.0001.

4.2.3.3 Rab35 (but not Rab27) is required for production of migration-altering microvesicles

Both Rab27a and Rab27b have important roles in the release of MVB-derived exosomes (Ostrowski et al., 2010). We, therefore, determined whether expression of Rab27a and Rab27b are required for donor p53^{R273H}-expressing cells to produce conditioned medium that is capable of influencing the migration of H1299 recipient cells. Combined knockdown of Rab27a (verified by Western blotting) and Rab27b (verified using qPCR) did not affect the ability of mutant p53-expressing cells to produce conditioned medium that was capable of suppressing the FMI of p53^{-/-} H1299 cells (figure 4-10 A - C). We, therefore, investigated other Rab subfamily GTPases that have been shown to influence microvesicle production. Although less well-characterised than the Rab27s, Rab35 is known to influence cell migration and invasion (Zhu et al., 2013, Allaire et al., 2013) and one report indicates that Rab35 contributes to MVB-derived exosome production (Hsu et al., 2010). We knocked down Rab35 in mutant p53-expressing donor cells for 72 hours (Figure 4-10 F) and found that this significantly reduced the ability of conditioned medium (Figure 4-10 D) and microvesicles (Figure 4-10 E) collected from these cells to suppress the FMI of recipient H1299 cells. Taken together, these data indicate that Rab35 is involved in production of microvesicles that contribute to the transfer of mutant p53's migratory gain-of-function between cells. By contrast, Rab27s, which are the Rab-GTPases with the most well-characterised role in microvesicle generation and release, do not contribute to this process.

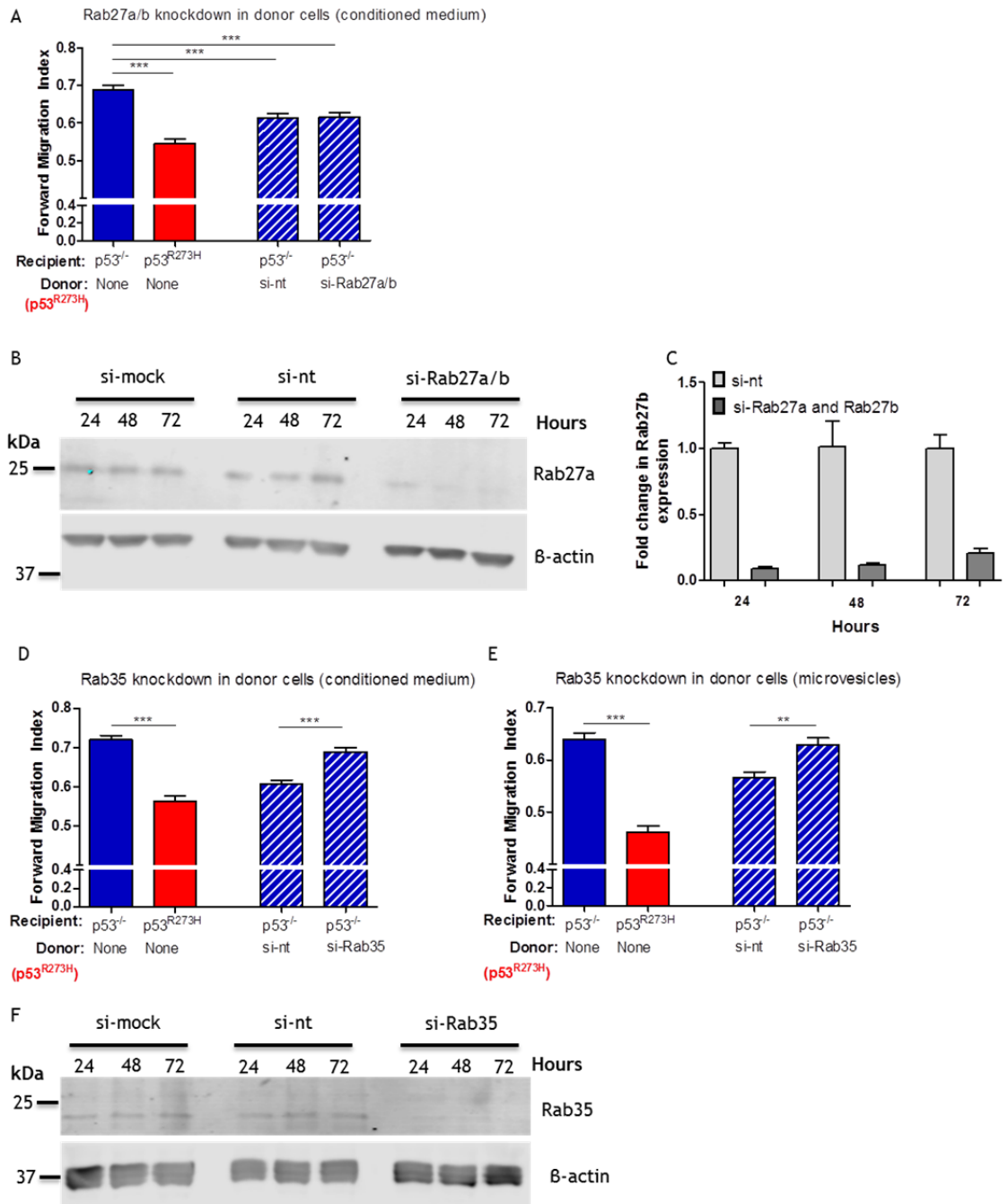


Figure 4-10: Rab35 (but not Rab27) is required for release of migration-altering microvesicles from mutant p53-expressing cells.

Conditioned medium (A & D) or microvesicles (E) were collected from p53^{R273H}-expressing H1299 cells which had been AMAXA transfected with siRNAs targeting Rab27a and Rab27b (si-Rab27a/b), Rab35 (si-Rab35) or a non-targeting control (si-nt). Conditioned medium or microvesicles from these cells were used to treat p53^{-/-} H1299 cells for 72 hours before re-plating on plastic to analyse the migration of cells closing the wound as in figure 4-1. n=3. Values are mean ± SEM. Kruskal Wallis. **p<0.001. ***p<0.0001. (B) Representative Western blot of si-Rab27a silencing in p53^{R273H}-expressing cells over 72 hours. (C) Representative mRNA knockdown of Rab27b in p53^{R273H}-expressing cells as determined by quantitative PCR (q-PCR). Briefly RNA was collected at 24, 48 and 72 hours after siRNA transfection. RNA was quantified and 1 µg was used to synthesise cDNA. 1 µl of cDNA was used for q-PCR with quantitect GAPDH control primers or Rab27b primers and Syber Green master mix. (F) Representative Western blot showing Rab35 silencing at 24, 48 and 72 hours after siRNA transfection of p53^{R273H}-expressing cells.

Despite our observations that they are functionally distinct, microvesicles released from Rab35 silenced p53^{R273H}-expressing cells, were physically indistinguishable from microvesicles collected from cells that express Rab35. Indeed, as shown in figure 4-11, knockdown of Rab35 did not alter the protein content (Qubit assay) (A), size (B + C) and particle concentration (D) (as determined by nanoparticle tracking analysis) of microvesicles purified by differential centrifugation. It is possible that any differences in the release of a minority sub-population of microvesicles, is not detectable using these approaches (as discussed in chapter 3). Alternatively Rab35 may have a role in sorting a specific functional cargo into the microvesicles rather than changing the quantity or size distribution of microvesicles released by p53^{R273H}-expressing cells.

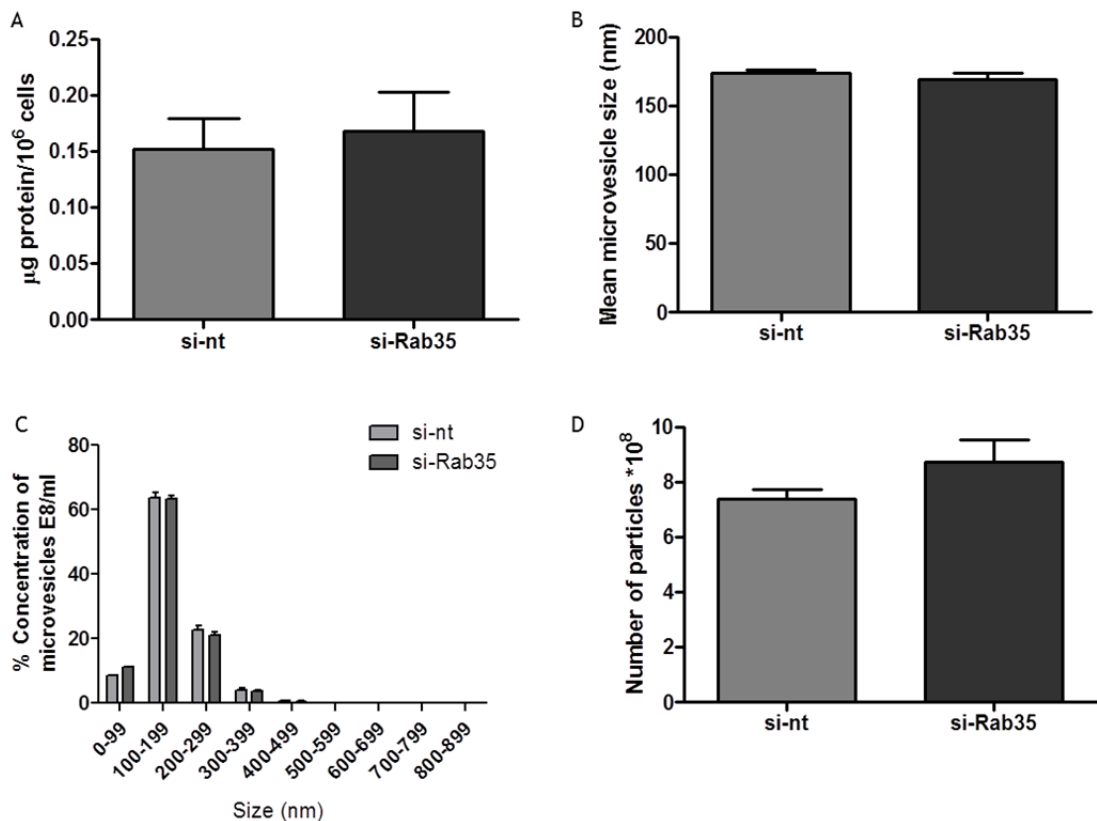


Figure 4-11: Rab35 silencing has no detectable influence on the number or size of microvesicles released from mutant p53-expressing cells.

Microvesicles were isolated from p53^{R273H}-expressing cells transfected with siRNAs targeting Rab35 (si-Rab35) or a non-targeting control (si-nt). Microvesicle protein content was determined using Qubit assay (A). NanoSight nanoparticle tracking analysis was used to determine the mean microvesicle size (B), size distribution (C) and particle concentration (C). n=2. Values are mean ± SEM.

4.2.3.4 Podocalyxin is required for production of microvesicles that influence receptor trafficking and migration in recipient cells

Our RNA sequencing analysis indicated that microvesicles from mutant p53-expressing cells influenced the endocytic trafficking and migratory characteristics of p53 null cells without detectably altering gene expression in these recipient cells. This indicated the possibility that microvesicles from mutant p53-expressing cells may act directly on the endomembrane system of recipient cells. Mass spectrometry indicated that podocalyxin (PODXL), a highly-charged sialomucin which is known to directly influence membrane organisation, was detectable in microvesicles isolated using differential centrifugation (Chapter 3). Furthermore, we reasoned that if PODXL was involved in functional microvesicle biogenesis, or if it were to be a candidate cargo protein that is packaged into microvesicles in a Rab35-dependent manner then it might, at least at some point in its progress through the endocytic pathway, associate physically with Rab35. To test for physical association between Rab35 and PODXL, we expressed GFP-tagged Rab35 in H1299 cells, immunoprecipitated this fusion protein using an antibody recognising GFP, and looked for the presence of PODXL in these immunoprecipitates using Western blotting. This analysis clearly indicated that PODXL co-immunoprecipitated with GFP-Rab35, but was not present in control immunoprecipitates in which cells were not transfected with GFP-Rab35 (Figure 4-12).

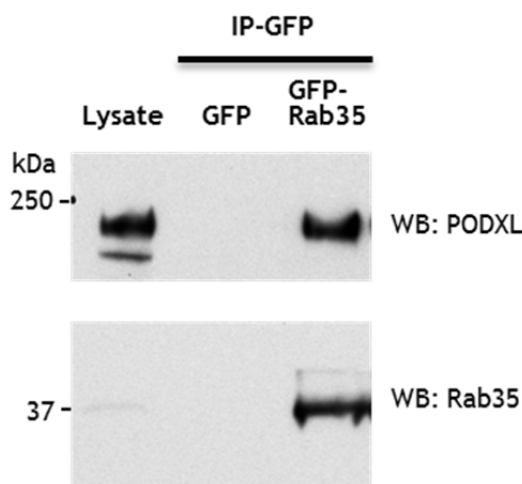


Figure 4-12: Podocalyxin co-immunoprecipitates with GFP-Rab35.

H1299 cells were transfected with GFP-Rab35 or GFP control. 24 hours following transfection, cells were lysed in a buffer containing 0.15% Tween-20. GFP was immunoprecipitated (IP) from lysates using magnetic beads conjugated to an antibody recognising GFP. Immunoprecipitated proteins were separated by SDS-PAGE, GFP-Rab35 and podocalyxin were detected by Western blotting (WB). n=2.

This potential physical association between Rab35 and PODXL lead us to investigate whether PODXL contributed to the ability of p53^{R273H}-expressing cells to generate microvesicles with the capacity to influence integrin receptor trafficking and cell migration. Microvesicles were purified from mutant p53-expressing cells in which PODXL had been knocked down using siRNA (Figure 4-13 C). Microvesicles from PODXL knockdown H1299-p53^{R273H} cells had a significantly reduced capacity to promote integrin recycling and to reduce the FMI of p53^{-/-} cells, indicating that PODXL is a key factor responsible for transmitting mutant p53's gain-of-function phenotype between cells (Figure 4-13 A + B).

In addition to looking at microvesicle-mediated transfer of receptor trafficking and migratory characteristics to other cells, we also investigated the consequences of PODXL knockdown on the behaviour of the mutant p53-expressing cells themselves. Interestingly, knockdown of PODXL strongly suppressed integrin recycling in H1299-p53^{R273H} cells to levels that were similar to those found in p53 null cells (Figure 4-13 E). Moreover, siRNA of PODXL significantly increased the FMI of p53^{R273H}-expressing H1299 cells, whereas control siRNA was ineffective this regard (Figure 4-13 D).

These data indicate that, not only is PODXL required to transfer aspects of mutant p53's gain-of-function phenotype to other cells, but that it is required for maintenance of the receptor trafficking and migratory phenotypes of the mutant p53-expressing cells themselves. This observation raises the possibility that an autocrine mechanism (in which mutant p53-expressing cells are influenced by microvesicles that they themselves have produced) may form an essential link between mutant p53 expression and the receptor trafficking and migratory machinery.

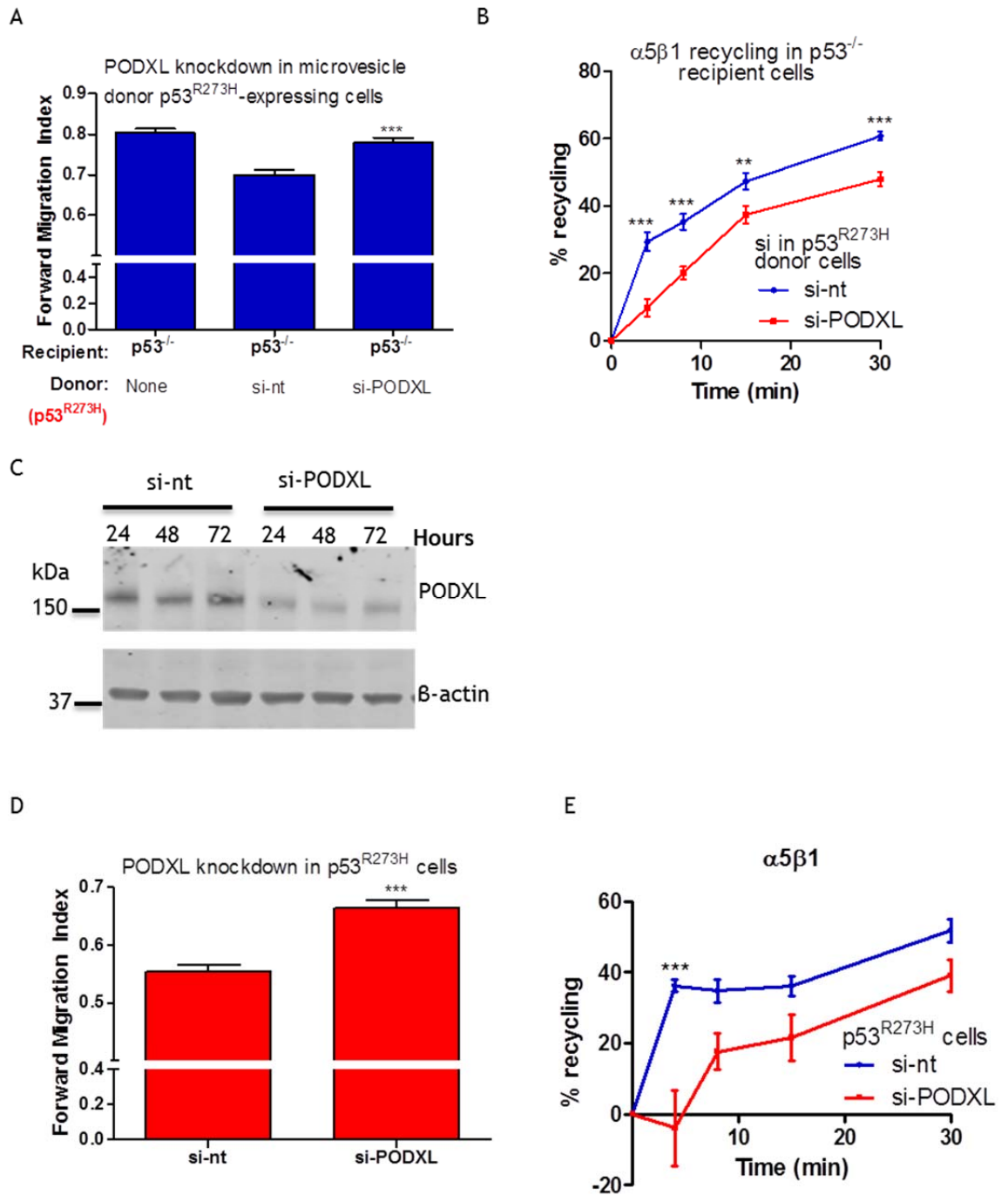


Figure 4-13: Podocalyxin is necessary for mutant p53 gain-of-function phenotype, and for transfer of the mutant p53 phenotype to p53^{-/-} cells via a microvesicle vector.

(A + B) p53^{R273H} cells were transfected with siRNA targeting PODXL (si-PODXL) or a non-targeting control (si-nt). Microvesicles were collected from these cells and used to treat p53^{-/-} cells. 24 hours later cells were wounded and their migration closing the wound was analysed by time-lapse microscopy as detailed in figure 4-1, maintaining the presence of microvesicles. n=3. Values are mean \pm SEM. Kruskal Wallis. ***p<0.0001 (A). Alternatively cells were plated onto plastic for a recycling assay as detailed in figure 4-7. n=3. Values are mean \pm SEM. Two way ANOVA. **p<0.01. ***p<0.001 (B). (C) Representative Western blot of PODXL knockdown in microvesicle donor p53^{R273H}-expressing cells at 24, 48 and 72 hours after AMAXA si-PODXL transfection. (D + E) p53^{R273H} cells were transfected with siRNA targeting PODXL (si-PODXL) or a non-targeting control (si-nt). 24 hours following this, the FMI of cell migration into scratch-wounds was analysed as described in figure 4-1 and the integrin recycling rates were analysed as described in figure 4-7. (D) n=3. Values are mean \pm SEM. Mann-Whitney. ***p<0.0001. (E) n=2. Values are mean \pm SEM. Two way ANOVA. ***p<0.001. Recycling assays done by Jim Norman, the Beatson Institute for Cancer Research.

4.2.3.5 Rab35 maintains the mutant p53 gain-of-function phenotype via an autocrine mechanism

The observations made in the previous sections indicate the possibility that microvesicle-mediated autocrine and paracrine mechanisms may contribute to the manifestation of mutant p53's gain-of-function phenotype. We therefore investigated the possibility that microvesicles from p53^{R273H}-expressing cells may be able to influence microvesicle production in other cells. Figure 4-14 (A) shows that a significant reduction in FMI is detectable even when microvesicles from mutant p53-expressing cells were added to recipient p53^{-/-} cells at the point of introducing the scratch-wound. This microvesicle-induced alteration to the FMI was then subsequently detectable for up to 96 hours following a 72 hour microvesicle pre-treatment even though cells were returned to normal tissue culture medium (Figure 4-14 B). We had previously found that microvesicles from p53^{R273H}-expressing cells did not change gene expression in recipient p53^{-/-} cells. Additionally PODXL is necessary for both the mutant p53 gain-of-function phenotype, as well as the mutant p53 non-cell-autonomous phenotype transfer to other cells. We therefore hypothesised that such a long-term change in cell migration could be maintained by an autocrine feed-forward mechanism.

To test this hypothesis, conditioned medium was collected from p53^{-/-} cells that had been previously pre-treated with microvesicles from p53^{-/-} or p53^{R273H}-expressing cells. The conditioned medium collected from these cells were then used to pre-treat other p53^{-/-} cells whose migratory behaviour we then examined. Conditioned medium from p53^{-/-} cells pre-treated with conditioned medium from p53^{R273H}-expressing cells, was able to decrease the FMI (i.e. transmit the mutant p53 gain-of-function phenotype) to p53^{-/-} cells (Figure 4-14 C). This suggested that p53^{-/-} cells may be educated by microvesicles from p53^{R273H}-expressing cells to themselves produce phenotype-altering microvesicles. A mechanism such as this may allow long-term maintenance of the mutant p53 phenotype within a population of cells which do not all express mutant p53 in an autocrine/paracrine fashion.

As already described in previous figures, the release of functional microvesicles from p53^{R273H}-expressing cells was found to be dependent on Rab35 and PODXL. Interestingly, siRNA of Rab35 opposed the mutant p53-driven reduction in FMI,

indicating that the generation of the mutant p53's phenotype in the mutant p53-expressing cells themselves was dependent upon expression of Rab35 as well as PODXL. The silencing of Rab35 in p53^{R273H} expressing cells resulted in an increase in the persistence of migration, reminiscent to the p53^{-/-} cells' migratory phenotype (Figure 4-14 D). Interestingly, the loss of mutant p53 migratory phenotype upon Rab35 silencing was partially restored by addition of p53^{R273H} microvesicles. Overall these data indicate that maintenance of the mutant p53 phenotype was reliant upon Rab35 and PODXL dependent release of microvesicles which initiate an autocrine positive feedback loop upon recipient cells driving increased integrin recycling and consequent migration and invasion (D).

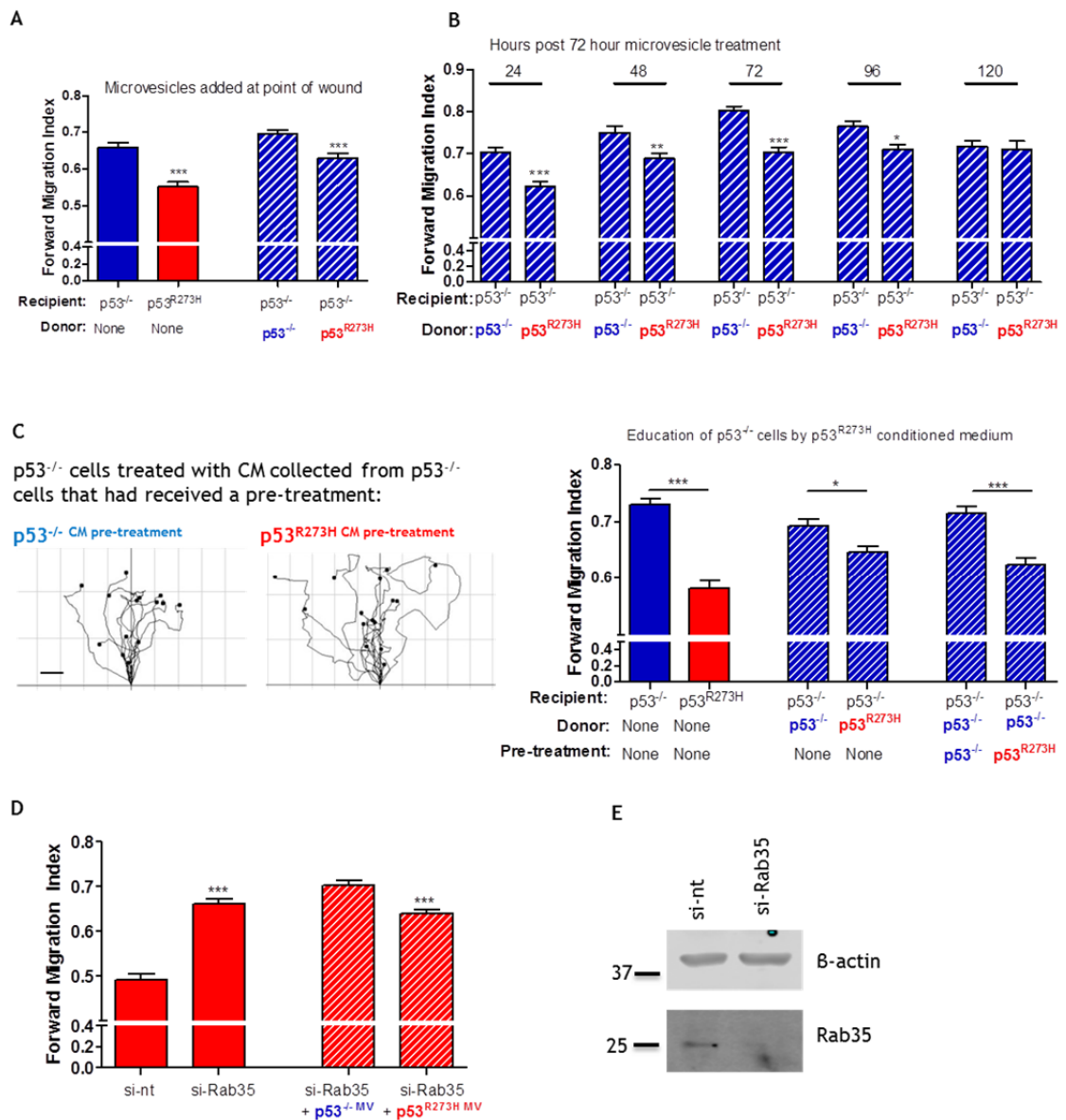


Figure 4-14: The mutant p53 gain-of-function migratory phenotype is maintained in p53^{R273H}-expressing cells and in microvesicle-educated p53^{-/-} cells in an autocrine/paracrine fashion. (A) p53^{-/-} cells were plated for wound healing, 24 hours later at the point of wounding, p53^{-/-} or p53^{R273H} microvesicles were spiked into the medium. Cells were then subject to time-lapse analysis of wound closure as in figure 4-1. n=3. Values are mean ± SEM. Kruskal Wallis. ***p<0.0001. (B) p53^{-/-} cells were pre-treated for 72 hours with p53^{-/-} or p53^{R273H} microvesicles. After microvesicle pre-treatment cells were returned back to a normal tissue culture regimen. Each day after pre-treatment the cells were plated for wound healing analysis as in figure 4-1 until the effect on migration was no longer apparent. n=2. Values are mean ± SEM. Kruskal Wallis. *p<0.01. **p<0.001. ***p<0.0001. (C) Conditioned medium was collected from p53^{-/-} cells that had been pre-treated for 72 hours with p53^{-/-} or p53^{R273H} conditioned medium. Collected conditioned medium was used to treat p53^{-/-} cells for 72 hours, cells were then plated onto plastic. Cells were then wounded and their migration closing the wound tracked as described in figure 4-1. n=2. Values are mean ± SEM. Kruskal Wallis. *p<0.01. ***p<0.0001. (D) p53^{R273H}-expressing cells were transfected with si-Rab35 or control si-nt. Concomitantly Rab35 silenced cells were treated with microvesicles from p53^{R273H}-expressing or p53^{-/-} cells. 24 hours later cells were wounded and migration during wound closure was analysed as in figure 4-1. n=3. Values are mean ± SEM. Kruskal Wallis. ***p<0.0001. (E) Representative Western blot showing silencing of Rab35 24 hours after siRNA transfection targeting si-Rab35 or control si-nt.

4.3 Discussion

4.3.1 Mutant p53 microvesicles

Here we show that the mutant p53 gain-of-function migratory and invasive phenotype is non-cell-autonomous and can be transferred to cells that are null for p53^{-/-} via a microvesicle vector. This expands the findings of Neilsen and colleagues, who found that conditioned medium collected from mutant p53 expressing cells increases the invasive capacity of cells null for p53 (Neilsen et al., 2011). Although cancer cells expressing oncogenes other than mutant p53 can release microvesicles that have the ability to alter the phenotype of neighbouring cells, this is the first time that mutant p53 has been shown to have such a role (Al-Nedawi et al., 2008, Skog et al., 2008, Demory Beckler et al., 2013).

4.3.1.1 Mutant p53 microvesicle release

Past studies indicate that wild-type p53 (but not mutant p53) promotes MVB-derived exosome release by regulating TSAP6 expression (Lespagnol et al., 2008, Yu et al., 2006). To exclude any involvement of TSAP6 in microvesicle release from mutant p53 cells, we confirmed that TSAP6 is not under mutant p53 transcriptional control. The TSAP6 mRNA transcript and protein levels do not differ between p53^{-/-} and p53^{R273H} expressing cells (data not shown).

To identify the mechanism through which microvesicles were released we tested a variety of Rab-GTPase proteins that are involved in MVB-derived exosome release (previously described in chapter 1) - namely Rab27a, Rab27b and Rab35 (Hsu et al., 2010, Savina et al., 2002, Ostrowski et al., 2010). We identified that Rab35 expression is essential for the release of functional microvesicles from p53^{R273H} expressing cells. This finding is in agreement with previous reports which find Rab35 to have a role in MVB-derived exosome release in oligodendrocytes, and has added to the literature a new role of Rab35 in the release of functional microvesicles from cancer cells (Hsu et al., 2010, Fruhbeis et al., 2013a).

4.3.1.2 Provenance of microvesicles from mutant p53 expressing cells

As Rab35 has previously been shown to be involved in the release of MVB-derived exosomes, one may speculate that the functional microvesicles released by mutant p53-expressing cells may be of endosomal origin (Hsu et al., 2010, Fruhbeis et al., 2013a). Furthermore, data from transmission electron microscopy suggested that p53^{R273H}-expressing cells release a specific sub-population of microvesicles which are less than 50 nm in diameter (chapter 3), indicating the possibility that the functional phenotype-altering microvesicles released from p53^{R273H} cells may be MVB-derived exosomes. However due to the lack of specific MVB-derived exosome markers, further analysis will be necessary to determine the lineage of the phenotype-altering microvesicles released by mutant p53-expressing cells. Separating different microvesicle populations by size using immuno-affinity capture (as discussed in chapter 3) may allow identification of specific phenotype-altering microvesicle populations and aid the analysis/speculation of whether functionally active microvesicles are MVB-derived exosomes or plasma membrane-shed microvesicles. To further support this, analysis of the dynamics of Rab35-positive endosomes in mutant p53-expressing cells may help to identify any role Rab35 may have in the transport and docking of MVB endosomes to the plasma membrane (Hsu et al., 2010).

4.3.1.3 Microvesicles from p53 null cells

It is interesting to consider what effect microvesicles released by p53^{-/-} cells may have upon neighbouring cells. Preliminary data suggests that when p53^{R273H} expressing cells are treated with microvesicles from p53^{-/-} cells, they start to migrate with a higher forward migration index (i.e. more like a cell null for p53). This warrants further investigation. If cancer cells null for p53 can release microvesicles that can reverse the malignant migratory phenotype of mutant p53-expressing cells, then perhaps it will be interesting to further investigate the tumour suppressing attributes of microvesicles from non-cancerous cells or from non-cancerous cells that have p53 activation. If non-cancerous cells/activation of tumour suppressors can indeed promote the release of microvesicles that can reverse malignant phenotypes of cancer cells, this could be an exciting avenue for the development of novel therapeutic strategies.

4.3.2 How are mutant p53 microvesicles exerting their effects?

4.3.2.1 Transcriptional regulation

Previous reports have shown that mutant p53 expression dramatically changes the gene expression profile of cells (O'Farrell et al., 2004). Some changes in gene expression have been directly linked to the mutant p53 gain-of-function phenotype, and this is discussed in detail in chapter 1 (Di Agostino et al., 2006, Weisz et al., 2004). The results from our in-depth RNASeq screen agrees with past literature as we also find that p53^{R273H} cells have a very different mRNA expression profile than p53^{-/-} cells. However, we found that p53^{-/-} cells treated with p53^{R273H} microvesicles did not have detectably altered mRNA expression, even though these cells had acquired the mutant p53 gain-of-function migratory phenotype. This disagrees with past literature as it indicates that certain cell migratory and invasive characteristics that constitute the mutant p53 gain-of-function phenotype do not rely upon gene expression changes in the cell.

4.3.2.2 Podocalyxin

Rab35 is necessary for release of functional microvesicles from p53^{R273H}-expressing cells. Our immunoprecipitation and siRNA experiments indicate that there is physical and functional interaction between Rab35 and PODXL. We found this interesting as it is possible to envisage how a negatively charged sialomucin such as PODXL could have an important role in microvesicle biogenesis, or alternatively microvesicles rich in PODXL could have an important functional effect in the extracellular environment (discussed in detail next). We identified from RNA sequencing and by Western blot analysis that PODXL mRNA and protein levels are similar in p53^{-/-} and p53^{R273H}-expressing cells (data not shown). PODXL could be detected in microvesicles from both p53^{-/-} and p53^{R273H}-expressing cells by mass spectrometry, however due to detection limitations, we have so far not been able to detect PODXL in microvesicles by Western blot. Upon silencing of PODXL in p53^{R273H} expressing cells, functional phenotype-altering microvesicles are no longer released into the extracellular environment, and therefore cannot alter the receptor trafficking rate and migration of p53^{-/-} cells. Furthermore, PODXL expression is essential for maintenance of the mutant p53 gain-of-function phenotype itself.

PODXL is a highly glycosylated transmembrane sialomucin which has a functionally important negative charge associated with it. PODXL has a well-defined role in kidney podocyte development and function, where it acts as an anti-adhesive molecule (Nielsen and McNagny, 2009). PODXL expression in podocytes is essential for the efficient filtration of urine via a charge-selective barrier. Its expression is also important for cell morphogenesis and the structural integrity and spacing of the podocyte membrane structure (Doyonnas et al., 2001, Nielsen and McNagny, 2009). Conversely PODXL has a pro-adhesive role in vasculature endothelium where it promotes tethering of lymphocytes to the vasculature via their ligand L-selectin, maintaining normal immune surveillance and response (Sasseti et al., 1998, Baumheter et al., 1993).

4.3.2.3 Podocalyxin and cancer

It is well characterised that PODXL is aberrantly expressed in several cancer types, most commonly very aggressive types of breast cancer, prostate cancer and leukaemia (Somasiri et al., 2004, Kelley et al., 2005, Casey et al., 2006). PODXL has been identified as being secreted into the extracellular space by cleavage, or released in microvesicles from Chinese hamster ovary cells (CHO) and human tetra-1 tumour cells. However this report did not demonstrate a function of either secreted PODXL fragments or released PODXL containing microvesicles (Fernandez et al., 2011).

4.3.2.4 Podocalyxin hypothesis

So what role does PODXL have in mutant p53 phenotype altering microvesicles? Primarily, sialic acid molecules have been shown to have an impact on membrane curvature, therefore the highly sialylated PODXL could potentially contribute to microvesicle biogenesis (Schmid-Schonbein et al., 1986b). Supporting this hypothesis, membrane curvature manipulation involving ceramide and sphingomyelinase activity has been implicated as having a role in MVB-derived exosome biogenesis (Trajkovic et al., 2008).

Alternatively it is interesting to consider the role of the microvesicle glycocalyx in p53^{R273H} microvesicle biogenesis. Microvesicles have been identified as having a conserved glycocalyx signature; they are enriched in high mannose, sialic acid

and N-linked glycans (Batista et al., 2011). The work by Batista and colleagues, speculated that the microvesicle glycocalyx signature is indicative of a new microvesicle biogenesis pathway which originates from a specific membrane domain where glycosylation has a role in protein sorting into microvesicles. PODXL is a highly glycosylated sialomucin and its presence could contribute to the glycocalyx of microvesicles. However, detection of differences in the glycocalyx of microvesicles is something that would be difficult to detect by mass spectrometry. Additionally, the functional effect of PODXL in microvesicle biogenesis may be dependent upon its glycosylation rather than its concentration in the microvesicles. This could account for the observation that equal quantities of PODXL was detected in p53^{-/-} and p53^{R273H} microvesicles by mass spectrometry. In the future it would be interesting to investigate the glycocalyx of microvesicles released by p53^{R273H} cells versus p53^{-/-} cells, and to determine the role PODXL (and its glycosylation state) may have in the biogenesis and content of functional microvesicles released from mutant p53-expressing cells.

Due to the negative charge associated with PODXL, its presence in microvesicles may have a functional impact upon microvesicle uptake into recipient cells. This is supported by a study which found that removal of negatively charged sialic acid from the surface of microvesicles can slightly increase (although not significantly) the uptake of microvesicles into recipient cells (Escrevente et al., 2011). We do not yet know the mechanism by which microvesicles are taken up into H1299 p53^{-/-} cells, although preliminary data suggests that microvesicles released by p53^{R273H}-expressing cells are taken up into the cell at an increased rate compared to those from p53^{-/-} cells. It should also be considered that if negatively charged microvesicles are taken up into cells by endocytosis, they could alter the physiology of the endosomal compartment. If endosomes become filled with negatively charged microvesicles, the sorting and recycling of their cargoes could be altered. To investigate this, the localisation and dynamics of PODXL positive microvesicles within the endosomal compartment would need to be closely investigated.

Finally it is important to consider the role of PODXL in epithelial cell polarity of MDCK cells. Upon initiation of integrin signalling at the ECM interface, PKCB11 phosphorylates the PODXL/Ezrin/NHERF1 complex initiating its translocation to

the apical membrane promoting epithelial polarity in lumen formation. Loss of PODXL disrupts this process and the polarised lumen formation of epithelial structures, and instead promotes front-rear polarity and motility (Bryant et al., 2014). Therefore it is important to consider that fusion of podocalyxin-containing microvesicles with the plasma membrane of recipient $p53^{-/-}$ cells, or their fusion with the endosome limiting membrane after endocytosis, could initiate the association of PODXL with other transmembrane receptors initiating intracellular signalling cascades and changing the recipient cell behaviour.

4.3.3 Mutant p53 microvesicles: Role in cell education and autocrine signalling

4.3.3.1 Microvesicles and education of neighbouring cells

As well as transferring the mutant p53 phenotype to neighbouring cells, microvesicles released from $p53^{R273H}$ cells also play a role in educating the recipient $p53^{-/-}$ cells. Recipient $p53^{-/-}$ cells are educated by $p53^{R273H}$ microvesicles in a paracrine fashion, to display the mutant p53 gain-of-function migratory phenotype quickly after initial exposure to the microvesicles. Importantly, $p53^{-/-}$ cells form a memory of the phenotype, enabling the mutant p53-like migration to be maintained in the long term even with no exposure to the original microvesicles. This memory is maintained because the educated $p53^{-/-}$ cells release similar phenotype-altering microvesicles into the extracellular environment as do $p53^{R273H}$ cells. The education of cells by microvesicles has previously been shown in various systems. For example, melanoma MVB-derived exosomes have been shown to be able to irreversibly educate bone marrow progenitor cells and promote their mobilisation to a metastatic site to initiate the metastatic niche formation (Peinado et al., 2012).

The educating ability of microvesicles released by mutant p53 expressing cells is potentially an important concept in a cancer setting. Education of neighbouring cells null for p53 by microvesicles released from mutant p53 expressing cells could support tumour growth, or even facilitate metastasis to a distant site. A small number of cells forming a micro-metastasis in a distant organ could educate its surrounding cells to support the metastatic tumour growth. This

idea will be the next important thing to investigate *in vivo* and is discussed in chapter 5.

4.3.3.2 Microvesicles and their autocrine role

Microvesicles that are released from mutant p53-expressing cells in a Rab35-dependent manner are also essential for maintenance of the intrinsic mutant p53 migratory phenotype via an autocrine positive feedback mechanism. A similar concept of microvesicle-mediated autocrine signalling was recently discussed in a study which found that polarised and persistent cell migration was maintained *in vivo* by an autocrine Rab27a dependent MVB-derived exosome release (Sung et al., 2015). Additionally glioblastoma microvesicles have been identified as having a self-promoting role by stimulating the proliferation of neighbouring glioblastoma cells (Skog et al., 2008). Furthermore displaying an even more complex autocrine role of microvesicles in a tumour environment, breast cancer cells secrete Wnt11 in an autocrine fashion, however the Wnt11 only becomes useful upon tethering of Wnt11 to fibroblast released MVB-derived exosomes. These fibroblast MBV-derived exosomes are subsequently taken up again by breast cancer cells and the tethered Wnt11 stimulates the planar cell polarity signalling pathway enhancing the invasive breast cancer cell phenotype (Luga et al., 2012). These studies taken together with ours, demonstrate a new emerging role of microvesicle release and consequent autocrine feedback upon recipient cells, in maintaining specific cell behaviours and responses within a complex microenvironment.

4.4 Conclusion

Figure 4-15 shows a schematic representation of the new mutant p53 gain-of-function model we have identified. Mutant p53 drives the release of functional microvesicles which is dependent upon the expression of both Rab35 and PODXL (A). These microvesicles can transfer the mutant p53 gain-of-function migratory and invasive phenotype it to p53^{-/-} cells in a paracrine signalling fashion (B). The microvesicles drive RCP and DGK dependent integrin and receptor tyrosine kinase trafficking, and these recipient cells consequently exhibit less persistent cell migration and increased invasion. Microvesicles from p53^{R273H}-expressing cells educate p53^{-/-} cells to release similar phenotype-altering microvesicles

maintaining the mutant p53 gain-of-function phenotype within the cell population. Importantly, we found that both PODXL and Rab35 are essential for the mutant p53 phenotype to be maintained in a microvesicle mediated autocrine positive feedback mechanism (C).

A: Cells expressing p53^{R273H} release phenotype altering microvesicles which is dependent upon Rab35 and PODXL expression

B: Paracrine education of recipient p53^{-/-} cells to transfer and maintain the mutant p53 migratory phenotype

C: Self maintenance of p53^{R273H} phenotype in a microvesicle mediated autocrine fashion

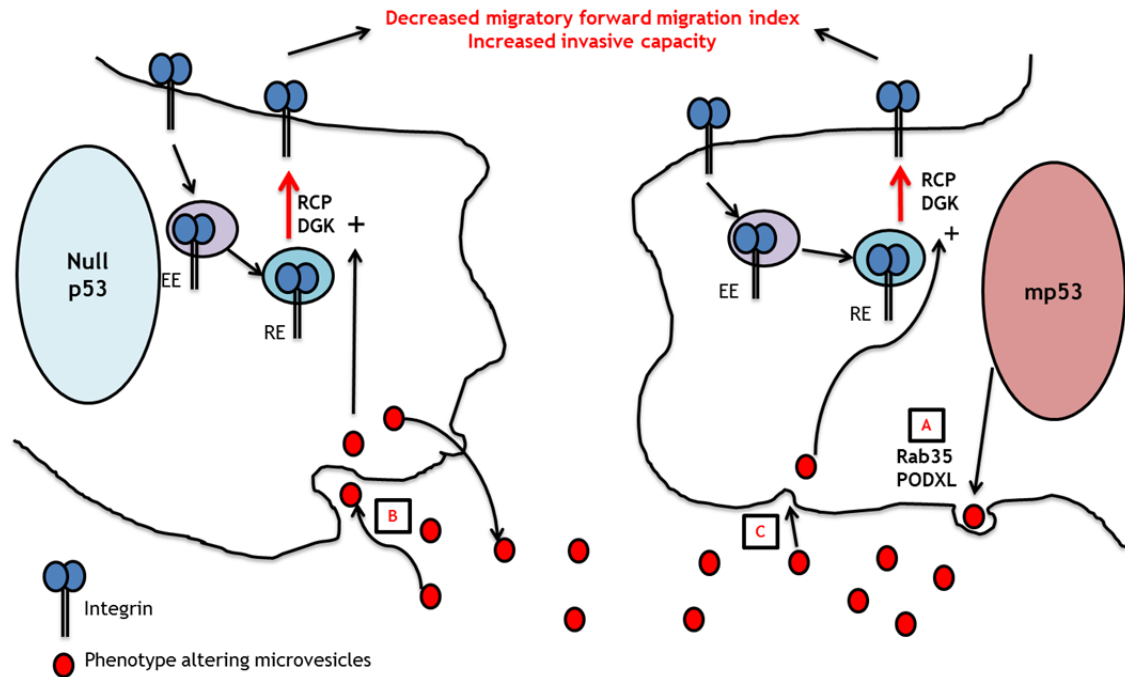


Figure 4-15: Diagram illustrating mutant p53 non-cell-autonomous gain-of-function invasive phenotype model.

Mutant p53 drives the release of microvesicles in a Rab35 and PODXL dependent manner. The microvesicles are necessary to feedback in an autocrine fashion onto mutant p53 expressing cells and maintain their high rate of RCP/DGK α -dependent integrin recycling to enable their invasive and migratory phenotype to be maintained. Additionally, microvesicles released from mutant p53-expressing cells have a dual role as they can also transmit mutant p53's gain-of-function invasive phenotype to neighbouring cells that are null for p53 in a paracrine fashion. Microvesicles from p53^{R273H}-expressing cells educate p53^{-/-} cells to release the same phenotype altering microvesicles into the extracellular environment allowing the phenotype to be sustained in an autocrine fashion.

5 Final discussion

We have identified a novel role of microvesicles released by mutant p53 expressing cells, in educating neighbouring cells null for p53 to display a mutant p53 migratory and invasive phenotype. This mutant p53-driven cell communication may have an important role *in vivo*; it could facilitate the maintenance of the mutant p53 gain-of-function phenotype within a population of heterogeneous cancer cells. We have also identified a novel aspect to the cell-intrinsic mechanism of the mutant p53 gain-of-function phenotype. Mutant p53 gain-of-function is not dependent on the mRNA expression changes that mutant p53 exerts, rather it appears to be maintained by an autocrine positive feedback loop mediated by microvesicles. This autocrine loop drives RCP and DGK α -dependent integrin and receptor tyrosine kinase recycling to promote a pro-invasive phenotype. This final chapter will review these main findings and discuss how they have contributed to, and fit within, the fields of microvesicle cell communication in cell migration and the mutant p53 gain-of-function phenotype.

5.1 Microvesicles from mutant p53-expressing cells and their role in cell migration

5.1.1 Microvesicles and cell migration

We have added more evidence to the literature supporting the involvement of oncogene-driven microvesicle release, in transferring oncogenic properties to other cells. Microvesicles have important roles in the regulation of cell migration, either by altering recipient cell behaviour or by exerting their effects within the extracellular environment (reviewed in figure 5-1). For example, the Rab27a-dependent release of MVB-derived exosomes from cancer cells co-ordinates focal adhesion assembly and directional cell migration *in vivo* (Sung et al., 2015). Furthermore MVB-derived exosomes released by fibroblasts contribute to cancer cell migration by driving autocrine planar cell polarity wnt signalling in breast cancer cells (Luga et al., 2012). Finally metalloproteinase and integrin loaded tumour-shed microvesicles are effective in enhancing invasive cell migration by binding to, and degrading the extracellular matrix (Muralidharan-Chari et al., 2009).

5.1.1.1 Microvesicles from mutant p53-expressing cells and cell migration: Integrins

We show that microvesicles released by mutant p53-expressing cells impact upon cell migration by increasing integrin and receptor tyrosine kinase recycling to the plasma membrane. This is a function of cancer cell-derived microvesicles that has not been previously identified. Nevertheless, macrophage-derived MVB-derived exosomes promote the internalisation of endothelial integrin $\beta 1$ to the lysosomal compartment for degradation, inhibiting cell migration (Lee et al., 2014). Although this study is conflicting with ours, it is not related to cancer cell migration. It does however support our study in identifying a potential role of microvesicles in altering recipient cell integrin and receptor tyrosine kinase trafficking.

The mode of migration that microvesicles released by mutant p53-expressing cells foster in recipient cells is highly integrin-dependent. Sung and colleagues recently showed that microvesicle release coincides with focal adhesion assembly and directional migration (Sung et al., 2015). Therefore it would be interesting to identify the impact that microvesicles from mutant p53 expressing cells have upon focal adhesion assembly and disassembly. Microvesicle-mediated alteration of focal adhesion dynamics could consequently have an impact on the rate of integrin recycling to the plasma membrane to support an invasive mode of migration.

Finally $\beta 1$ integrin has been hypothesised to have an important role in directing microvesicles to degrade the extracellular matrix (Dolo et al., 1998, Muralidharan-Chari et al., 2009). Microvesicles released by mutant p53 expressing cells are rich in $\beta 1$ integrin as well as several other integrins (although it is not known whether the integrins are active or not). Therefore there is a possibility that these microvesicles exert their functional effects in the extracellular environment by binding to the extracellular matrix. However preliminary data does suggest the mutant p53-expressing cell derived microvesicles are taken up into the cell to exert their effects (data not shown). Additionally the effects of microvesicles from mutant p53 expressing cells are apparent when cells migrate both on plastic as well as on 3D matrices (data not

shown), therefore it is likely that their phenotype-altering capacity is not dependent on microvesicle interaction with the extracellular matrix.

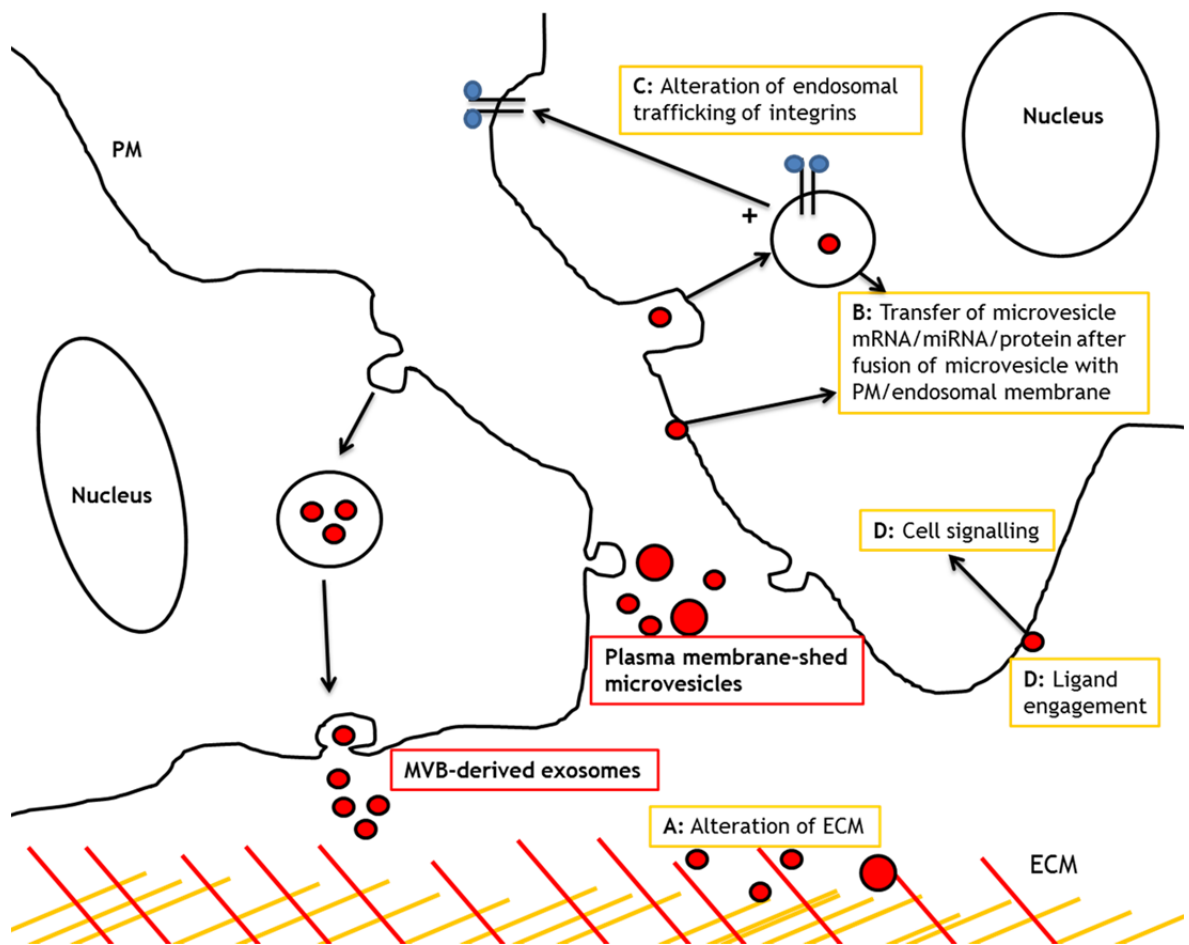


Figure 5-1: Diagram of potential mechanisms through which microvesicles influence cell migration.

When microvesicles are released into the extracellular environment they can affect recipient cell migration in several different ways. Microvesicles can interact with and degrade the extracellular matrix to facilitate cell migration (A). Microvesicles may fuse with the plasma membrane/endosome limiting membrane after uptake into the cell, enabling their contents to be released and consequently initiate a signalling cascade or a change the cells' protein/mRNA/gene expression profile (B). Alternatively they may be endocytosed and reside within the endosomal system where they have a positive impact on integrin recycling (C). Finally they may hypothetically interact via a ligand-receptor interaction on the plasma membrane of the recipient cell to trigger a signalling cascade altering cell migration (D).

5.1.2 Microvesicles and cell migration and metastasis *in-vivo*: future aims

The non-cell-autonomous nature of the mutant p53 invasive phenotype is a new area of study, and with that come several ideas that would be important to investigate in the near future. Primarily the impact of microvesicles released by mutant p53 expressing cells on the immune system needs to be investigated. It was recently shown that pancreatic cancer cell-derived, miRNA rich,

microvesicles have the ability to transform fibroblasts into cancer-associated fibroblasts that promote cancer progression (Pang et al., 2015). In initial studies aimed at determining whether immortalised fibroblasts may be activated by microvesicles from mutant p53-expressing cells, we were unable to detect any apparent alteration in smooth muscle actin expression after a mutant p53 microvesicle pre-treatment (data not shown), indicating that these microvesicles do not promote conversion to a myofibroblast-like phenotype. However, as immortalised cells are thought to be partially-activated, these experiments should be repeated with primary cultured fibroblasts. It would also be worthwhile investigating if microvesicles from mutant p53-expressing cells have any impact on immune cell tumour infiltration *in vivo* by increasing the migratory capacity/recruitment of neutrophils to support tumour growth (Bobrie et al., 2012).

Investigation of the role mutant p53 microvesicles play in cell migration and metastasis *in vivo* is an equally important strategy. One way to do this is elegantly demonstrated by a recent study by Zomer and colleagues which showed the transfer of malignant cancer cell-derived microvesicles to recipient benign cancer cells *in vivo* using the Cre-loxP system. Cre-recombinase expressing metastatic cancer cells released microvesicles that contain the Cre recombinase protein product, which when taken up by benign cancer cells that can express GFP under Cre-recombinase control, results in GFP expression in the benign cancer cells. Therefore cancer cells that have taken up metastatic cell-derived microvesicles could be detected by their GFP expression and any changes in their phenotype could then be analysed. The non-metastatic tumour cells after uptake of metastatic cell-derived microvesicles displayed more metastatic migratory behaviour (Zomer et al., 2015). This strategy would be useful to identify mutant p53 microvesicle uptake and functional effects *in vivo*. A second informative strategy to analyse the role of mutant p53 microvesicles *in vivo* would be to carry out experiments similar to those published by David Lydon's lab. These *in vivo* experiments used cancer cell-derived exosomes to 'educate' the mouse bone marrow/stromal cells prior to introduction of cancer cells as syngeneic xenografts (Peinado et al., 2012, Costa-Silva et al., 2015). Education of bone marrow/stromal cells initiated pre-metastatic niche formation which enhanced the homing of the xenografted cancer cells to the primed organ.

This type of experiment would enable identification of whether mutant p53 microvesicles are able to promote metastasis by educating cells at distant sites within the organism, and priming organs for metastasis. *In vivo* experiments in which microvesicles are introduced by supraorbital or tail vein injection whilst tumours are growing would also be informative, and could enable analysis of the pro-tumorigenic and metastasis-promoting capacity of systemic circulating microvesicles. As we know that microvesicles from mutant p53-expressing MCF7 breast cancer cells have a substantial effect upon H1299 cell migration, it would perhaps be beneficial to use the MMTV-polyoma middle T breast cancer mouse model that is already established in the lab to analyse the effects of regular tail vein injections of microvesicles from mutant p53-expressing cells on breast tumour growth and metastases. For shorter term experiments, cancer cell xenografts with or without microvesicle treatment could also be attempted.

If microvesicles from mutant p53-expressing cells are important in the metastasis process, these could represent a new potential anti-metastatic therapeutic target. Microvesicle removal from the blood to prevent further cell education and tumour progression/metastasis could be an option. Indeed, this is a hypothetical cancer therapy which has been discussed in detail by Marleau and colleagues (Marleau et al., 2012).

5.1.3 Microvesicles as diagnostic biomarkers

Microvesicle biomarkers are an emerging field of cancer research. It is widely accepted that lung and ovarian cancer patients display increased levels of microvesicles in circulating blood (Caby et al., 2005, Rabinowits et al., 2009). Not only does this indicate a potentially important role of microvesicle release in cancer pathology, but also reveals the potential for using microvesicles from patient blood as diagnostic biomarkers. For example microvesicles isolated from the blood of pancreatic cancer patients contain mutant p53 and mutant KRAS genomic DNA which may eventually serve as an effective diagnostic biomarker (Kahlert et al., 2014), and more recently measurement of circulating glypican-1-rich exosomes has been shown to assist detection of early pancreatic cancer (Melo et al., 2015). Other promising studies for diagnostic biomarkers show that prostate cancer-derived exosomes isolated from urine have an interesting pro-cancerous protein signature (Nilsson et al., 2009), and microvesicles from the

blood of ovarian cancer patients contain a specific/unique miRNA signature (Manterola et al., 2014).

Microvesicles released by mutant p53 cells may be important for cell communication in many different cancer types. Preliminary indications suggest this may be true as we have found that lung, ovarian and breast cancer cell lines are involved in either release of phenotype altering microvesicles from mutant p53-expressing cells, or can respond to microvesicles released by mutant p53-expressing cells and display a mutant p53 gain-of-function phenotype. Therefore microvesicles from mutant p53-expressing cancer cells may be present in the circulation of many patients and this may be useful as a diagnostic tool. Despite the fact that we have been unable to identify differences in the protein and lipid constituents of microvesicle preparations from p53 null and mutant p53-expressing cells, with more sophisticated vesicle fractionation approaches it may be possible to isolate the functional microvesicles from mutant p53-expressing cells and determine whether they have a distinguishing protein signature. Other promising diagnostic signatures may arise from analysing the miRNA content of microvesicles derived from mutant p53-expressing cells. We think that microvesicular miRNA is not participating in the mutant p53 phenotype transfer, because the mRNA expression profile of p53 null cells does not detectably alter following treatment with microvesicles from mutant p53-expressing cells. Nevertheless, because mutant p53 down regulates DICER expression and mature miRNA processing, there is a possibility that mutant p53 microvesicles have a very distinct miRNA profile/signature which could be used as a diagnostic marker enabling early diagnosis of mutant p53 expressing cancers from patient blood (Muller et al., 2014).

5.2 Mutant p53 gain-of-function mechanism

5.2.1 p63 and the mutant p53 gain-of-function

The transcription factor p63 is a tumour suppressor whose expression is often lost in cancer (Urist et al., 2002). Indeed, tumours spontaneously form in p63 knockout mice (Flores et al., 2005). Mutant p53's gain-of-function invasive phenotype in part arises from its inhibition of p63 tumour suppressing activity

(Noske et al., 2009, Muller et al., 2014). This is thought to be due to direct interaction of mutant p53 with p63 (Gaiddon et al., 2001, Strano et al., 2002).

Past studies have shown that mutant p53-driven integrin and receptor tyrosine kinase recycling, and the enhanced migration and invasion that is a consequence of this, can be both dependent and independent of inhibition of p63 via mutant p53 (Muller et al., 2009, Muller et al., 2013, Muller et al., 2014, Adorno et al., 2009). So far p63 has not been linked to microvesicle biology, however the possibility that p63 is involved in the generation of functionally active microvesicles by mutant p53-expressing cells, or is necessary for recipient cells to alter their migratory phenotype in response to microvesicles from mutant p53-expressing cells needs to be investigated.

5.2.2 Achieving mutant p53 gain-of-function without alterations to mRNA expression

The mutant p53 gain-of-function migratory phenotype has long thought to be due to the transcriptional changes that occur upon p53 mutation. Not only does p53 lose its wild-type tumour suppressing transcriptional properties, but it may gain some new transcriptional properties (O'Farrell et al., 2004). There has been several studies already discussed in chapter 1 associating mutant p53's transcriptional properties with the gain-of-function migratory phenotype (Di Agostino et al., 2006).

Our data agree with past studies showing mutant p53 expression causes a huge change in global mRNA expression, and it is possible that the generation of phenotype-altering microvesicles involves some of these mRNA expression changes. However, an interesting aspect to our study is that, using a highly sensitive RNA sequencing approach, we are unable to detect any mRNA expression changes that are associated with the response of recipient cells to prolonged (72 hr) exposures to microvesicles from mutant p53-expressing cells. This indicates that the changes to the receptor trafficking and migratory machinery that are necessary to implement mutant p53's phenotype may not require, nor be mediated by, any alterations to mRNA expression. This is somewhat puzzling - particularly as one considers that altered receptor tyrosine kinase trafficking and signalling might be expected to alter expression of genes

downstream of signalling modules such as the PI3K-Akt axis. Of course, one needs to consider the possibility that some miRNAs that are transferred via microvesicles may alter mRNA translation without detectably changing transcript level. However, the rapidity with which mutant p53's migratory phenotype is apparent following microvesicle addition tends to argue against this. Indeed, we observe suppression of the FMI very quickly following addition of microvesicles from mutant p53-expressing cells, and this allows very little time for miRNA delivery and alteration to translation to influence cell migration. Rather, our data are more consistent with a mechanism through which the influence of microvesicles on cell migration is mediated via relatively direct effects on the cell's receptor trafficking machinery.

Another intriguing aspect of our findings is that recipient cells appear to be educated by microvesicles from mutant p53 expressing cells to produce phenotype-altering microvesicles even in the absence of detectable alterations to mRNA expression. Thus it appears that not only the migratory response of cells to microvesicles, but also some of the cell's capacity to produce phenotype altering microvesicles is regulated in a way that doesn't seem to involve altered mRNA expression. This indicates the possibility that many (if not all) of the mutant p53-driven gene expression changes that have previously been identified using microarray and RNA sequencing approaches may not be relevant to the implementation of the invasive phenotype.

5.2.3 The roles of Rab35 and PODXL in microvesicle production and function

We have established that Rab35 and PODXL are key to the release of phenotype-altering microvesicles from mutant p53-expressing cells. Active Rab35 levels in p53^{-/-} and p53^{R273H}-expressing cells were analysed by immunoprecipitation using an antibody specific to the active Rab35-GTPase form. Preliminary data from these experiments (not shown) suggests that there is no difference in the quantity of active Rab35 present in p53^{-/-} and p53^{R273H} cells. Additionally Rab35 and PODXL have been shown to directly associate with one another in H1299 cells by immunoprecipitation of Rab35-GFP. It will be interesting to determine the influence of mutant p53 expression upon Rab35 interaction with PODXL, and to identify the overall interactome of Rab35. Perhaps PODXL will be identified

as having an altered interaction with Rab35 when mutant p53 is expressed. The interaction between, and co-ordination of PODXL and Rab35 functions may be important for the release of functional microvesicles.

As to how the Rab35-PODXL dependent functional microvesicles actually drive integrin recycling in p53^{R273H} and p53^{-/-} cells is not yet known. Several hypotheses are discussed in chapter 4. To reiterate, Rab35 is thought to drive the release of MVB-derived exosomes from a cell by aiding the transport/docking of MVBs to the plasma membrane (Hsu et al., 2010). Work into the localisation of Rab35 within the endosomal compartment is necessary to further investigate the hypothesis. The highly glycosylated protein PODXL could have a role in microvesicle biogenesis by promoting membrane curvature (Schmid-Schonbein et al., 1986a). Alternatively PODXL could have a role in sorting of specific cargo into the microvesicles dependent upon its glycosylation state and localisation in the cell as hypothesised by (Batista et al., 2011). Additionally the negative charge that PODXL would be expected to impart to microvesicles may influence their uptake into recipient cells (Escrevente et al., 2011). Alternatively, endocytosis of PODXL-containing microvesicles could introduce negative charge into the lumen of the endosomal system. This negative charge may influence endosome dynamics via effects on membrane curvature, membrane spacing and protein interactions. Such phenomena could influence the sorting of endosomal cargoes and/or shuttling of endosomes to the plasma membrane altering integrin and receptor tyrosine kinase trafficking rates. The importance of PODXL's acidic nature may be investigated by removal of these negatively charged sialic acid carbohydrate chains from the microvesicle surface - this could be achieved using enzymes such as neuraminidases - and then testing the capacity of these desialylated microvesicles to influence receptor trafficking and cell migration (Escrevente et al., 2011).

5.2.4 Autocrine and paracrine maintenance of the mutant p53 phenotype

This study, along with others already discussed, has shed light on the maintenance of a cell's invasive phenotype by microvesicle release and autocrine positive feedback signalling (Sung et al., 2015). We have also identified that microvesicles from mutant p53 expressing cells play a role in

paracrine education of other cells so that they themselves form a memory and are able to maintain the mutant p53 phenotype in the same autocrine fashion as mutant p53 cells themselves. The next challenge is to determine whether this autocrine/paracrine cell communication by mutant p53 microvesicles occurs *in vivo*.

5.2.4.1 Autocrine maintenance and paracrine transfer of the mutant p53 phenotype *in vivo*: future aims

Elucidation of the mechanism for autocrine maintenance and paracrine transfer of the mutant p53 phenotype *in vivo* is an exciting prospect. One experiment that has already been attempted, and will be tried again, is to inject PDAC p53^{-/-} cells into one flank of a mouse and PDAC p53^{R172H} cells into the opposite flank. Tumour growth will be monitored to determine whether presence of a mutant p53 expressing tumour in one flank has any impact upon the invasive growth of the p53^{-/-} expressing tumour in the opposite flank. If the microvesicles released by the mutant p53 cells are able to provide autocrine and paracrine maintenance of the mutant p53 phenotype, you would expect p53^{-/-} tumours to develop a more invasive phenotype.

To determine whether microvesicles from mutant p53-expressing cells are relevant in a clinical setting, it would be useful to collect microvesicles from the blood of patients with mutant p53-expressing cancers and compare the properties of those with those from patients with cancer that do not have p53 mutations and from healthy individuals. The microvesicles collected from patient blood could then be used to determine whether they can influence the migratory and invasive behaviour of p53^{-/-} cells *ex vivo*. If so, this would provide further evidence that mutant p53 tumour derived microvesicles have an autocrine/paracrine role in supporting cancer progression.

If the autocrine/paracrine role of mutant p53 could be demonstrated *in vivo* and had clinical relevance, it would next be desirable to develop strategies to oppose the autocrine ability of mutant p53 expressing tumours to maintain their own phenotype and paracrine ability to educate neighbouring cells *in vivo*. Inhibition or disruption of this autocrine loop would theoretically allow the tumour and neighbouring cells to revert to a less invasive phenotype, as we have

shown can occur *in vitro* after Rab35 or PODXL silencing. This strategy could potentially decrease tumour growth and inhibit metastasis. To test this, Rab35 could be stably removed from mutant p53 expressing cells using CRISPR gene deletion. This would enable analysis of mutant p53 tumour growth with or without Rab35 expression *in vivo* using xenografts. If Rab35 expression depletion results in smaller tumours and fewer metastases because of a microvesicle release defect, then co-injection of mutant p53 cell derived microvesicles into the Rab35 deficient mouse tumours should rescue tumour growth, demonstrating the necessity of the microvesicle autocrine maintenance of the mutant p53 gain-of-function phenotype and how useful disruption of the microvesicle autocrine loop would be.

Overall (as summarised in figure 5-2) this project has shed light on the role played by mutant p53 mediated microvesicle release and function in cell migration, as well as adding new knowledge regarding the mutant p53 gain-of-function phenotype. It is a novel and exciting area of research that is worthy of more investigation and could lead to the discovery of new biomarkers for diagnosis of cancer or even new targets for anti-metastasis cancer therapies.

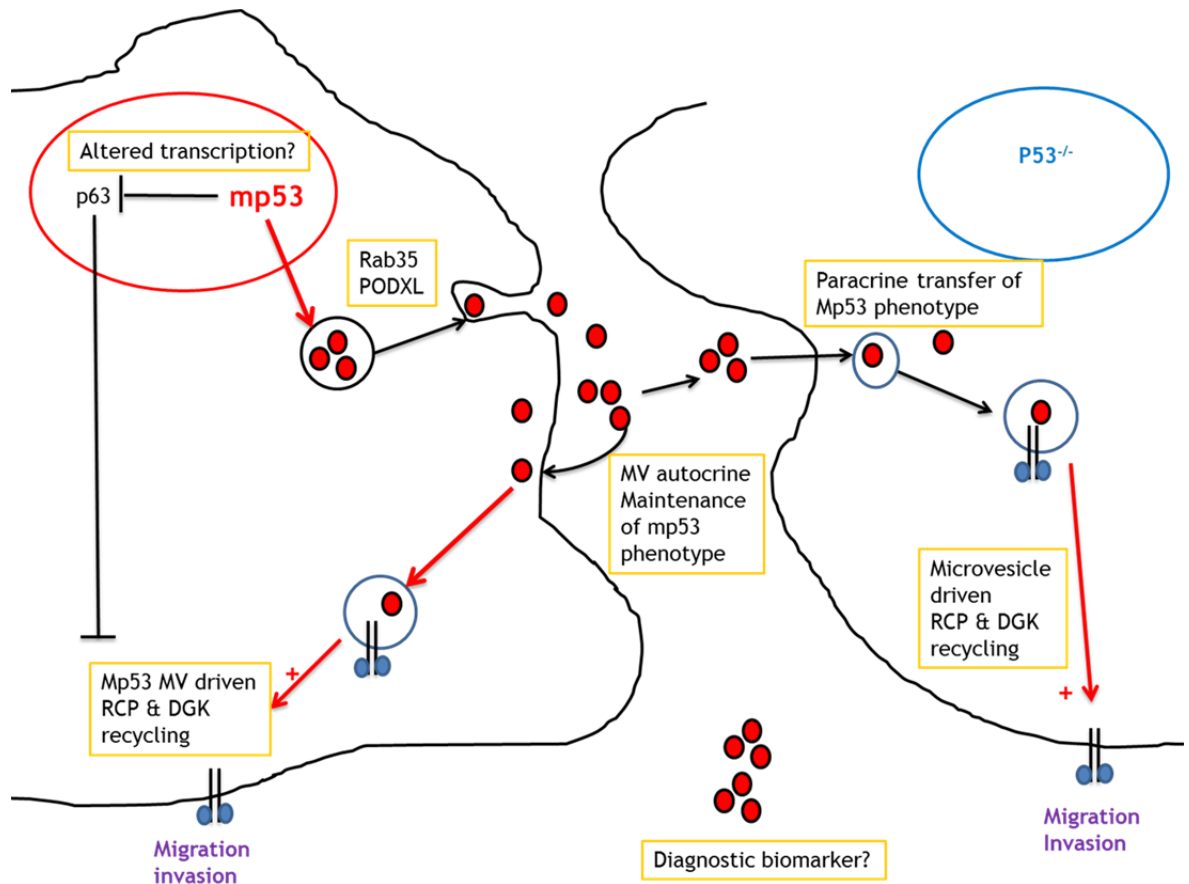


Figure 5-2: A proposed mechanism for p53 gain-of-function.

The diagram depicts various published, as well as newly-discovered, mechanistic aspects of the mutant p53 gain-of-function phenotype. It is already known that altered transcription following mutant p53 expression can contribute to the mutant p53 gain-of-function phenotype (O'Farrell et al., 2004). Additionally mutant p53 drives RCP and DGK α -dependent integrin and receptor tyrosine kinase trafficking and signalling to enhance migration, invasion and metastasis in a p63-dependent and independent fashion (Noske et al., 2009, Muller et al., 2014). We identify a new mechanism of mutant p53 gain-of-function invasive phenotype, whereby the Rab35 and PODXL-dependent release of microvesicles drives integrin trafficking in an RCP and DGK α -dependent manner in an autocrine positive feedback signalling pathway. Additionally these extracellular microvesicles have the ability to transfer this phenotype to neighbouring cells null for p53. We find that the response of recipient cells to microvesicles from mutant p53-expressing cells is not associated with detectable changes in mRNA expression. The mutant p53 expressing cell-derived microvesicles educate cells null for p53 to release the same phenotype altering microvesicles into the extracellular environment allowing long term maintenance of the invasive gain-of-function phenotype in an autocrine fashion. There is potential to identify whether it would be useful to inhibit the release of these microvesicles, remove them from circulation or block their activity to constitute a new therapy to treat mutant p53-expressing cancers. Additionally microvesicles released from mutant p53 expressing cancer cells could be collected from patient blood samples and used as biomarkers for cancer diagnosis.

List of references

- ADORNO, M., CORDENONSI, M., MONTAGNER, M., DUPONT, S., WONG, C., HANN, B., SOLARI, A., BOBISSE, S., RONDINA, M. B., GUZZARDO, V., PARENTI, A. R., ROSATO, A., BICCIATO, S., BALMAIN, A. & PICCOLO, S. 2009. A Mutant-p53/Smad complex opposes p63 to empower TGFbeta-induced metastasis. *Cell*, 137, 87-98.
- AL-NEDAWI, K., MEEHAN, B., MICALLEF, J., LHOTAK, V., MAY, L., GUHA, A. & RAK, J. 2008. Intercellular transfer of the oncogenic receptor EGFRvIII by microvesicles derived from tumour cells. *Nature cell biology*, 10, 619-24.
- ALLAIRE, P. D., SEYED SADR, M., CHAINEAU, M., SEYED SADR, E., KONEFAL, S., FOTOUHI, M., MARET, D., RITTER, B., DEL MAESTRO, R. F. & MCPHERSON, P. S. 2013. Interplay between Rab35 and Arf6 controls cargo recycling to coordinate cell adhesion and migration. *Journal of cell science*, 126, 722-31.
- ALONI-GRINSTEIN, R., SHETZER, Y., KAUFMAN, T. & ROTTER, V. 2014. p53: the barrier to cancer stem cell formation. *FEBS Lett*, 588, 2580-9.
- AMZALLAG, N., PASSER, B. J., ALLANIC, D., SEGURA, E., THERY, C., GOUD, B., AMSON, R. & TELERMAN, A. 2004. TSAP6 facilitates the secretion of translationally controlled tumor protein/histamine-releasing factor via a nonclassical pathway. *J Biol Chem*, 279, 46104-12.
- ANDRE, F., SCHATZ, N. E., MOVASSAGH, M., FLAMENT, C., PAUTIER, P., MORICE, P., POMEL, C., LHOMME, C., ESCUDIER, B., LE CHEVALIER, T., TURSZ, T., AMIGORENA, S., RAPOSO, G., ANGEVIN, E. & ZITVOGEL, L. 2002. Malignant effusions and immunogenic tumour-derived exosomes. *Lancet*, 360, 295-305.
- ANDREOLA, G., RIVOLTINI, L., CASTELLI, C., HUBER, V., PEREGO, P., DEHO, P., SQUARCINA, P., ACCORNERO, P., LOZUPONE, F., LUGINI, L., STRINGARO, A., MOLINARI, A., ARANCIA, G., GENTILE, M., PARMIANI, G. & FAIS, S. 2002. Induction of lymphocyte apoptosis by tumor cell secretion of FasL-bearing microvesicles. *J Exp Med*, 195, 1303-16.
- ANO BOM, A. P., RANGEL, L. P., COSTA, D. C., DE OLIVEIRA, G. A., SANCHES, D., BRAGA, C. A., GAVA, L. M., RAMOS, C. H., CEPEDA, A. O., STUMBO, A. C., DE MOURA GALLO, C. V., CORDEIRO, Y. & SILVA, J. L. 2012. Mutant p53 aggregates into prion-like amyloid oligomers and fibrils: implications for cancer. *J Biol Chem*, 287, 28152-62.
- BAPTISTE, N., FRIEDLANDER, P., CHEN, X. & PRIVES, C. 2002. The proline-rich domain of p53 is required for cooperation with anti-neoplastic agents to promote apoptosis of tumor cells. *Oncogene*, 21, 9-21.
- BARAK, Y., JUVEN, T., HAFFNER, R. & OREN, M. 1993. mdm2 expression is induced by wild type p53 activity. *EMBO J*, 12, 461-8.
- BARRES, C., BLANC, L., BETTE-BOBILLO, P., ANDRE, S., MAMOUN, R., GABIUS, H. J. & VIDAL, M. 2010. Galectin-5 is bound onto the surface of rat reticulocyte exosomes and modulates vesicle uptake by macrophages. *Blood*, 115, 696-705.
- BATAGOV, A. O., KUZNETSOV, V. A. & KUROCHKIN, I. V. 2011. Identification of nucleotide patterns enriched in secreted RNAs as putative cis-acting elements targeting them to exosome nano-vesicles. *BMC Genomics*, 12 Suppl 3, S18.
- BATISTA, B. S., ENG, W. S., PILOBELLO, K. T., HENDRICKS-MUNOZ, K. D. & MAHAL, L. K. 2011. Identification of a conserved glycan signature for microvesicles. *J Proteome Res*, 10, 4624-33.

- BAUMHETER, S., SINGER, M. S., HENZEL, W., HEMMERICH, S., RENZ, M., ROSEN, S. D. & LASKY, L. A. 1993. Binding of L-selectin to the vascular sialomucin CD34. *Science*, 262, 436-8.
- BECKETT, K., MONIER, S., PALMER, L., ALEXANDRE, C., GREEN, H., BONNEIL, E., RAPOSO, G., THIBAUT, P., LE BORGNE, R. & VINCENT, J. P. 2013. Drosophila S2 cells secrete wingless on exosome-like vesicles but the wingless gradient forms independently of exosomes. *Traffic*, 14, 82-96.
- BENSAAD, K., TSURUTA, A., SELAK, M. A., VIDAL, M. N., NAKANO, K., BARTRONS, R., GOTTLIEB, E. & VOUSDEN, K. H. 2006. TIGAR, a p53-inducible regulator of glycolysis and apoptosis. *Cell*, 126, 107-20.
- BHATNAGAR, S. & SCHOREY, J. S. 2007. Exosomes released from infected macrophages contain Mycobacterium avium glycopeptidolipids and are proinflammatory. *J Biol Chem*, 282, 25779-89.
- BHUIN, T. & ROY, J. K. 2014. Rab proteins: the key regulators of intracellular vesicle transport. *Exp Cell Res*, 328, 1-19.
- BIANCO, F., PERROTTA, C., NOVELLINO, L., FRANCOLINI, M., RIGANTI, L., MENNA, E., SAGLIETTI, L., SCHUCHMAN, E. H., FURLAN, R., CLEMENTI, E., MATTEOLI, M. & VERDERIO, C. 2009. Acid sphingomyelinase activity triggers microparticle release from glial cells. *EMBO J*, 28, 1043-54.
- BOBRIE, A., KRUMEICH, S., REYAL, F., RECCHI, C., MOITA, L. F., SEABRA, M. C., OSTROWSKI, M. & THERY, C. 2012. Rab27a supports exosome-dependent and -independent mechanisms that modify the tumor microenvironment and can promote tumor progression. *Cancer research*, 72, 4920-30.
- BOLOS, V., PEINADO, H., PEREZ-MORENO, M. A., FRAGA, M. F., ESTELLER, M. & CANO, A. 2003. The transcription factor Slug represses E-cadherin expression and induces epithelial to mesenchymal transitions: a comparison with Snail and E47 repressors. *Journal of cell science*, 116, 499-511.
- BOOTH, A. M., FANG, Y., FALLON, J. K., YANG, J. M., HILDRETH, J. E. & GOULD, S. J. 2006. Exosomes and HIV Gag bud from endosome-like domains of the T cell plasma membrane. *The Journal of cell biology*, 172, 923-35.
- BRIDGEWATER, R. E., NORMAN, J. C. & CASWELL, P. T. 2012. Integrin trafficking at a glance. *Journal of cell science*, 125, 3695-701.
- BROSH, R. & ROTTER, V. 2009. When mutants gain new powers: news from the mutant p53 field. *Nat Rev Cancer*, 9, 701-13.
- BROUWERS, J. F., AALBERTS, M., JANSEN, J. W., VAN NIEL, G., WAUBEN, M. H., STOUT, T. A., HELMS, J. B. & STOORVOGEL, W. 2013. Distinct lipid compositions of two types of human prostasomes. *Proteomics*, 13, 1660-6.
- BRYANT, D. M., ROIGNOT, J., DATTA, A., OVEREEM, A. W., KIM, M., YU, W., PENG, X., EASTBURN, D. J., EWALD, A. J., WERB, Z. & MOSTOV, K. E. 2014. A molecular switch for the orientation of epithelial cell polarization. *Dev Cell*, 31, 171-87.
- BUDANOV, A. V. & KARIN, M. 2008. p53 target genes sestrin1 and sestrin2 connect genotoxic stress and mTOR signaling. *Cell*, 134, 451-60.
- BYKOV, V. J., ISSAEVA, N., SHILOV, A., HULTCRANTZ, M., PUGACHEVA, E., CHUMAKOV, P., BERGMAN, J., WIMAN, K. G. & SELIVANOVA, G. 2002. Restoration of the tumor suppressor function to mutant p53 by a low-molecular-weight compound. *Nature medicine*, 8, 282-8.
- CABY, M. P., LANKAR, D., VINCEDEAU-SCHERRER, C., RAPOSO, G. & BONNEROT, C. 2005. Exosomal-like vesicles are present in human blood plasma. *Int Immunol*, 17, 879-87.

- CAI, H., REINISCH, K. & FERRO-NOVICK, S. 2007. Coats, tethers, Rabs, and SNAREs work together to mediate the intracellular destination of a transport vesicle. *Dev Cell*, 12, 671-82.
- CALDERWOOD, D. A., FUJIOKA, Y., DE PEREDA, J. M., GARCIA-ALVAREZ, B., NAKAMOTO, T., MARGOLIS, B., MCGLADE, C. J., LIDDINGTON, R. C. & GINSBERG, M. H. 2003. Integrin beta cytoplasmic domain interactions with phosphotyrosine-binding domains: a structural prototype for diversity in integrin signaling. *Proc Natl Acad Sci U S A*, 100, 2272-7.
- CAMPBELL, H. G., MEHTA, R., NEUMANN, A. A., RUBIO, C., BAIRD, M., SLATTER, T. L. & BRAITHWAITE, A. W. 2013. Activation of p53 following ionizing radiation, but not other stressors, is dependent on the proline-rich domain (PRD). *Oncogene*, 32, 827-36.
- CASEY, G., NEVILLE, P. J., LIU, X., PLUMMER, S. J., CICEK, M. S., KRUMROY, L. M., CURRAN, A. P., MCGREEVY, M. R., CATALONA, W. J., KLEIN, E. A. & WITTE, J. S. 2006. Podocalyxin variants and risk of prostate cancer and tumor aggressiveness. *Human molecular genetics*, 15, 735-41.
- CASWELL, P. T., CHAN, M., LINDSAY, A. J., MCCAFFREY, M. W., BOETTIGER, D. & NORMAN, J. C. 2008. Rab-coupling protein coordinates recycling of alpha5beta1 integrin and EGFR1 to promote cell migration in 3D microenvironments. *The Journal of cell biology*, 183, 143-55.
- CASWELL, P. T., SPENCE, H. J., PARSONS, M., WHITE, D. P., CLARK, K., CHENG, K. W., MILLS, G. B., HUMPHRIES, M. J., MESSENT, A. J., ANDERSON, K. I., MCCAFFREY, M. W., OZANNE, B. W. & NORMAN, J. C. 2007. Rab25 associates with alpha5beta1 integrin to promote invasive migration in 3D microenvironments. *Dev Cell*, 13, 496-510.
- CAULIN, C., NGUYEN, T., LANG, G. A., GOEPFERT, T. M., BRINKLEY, B. R., CAI, W. W., LOZANO, G. & ROOP, D. R. 2007. An inducible mouse model for skin cancer reveals distinct roles for gain- and loss-of-function p53 mutations. *J Clin Invest*, 117, 1893-901.
- CHAIROUNGDUA, A., SMITH, D. L., POCHARD, P., HULL, M. & CAPLAN, M. J. 2010. Exosome release of beta-catenin: a novel mechanism that antagonizes Wnt signaling. *The Journal of cell biology*, 190, 1079-91.
- CHENG, K. W., LAHAD, J. P., KUO, W. L., LAPUK, A., YAMADA, K., AUERSPERG, N., LIU, J., SMITH-MCCUNE, K., LU, K. H., FISHMAN, D., GRAY, J. W. & MILLS, G. B. 2004. The RAB25 small GTPase determines aggressiveness of ovarian and breast cancers. *Nature medicine*, 10, 1251-6.
- CHO, Y., GORINA, S., JEFFREY, P. D. & PAVLETICH, N. P. 1994. Crystal structure of a p53 tumor suppressor-DNA complex: understanding tumorigenic mutations. *Science*, 265, 346-55.
- CHRISTOFORIDES, C., RAINERO, E., BROWN, K. K., NORMAN, J. C. & TOKER, A. 2012. PKD controls alpha5beta3 integrin recycling and tumor cell invasive migration through its substrate Rabaptin-5. *Developmental cell*, 23, 560-72.
- CLARK, A. G. & VIGNJEVIC, D. M. 2015. Modes of cancer cell invasion and the role of the microenvironment. *Curr Opin Cell Biol*, 36, 13-22.
- COLOMBO, M., RAPOSO, G. & THERY, C. 2014. Biogenesis, secretion, and intercellular interactions of exosomes and other extracellular vesicles. *Annual review of cell and developmental biology*, 30, 255-89.
- CONDE-VANCELLS, J., RODRIGUEZ-SUAREZ, E., EMBADE, N., GIL, D., MATTHIESEN, R., VALLE, M., ELORTZA, F., LU, S. C., MATO, J. M. & FALCON-PEREZ, J. M. 2008. Characterization and comprehensive proteome profiling of exosomes secreted by hepatocytes. *J Proteome Res*, 7, 5157-66.

- COSTA-SILVA, B., AIELLO, N. M., OCEAN, A. J., SINGH, S., ZHANG, H., THAKUR, B. K., BECKER, A., HOSHINO, A., MARK, M. T., MOLINA, H., XIANG, J., ZHANG, T., THEILEN, T. M., GARCIA-SANTOS, G., WILLIAMS, C., ARARSO, Y., HUANG, Y., RODRIGUES, G., SHEN, T. L., LABORI, K. J., LOTHE, I. M., KURE, E. H., HERNANDEZ, J., DOUSSOT, A., EBBESEN, S. H., GRANDGENETT, P. M., HOLLINGSWORTH, M. A., JAIN, M., MALLYA, K., BATRA, S. K., JARNAGIN, W. R., SCHWARTZ, R. E., MATEI, I., PEINADO, H., STANGER, B. Z., BROMBERG, J. & LYDEN, D. 2015. Pancreatic cancer exosomes initiate pre-metastatic niche formation in the liver. *Nature cell biology*, 17, 816-26.
- CRAWFORD, N. 1971. The presence of contractile proteins in platelet microparticles isolated from human and animal platelet-free plasma. *Br J Haematol*, 21, 53-69.
- CROSS, B., CHEN, L., CHENG, Q., LI, B., YUAN, Z. M. & CHEN, J. 2011. Inhibition of p53 DNA binding function by the MDM2 protein acidic domain. *J Biol Chem*, 286, 16018-29.
- DAMERON, K. M., VOLPERT, O. V., TAINSKY, M. A. & BOUCK, N. 1994. Control of angiogenesis in fibroblasts by p53 regulation of thrombospondin-1. *Science*, 265, 1582-4.
- DE JONG, O. G., VERHAAR, M. C., CHEN, Y., VADER, P., GREMMELS, H., POSTHUMA, G., SCHIFFELERS, R. M., GUCEK, M. & VAN BALKOM, B. W. 2012. Cellular stress conditions are reflected in the protein and RNA content of endothelial cell-derived exosomes. *J Extracell Vesicles*, 1.
- DE WEVER, O., NGUYEN, Q. D., VAN HOORDE, L., BRACKE, M., BRUYNEEL, E., GESPACH, C. & MAREEL, M. 2004. Tenascin-C and SF/HGF produced by myofibroblasts in vitro provide convergent pro-invasive signals to human colon cancer cells through RhoA and Rac. *FASEB J*, 18, 1016-8.
- DELEO, A. B., JAY, G., APPELLA, E., DUBOIS, G. C., LAW, L. W. & OLD, L. J. 1979. Detection of a transformation-related antigen in chemically induced sarcomas and other transformed cells of the mouse. *Proc Natl Acad Sci U S A*, 76, 2420-4.
- DEMORY BECKLER, M., HIGGINBOTHAM, J. N., FRANKLIN, J. L., HAM, A. J., HALVEY, P. J., IMASUEN, I. E., WHITWELL, C., LI, M., LIEBLER, D. C. & COFFEY, R. J. 2013. Proteomic analysis of exosomes from mutant KRAS colon cancer cells identifies intercellular transfer of mutant KRAS. *Molecular & cellular proteomics : MCP*, 12, 343-55.
- DEREGIBUS, M. C., CANTALUPPI, V., CALOGERO, R., LO IACONO, M., TETTA, C., BIANCONE, L., BRUNO, S., BUSSOLATI, B. & CAMUSSI, G. 2007. Endothelial progenitor cell derived microvesicles activate an angiogenic program in endothelial cells by a horizontal transfer of mRNA. *Blood*, 110, 2440-8.
- DERKSEN, P. W., LIU, X., SARIDIN, F., VAN DER GULDEN, H., ZEVENHOVEN, J., EVERS, B., VAN BEIJNUM, J. R., GRIFFIOEN, A. W., VINK, J., KRIMPENFORT, P., PETERSE, J. L., CARDIFF, R. D., BERNS, A. & JONKERS, J. 2006. Somatic inactivation of E-cadherin and p53 in mice leads to metastatic lobular mammary carcinoma through induction of anoikis resistance and angiogenesis. *Cancer Cell*, 10, 437-49.
- DI AGOSTINO, S., STRANO, S., EMILIOZZI, V., ZERBINI, V., MOTTOLESE, M., SACCHI, A., BLANDINO, G. & PIAGGIO, G. 2006. Gain of function of mutant p53: the mutant p53/NF-Y protein complex reveals an aberrant transcriptional mechanism of cell cycle regulation. *Cancer Cell*, 10, 191-202.

- DI BLASIO, L., DROETTO, S., NORMAN, J., BUSSOLINO, F. & PRIMO, L. 2010. Protein kinase D1 regulates VEGF-A-induced alphavbeta3 integrin trafficking and endothelial cell migration. *Traffic*, 11, 1107-18.
- DI VIZIO, D., KIM, J., HAGER, M. H., MORELLO, M., YANG, W., LAFARGUE, C. J., TRUE, L. D., RUBIN, M. A., ADAM, R. M., BEROUKHIM, R., DEMICHELIS, F. & FREEMAN, M. R. 2009. Oncosome formation in prostate cancer: association with a region of frequent chromosomal deletion in metastatic disease. *Cancer research*, 69, 5601-9.
- DITTMER, D., PATI, S., ZAMBETTI, G., CHU, S., TERESKY, A. K., MOORE, M., FINLAY, C. & LEVINE, A. J. 1993. Gain of function mutations in p53. *Nat Genet*, 4, 42-6.
- DOLO, V., GINESTRA, A., CASSARA, D., VIOLINI, S., LUCANIA, G., TORRISI, M. R., NAGASE, H., CANEVARI, S., PAVAN, A. & VITTORELLI, M. L. 1998. Selective localization of matrix metalloproteinase 9, beta1 integrins, and human lymphocyte antigen class I molecules on membrane vesicles shed by 8701-BC breast carcinoma cells. *Cancer research*, 58, 4468-74.
- DOLO, V., GINESTRA, A., GHERSI, G., NAGASE, H. & VITTORELLI, M. L. 1994. Human breast carcinoma cells cultured in the presence of serum shed membrane vesicles rich in gelatinolytic activities. *J Submicrosc Cytol Pathol*, 26, 173-80.
- DONEHOWER, L. A., HARVEY, M., SLAGLE, B. L., MCARTHUR, M. J., MONTGOMERY, C. A., JR., BUTEL, J. S. & BRADLEY, A. 1992. Mice deficient for p53 are developmentally normal but susceptible to spontaneous tumours. *Nature*, 356, 215-21.
- DOYONNAS, R., KERSHAW, D. B., DUHME, C., MERKENS, H., CHELLIAH, S., GRAF, T. & MCNAGNY, K. M. 2001. Anuria, omphalocele, and perinatal lethality in mice lacking the CD34-related protein podocalyxin. *J Exp Med*, 194, 13-27.
- DOZYNKIEWICZ, M. A., JAMIESON, N. B., MACPHERSON, I., GRINDLAY, J., VAN DEN BERGHE, P. V., VON THUN, A., MORTON, J. P., GOURLEY, C., TIMPSON, P., NIXON, C., MCKAY, C. J., CARTER, R., STRACHAN, D., ANDERSON, K., SANSOM, O. J., CASWELL, P. T. & NORMAN, J. C. 2012. Rab25 and CLIC3 collaborate to promote integrin recycling from late endosomes/lysosomes and drive cancer progression. *Dev Cell*, 22, 131-45.
- DULIC, V., KAUFMANN, W. K., WILSON, S. J., TLSTY, T. D., LEES, E., HARPER, J. W., ELLEDGE, S. J. & REED, S. I. 1994. p53-dependent inhibition of cyclin-dependent kinase activities in human fibroblasts during radiation-induced G1 arrest. *Cell*, 76, 1013-23.
- DVORAK, H. F., QUAY, S. C., ORENSTEIN, N. S., DVORAK, A. M., HAHN, P., BITZER, A. M. & CARVALHO, A. C. 1981. Tumor shedding and coagulation. *Science*, 212, 923-4.
- ELIYAHU, D., MICHALOVITZ, D., ELIYAHU, S., PINHASI-KIMHI, O. & OREN, M. 1989. Wild-type p53 can inhibit oncogene-mediated focus formation. *Proc Natl Acad Sci U S A*, 86, 8763-7.
- ESCREVENTE, C., KELLER, S., ALTEVOGT, P. & COSTA, J. 2011. Interaction and uptake of exosomes by ovarian cancer cells. *BMC Cancer*, 11, 108.
- ESCUDIER, B., DORVAL, T., CHAPUT, N., ANDRE, F., CABY, M. P., NOVAULT, S., FLAMENT, C., LÉBOULAIRE, C., BORG, C., AMIGORENA, S., BOCCACCIO, C., BONNEROT, C., DHELLIN, O., MOVASSAGH, M., PIPERNO, S., ROBERT, C., SERRA, V., VALENTE, N., LE PECQ, J. B., SPATZ, A., LANTZ, O., TURSZ, T., ANGEVIN, E. & ZITVOGEL, L. 2005. Vaccination of metastatic melanoma patients with autologous dendritic cell (DC) derived-exosomes: results of the first phase I clinical trial. *J Transl Med*, 3, 10.

- EZRATTY, E. J., BERTAUX, C., MARCANTONIO, E. E. & GUNDERSEN, G. G. 2009. Clathrin mediates integrin endocytosis for focal adhesion disassembly in migrating cells. *The Journal of cell biology*, 187, 733-47.
- FADER, C. M., SANCHEZ, D. G., MESTRE, M. B. & COLOMBO, M. I. 2009. TI-VAMP/VAMP7 and VAMP3/cellubrevin: two v-SNARE proteins involved in specific steps of the autophagy/multivesicular body pathways. *Biochim Biophys Acta*, 1793, 1901-16.
- FAURE, J., LACHENAL, G., COURT, M., HIRRLINGER, J., CHATELLARD-CAUSSE, C., BLOT, B., GRANGE, J., SCHOEHN, G., GOLDBERG, Y., BOYER, V., KIRCHHOFF, F., RAPOSO, G., GARIN, J. & SADOUL, R. 2006. Exosomes are released by cultured cortical neurones. *Mol Cell Neurosci*, 31, 642-8.
- FENG, D., ZHAO, W. L., YE, Y. Y., BAI, X. C., LIU, R. Q., CHANG, L. F., ZHOU, Q. & SUI, S. F. 2010. Cellular internalization of exosomes occurs through phagocytosis. *Traffic*, 11, 675-87.
- FERNANDEZ, D., LARRUCEA, S., NOWAKOWSKI, A., PERICACHO, M., PARRILLA, R. & AYUSO, M. S. 2011. Release of podocalyxin into the extracellular space. Role of metalloproteinases. *Biochim Biophys Acta*, 1813, 1504-10.
- FISHER, S., BARRY, A., ABREU, J., MINIE, B., NOLAN, J., DELOREY, T. M., YOUNG, G., FENNELL, T. J., ALLEN, A., AMBROGIO, L., BERLIN, A. M., BLUMENSTIEL, B., CIBULSKIS, K., FRIEDRICH, D., JOHNSON, R., JUHN, F., REILLY, B., SHAMMAS, R., STALKER, J., SYKES, S. M., THOMPSON, J., WALSH, J., ZIMMER, A., ZWIRKO, Z., GABRIEL, S., NICOL, R. & NUSBAUM, C. 2011. A scalable, fully automated process for construction of sequence-ready human exome targeted capture libraries. *Genome biology*, 12, R1.
- FITZNER, D., SCHNAARS, M., VAN ROSSUM, D., KRISHNAMOORTHY, G., DIBAJ, P., BAKHTI, M., REGEN, T., HANISCH, U. K. & SIMONS, M. 2011. Selective transfer of exosomes from oligodendrocytes to microglia by macropinocytosis. *Journal of cell science*, 124, 447-58.
- FLORES, E. R., SENGUPTA, S., MILLER, J. B., NEWMAN, J. J., BRONSON, R., CROWLEY, D., YANG, A., MCKEON, F. & JACKS, T. 2005. Tumor predisposition in mice mutant for p63 and p73: evidence for broader tumor suppressor functions for the p53 family. *Cancer Cell*, 7, 363-73.
- FOLCH, J., LEES, M. & SLOANE STANLEY, G. H. 1957. A simple method for the isolation and purification of total lipides from animal tissues. *J Biol Chem*, 226, 497-509.
- FREED-PASTOR, W. A., MIZUNO, H., ZHAO, X., LANGEROD, A., MOON, S. H., RODRIGUEZ-BARRUECO, R., BARSOTTI, A., CHICAS, A., LI, W., POLOTSKAIA, A., BISSELL, M. J., OSBORNE, T. F., TIAN, B., LOWE, S. W., SILVA, J. M., BORRESEN-DALE, A. L., LEVINE, A. J., BARGONETTI, J. & PRIVES, C. 2012. Mutant p53 disrupts mammary tissue architecture via the mevalonate pathway. *Cell*, 148, 244-58.
- FREED-PASTOR, W. A. & PRIVES, C. 2012. Mutant p53: one name, many proteins. *Genes Dev*, 26, 1268-86.
- FRIEDL, P. & ALEXANDER, S. 2011. Cancer invasion and the microenvironment: plasticity and reciprocity. *Cell*, 147, 992-1009.
- FRUHBEL, C., FROHLICH, D., KUO, W. P., AMPHORN, J., THILEMANN, S., SAAB, A. S., KIRCHHOFF, F., MOBIUS, W., GOEBBELS, S., NAVE, K. A., SCHNEIDER, A., SIMONS, M., KLUGMANN, M., TROTTER, J. & KRAMER-ALBERS, E. M. 2013a. Neurotransmitter-triggered transfer of exosomes mediates oligodendrocyte-neuron communication. *PLoS Biol*, 11, e1001604.

- FRUHBEIS, C., FROHLICH, D., KUO, W. P. & KRAMER-ALBERS, E. M. 2013b. Extracellular vesicles as mediators of neuron-glia communication. *Front Cell Neurosci*, 7, 182.
- FUTTER, C. E., COLLINSON, L. M., BACKER, J. M. & HOPKINS, C. R. 2001. Human VPS34 is required for internal vesicle formation within multivesicular endosomes. *The Journal of cell biology*, 155, 1251-64.
- GADEA, G., DE TOLEDO, M., ANGUILLE, C. & ROUX, P. 2007. Loss of p53 promotes RhoA-ROCK-dependent cell migration and invasion in 3D matrices. *The Journal of cell biology*, 178, 23-30.
- GAIDDON, C., LOKSHIN, M., AHN, J., ZHANG, T. & PRIVES, C. 2001. A subset of tumor-derived mutant forms of p53 down-regulate p63 and p73 through a direct interaction with the p53 core domain. *Mol Cell Biol*, 21, 1874-87.
- GATZ, S. A. & WIESMULLER, L. 2006. p53 in recombination and repair. *Cell death and differentiation*, 13, 1003-16.
- GOCHEVA, V., WANG, H. W., GADEA, B. B., SHREE, T., HUNTER, K. E., GARFALL, A. L., BERMAN, T. & JOYCE, J. A. 2010. IL-4 induces cathepsin protease activity in tumor-associated macrophages to promote cancer growth and invasion. *Genes Dev*, 24, 241-55.
- GOHLER, T., JAGER, S., WARNECKE, G., YASUDA, H., KIM, E. & DEPPERT, W. 2005. Mutant p53 proteins bind DNA in a DNA structure-selective mode. *Nucleic Acids Res*, 33, 1087-100.
- GOLDSTEIN, I. & ROTTER, V. 2012. Regulation of lipid metabolism by p53 - fighting two villains with one sword. *Trends Endocrinol Metab*, 23, 567-75.
- GOSWAMI, S., SAHAI, E., WYCKOFF, J. B., CAMMER, M., COX, D., PIXLEY, F. J., STANLEY, E. R., SEGALL, J. E. & CONDEELIS, J. S. 2005. Macrophages promote the invasion of breast carcinoma cells via a colony-stimulating factor-1/epidermal growth factor paracrine loop. *Cancer research*, 65, 5278-83.
- GRANER, M. W., ALZATE, O., DECHKOVSKAIA, A. M., KEENE, J. D., SAMPSON, J. H., MITCHELL, D. A. & BIGNER, D. D. 2009. Proteomic and immunologic analyses of brain tumor exosomes. *FASEB J*, 23, 1541-57.
- GRIMSHAW, M. J., HAGEMANN, T., AYHAN, A., GILLETT, C. E., BINDER, C. & BALKWILL, F. R. 2004. A role for endothelin-2 and its receptors in breast tumor cell invasion. *Cancer research*, 64, 2461-8.
- GROSS, J. C., CHAUDHARY, V., BARTSCHERER, K. & BOUTROS, M. 2012. Active Wnt proteins are secreted on exosomes. *Nature cell biology*, 14, 1036-45.
- GUALBERTO, A., ALDAPE, K., KOZAKIEWICZ, K. & TLSTY, T. D. 1998. An oncogenic form of p53 confers a dominant, gain-of-function phenotype that disrupts spindle checkpoint control. *Proc Natl Acad Sci U S A*, 95, 5166-71.
- HANAHAH, D. & WEINBERG, R. A. 2011. Hallmarks of cancer: the next generation. *Cell*, 144, 646-74.
- HANSON, P. I. & CASHIKAR, A. 2012. Multivesicular body morphogenesis. *Annual review of cell and developmental biology*, 28, 337-62.
- HARDING, C., HEUSER, J. & STAHL, P. 1983. Receptor-mediated endocytosis of transferrin and recycling of the transferrin receptor in rat reticulocytes. *The Journal of cell biology*, 97, 329-39.
- HAUPT, Y., MAYA, R., KAZAZ, A. & OREN, M. 1997. Mdm2 promotes the rapid degradation of p53. *Nature*, 387, 296-9.
- HENNIGAN, R. F., HAWKER, K. L. & OZANNE, B. W. 1994. Fos-transformation activates genes associated with invasion. *Oncogene*, 9, 3591-600.

- HINDS, P., FINLAY, C. & LEVINE, A. J. 1989. Mutation is required to activate the p53 gene for cooperation with the ras oncogene and transformation. *J Virol*, 63, 739-46.
- HINDS, P. W., FINLAY, C. A., QUARTIN, R. S., BAKER, S. J., FEARON, E. R., VOGELSTEIN, B. & LEVINE, A. J. 1990. Mutant p53 DNA clones from human colon carcinomas cooperate with ras in transforming primary rat cells: a comparison of the "hot spot" mutant phenotypes. *Cell Growth Differ*, 1, 571-80.
- HINGORANI, S. R., WANG, L., MULTANI, A. S., COMBS, C., DERAMAUDT, T. B., HRUBAN, R. H., RUSTGI, A. K., CHANG, S. & TUVESON, D. A. 2005. Trp53R172H and KrasG12D cooperate to promote chromosomal instability and widely metastatic pancreatic ductal adenocarcinoma in mice. *Cancer Cell*, 7, 469-83.
- HOOD, J. L., SAN, R. S. & WICKLINE, S. A. 2011. Exosomes released by melanoma cells prepare sentinel lymph nodes for tumor metastasis. *Cancer research*, 71, 3792-801.
- HOWES, M. T., KIRKHAM, M., RICHES, J., CORTESE, K., WALSER, P. J., SIMPSON, F., HILL, M. M., JONES, A., LUNDMARK, R., LINDSAY, M. R., HERNANDEZ-DEVIEZ, D. J., HADZIC, G., MCCLUSKEY, A., BASHIR, R., LIU, L., PILCH, P., MCMAHON, H., ROBINSON, P. J., HANCOCK, J. F., MAYOR, S. & PARTON, R. G. 2010. Clathrin-independent carriers form a high capacity endocytic sorting system at the leading edge of migrating cells. *The Journal of cell biology*, 190, 675-91.
- HSU, C., MOROHASHI, Y., YOSHIMURA, S., MANRIQUE-HOYOS, N., JUNG, S., LAUTERBACH, M. A., BAKHTI, M., GRONBORG, M., MOBIUS, W., RHEE, J., BARR, F. A. & SIMONS, M. 2010. Regulation of exosome secretion by Rab35 and its GTPase-activating proteins TBC1D10A-C. *The Journal of cell biology*, 189, 223-32.
- HU, W., FENG, Z. & LEVINE, A. J. 2012. The Regulation of Multiple p53 Stress Responses is Mediated through MDM2. *Genes Cancer*, 3, 199-208.
- HUGEL, B., MARTINEZ, M. C., KUNZELMANN, C. & FREYSSINET, J. M. 2005. Membrane microparticles: two sides of the coin. *Physiology (Bethesda)*, 20, 22-7.
- HUMPHRIES, J. D., BYRON, A. & HUMPHRIES, M. J. 2006. Integrin ligands at a glance. *Journal of cell science*, 119, 3901-3.
- HYNES, R. O. 2002. Integrins: bidirectional, allosteric signaling machines. *Cell*, 110, 673-87.
- IKONEN, E. 2001. Roles of lipid rafts in membrane transport. *Curr Opin Cell Biol*, 13, 470-7.
- ISMAIL, N., WANG, Y., DAKHLALLAH, D., MOLDOVAN, L., AGARWAL, K., BATTE, K., SHAH, P., WISLER, J., EUBANK, T. D., TRIDANDAPANI, S., PAULAITIS, M. E., PIPER, M. G. & MARSH, C. B. 2013. Macrophage microvesicles induce macrophage differentiation and miR-223 transfer. *Blood*, 121, 984-95.
- JACQUEMET, G., GREEN, D. M., BRIDGEWATER, R. E., VON KRIEGSHEIM, A., HUMPHRIES, M. J., NORMAN, J. C. & CASWELL, P. T. 2013. RCP-driven alpha5beta1 recycling suppresses Rac and promotes RhoA activity via the RacGAP1-IQGAP1 complex. *The Journal of cell biology*, 202, 917-35.
- JOHNSTONE, R. M., ADAM, M., HAMMOND, J. R., ORR, L. & TURBIDE, C. 1987. Vesicle formation during reticulocyte maturation. Association of plasma membrane activities with released vesicles (exosomes). *J Biol Chem*, 262, 9412-20.

- JOHNSTONE, R. M., MATHEW, A., MASON, A. B. & TENG, K. 1991. Exosome formation during maturation of mammalian and avian reticulocytes: evidence that exosome release is a major route for externalization of obsolete membrane proteins. *J Cell Physiol*, 147, 27-36.
- KAHLERT, C., MELO, S. A., PROTOPOPOV, A., TANG, J., SETH, S., KOCH, M., ZHANG, J., WEITZ, J., CHIN, L., FUTREAL, A. & KALLURI, R. 2014. Identification of double-stranded genomic DNA spanning all chromosomes with mutated KRAS and p53 DNA in the serum exosomes of patients with pancreatic cancer. *J Biol Chem*, 289, 3869-75.
- KARNOUB, A. E., DASH, A. B., VO, A. P., SULLIVAN, A., BROOKS, M. W., BELL, G. W., RICHARDSON, A. L., POLYAK, K., TUBO, R. & WEINBERG, R. A. 2007. Mesenchymal stem cells within tumour stroma promote breast cancer metastasis. *Nature*, 449, 557-63.
- KAWAUCHI, K., ARAKI, K., TOBIUME, K. & TANAKA, N. 2008. p53 regulates glucose metabolism through an IKK-NF-kappaB pathway and inhibits cell transformation. *Nature cell biology*, 10, 611-8.
- KELLEY, T. W., HUNTSMAN, D., MCNAGNY, K. M., ROSKELLEY, C. D. & HSI, E. D. 2005. Podocalyxin: a marker of blasts in acute leukemia. *American journal of clinical pathology*, 124, 134-42.
- KHALIL, A. A. & FRIEDL, P. 2010. Determinants of leader cells in collective cell migration. *Integr Biol (Camb)*, 2, 568-74.
- KIARIS, H., CHATZISTAMOU, I., TRIMIS, G., FRANGOUPLEMMENOU, M., PAFITIKONDI, A. & KALOFOUTIS, A. 2005. Evidence for nonautonomous effect of p53 tumor suppressor in carcinogenesis. *Cancer research*, 65, 1627-30.
- KILPINEN, L., IMPOLA, U., SANKKILA, L., RITAMO, I., AATONEN, M., KILPINEN, S., TUIMALA, J., VALMU, L., LEVIJOKI, J., FINCKENBERG, P., SILJANDER, P., KANKURI, E., MERVAALA, E. & LAITINEN, S. 2013. Extracellular membrane vesicles from umbilical cord blood-derived MSC protect against ischemic acute kidney injury, a feature that is lost after inflammatory conditioning. *J Extracell Vesicles*, 2.
- KLYMKOWSKY, M. W. & SAVAGNER, P. 2009. Epithelial-mesenchymal transition: a cancer researcher's conceptual friend and foe. *Am J Pathol*, 174, 1588-93.
- KOLES, K., NUNNARI, J., KORKUT, C., BARRIA, R., BREWER, C., LI, Y., LESZYK, J., ZHANG, B. & BUDNIK, V. 2012. Mechanism of evenness interrupted (Evi)-exosome release at synaptic boutons. *J Biol Chem*, 287, 16820-34.
- KOMAROVA, E. A., DIATCHENKO, L., ROKHLIN, O. W., HILL, J. E., WANG, Z. J., KRIVOKRYSENKO, V. I., FEINSTEIN, E. & GUDKOV, A. V. 1998. Stress-induced secretion of growth inhibitors: a novel tumor suppressor function of p53. *Oncogene*, 17, 1089-96.
- KOMAROVA, E. A., KRIVOKRYSENKO, V., WANG, K., NEZNANOV, N., CHERNOV, M. V., KOMAROV, P. G., BRENNAN, M. L., GOLOVKINA, T. V., ROKHLIN, O. W., KUPRASH, D. V., NEDOSPASOV, S. A., HAZEN, S. L., FEINSTEIN, E. & GUDKOV, A. V. 2005. p53 is a suppressor of inflammatory response in mice. *FASEB J*, 19, 1030-2.
- KRAVCHENKO, J. E., ILYINSKAYA, G. V., KOMAROV, P. G., AGAPOVA, L. S., KOCHETKOV, D. V., STROM, E., FROLOVA, E. I., KOVRIGA, I., GUDKOV, A. V., FEINSTEIN, E. & CHUMAKOV, P. M. 2008. Small-molecule RETRA suppresses mutant p53-bearing cancer cells through a p73-dependent salvage pathway. *Proc Natl Acad Sci U S A*, 105, 6302-7.
- KUCHARZEWSKA, P., CHRISTIANSON, H. C., WELCH, J. E., SVENSSON, K. J., FREDLUND, E., RINGNER, M., MORGELIN, M., BOURSEAU-GUILMAIN, E., BENGZON, J. & BELTING, M. 2013. Exosomes reflect the hypoxic status of

- glioma cells and mediate hypoxia-dependent activation of vascular cells during tumor development. *Proc Natl Acad Sci U S A*, 110, 7312-7.
- KUSSIE, P. H., GORINA, S., MARECHAL, V., ELENBAAS, B., MOREAU, J., LEVINE, A. J. & PAVLETICH, N. P. 1996. Structure of the MDM2 oncoprotein bound to the p53 tumor suppressor transactivation domain. *Science*, 274, 948-53.
- LAKSHMINARAYAN, R., WUNDER, C., BECKEN, U., HOWES, M. T., BENZING, C., ARUMUGAM, S., SALES, S., ARIOTTI, N., CHAMBON, V., LAMAZE, C., LOEW, D., SHEVCHENKO, A., GAUS, K., PARTON, R. G. & JOHANNES, L. 2014. Galectin-3 drives glycosphingolipid-dependent biogenesis of clathrin-independent carriers. *Nature cell biology*, 16, 595-606.
- LANE, D. P. & CRAWFORD, L. V. 1979. T antigen is bound to a host protein in SV40-transformed cells. *Nature*, 278, 261-3.
- LANG, G. A., IWAKUMA, T., SUH, Y. A., LIU, G., RAO, V. A., PARANT, J. M., VALENTIN-VEGA, Y. A., TERZIAN, T., CALDWELL, L. C., STRONG, L. C., EL-NAGGAR, A. K. & LOZANO, G. 2004. Gain of function of a p53 hot spot mutation in a mouse model of Li-Fraumeni syndrome. *Cell*, 119, 861-72.
- LAPTENKO, O. & PRIVES, C. 2006. Transcriptional regulation by p53: one protein, many possibilities. *Cell death and differentiation*, 13, 951-61.
- LAULAGNIER, K., VINCENT-SCHNEIDER, H., HAMDY, S., SUBRA, C., LANKAR, D. & RECORD, M. 2005. Characterization of exosome subpopulations from RBL-2H3 cells using fluorescent lipids. *Blood Cells Mol Dis*, 35, 116-21.
- LEE, H. D., KIM, Y. H. & KIM, D. S. 2014. Exosomes derived from human macrophages suppress endothelial cell migration by controlling integrin trafficking. *Eur J Immunol*, 44, 1156-69.
- LEGATE, K. R., WICKSTROM, S. A. & FASSLER, R. 2009. Genetic and cell biological analysis of integrin outside-in signaling. *Genes Dev*, 23, 397-418.
- LESPAGNOL, A., DUFLAUT, D., BEEKMAN, C., BLANC, L., FIUCCI, G., MARINE, J. C., VIDAL, M., AMSON, R. & TELERMAN, A. 2008. Exosome secretion, including the DNA damage-induced p53-dependent secretory pathway, is severely compromised in TSAP6/Steap3-null mice. *Cell death and differentiation*, 15, 1723-33.
- LEVINE, A. J. & OREN, M. 2009. The first 30 years of p53: growing ever more complex. *Nat Rev Cancer*, 9, 749-58.
- LEVINE, A. J., TOMASINI, R., MCKEON, F. D., MAK, T. W. & MELINO, G. 2011. The p53 family: guardians of maternal reproduction. *Nat Rev Mol Cell Biol*, 12, 259-65.
- LI, D., MARCHENKO, N. D. & MOLL, U. M. 2011. SAHA shows preferential cytotoxicity in mutant p53 cancer cells by destabilizing mutant p53 through inhibition of the HDAC6-Hsp90 chaperone axis. *Cell death and differentiation*, 18, 1904-13.
- LI, J., JUNYU, LIU, A. & WANG, Y. 2014. beta-Element against human lung cancer via up-regulation of P53 protein expression to promote the release of exosome. *Lung Cancer*, 86, 144-50.
- LI, R., SUTPHIN, P. D., SCHWARTZ, D., MATAS, D., ALMOG, N., WOLKOWICZ, R., GOLDFINGER, N., PEI, H., PROKOCIMER, M. & ROTTER, V. 1998. Mutant p53 protein expression interferes with p53-independent apoptotic pathways. *Oncogene*, 16, 3269-77.
- LINZER, D. I. & LEVINE, A. J. 1979. Characterization of a 54K dalton cellular SV40 tumor antigen present in SV40-transformed cells and uninfected embryonal carcinoma cells. *Cell*, 17, 43-52.
- LLORENTE, A., SKOTLAND, T., SYLVANNE, T., KAUKANEN, D., ROG, T., ORLOWSKI, A., VATTULAINEN, I., EKROOS, K. & SANDVIG, K. 2013.

- Molecular lipidomics of exosomes released by PC-3 prostate cancer cells. *Biochim Biophys Acta*, 1831, 1302-9.
- LORENTZEN, A., BAMBER, J., SADOK, A., ELSON-SCHWAB, I. & MARSHALL, C. J. 2011. An ezrin-rich, rigid uropod-like structure directs movement of amoeboid blebbing cells. *Journal of cell science*, 124, 1256-67.
- LOTEM, J. & SACHS, L. 1995. A mutant p53 antagonizes the deregulated c-myc-mediated enhancement of apoptosis and decrease in leukemogenicity. *Proc Natl Acad Sci U S A*, 92, 9672-6.
- LOTVALL, J., HILL, A. F., HOCHBERG, F., BUZAS, E. I., DI VIZIO, D., GARDINER, C., GHO, Y. S., KUROCHKIN, I. V., MATHIVANAN, S., QUESENBERRY, P., SAHOO, S., TAHARA, H., WAUBEN, M. H., WITWER, K. W. & THERY, C. 2014. Minimal experimental requirements for definition of extracellular vesicles and their functions: a position statement from the International Society for Extracellular Vesicles. *J Extracell Vesicles*, 3, 26913.
- LUDWIG, R. L., BATES, S. & VOUSDEN, K. H. 1996. Differential activation of target cellular promoters by p53 mutants with impaired apoptotic function. *Mol Cell Biol*, 16, 4952-60.
- LUGA, V., ZHANG, L., VILORIA-PETIT, A. M., OGUNJIMI, A. A., INANLOU, M. R., CHIU, E., BUCHANAN, M., HOSEIN, A. N., BASIK, M. & WRANA, J. L. 2012. Exosomes mediate stromal mobilization of autocrine Wnt-PCP signaling in breast cancer cell migration. *Cell*, 151, 1542-56.
- LUJAMBIO, A., AKKARI, L., SIMON, J., GRACE, D., TSCHAHARGANEH, D. F., BOLDEN, J. E., ZHAO, Z., THAPAR, V., JOYCE, J. A., KRIZHANOVSKY, V. & LOWE, S. W. 2013. Non-cell-autonomous tumor suppression by p53. *Cell*, 153, 449-60.
- LUKASHCHUK, N. & VOUSDEN, K. H. 2007. Ubiquitination and degradation of mutant p53. *Mol Cell Biol*, 27, 8284-95.
- MA, W., SUNG, H. J., PARK, J. Y., MATOBA, S. & HWANG, P. M. 2007. A pivotal role for p53: balancing aerobic respiration and glycolysis. *J Bioenerg Biomembr*, 39, 243-6.
- MAI, A., VELTEL, S., PELLINEN, T., PADZIK, A., COFFEY, E., MARJOMAKI, V. & IVASKA, J. 2011. Competitive binding of Rab21 and p120RasGAP to integrins regulates receptor traffic and migration. *The Journal of cell biology*, 194, 291-306.
- MANTEROLA, L., GURUCEAGA, E., GALLEGRO PEREZ-LARRAYA, J., GONZALEZ-HUARRIZ, M., JAUREGUI, P., TEJADA, S., DIEZ-VALLE, R., SEGURA, V., SAMPRON, N., BARRENA, C., RUIZ, I., AGIRRE, A., AYUSO, A., RODRIGUEZ, J., GONZALEZ, A., XIPELL, E., MATHEU, A., LOPEZ DE MUNAIN, A., TUNON, T., ZAZPE, I., GARCIA-FONCILLAS, J., PARIS, S., DELATTRE, J. Y. & ALONSO, M. M. 2014. A small noncoding RNA signature found in exosomes of GBM patient serum as a diagnostic tool. *Neuro Oncol*, 16, 520-7.
- MAO, S., SUN, Q., XIAO, H., ZHANG, C. & LI, L. 2015. Secreted miR-34a in astrocytic shedding vesicles enhanced the vulnerability of dopaminergic neurons to neurotoxins by targeting Bcl-2. *Protein Cell*.
- MARGADANT, C., MONSUUR, H. N., NORMAN, J. C. & SONNENBERG, A. 2011. Mechanisms of integrin activation and trafficking. *Curr Opin Cell Biol*, 23, 607-14.
- MARINE, J. C. & LOZANO, G. 2010. Mdm2-mediated ubiquitylation: p53 and beyond. *Cell death and differentiation*, 17, 93-102.
- MARLEAU, A. M., CHEN, C. S., JOYCE, J. A. & TULLIS, R. H. 2012. Exosome removal as a therapeutic adjuvant in cancer. *J Transl Med*, 10, 134.

- MATHIVANAN, S., FAHNER, C. J., REID, G. E. & SIMPSON, R. J. 2012. ExoCarta 2012: database of exosomal proteins, RNA and lipids. *Nucleic Acids Res*, 40, D1241-4.
- MATHIVANAN, S., JI, H. & SIMPSON, R. J. 2010a. Exosomes: extracellular organelles important in intercellular communication. *Journal of proteomics*, 73, 1907-20.
- MATHIVANAN, S., LIM, J. W., TAURO, B. J., JI, H., MORITZ, R. L. & SIMPSON, R. J. 2010b. Proteomics analysis of A33 immunoaffinity-purified exosomes released from the human colon tumor cell line LIM1215 reveals a tissue-specific protein signature. *Molecular & cellular proteomics : MCP*, 9, 197-208.
- MAYA, R., BALASS, M., KIM, S. T., SHKEDY, D., LEAL, J. F., SHIFMAN, O., MOAS, M., BUSCHMANN, T., RONAI, Z., SHILOH, Y., KASTAN, M. B., KATZIR, E. & OREN, M. 2001. ATM-dependent phosphorylation of Mdm2 on serine 395: role in p53 activation by DNA damage. *Genes Dev*, 15, 1067-77.
- MAYOR, S. & PAGANO, R. E. 2007. Pathways of clathrin-independent endocytosis. *Nat Rev Mol Cell Biol*, 8, 603-12.
- MCMAHON, H. T. & BOUCROT, E. 2011. Molecular mechanism and physiological functions of clathrin-mediated endocytosis. *Nat Rev Mol Cell Biol*, 12, 517-33.
- MEEK, D. W. 2015. Regulation of the p53 response and its relationship to cancer. *Biochem J*, 469, 325-46.
- MELO, S. A., LUECKE, L. B., KAHLERT, C., FERNANDEZ, A. F., GAMMON, S. T., KAYE, J., LEBLEU, V. S., MITTENDORF, E. A., WEITZ, J., RAHBARI, N., REISSFELDER, C., PILARSKY, C., FRAGA, M. F., PIWNICA-WORMS, D. & KALLURI, R. 2015. Glypican-1 identifies cancer exosomes and detects early pancreatic cancer. *Nature*, 523, 177-82.
- MILNER, J. & MEDCALF, E. A. 1991. Cotranslation of activated mutant p53 with wild type drives the wild-type p53 protein into the mutant conformation. *Cell*, 65, 765-74.
- MONLEON, I., MARTINEZ-LORENZO, M. J., MONTEAGUDO, L., LASIERRA, P., TAULES, M., ITURRALDE, M., PINEIRO, A., LARRAD, L., ALAVA, M. A., NAVAL, J. & ANEL, A. 2001. Differential secretion of Fas ligand- or APO2 ligand/TNF-related apoptosis-inducing ligand-carrying microvesicles during activation-induced death of human T cells. *J Immunol*, 167, 6736-44.
- MONTECALVO, A., LARREGINA, A. T., SHUFESKY, W. J., STOLZ, D. B., SULLIVAN, M. L., KARLSSON, J. M., BATY, C. J., GIBSON, G. A., ERDOS, G., WANG, Z., MILOSEVIC, J., TKACHEVA, O. A., DIVITO, S. J., JORDAN, R., LYONS-WEILER, J., WATKINS, S. C. & MORELLI, A. E. 2012. Mechanism of transfer of functional microRNAs between mouse dendritic cells via exosomes. *Blood*, 119, 756-66.
- MORELLI, A. E., LARREGINA, A. T., SHUFESKY, W. J., SULLIVAN, M. L., STOLZ, D. B., PAPWORTH, G. D., ZAHORCHAK, A. F., LOGAR, A. J., WANG, Z., WATKINS, S. C., FALO, L. D., JR. & THOMSON, A. W. 2004. Endocytosis, intracellular sorting, and processing of exosomes by dendritic cells. *Blood*, 104, 3257-66.
- MORSE, M. A., GARST, J., OSADA, T., KHAN, S., HOBEIKA, A., CLAY, T. M., VALENTE, N., SHREENIWAS, R., SUTTON, M. A., DELCAYRE, A., HSU, D. H., LE PECQ, J. B. & LYERLY, H. K. 2005. A phase I study of dexosome immunotherapy in patients with advanced non-small cell lung cancer. *J Transl Med*, 3, 9.

- MORTON, J. P., TIMPSON, P., KARIM, S. A., RIDGWAY, R. A., ATHINEOS, D., DOYLE, B., JAMIESON, N. B., OIEN, K. A., LOWY, A. M., BRUNTON, V. G., FRAME, M. C., EVANS, T. R. & SANSOM, O. J. 2010. Mutant p53 drives metastasis and overcomes growth arrest/senescence in pancreatic cancer. *Proc Natl Acad Sci U S A*, 107, 246-51.
- MULLER, P. A., CASWELL, P. T., DOYLE, B., IWANICKI, M. P., TAN, E. H., KARIM, S., LUKASHCHUK, N., GILLESPIE, D. A., LUDWIG, R. L., GOSSELIN, P., CROMER, A., BRUGGE, J. S., SANSOM, O. J., NORMAN, J. C. & VOUSDEN, K. H. 2009. Mutant p53 drives invasion by promoting integrin recycling. *Cell*, 139, 1327-41.
- MULLER, P. A., TRINIDAD, A. G., CASWELL, P. T., NORMAN, J. C. & VOUSDEN, K. H. 2014. Mutant p53 regulates Dicer through p63-dependent and -independent mechanisms to promote an invasive phenotype. *J Biol Chem*, 289, 122-32.
- MULLER, P. A., TRINIDAD, A. G., TIMPSON, P., MORTON, J. P., ZANIVAN, S., VAN DEN BERGHE, P. V., NIXON, C., KARIM, S. A., CASWELL, P. T., NOLL, J. E., COFFILL, C. R., LANE, D. P., SANSOM, O. J., NEILSEN, P. M., NORMAN, J. C. & VOUSDEN, K. H. 2013. Mutant p53 enhances MET trafficking and signalling to drive cell scattering and invasion. *Oncogene*, 32, 1252-65.
- MURALIDHARAN-CHARI, V., CLANCY, J., PLOU, C., ROMAO, M., CHAVRIER, P., RAPOSO, G. & D'SOUZA-SCHOREY, C. 2009. ARF6-regulated shedding of tumor cell-derived plasma membrane microvesicles. *Current biology : CB*, 19, 1875-85.
- NANBO, A., KAWANISHI, E., YOSHIDA, R. & YOSHIYAMA, H. 2013. Exosomes derived from Epstein-Barr virus-infected cells are internalized via caveola-dependent endocytosis and promote phenotypic modulation in target cells. *J Virol*, 87, 10334-47.
- NEILSEN, P. M., NOLL, J. E., SUETANI, R. J., SCHULZ, R. B., AL-EJEH, F., EVDOKIOU, A., LANE, D. P. & CALLEN, D. F. 2011. Mutant p53 uses p63 as a molecular chaperone to alter gene expression and induce a pro-invasive secretome. *Oncotarget*, 2, 1203-17.
- NIELSEN, J. S. & MCNAGNY, K. M. 2009. The role of podocalyxin in health and disease. *J Am Soc Nephrol*, 20, 1669-76.
- NILSSON, J., SKOG, J., NORDSTRAND, A., BARANOV, V., MINCHEVA-NILSSON, L., BREAKEFIELD, X. O. & WIDMARK, A. 2009. Prostate cancer-derived urine exosomes: a novel approach to biomarkers for prostate cancer. *Br J Cancer*, 100, 1603-7.
- NISHIMURA, T. & KAIBUCHI, K. 2007. Numb controls integrin endocytosis for directional cell migration with aPKC and PAR-3. *Dev Cell*, 13, 15-28.
- NOSKE, A., LIPKA, S., BUDCZIES, J., MULLER, K., LODDENKEMPER, C., BUHR, H. J. & KRUSCHEWSKI, M. 2009. Combination of p53 expression and p21 loss has an independent prognostic impact on sporadic colorectal cancer. *Oncology reports*, 22, 3-9.
- O'FARRELL, T. J., GHOSH, P., DOBASHI, N., SASAKI, C. Y. & LONGO, D. L. 2004. Comparison of the effect of mutant and wild-type p53 on global gene expression. *Cancer research*, 64, 8199-207.
- OFIR-ROSENFELD, Y., BOGGS, K., MICHAEL, D., KASTAN, M. B. & OREN, M. 2008. Mdm2 regulates p53 mRNA translation through inhibitory interactions with ribosomal protein L26. *Mol Cell*, 32, 180-9.
- OLIVE, K. P., TUVESON, D. A., RUHE, Z. C., YIN, B., WILLIS, N. A., BRONSON, R. T., CROWLEY, D. & JACKS, T. 2004. Mutant p53 gain of function in two mouse models of Li-Fraumeni syndrome. *Cell*, 119, 847-60.

- OLIVIER, M., GOLDFAR, D. E., SODHA, N., OHGAKI, H., KLEIHUES, P., HAINAUT, P. & EELES, R. A. 2003. Li-Fraumeni and related syndromes: correlation between tumor type, family structure, and TP53 genotype. *Cancer research*, 63, 6643-50.
- OSTROWSKI, M., CARMO, N. B., KRUMEICH, S., FANGET, I., RAPOSO, G., SAVINA, A., MOITA, C. F., SCHAUER, K., HUME, A. N., FREITAS, R. P., GOUD, B., BENARROCH, P., HACHOEN, N., FUKUDA, M., DESNOS, C., SEABRA, M. C., DARCHEN, F., AMIGORENA, S., MOITA, L. F. & THERY, C. 2010. Rab27a and Rab27b control different steps of the exosome secretion pathway. *Nature cell biology*, 12, 19-30; sup pp 1-13.
- PAN, B. T. & JOHNSTONE, R. M. 1983. Fate of the transferrin receptor during maturation of sheep reticulocytes in vitro: selective externalization of the receptor. *Cell*, 33, 967-78.
- PAN, B. T., TENG, K., WU, C., ADAM, M. & JOHNSTONE, R. M. 1985. Electron microscopic evidence for externalization of the transferrin receptor in vesicular form in sheep reticulocytes. *The Journal of cell biology*, 101, 942-8.
- PANG, W., SU, J., WANG, Y., FENG, H., DAI, X., YUAN, Y., CHEN, X. & YAO, W. 2015. Pancreatic Cancer-Secreted miR-155 implicates in the Conversion from Normal Fibroblasts to Cancer-Associated Fibroblasts. *Cancer Sci*.
- PAROLINI, I., FEDERICI, C., RAGGI, C., LUGINI, L., PALLESCHI, S., DE MILITO, A., COSCIA, C., IESSI, E., LOGOZZI, M., MOLINARI, A., COLONE, M., TATTI, M., SARGIACOMO, M. & FAIS, S. 2009. Microenvironmental pH is a key factor for exosome traffic in tumor cells. *J Biol Chem*, 284, 34211-22.
- PASQUET, J. M., DACHARY-PRIGENT, J. & NURDEN, A. T. 1996. Calcium influx is a determining factor of calpain activation and microparticle formation in platelets. *Eur J Biochem*, 239, 647-54.
- PEGTEL, D. M., COSMOPOULOS, K., THORLEY-LAWSON, D. A., VAN EIJNDHOVEN, M. A., HOPMANS, E. S., LINDENBERG, J. L., DE GRUIJL, T. D., WURDINGER, T. & MIDDELDORP, J. M. 2010. Functional delivery of viral miRNAs via exosomes. *Proc Natl Acad Sci U S A*, 107, 6328-33.
- PEINADO, H., ALECKOVIC, M., LAVOTSHKIN, S., MATEI, I., COSTA-SILVA, B., MORENO-BUENO, G., HERGUETA-REDONDO, M., WILLIAMS, C., GARCIA-SANTOS, G., GHAJAR, C., NITADORI-HOSHINO, A., HOFFMAN, C., BADAL, K., GARCIA, B. A., CALLAHAN, M. K., YUAN, J., MARTINS, V. R., SKOG, J., KAPLAN, R. N., BRADY, M. S., WOLCHOK, J. D., CHAPMAN, P. B., KANG, Y., BROMBERG, J. & LYDEN, D. 2012. Melanoma exosomes educate bone marrow progenitor cells toward a pro-metastatic phenotype through MET. *Nature medicine*, 18, 883-91.
- PELED, A., ZIPORI, D. & ROTTER, V. 1996. Cooperation between p53-dependent and p53-independent apoptotic pathways in myeloid cells. *Cancer research*, 56, 2148-56.
- PEREZ-HERNANDEZ, D., GUTIERREZ-VAZQUEZ, C., JORGE, I., LOPEZ-MARTIN, S., URSA, A., SANCHEZ-MADRID, F., VAZQUEZ, J. & YANEZ-MO, M. 2013. The intracellular interactome of tetraspanin-enriched microdomains reveals their function as sorting machineries toward exosomes. *J Biol Chem*, 288, 11649-61.
- PETITJEAN, A., MATHE, E., KATO, S., ISHIOKA, C., TAVTIGIAN, S. V., HAINAUT, P. & OLIVIER, M. 2007. Impact of mutant p53 functional properties on TP53 mutation patterns and tumor phenotype: lessons from recent developments in the IARC TP53 database. *Hum Mutat*, 28, 622-9.
- PIPER, R. C. & KATZMANN, D. J. 2007. Biogenesis and function of multivesicular bodies. *Annual review of cell and developmental biology*, 23, 519-47.

- POLLARD, T. D. & BORISY, G. G. 2003. Cellular motility driven by assembly and disassembly of actin filaments. *Cell*, 112, 453-65.
- POUTSIKA, D. D., SCHRODER, E. W., TAYLOR, D. D., LEVY, E. M. & BLACK, P. H. 1985. Membrane vesicles shed by murine melanoma cells selectively inhibit the expression of Ia antigen by macrophages. *J Immunol*, 134, 138-44.
- POWELKA, A. M., SUN, J., LI, J., GAO, M., SHAW, L. M., SONNENBERG, A. & HSU, V. W. 2004. Stimulation-dependent recycling of integrin beta1 regulated by ARF6 and Rab11. *Traffic*, 5, 20-36.
- RABESANDRATANA, H., TOUTANT, J. P., REGGIO, H. & VIDAL, M. 1998. Decay-accelerating factor (CD55) and membrane inhibitor of reactive lysis (CD59) are released within exosomes during In vitro maturation of reticulocytes. *Blood*, 91, 2573-80.
- RABINOWITS, G., GERCEL-TAYLOR, C., DAY, J. M., TAYLOR, D. D. & KLOECKER, G. H. 2009. Exosomal microRNA: a diagnostic marker for lung cancer. *Clin Lung Cancer*, 10, 42-6.
- RAINERO, E., CASWELL, P. T., MULLER, P. A., GRINDLAY, J., MCCAFFREY, M. W., ZHANG, Q., WAKELAM, M. J., VOUSDEN, K. H., GRAZIANI, A. & NORMAN, J. C. 2012. Diacylglycerol kinase alpha controls RCP-dependent integrin trafficking to promote invasive migration. *The Journal of cell biology*, 196, 277-95.
- RAMSAY, A. G., KEPPLER, M. D., JAZAYERI, M., THOMAS, G. J., PARSONS, M., VIOLETTE, S., WEINREB, P., HART, I. R. & MARSHALL, J. F. 2007. HS1-associated protein X-1 regulates carcinoma cell migration and invasion via clathrin-mediated endocytosis of integrin alphavbeta6. *Cancer research*, 67, 5275-84.
- RAN, F. A., HSU, P. D., LIN, C. Y., GOOTENBERG, J. S., KONERMANN, S., TREVINO, A. E., SCOTT, D. A., INOUE, A., MATOBA, S., ZHANG, Y. & ZHANG, F. 2013. Double nicking by RNA-guided CRISPR Cas9 for enhanced genome editing specificity. *Cell*, 154, 1380-9.
- RAPOSO, G., NIJMAN, H. W., STOORVOGEL, W., LIEJENDEKKER, R., HARDING, C. V., MELIEF, C. J. & GEUZE, H. J. 1996. B lymphocytes secrete antigen-presenting vesicles. *J Exp Med*, 183, 1161-72.
- RAPOSO, G. & STOORVOGEL, W. 2013. Extracellular vesicles: exosomes, microvesicles, and friends. *The Journal of cell biology*, 200, 373-83.
- RATAJCZAK, J., MIEKUS, K., KUCIA, M., ZHANG, J., RECA, R., DVORAK, P. & RATAJCZAK, M. Z. 2006. Embryonic stem cell-derived microvesicles reprogram hematopoietic progenitors: evidence for horizontal transfer of mRNA and protein delivery. *Leukemia*, 20, 847-56.
- RESTLE, A., FARBER, M., BAUMANN, C., BOHRINGER, M., SCHEIDTMANN, K. H., MULLER-TIDOW, C. & WIESMULLER, L. 2008. Dissecting the role of p53 phosphorylation in homologous recombination provides new clues for gain-of-function mutants. *Nucleic Acids Res*, 36, 5362-75.
- ROBERTS, M., BARRY, S., WOODS, A., VAN DER SLUIJS, P. & NORMAN, J. 2001. PDGF-regulated rab4-dependent recycling of alphavbeta3 integrin from early endosomes is necessary for cell adhesion and spreading. *Current biology : CB*, 11, 1392-402.
- ROBERTS, M. S., WOODS, A. J., DALE, T. C., VAN DER SLUIJS, P. & NORMAN, J. C. 2004. Protein kinase B/Akt acts via glycogen synthase kinase 3 to regulate recycling of alpha v beta 3 and alpha 5 beta 1 integrins. *Mol Cell Biol*, 24, 1505-15.

- ROTTER, V. 1983. p53, a transformation-related cellular-encoded protein, can be used as a biochemical marker for the detection of primary mouse tumor cells. *Proc Natl Acad Sci U S A*, 80, 2613-7.
- SAHAI, E. 2005. Mechanisms of cancer cell invasion. *Curr Opin Genet Dev*, 15, 87-96.
- SAHAI, E. & MARSHALL, C. J. 2003. Differing modes of tumour cell invasion have distinct requirements for Rho/ROCK signalling and extracellular proteolysis. *Nature cell biology*, 5, 711-9.
- SAMENI, M., DOSESCU, J., MOIN, K. & SLOANE, B. F. 2003. Functional imaging of proteolysis: stromal and inflammatory cells increase tumor proteolysis. *Mol Imaging*, 2, 159-75.
- SASSETTI, C., TANGEMANN, K., SINGER, M. S., KERSHAW, D. B. & ROSEN, S. D. 1998. Identification of podocalyxin-like protein as a high endothelial venule ligand for L-selectin: parallels to CD34. *J Exp Med*, 187, 1965-75.
- SAUNDERSON, S. C., DUNN, A. C., CROCKER, P. R. & MCLELLAN, A. D. 2014. CD169 mediates the capture of exosomes in spleen and lymph node. *Blood*, 123, 208-16.
- SAVINA, A., VIDAL, M. & COLOMBO, M. I. 2002. The exosome pathway in K562 cells is regulated by Rab11. *Journal of cell science*, 115, 2505-15.
- SCHMID-SCHONBEIN, H., HEIDTMANN, H. & GREBE, R. 1986a. Spectrin, red cell shape and deformability. I. Membrane curvature in genetic spectrin deficiency. *Blut*, 52, 131-47.
- SCHMID-SCHONBEIN, H., HEIDTMANN, H. & GREBE, R. 1986b. Spectrin, red cell shape and deformability. II. The antagonistic action of spectrin and sialic acid residues in determining membrane curvature in genetic spectrin deficiency in mice. *Blut*, 52, 149-64.
- SEGURA, E., GUERIN, C., HOGG, N., AMIGORENA, S. & THERY, C. 2007. CD8+ dendritic cells use LFA-1 to capture MHC-peptide complexes from exosomes in vivo. *J Immunol*, 179, 1489-96.
- SEGURA, E., NICCO, C., LOMBARD, B., VERON, P., RAPOSO, G., BATTEUX, F., AMIGORENA, S. & THERY, C. 2005. ICAM-1 on exosomes from mature dendritic cells is critical for efficient naive T-cell priming. *Blood*, 106, 216-23.
- SELIVANOVA, G., IOTSOVA, V., OKAN, I., FRITSCHKE, M., STROM, M., GRONER, B., GRAFSTROM, R. C. & WIMAN, K. G. 1997. Restoration of the growth suppression function of mutant p53 by a synthetic peptide derived from the p53 C-terminal domain. *Nature medicine*, 3, 632-8.
- SHIH, J. Y., TSAI, M. F., CHANG, T. H., CHANG, Y. L., YUAN, A., YU, C. J., LIN, S. B., LIOU, G. Y., LEE, M. L., CHEN, J. J., HONG, T. M., YANG, S. C., SU, J. L., LEE, Y. C. & YANG, P. C. 2005. Transcription repressor slug promotes carcinoma invasion and predicts outcome of patients with lung adenocarcinoma. *Clin Cancer Res*, 11, 8070-8.
- SHIOTA, M., IZUMI, H., ONITSUKA, T., MIYAMOTO, N., KASHIWAGI, E., KIDANI, A., HIRANO, G., TAKAHASHI, M., NAITO, S. & KOHNO, K. 2008. Twist and p53 reciprocally regulate target genes via direct interaction. *Oncogene*, 27, 5543-53.
- SILVA, J. L., RANGEL, L. P., COSTA, D. C., CORDEIRO, Y. & DE MOURA GALLO, C. V. 2013. Expanding the prion concept to cancer biology: dominant-negative effect of aggregates of mutant p53 tumour suppressor. *Biosci Rep*, 33.
- SIMPSON, R. J., KALRA, H. & MATHIVANAN, S. 2012. ExoCarta as a resource for exosomal research. *J Extracell Vesicles*, 1.

- SKOG, J., WURDINGER, T., VAN RIJN, S., MEIJER, D. H., GAINCHE, L., SENA-ESTEVEZ, M., CURRY, W. T., JR., CARTER, B. S., KRICHEVSKY, A. M. & BREAKEYFIELD, X. O. 2008. Glioblastoma microvesicles transport RNA and proteins that promote tumour growth and provide diagnostic biomarkers. *Nature cell biology*, 10, 1470-6.
- SODERBERG, A., BARRAL, A. M., SODERSTROM, M., SANDER, B. & ROSEN, A. 2007. Redox-signaling transmitted in trans to neighboring cells by melanoma-derived TNF-containing exosomes. *Free Radic Biol Med*, 43, 90-9.
- SOLOMON, H., BUGANIM, Y., KOGAN-SAKIN, I., POMERANIEC, L., ASSIA, Y., MADAR, S., GOLDSTEIN, I., BROSH, R., KALO, E., BEATUS, T., GOLDFINGER, N. & ROTTER, V. 2012. Various p53 mutant proteins differently regulate the Ras circuit to induce a cancer-related gene signature. *Journal of cell science*, 125, 3144-52.
- SOMASIRI, A., NIELSEN, J. S., MAKRETSOV, N., MCCOY, M. L., PRENTICE, L., GILKS, C. B., CHIA, S. K., GELMON, K. A., KERSHAW, D. B., HUNTSMAN, D. G., MCNAGNY, K. M. & ROSKELLEY, C. D. 2004. Overexpression of the anti-adhesin podocalyxin is an independent predictor of breast cancer progression. *Cancer research*, 64, 5068-73.
- SOO, C. Y., SONG, Y., ZHENG, Y., CAMPBELL, E. C., RICHES, A. C., GUNN-MOORE, F. & POWIS, S. J. 2012. Nanoparticle tracking analysis monitors microvesicle and exosome secretion from immune cells. *Immunology*, 136, 192-7.
- STEGMAYR, B. & RONQUIST, G. 1982. Promotive effect on human sperm progressive motility by prostasomes. *Urol Res*, 10, 253-7.
- STENMARK, H. 2009. Rab GTPases as coordinators of vesicle traffic. *Nat Rev Mol Cell Biol*, 10, 513-25.
- STOORVOGEL, W., STROUS, G. J., GEUZE, H. J., OORSCHOT, V. & SCHWARTZ, A. L. 1991. Late endosomes derive from early endosomes by maturation. *Cell*, 65, 417-27.
- STRANO, S., FONTEMAGGI, G., COSTANZO, A., RIZZO, M. G., MONTI, O., BACCARINI, A., DEL SAL, G., LEVRERO, M., SACCHI, A., OREN, M. & BLANDINO, G. 2002. Physical interaction with human tumor-derived p53 mutants inhibits p63 activities. *J Biol Chem*, 277, 18817-26.
- SUH, Y. A., POST, S. M., ELIZONDO-FRAIRE, A. C., MACCIO, D. R., JACKSON, J. G., EL-NAGGAR, A. K., VAN PELT, C., TERZIAN, T. & LOZANO, G. 2011. Multiple stress signals activate mutant p53 in vivo. *Cancer research*, 71, 7168-75.
- SUNG, B. H., KETOVA, T., HOSHINO, D., ZIJLSTRA, A. & WEAVER, A. M. 2015. Directional cell movement through tissues is controlled by exosome secretion. *Nat Commun*, 6, 7164.
- SVENSSON, K. J., CHRISTIANSON, H. C., WITTRUP, A., BOURSEAU-GUILMAIN, E., LINDQVIST, E., SVENSSON, L. M., MORGELIN, M. & BELTING, M. 2013. Exosome uptake depends on ERK1/2-heat shock protein 27 signaling and lipid Raft-mediated endocytosis negatively regulated by caveolin-1. *J Biol Chem*, 288, 17713-24.
- TALMADGE, J. E. & FIDLER, I. J. 2010. AACR centennial series: the biology of cancer metastasis: historical perspective. *Cancer research*, 70, 5649-69.
- TAN, S. S., YIN, Y., LEE, T., LAI, R. C., YEO, R. W., ZHANG, B., CHOO, A. & LIM, S. K. 2013. Therapeutic MSC exosomes are derived from lipid raft microdomains in the plasma membrane. *J Extracell Vesicles*, 2.
- TAURO, B. J., GREENING, D. W., MATHIAS, R. A., JI, H., MATHIVANAN, S., SCOTT, A. M. & SIMPSON, R. J. 2012. Comparison of ultracentrifugation, density gradient separation, and immunoaffinity capture methods for

- isolating human colon cancer cell line LIM1863-derived exosomes. *Methods*, 56, 293-304.
- TAYLOR, D. D. & GERCEL-TAYLOR, C. 2005. Tumour-derived exosomes and their role in cancer-associated T-cell signalling defects. *Br J Cancer*, 92, 305-11.
- TAYLOR, D. D. & GERCEL-TAYLOR, C. 2008. MicroRNA signatures of tumor-derived exosomes as diagnostic biomarkers of ovarian cancer. *Gynecol Oncol*, 110, 13-21.
- TECKCHANDANI, A., MULKEARNS, E. E., RANDOLPH, T. W., TOIDA, N. & COOPER, J. A. 2012. The clathrin adaptor Dab2 recruits EH domain scaffold proteins to regulate integrin beta1 endocytosis. *Mol Biol Cell*, 23, 2905-16.
- TERZIAN, T., SUH, Y. A., IWAKUMA, T., POST, S. M., NEUMANN, M., LANG, G. A., VAN PELT, C. S. & LOZANO, G. 2008. The inherent instability of mutant p53 is alleviated by Mdm2 or p16INK4a loss. *Genes Dev*, 22, 1337-44.
- THERY, C., AMIGORENA, S., RAPOSO, G. & CLAYTON, A. 2006a. Isolation and characterization of exosomes from cell culture supernatants and biological fluids. *Current protocols in cell biology / editorial board, Juan S. Bonifacino ... [et al.]*, Chapter 3, Unit 3 22.
- THERY, C., BOUSSAC, M., VERON, P., RICCIARDI-CASTAGNOLI, P., RAPOSO, G., GARIN, J. & AMIGORENA, S. 2001. Proteomic analysis of dendritic cell-derived exosomes: a secreted subcellular compartment distinct from apoptotic vesicles. *J Immunol*, 166, 7309-18.
- THERY, C., DUBAN, L., SEGURA, E., VERON, P., LANTZ, O. & AMIGORENA, S. 2002. Indirect activation of naive CD4+ T cells by dendritic cell-derived exosomes. *Nat Immunol*, 3, 1156-62.
- THERY, C., REGNAULT, A., GARIN, J., WOLFERS, J., ZITVOGEL, L., RICCIARDI-CASTAGNOLI, P., RAPOSO, G. & AMIGORENA, S. 1999. Molecular characterization of dendritic cell-derived exosomes. Selective accumulation of the heat shock protein hsc73. *The Journal of cell biology*, 147, 599-610.
- THERY, M., RACINE, V., PIEL, M., PEPIN, A., DIMITROV, A., CHEN, Y., SIBARITA, J. B. & BORNENS, M. 2006b. Anisotropy of cell adhesive microenvironment governs cell internal organization and orientation of polarity. *Proc Natl Acad Sci U S A*, 103, 19771-6.
- TIMPSON, P., MCGHEE, E. J., MORTON, J. P., VON KRIEGSHEIM, A., SCHWARZ, J. P., KARIM, S. A., DOYLE, B., QUINN, J. A., CARRAGHER, N. O., EDWARD, M., OLSON, M. F., FRAME, M. C., BRUNTON, V. G., SANSOM, O. J. & ANDERSON, K. I. 2011. Spatial regulation of RhoA activity during pancreatic cancer cell invasion driven by mutant p53. *Cancer research*, 71, 747-57.
- TRAJKOVIC, K., HSU, C., CHIANTIA, S., RAJENDRAN, L., WENZEL, D., WIELAND, F., SCHWILLE, P., BRUGGER, B. & SIMONS, M. 2008. Ceramide triggers budding of exosome vesicles into multivesicular endosomes. *Science*, 319, 1244-7.
- TRAMS, E. G., LAUTER, C. J., SALEM, N., JR. & HEINE, U. 1981. Exfoliation of membrane ecto-enzymes in the form of micro-vesicles. *Biochim Biophys Acta*, 645, 63-70.
- UPLA, P., MARJOMAKI, V., KANKAANPAA, P., IVASKA, J., HYYPIA, T., VAN DER GOOT, F. G. & HEINO, J. 2004. Clustering induces a lateral redistribution of alpha 2 beta 1 integrin from membrane rafts to caveolae and subsequent protein kinase C-dependent internalization. *Mol Biol Cell*, 15, 625-36.

- URIST, M. J., DI COMO, C. J., LU, M. L., CHARYTONOWICZ, E., VERBEL, D., CRUM, C. P., INCE, T. A., MCKEON, F. D. & CORDON-CARDO, C. 2002. Loss of p63 expression is associated with tumor progression in bladder cancer. *Am J Pathol*, 161, 1199-206.
- VALADI, H., EKSTROM, K., BOSSIOS, A., SJOSTRAND, M., LEE, J. J. & LOTVALL, J. O. 2007. Exosome-mediated transfer of mRNAs and microRNAs is a novel mechanism of genetic exchange between cells. *Nature cell biology*, 9, 654-9.
- VAN NGUYEN, T., PUEBLA-OSORIO, N., PANG, H., DUJKA, M. E. & ZHU, C. 2007. DNA damage-induced cellular senescence is sufficient to suppress tumorigenesis: a mouse model. *J Exp Med*, 204, 1453-61.
- VAN NIEL, G., RAPOSO, G., CANDALH, C., BOUSSAC, M., HERSHBERG, R., CERF-BENSUSSAN, N. & HEYMAN, M. 2001. Intestinal epithelial cells secrete exosome-like vesicles. *Gastroenterology*, 121, 337-49.
- VENTURA, A., KIRSCH, D. G., MCLAUGHLIN, M. E., TUVESON, D. A., GRIMM, J., LINTAULT, L., NEWMAN, J., RECZEK, E. E., WEISSELEDER, R. & JACKS, T. 2007. Restoration of p53 function leads to tumour regression in vivo. *Nature*, 445, 661-5.
- VERWEIJ, F. J., VAN EIJNDHOVEN, M. A., HOPMANS, E. S., VENDRIG, T., WURDINGER, T., CAHIR-MCFARLAND, E., KIEFF, E., GEERTS, D., VAN DER KANT, R., NEEFJES, J., MIDDELDORP, J. M. & PEGTEL, D. M. 2011. LMP1 association with CD63 in endosomes and secretion via exosomes limits constitutive NF-kappaB activation. *EMBO J*, 30, 2115-29.
- VIAL, E., SAHAI, E. & MARSHALL, C. J. 2003. ERK-MAPK signaling coordinately regulates activity of Rac1 and RhoA for tumor cell motility. *Cancer Cell*, 4, 67-79.
- VOGELSTEIN, B., LANE, D. & LEVINE, A. J. 2000. Surfing the p53 network. *Nature*, 408, 307-10.
- VOJTESEK, B., BARTEK, J., MIDGLEY, C. A. & LANE, D. P. 1992. An immunochemical analysis of the human nuclear phosphoprotein p53. New monoclonal antibodies and epitope mapping using recombinant p53. *Journal of immunological methods*, 151, 237-44.
- VOUSDEN, K. H. & LANE, D. P. 2007. p53 in health and disease. *Nat Rev Mol Cell Biol*, 8, 275-83.
- VOUSDEN, K. H. & LU, X. 2002. Live or let die: the cell's response to p53. *Nat Rev Cancer*, 2, 594-604.
- VOUSDEN, K. H. & PRIVES, C. 2009. Blinded by the Light: The Growing Complexity of p53. *Cell*, 137, 413-31.
- VOUSDEN, K. H. & RYAN, K. M. 2009. p53 and metabolism. *Nat Rev Cancer*, 9, 691-700.
- WANG, B., FENG, P., XIAO, Z. & REN, E. C. 2009a. LIM and SH3 protein 1 (Lasp1) is a novel p53 transcriptional target involved in hepatocellular carcinoma. *J Hepatol*, 50, 528-37.
- WANG, S. P., WANG, W. L., CHANG, Y. L., WU, C. T., CHAO, Y. C., KAO, S. H., YUAN, A., LIN, C. W., YANG, S. C., CHAN, W. K., LI, K. C., HONG, T. M. & YANG, P. C. 2009b. p53 controls cancer cell invasion by inducing the MDM2-mediated degradation of Slug. *Nature cell biology*, 11, 694-704.
- WANG, T., GILKES, D. M., TAKANO, N., XIANG, L., LUO, W., BISHOP, C. J., CHATURVEDI, P., GREEN, J. J. & SEMENZA, G. L. 2014. Hypoxia-inducible factors and RAB22A mediate formation of microvesicles that stimulate breast cancer invasion and metastasis. *Proc Natl Acad Sci U S A*, 111, E3234-42.

- WANG, T. Y., HAN, Z. M., CHAI, Y. R. & ZHANG, J. H. 2010. A mini review of MAR-binding proteins. *Mol Biol Rep*, 37, 3553-60.
- WANG, W., GOSWAMI, S., LAPIDUS, K., WELLS, A. L., WYCKOFF, J. B., SAHAI, E., SINGER, R. H., SEGALL, J. E. & CONDEELIS, J. S. 2004. Identification and testing of a gene expression signature of invasive carcinoma cells within primary mammary tumors. *Cancer research*, 64, 8585-94.
- WANG, X., WANG, J. & JIANG, X. 2011. MdmX protein is essential for Mdm2 protein-mediated p53 polyubiquitination. *J Biol Chem*, 286, 23725-34.
- WEBER, J. D., TAYLOR, L. J., ROUSSEL, M. F., SHERR, C. J. & BAR-SAGI, D. 1999. Nucleolar Arf sequesters Mdm2 and activates p53. *Nature cell biology*, 1, 20-6.
- WEISZ, L., ZALCENSTEIN, A., STAMBOLSKY, P., COHEN, Y., GOLDFINGER, N., OREN, M. & ROTTER, V. 2004. Transactivation of the EGR1 gene contributes to mutant p53 gain of function. *Cancer research*, 64, 8318-27.
- WHITE, D. P., CASWELL, P. T. & NORMAN, J. C. 2007. alpha v beta3 and alpha5beta1 integrin recycling pathways dictate downstream Rho kinase signaling to regulate persistent cell migration. *The Journal of cell biology*, 177, 515-25.
- WILL, K., WARNECKE, G., WIESMULLER, L. & DEPERT, W. 1998. Specific interaction of mutant p53 with regions of matrix attachment region DNA elements (MARs) with a high potential for base-unpairing. *Proc Natl Acad Sci U S A*, 95, 13681-6.
- WOLF, K., MULLER, R., BORGMANN, S., BROCKER, E. B. & FRIEDL, P. 2003. Amoeboid shape change and contact guidance: T-lymphocyte crawling through fibrillar collagen is independent of matrix remodeling by MMPs and other proteases. *Blood*, 102, 3262-9.
- WOLFERS, J., LOZIER, A., RAPOSO, G., REGNAULT, A., THERY, C., MASURIER, C., FLAMENT, C., POUZIEUX, S., FAURE, F., TURSZ, T., ANGEVIN, E., AMIGORENA, S. & ZITVOGEL, L. 2001. Tumor-derived exosomes are a source of shared tumor rejection antigens for CTL cross-priming. *Nature medicine*, 7, 297-303.
- WUBBOLTS, R., LECKIE, R. S., VEENHUIZEN, P. T., SCHWARZMANN, G., MOBIUS, W., HOERNSCHEMEYER, J., SLOT, J. W., GEUZE, H. J. & STOOORVOGEL, W. 2003. Proteomic and biochemical analyses of human B cell-derived exosomes. Potential implications for their function and multivesicular body formation. *J Biol Chem*, 278, 10963-72.
- XIA, M. & LAND, H. 2007. Tumor suppressor p53 restricts Ras stimulation of RhoA and cancer cell motility. *Nat Struct Mol Biol*, 14, 215-23.
- XUE, W., ZENDER, L., MIETHING, C., DICKINS, R. A., HERNANDO, E., KRIZHANOVSKY, V., CORDON-CARDO, C. & LOWE, S. W. 2007. Senescence and tumour clearance is triggered by p53 restoration in murine liver carcinomas. *Nature*, 445, 656-60.
- YOON, S. O., SHIN, S. & MERCURIO, A. M. 2005. Hypoxia stimulates carcinoma invasion by stabilizing microtubules and promoting the Rab11 trafficking of the alpha6beta4 integrin. *Cancer research*, 65, 2761-9.
- YU, J., WANG, Z., KINZLER, K. W., VOGELSTEIN, B. & ZHANG, L. 2003. PUMA mediates the apoptotic response to p53 in colorectal cancer cells. *Proc Natl Acad Sci U S A*, 100, 1931-6.
- YU, X., HARRIS, S. L. & LEVINE, A. J. 2006. The regulation of exosome secretion: a novel function of the p53 protein. *Cancer research*, 66, 4795-801.
- ZHU, Y., SHEN, T., LIU, J., ZHENG, J., ZHANG, Y., XU, R., SUN, C., DU, J., CHEN, Y. & GU, L. 2013. Rab35 is required for Wnt5a/Dvl2-induced Rac1

- activation and cell migration in MCF-7 breast cancer cells. *Cell Signal*, 25, 1075-85.
- ZITVOGEL, L., REGNAULT, A., LOZIER, A., WOLFERS, J., FLAMENT, C., TENZA, D., RICCIARDI-CASTAGNOLI, P., RAPOSO, G. & AMIGORENA, S. 1998. Eradication of established murine tumors using a novel cell-free vaccine: dendritic cell-derived exosomes. *Nature medicine*, 4, 594-600.
- ZOMER, A., MAYNARD, C., VERWEIJ, F. J., KAMERMANS, A., SCHAFFER, R., BEERLING, E., SCHIFFELERS, R. M., DE WIT, E., BERENQUER, J., ELLENBROEK, S. I., WURDINGER, T., PEGTEL, D. M. & VAN RHEENEN, J. 2015. In Vivo imaging reveals extracellular vesicle-mediated phenocopying of metastatic behavior. *Cell*, 161, 1046-57.
- ZYLBERSZTEJN, K. & GALLI, T. 2011. Vesicular traffic in cell navigation. *FEBS J*, 278, 4497-505.